WARWICK
THE UNIVERSITY OF WARWICK

A Thesis Submitted for the Degree of PhD at the University of Warwick

Permanent WRAP URL:
http://wrap.warwick.ac.uk/106502

Copyright and reuse:
This thesis is made available online and is protected by original copyright.
Please scroll down to view the document itself.
Please refer to the repository record for this item for information to help you to cite it.
Our policy information is available from the repository home page.

For more information, please contact the WRAP Team at: wrap@warwick.ac.uk

warwick.ac.uk/lib-publications

Highly branched and hyperbranched polymers: Synthesis, characterisation, and application in nucleic acid delivery

Alexander B. Cook

A thesis submitted in partial fulfilment of the requirements for the degree of

Doctor of Philosophy in Chemistry

Department of Chemistry

University of Warwick

February 2018

Table of Contents

List of Figures

List of Tables

List of Schemes

List of publications

- Branched and Dendritic Polymer Architectures: Functional Nanomaterials for Therapeutic Delivery (Chapter 1 - review)
  AB Cook, S Perrier
  To be submitted

- Hyperbranched Polymers with High Degrees of Branching and Low Dispersity Values: Pushing the Limits of Thiol–Yne Chemistry (Chapter 2)
  AB Cook, R Barbey, JA Burns, S Perrier
  Macromolecules, **2016**, 49 (4), 1296-1304

- Well-Defined Hyperstar Copolymers Based on a Hyperbranched Thiol-Yne Core and a Poly(2-oxazoline) Shell for Biomedical Applications (Chapter 2)
  M Hartlieb, T Floyd, **AB Cook**, C Sanchez-Cano, S Catrouillet, JA Burns, S Perrier
  Polymer Chemistry, **2017**, 8, 2041-2054

- Hyperbranched Poly(ethyleneimine-co-oxazoline) by Thiol-Yne Chemistry for Non-Viral Gene Delivery: Investigating the Role of Polymer Architecture (Chapter 3)
  AB Cook, R Peltier, J Zhang, P Gurnani, J Tanaka, JA Burns, R Dallman, M Hartlieb, S Perrier
  To be submitted

- Cationic and Hydrolysable Branched Polymers by RAFT for Complexation and Release of dsRNA (Chapter 4)
  AB Cook, R Peltier, M Hartlieb, R Whitfield, G Moriceau, JA Burns, DM Haddleton, S Perrier
  To be submitted

- Branched Poly(trimethylphosphonium ethylacrylate-co-PEGA) by RAFT: Alternative to Cationic Polyammoniums for Nucleic Acid Complexation (Chapter 5)
  AB Cook, R Peltier, T Barlow, J Tanaka, JA Burns, S Perrier
  To be submitted

Abbreviations

AA	Acrylic acid
AFM	Atomic force microscopy
ATRP	Atom transfer radical polymerisation
BEA	Bromoethyl acrylate
Conv.	Conversion
CROP	Cationic ring-opening polymerisation
CRP	Controlled radical polymerization
CTA	Chain transfer agent
Đ	Dispersity
DEGDA	Di(ethylene glycol) diacrylate
DLS	Dynamic light scattering
DMF	*N*,*N*-dimethyl formamide
DMSO	Dimethyl sulfoxide
DMAEMA	2-(dimethylamino)ethyl methacrylate
DMAEA	2-(dimethylamino)ethyl acrylate
DMAPA	2-(dimethylamino)propyl acrylate
*d*n/*d*C	Incremental refractive index
DP	Degree of polymerization
DRI	Differential refractive index
dsRNA	Double stranded ribose nucleic acid
EGDMA	Ethylene glycol dimethacrylate
ESI—MS	Electrospray ionization mass spectroscopy
EtBr	Ethidium bromide
GFP	Green fluorescent protein
GPC	Gel permeation chromatography
IV	Intrinsic viscosity
KMHS	Kuhn Mark Houwink Sakurada
Log M	Log molecular weight
MALDI-ToF	Matrix assisted laser desorption ionisaton – time of flight

MALLS	Multi angle laser light scattering
MMA	Methyl methacrylate
M_n	Number average molecular weight
M_p	Peak molecular weight
M_w	Weight average molecular weight
MW	Molecular weight
MWD	Molecular weight distribution
NMP	Nitroxide mediated polymerization
NMR	Nuclear magnetic resonance (spectroscopy)
pDNA	Plasmid deoxyribose nucleic acid
PEG	Poly(ethylene glycol)
PEGA	Poly(ethylene glycol) acrylate
PEI	Poly(ethyleneimine)
PMMA	Poly(methyl methacrylate)
POx	Poly(oxazoline)
ppm	Parts per million
PS	Polystyrene
RAFT	Reversible addition fragmentation chain transfer (polymerisation)
RI	Refractive index
SCVP	Self-condensing vinyl polymerisation
SD	Standard deviation
SEC	Size exclusion chromatography
SLS	Static light scattering
THF	Tetrahydrofuran
Thiol-yne	Thiol-alkyne chemistry
TMP	Trimethylphosphine
TMA	Trimethylamine
UV	Ultraviolet
V_h	Hydrodynamic volume
XTT	2,3-Bis-(2-Methoxy-4-Nitro-5-Sulfophenyl)-2H-Tetrazolium-5-Carboxanilide)

Acknowledgements

To thank the very large number of people that have helped me to reach this point would be almost impossible, therefore, I shall acknowledge a few key people.

I am very grateful to Professor Sebastien Perrier for giving me this opportunity. He has taught me, both consciously and unconsciously, how thorough but also exciting science is done. I appreciate all his contributions of time, ideas, and funding to make my Ph.D. experience productive and stimulating. His positive encouragement and support has made my time spent studying for a PhD at Warwick both a pleasure and rewarding.

I would like to thank Dr James Burns and the Formulation Technology Group at Syngenta for their invaluable contributions and guidance throughout my research. In addition, I greatly appreciate the help and support of Professor David Haddleton during the project.

The members of the Perrier group, past and present, have contributed immensely to my personal and professional time at Warwick. The group has been a source of great friendship, as well as good advice and collaboration. (MLK, GG, JSM, JB, MH, RP, KK, SC, TB, SL, JZ, LM, AS, JG, AK, JR, RW, CSS, PG, CB, GM, JT, MG, RH, DL, SL, MA, AK, AL, SE, EM, TF, HS, RR, FB).

I would also like to thank all the talented and kind people of the Warwick polymer groups and the wider Department of Chemistry, including all of those who have since moved on.

The final thank you is to my family for their constant support.

Declaration

Experimental work contained in this thesis is original research carried out by the author, unless otherwise stated, in the Department of Chemistry at the University of Warwick, between October 2014 and December 2017. No material contained herein has been submitted for any other degree, or at any other institution.

Results from other authors are referenced in the usual manner throughout the text.

In addition, the AFM images in Chapter 3 were obtained by Dr Jungliang Zhang, the toxicity assay and GFP plasmid transfection results in Chapter 3 were obtained by Dr Raoul Peltier, and the GFP plasmid transfection results in Chapter 5 were obtained by Dr Raoul Peltier.

Signed: _____ Date:_____

Alexander B. Cook

Abstract

Polymer chemistry enables the design and development of synthetic cationic gene delivery systems with varying polymer architectures. Branched polymers have been shown to have advantages for drug delivery purposes including nucleic acid delivery. The objective of this work is to utilise advanced polymer synthesis methods to synthesise a range of cationic polymers with well controlled branched architectures and investigate their cytotoxicity, nucleic acid complexation, resulting polyplex morphology, and gene transfection efficiency.

Firstly, the synthesis of hyperbranched polymers using thiol-yne chemistry is explored with a semi-batch process to form hyperbranched polymers with well-defined molecular weights and dispersities. Following this, cationic moieties are introduced onto thiol-yne hyperbranched polymers using the ring opening polymerisation of 2-ethyloxazoline and an additional hydrolysis step to form PEI-POx copolymers with hyperbranched architectures. An investigation of plasmid DNA complexation, and *in vitro* toxicity and GFP plasmid gene transfection is then conducted.

RAFT polymerisation is then utilised to form highly branched polymer architectures by copolymerisation of a divinyl branching comonomer. This strategy has the advantage of being able to introduce tuneable degradation and nucleic acid release. Finally, the possibility of using RAFT to synthesise branched polymers with phosphonium cationic moieties is also investigated, and their DNA complexation, toxicity, and gene transfection efficiency compared to the equivalent cationic polyammoniums.

Overall, this thesis describes a number of advanced polymer synthesis methods to create hyperbranched and highly branched cationic polymers suitable for nucleic acid complexation, and also investigates their structure-function characteristics relating to aspects of nucleic acid delivery.

1.

Introduction

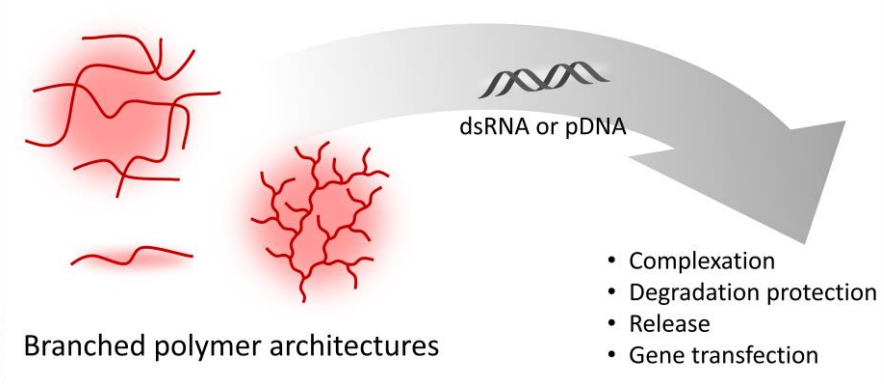

1.1 Nucleic acid therapy

Gene therapy involves the introduction of genetic material (i.e. nucleic acids: DNA, mRNA, dsRNA, siRNA) into target cells, with the goal of treating various forms of disease with genetic origins.[1,2] These nucleic acid therapies have the potential to treat a wide range of disease with currently limited therapeutic options including: cystic fibrosis, cancer, cardiovascular disease, hemophilia, and neurodegenerative disorders among others.[3-7] Another use for this nucleic acid technology lies in the agrochemical sector, in theory an individual species of pest could be targeted with complete specificity.

There are three main gene therapy strategies: 1) introduction of a DNA or mRNA to cells in order for it to transcribe a gene or protein that would otherwise not be produced; 2) introduction of a dsRNA or siRNA in order to induce the RNA interference pathway and silence production of a certain gene or protein of interest; 3) In recent years, the potential impact of gene therapy has been expanded even further by the development of CRISPR/Cas9 gene editing technology.[8,9] RNA interference (RNAi) is a biological process which involves the silencing of certain genes by RNA molecules, with high efficiency and specificity.[10] The mechanism results in the destruction of specific messenger RNA molecules. In 1998, the seminal study on RNA interference was conducted by Fire and Mello, and showed gene silencing in nematode worm *Caenorhabditis elegans*.[11] In recognition of the importance of this work they were awarded the Nobel Prize for medicine in 2006.

1.1.1 Delivery barriers

Naked nucleic acid formulations are in clinical trials for certain physiological environments like the brain, lung, and eye, however most tissues in the body require a delivery system to facilitate the transfection process.[12] This is due to multiple extracellular and intracellular delivery barriers that need to be overcome (**Figure 1.1**).[13-17]

Extracellular barriers to successful gene delivery include the problem of DNA and RNA having poor resistance to enzymes such as RNases and other nucleases. In agrochemical applications these enzymes can be present in the soil and also most pest midguts.[18] In human health applications these DNA and RNA degrading enzymes exist in the bloodstream.[1,19] Other extracellular barriers include recognition and clearance by the immune system, for example, macrophages can readily uptake polyplex nanoparticles.[20] In addition, RNA is hydrolytically unstable due to the additional hydroxyl group at the 2' position on the ribose compared to DNA.[15,21]

There are also a number of intracellular barriers that need to be surpassed before the desired exogenous genetic material can be incorporated into the new cell's machinery. Nucleic acids, and their vectors, typically enter the cell by endocytosis.[22] This process of crossing cellular membranes can depend to a large extent on size and charge, with naked DNA usually being too negatively charged to enter cells efficiently *via* endocytosis. Once inside the cell, the vector then needs to escape from the endosome.[23] The therapeutic nucleic acid needs to be released or become bioavailable in the cytosol, either for the mechanism of action to occur in the cytosol, or for diffusion through the cytosol to the nucleus. For successful DNA transfection the DNA needs to pass the double membrane nuclear envelope and enter the nucleus to be transcribed. Entry to the nucleus occurs through the nuclear pore complex through either passive or active transport mechanisms, again, with size being a determining factor.[24-26]

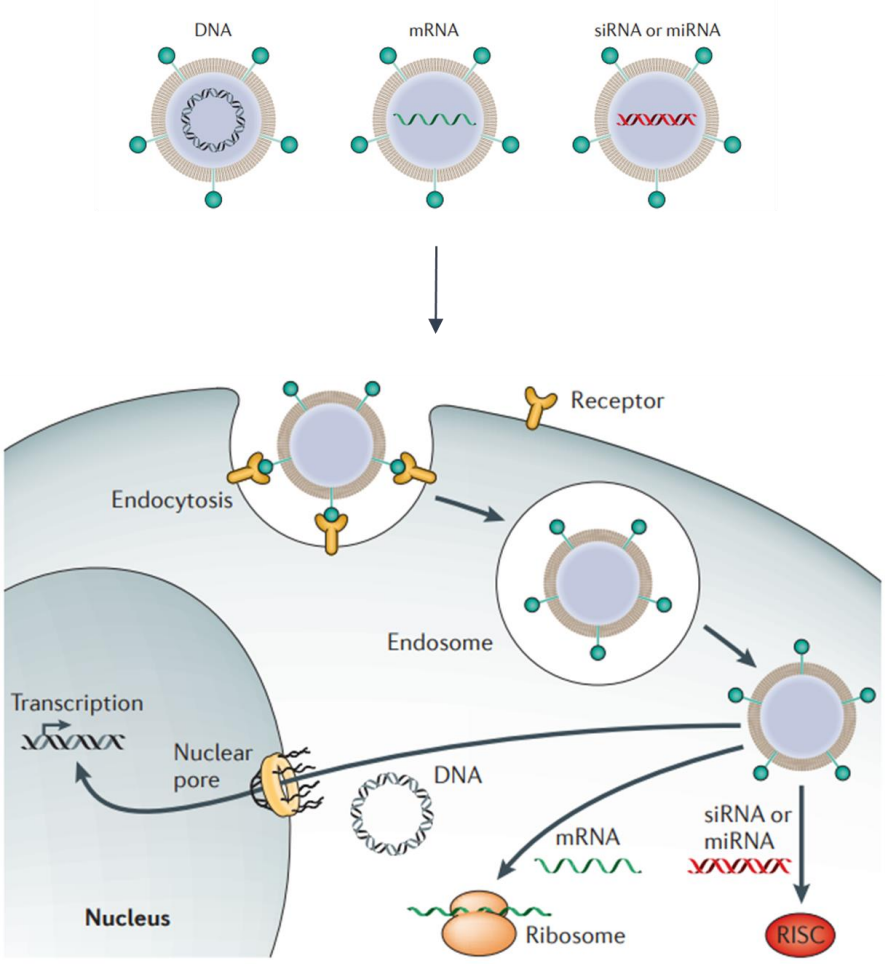

Figure 1.1. Pathway to successful intracellular delivery of nucleic acids. Figure adapted from reference [17].

1.1.2 Non-viral gene delivery

Various viral and non-viral vectors have been investigated for their potential to help overcome the mentioned delivery barriers. Viral vectors such as adeno associating viruses, retroviruses, and herpes simplex viruses have been studied extensively for nucleic acid protection and enhanced delivery, but have specific drawbacks including undesirable mutagenic and immunogenic effects.[27,28] Such drawbacks can be circumvented by using synthetic delivery vectors based on polymeric nanostructures of defined architecture for optimal binding of nucleic acids.[29] Synthetic vectors also have the benefits of reproducible and easily scalable production. The most popular commercial

gene delivery polymers are shown in **Figure 1.5**, and include linear polylysine, linear and branched polyethyleneimine (PEI), polyamidoamine dendrimers (PAMAM).

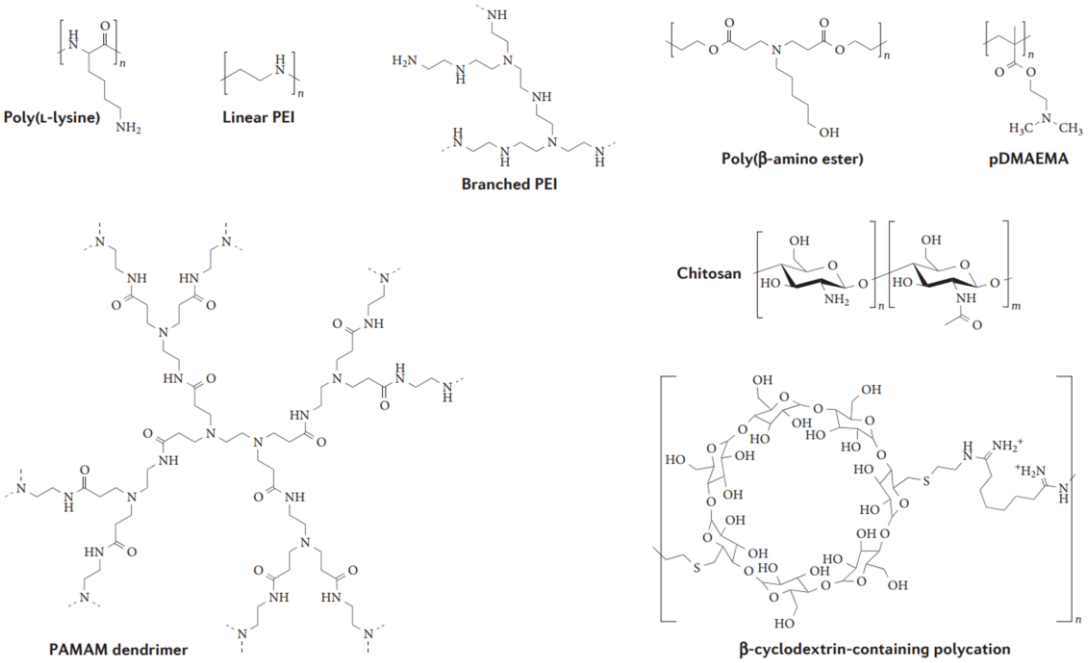

Figure 1.2. Structures of commercially available gene delivery polymers. Figure adapted from reference [17].

Linear polylysine was one of the first polymers utilized for gene delivery.[30] However its clinical application has been very limited, commonly thought to be due to poor escape from the endocytic pathway. Polyethyleneimine (PEI) was first used in 1995 and has since been well investigated as a carrier for nucleotides.[31] In one study, intrathecal administration of siRNA PEI complex was shown to silence a targeted pain receptor (NR2B) in rats.[32] PEI has been the subject of a number of successful *in vivo* gene delivery studies to a range of tissues, including the central nervous system, kidney, lung and various tumors. However translation of PEI in the clinic is currently limited, commonly thought to be due to high cytotoxicity related to its positive charge.

Chitosan and cationic cyclodextran based polymers have also been investigated for application in non-viral gene delivery systems.[4,33] The effect of polymer size, nature of amine protonation or quaternisation, and charge density on gene delivery and complex toxicity was reported. Both chitosan and amine modified cyclodextran are reported to be less cytotoxic than PEI.[29]

1.2. Polymer architecture

1.2.1. Increasing complexity

Polymers have a key role in drug delivery systems and have the potential to provide solutions by simplifying administration, reducing toxicities, and improving efficiencies through additional functionality.[34] The progression of polymer architectures from linear to more complex branched topologies by use of easily accessible chemistries while maintaining reasonably large scale production, offers further opportunities to improve therapeutic delivery.[35,36] Recent advances in polymer chemistry, including new step-growth polymerisation routes, continued advancement of controlled radical and ring-opening polymerisation methods, and further development of simple, high yielding, and orthogonal coupling chemistries, has brought unprecedented access to complex polymer architectures.[37,38] Branched polymers are a special class of polymer architecture characterised by their high branching densities.[39] The branched polymer topology imparts a number of favourable properties compared to their linear polymer equivalents including: high surface functionality, globular conformation, low intrinsic viscosities, high solubilities, and interesting rheological modifying properties.[39-41] This has led to branched polymers being increasingly important for biomedical applications over the past 20 – 30 years.[42-44]

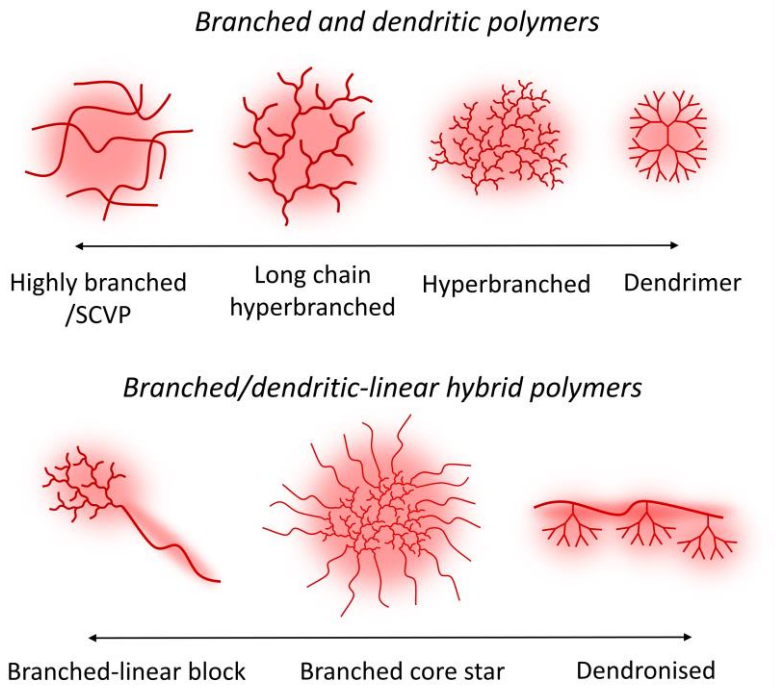

Figure 1.3. Cartoon representation of various branched polymer architectures able to be synthesised with modern polymerisation and coupling synthetic strategies.

In certain polymers such as thermosets and rubbers, branching is typically on a macrocscopic/crosslinked scale, leading to interesting physical properties of these materials. This thesis focuses of branching in soluble nanoscale forms, and will refer to branched polymers of the following definitions (illustrated in **Figure 2**). The term highly branched polymer refers to high frequency main chain branching of linear polymers, with the branch points in a highly branched polymer being distributed randomly throughout the polymer. The major advantage of highly branched polymers is their simple synthetic methodolgies. In general, the term dendritic polymer is used to refer to a class of branched polymers including dendrimers, dendrons, hyperbranched polymers, and hybrid variants containing dendrons and hyperbranched polymers. The term originates from the Greek word Dendron, δένδρον, which translates to tree. The various subclasses of dendritic polymers can be further defined. Dendrimers were first synthesised in laborious multi-step procedures, in the late 1970s and early 1980s, and are defined by their perfectly symmetrical and layered branching patterns (with no irregular or non-branching points, DB), and therefore single molecular weight with a dispersity of 1.[45-47]

$$DB = \frac{D + T}{D + T + L} \qquad (\boldsymbol{Equation\ 1})$$

Degree of branching (DB) was defined by Frechet and coworkers, **Equation 1**, where D, T and L are the fractions of dendritic, terminal or linear monomer segments in the resulting dendritic polymers (obtained from NMR spectroscopy).[48] Dendrimers have DB's of 1. Hyperbranched polymers are synthesized by step-growth polymerization via condensation or addition of AB_n monomers in one-pot reactions. Here, A and B are the two functionalities that can react with each other but not with themselves. In an AB_2 monomer system, the degree of branching is controlled by statistics and only reaches around 0.5, far from the value of 1 usually achieved with dendrimers.[49] Further functionality and control over branching distributions can be introduced by the AB_2 polymerisation of macromonomers leading to long chain hyperbranched polymers.[50] Recently, evolution of these branched topologies has progressed towards dendritic-linear hybrid polymers from combination of well controlled linear polymers with dendritic polymers, *via* creative coupling and polymerisation chemistries.[51] These structures include linear hybrids of dendrimers and hyperbranched polymers, and can be in the form of branched-linear block copolymers, branched-core star polymers, and dendronised polymers.

From a synthetic chemistry perspective, these structures can by produced from an ever expanding toolbox of polymer chemistry and coupling chemistry techniques. A summary of these procedures can be found in **Figure 3**. Dendrimer formation has typically proceeded using a series of iterative growth and activation steps.[52] Dendrimers can be synthesized following the divergent approach which can lead to branching irregularities at higher generations, and also the convergent approach, which was introduced in pioneering work by Fréchet and Hawker and can lead to higher purity.[53] Due to their structural precision this has been achieved with robust organic reactions, including amidification and esterification reactions (**Figure 3)**. Recently improvements to dendrimer synthesis, in terms of reaction times and purity, have been achieved using accelerated techniques based on efficient and orthogonal chemistries.[54]

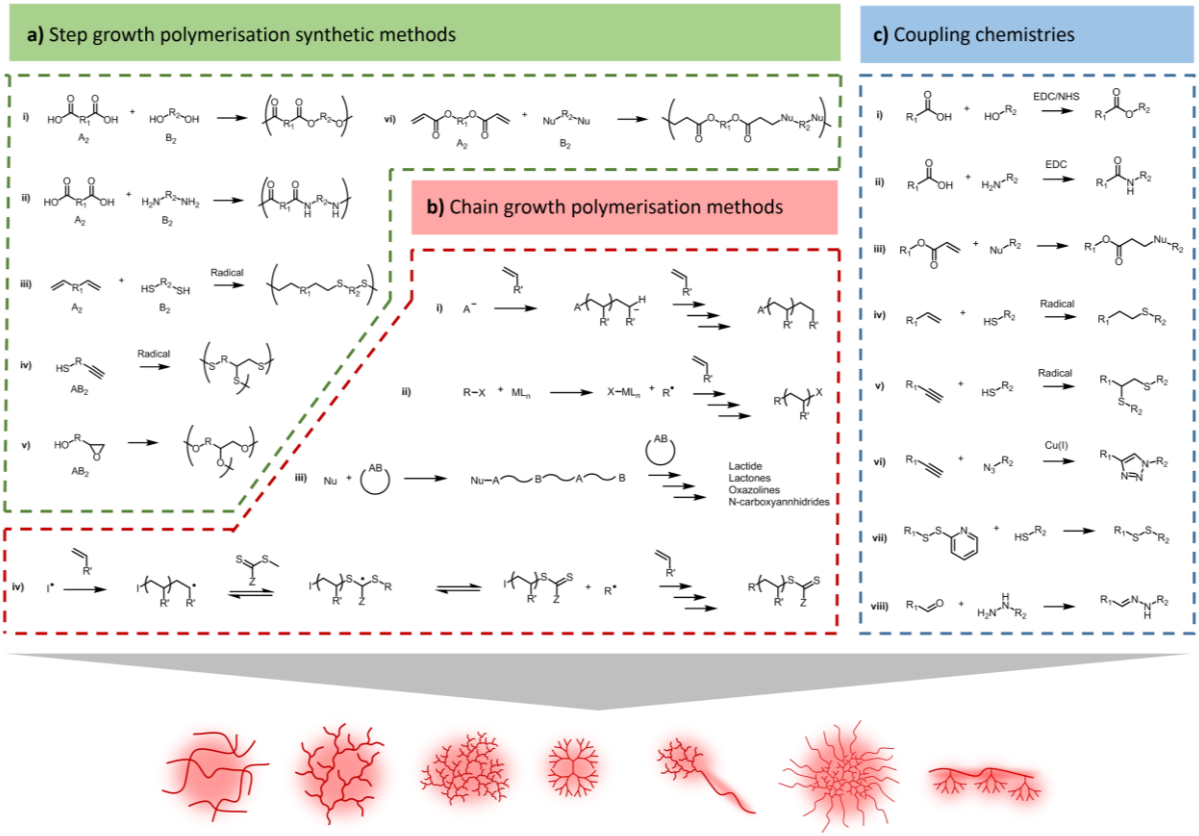

Figure 1.4. Schematic representations of some of the synthetic strategies to achieve branched polymer architectures with modern polymerisation and coupling synthetic strategies: **a)** branched and linear polymers via step growth polymerisations, i) esterification condensation, ii) amidification condensation, iii) thiol-ene addition, iv) thiol-yne addition, v) asymmetric epoxide ring opening, vi) michael addition type, **b)** branched and linear polymers via controlled chain growth polymerisations, i) living anionic, ii) Cu(0) radical polymerisations, iii) ring opening polymerisations, iv) RAFT polymerisation, **c)** various coupling strategies for formation of branched-linear hybrid materials, and also therapeutic conjugation, i) ester, ii) amide, iii) michael addition, iv) thiol-ene, v) thiol-yne, vi) azide-alkyne cycloaddition, vii) disulphide formation, viii) hydrazone.

Synthetic strategies for formation of highly branched and hyperbranched polymers arose as an alternative and simpler route to polymers with similar favourable properties to dendrimers, but without demanding multi-step syntheses and purifications. Hyperbranched polymers are synthesised by the step growth polymerisation of AB_n monomers (where $n \geq 2$), and also the step growth copolymerisation of combinations of

monomers, as in the $A_2 + B_m$ approach (where $m \geq 3$).[39] These reactions were theorised by Flory decades ago and require monomers different A and B functionalities that can react with each other but not with themselves.[55] Step growth polymerisations can also be performed with telechelic AB_2 macromonomers leading to long chain hyperbranched polymers.[56]

The design and synthesis of highly branched polymers by chain growth polymerisations is a more recent development in polymer chemistry. In the self-condensing vinyl polymerisation (SCVP) route, which was introduced by Fréchet and co-workers, a vinyl monomer bearing an initiating group can propagate through the vinyl bond and also form branching points through the initiating group.[57] This SCVP has been extended to RAFT, ATRP, NMP, and SCROP. Another popular chain growth strategy for highly branched polymers is the Strathclyde route, which involves the copolymerisation of vinyl monomers with small amounts of divinyl monomers and in the presence of a chain transfer agent.[58] Similarly to SCVP, this method has also been extended to the controlled radical polymerisations RAFT and ATRP. Linear polymers with pendant vinyl moieties are formed, which then have the opportunity to polymerise into other linear chains to form highly branched polymers.

Since the development of living anionic polymerisations by Szwarc in 1956, there have been many chain growth polymerisations developed for synthesis of linear polymers with controlled molecular weights, narrow molecular weight dispersities, and precise functionality.[59,60] RAFT polymerisation in particular is becoming increasingly popular for biomedical applications, in part due to its ease of use and compatibility with a wide range of monomers.[61] In addition to synthesis of highly branched polymers by chain growth methods as mentioned previously, by combining these chain growth systems with efficient coupling chemistries, researchers can now easily synthesise new types of branched-linear hybrid architectures including, branched-linear block copolymers, branched-core star polymers, and dendronised polymers. The expansion of highly efficient coupling chemistries, after the seminal work of the Sharpless group, has led to further options for synthesis of these types of architectures.[62] Available click-type reactions include, the Huisgen alkyne-azide cycloaddition, thiol-ene/yne radical

additions, various thiol-ene Michael additions, and tertiary isocyanate amine coupling among others.[37,63]

Therapeutic molecules can be carried by these polymer systems by two main methods: encapsulation with either hydrophobic or electrostatic interactions, and also covalent attachment to the polymeric carrier. Encapsulation methods have been widely investigated, and branched polymer architectures offer the benefits of having globular three-dimensional topologies capable of encapsulating high loadings of cargo. A benefit of this approach is the ability to obtain unimolecular micelle type of structures without concentration dependent disassembly at low concentrations.[64] However it can be difficult to control the release of molecules from the polymer. Many interesting chemistries (**Figure 3**) have been developed for covalent attachment guest molecules, including stimuli responsive linkers able to release therapeutic molecules on certain specific triggers, including pH, redox environments, glucose, and enzymatic cleavage.[65] Branched polymers also offer advantages for this drug attachment method, due to their high number of functionalisable groups on the periphery of the constructs.

Table 1.1. Summary of current state-of-the-art in branched polymer therapeutic delivery systems, including design strategies for various branched polymer architectures, and specific application details in drug/ gene delivery.

Architecture	Structure	Polymer synthetic method	Therapeutic conjugation method	Application	Ref
Highly branched Divinyl copolymerisation	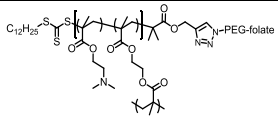	RAFT copolymerisation with divinyl monomer	Electrostatic nucleic acid complexation	Plasmid DNA delivery	66
	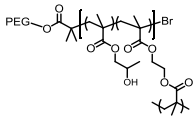	ATRP copolymerisation with divinyl monomer	Encapsulation of SPIONs	SPION delivery for therapy/diagnosis	67
	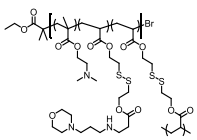	ATRP copolymerisation with divinyl monomer	Electrostatic nucleic acid complexation	Plasmid DNA delivery	68
SCVP	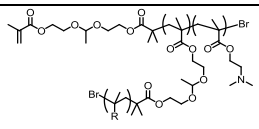	ATRP SCVP of degradable inimer and dmaema	Drug encapsulation	Niclosamide and amonafide drug delivery	69

	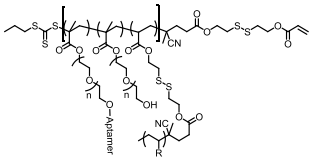	RAFT SCVP of Disulphide inimer and pegma	Hydrophobic drug encapsulation	Delivery of Dox to breast cancer cell line	70
	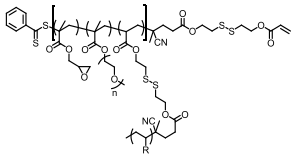	RAFT SCVP of Disulphide inimer and pegma/gma	covalent attachment, with acid and redox cleavable groups	Camptothecin intracellular delivery	71
	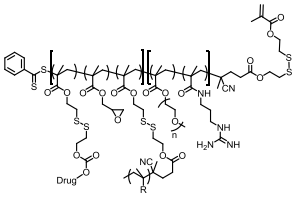	RAFT SCVP of Disulphide inimer and pegma/gma/cptm	Disulphide linked drug monomer (Gd MRI imaging via epoxide)	Camptothecin intracellular delivery	72
Hyperbranched AB_n	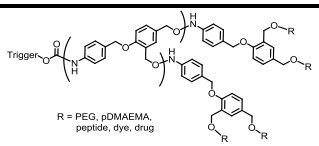	AB2 polycondensation (isocyanate-hydroxy)	Covalent attachment	Doxorubicin delivery and DNA delivery	73
	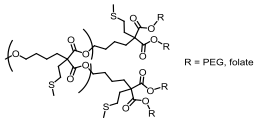	AB2 polycondensation	Hydrophobic drug encapsulation	Taxol anticancer therapy	74
	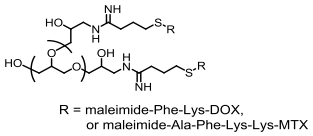	Ab2 ROP of epoxide containing glycidol	Enzyme cleavable covalent attachemnt	Doxorubicin and methotrexate anticancer drugs	75
	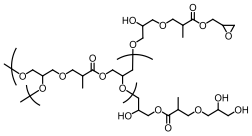	AB3 ROP of epoxide containing monomer	Ester linked covalent attachemnt	MTX anticancer drug	76
A_2+B_m	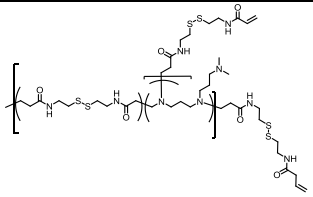	A2 +B3 Michael addition	Electrostatic nucleic acid complexation	Tumour siRNA delivery in vivo	77
	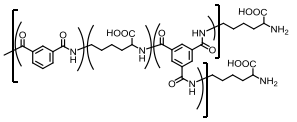	A2 +B2 +B3 polycondensation	Cell penetrating peptide mimick	Intracellular delivery via endosome disruption	78
	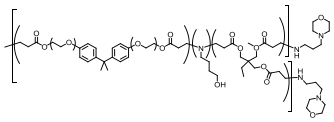	A2 +B2 +B3 Michael addition	Electrostatic nucleic acid complexation	Plasmid DNA delivery for skin gene therapy	79
Longchain hyperbranched	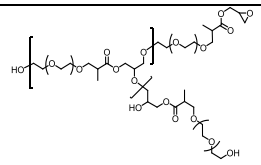	Proton transfer AB2 polymerisation	Ester linked covalent attachemnt	MTX anticancer drug	80

	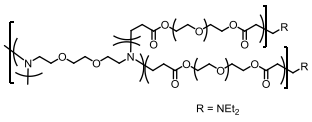	A2 +B4 Michael addition polymerisation	Electrostatic nucleic acid complexation	Plasmid DNA delivery	81
	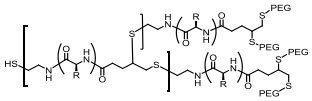	CROP and thiol-yne AB2 photoaddition polymerisation	Hydrophobic drug encapsulation	DOX drug release in vitro	82
Dendrimer	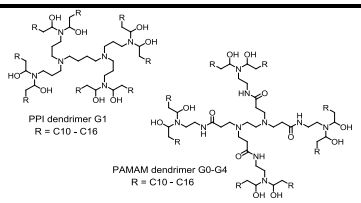	Divergent dendrimer synthesis (commercial) then michael addition modification	Electrostatic nucleic acid complexation	siRNA gene delivery to lung vasculature	83
	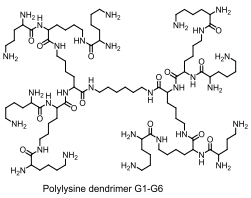	divergent strategy using standard peptide coupling chemistry	Electrostatic nucleic acid complexation	Plasmid DNA delivery	84
	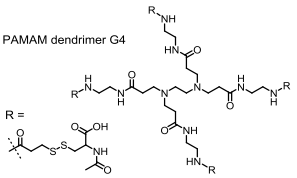	Divergent dendrimer synthesis (commercial) then activated ester coupling	Disulphide linked covalent attachment	NAC Anti inflamitory agent delivery to B2-V microglial cells	85
	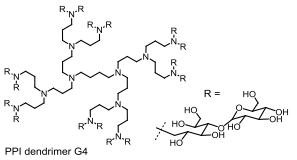	G4 PPI dendrimer Reductive amination coupling of maltose shell	Electrostatic drug complexation	fludarabine triphosphate delivery	86
	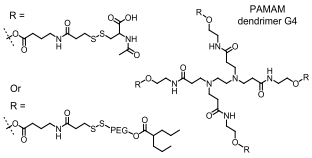	Divergent dendrimer synthesis (commercial) then pyBOPcoupling	Disulphide linked covalent attachment	NAC and Valproic acid Antiinflamitory	87
Branched-linear hybrid Branched-linear block	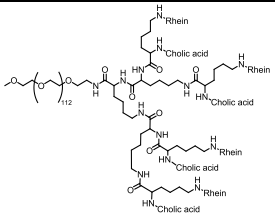	Divergent lysine Dendron synthesis and amidificaion with PEG and functionality	Hydrophobic drug encapsulation	Delivery of Dox to lymphoma tumour	88
	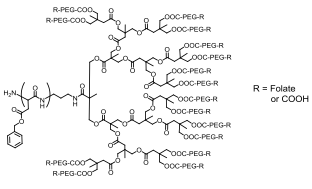	NCA ROP, divergent dendrimer synthesis, Activated ester coupling	Hydrophobic drug encapsulation	PTX drug delivery	89

	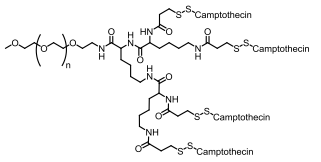	Commercial PEG, divergent dendrimer synthesis, activated ester coupling	Disulphide linked covalent attachment	Camptothecin delivery in vivo	90
	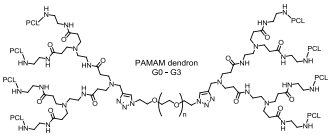	Alkyn azide click coupling of PAMAM dendrons and PEG	Hydrophobic drug encapsulation	DOXorubicin encapsulation and release	91
Branched-linear star	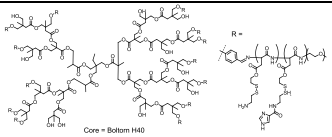	Polycondensation (commercial H40) ph sensitive polypeptide shell coupling	Electrostatic nucleic acid complexation	siRNA gene delivery	92
	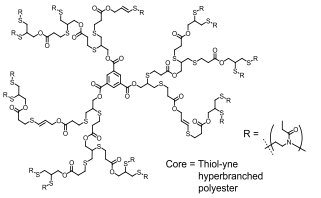	CROP and thiol-yne photoaddition polymerisation	Hydrophobic drug encapsulation	Hydrophobic dye as drug model	93
	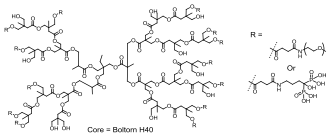	Polycondensation (commercial H40) activated ester PEG coupling	Hydrophobic drug encapsulation	Doxorubicin anticancer drug delivery	94
	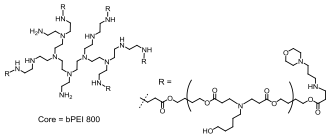	Azirine ROP (commercial PEI) Michael addition arm coupling	Electrostatic nucleic acid complexation	Plasmid DNA delivery	95
	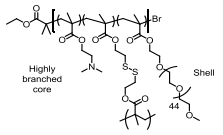	ATRP with divinyl comonomer	Electrostatic nucleic acid complexation	siRNA gene delivery to lung vasculature	96
Dendronised	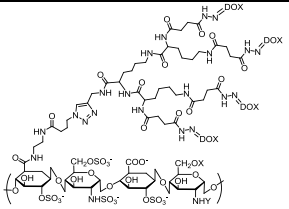	Divergent lysine dendron synthesis and azide alkyne click coupling to heparin	Covalent attachment, through acid cleavable hydrazone	Doxorubicin delivery in 4T1 breast tumor model	97
	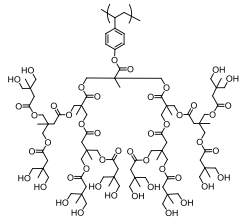	Polystyrene based backbone grafted with polyester dendrons	In vivo biodistribution studies with radiolabel	Radiolabel as proof-of-concept for drug delivery	98
	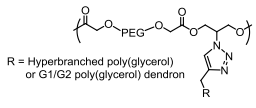	PEG azido polymer backbone grafted with polyglycerol dendrons	Hydrophobic drug encapsulation	Hydrophobic dye as drug model	99

1.2.2. Highly branched polymers

Synthesis of highly branched polymers by use of chain growth polymerisations, is a versatile and scalable approach for the synthesis of functional polymers.[40] Radical chain growth polymerisation methods have always produced branching in some cases through the radical polymerisation side reactions of intramolecular backbiting, intermolecular transfer to polymer, and polymerisation of vinyl terminated disproportionation products.[100] However, introduction of branching in radical polymerisations through design was more recently established.

1.2.2.1. Divinyl monomer copolymerisation

Network formation through the radical polymerisation of vinyl monomers with difunctional comonomers is analogous to step growth polymerisations of multifunctional monomers. These polymerisations have been considered theoretically by Flory and Stockmayer, among others.[101-104] Whilst considerable experimental work has also been carried out with various monomer pairs, including: MMA and EGDMA, styrene and divinyl benzene, vinyl acetate and divinyl adipate. Theory predicts that macroscopic crosslinking will occur when the number of difunctional branching monomers per polymer chain is greater than one. In practise there is often a discrepancy between the theory and the observed polymerisation gel points. Theoretical gel point values are generally underestimated due to pendant vinyl group of the multifunctional commoner species causing intramolecular cyclisation during the polymerisation or becoming less reactive as one group is polymerised and remaining as an unreacted pendant vinyl group throughout the polymerisation.[105] These free radical polymerisation systems are often difficult to predict and can require considerable optimisation in order to achieve high conversions without macroscopic gelation.[106,107]

However, in 2000 Sherrington *et al*., introduced an improvement to free radical polymerisations of divinyl monomers to form highly branched but soluble polymer architectures, by inclusion of thiol chain transfer agent (CTA).[58,108,109] This method,

known as the 'Strathclyde route', reduces the primary chain length, can delay gelation, and can allow inclusion of additional functionality through functional CTAs. Atom transfer radical polymerisation (ATRP) was then employed to synthesise similar branched polymers with a more controlled polymerisation.[108] The difunctional copolymer method to branched polymers was first employed with reversible addition fragmentation chain transfer (RAFT) polymerization by our group in 2005,[110,111] and further investigated by Armes and coworkers.[105]

Early work on application of these branched polymer systems to DNA delivery was established by the Davis group, who synthesised highly branched PDMAEMA-b-PEG using RAFT polymerisation.[112,113] The structures were formed with a redox sensitive divinyl comonomer, to yield high molecular weight polymers able to be cleaved into lower molecular weight polymer chains. Efficient binding of DNA was shown to occur through electrostatic interactions. This method has also been adopted by Thurecht *et al*. who have used the RAFT copolymerisation of DMAEMA and EGDMA to synthesise highly branched structures for a variety of biomedical applications including gene delivery.[66,114] Polymer ability to deliver DNA was investigated using in vitro cell uptake assays in HeLa cells with flow cytometry. Branched pDMAEMA conjugated with the targeting ligand Folate (overexpressed on HeLa cells) showed improved cell uptake compared to oligofectamine and non-folate branched pDMAEMA, however polymer toxicity was observed above N/P ratios of 10.

More recently, Rannard *et al*., have shown that ATRP copolymerisations with small amounts of EGDMA leads to branched polymers which can form stable nanoparticles with tuneable sizes and functionalities.[115] It was shown, with a gut epithelium model, that these nanoparticles are able to cross mucus barriers and have potential of use as orally-administered nanocarrier systems. Additionally, it has been demonstrated that these highly branched polymers, synthesised by ATRP, can form stable nanoparticle composites with super-paramagnetic iron oxide nanoparticles (SPIONs) with future uses for delivery of drugs, imaging agents, or hyperthermia agents within cancer therapies.[67]

Wang and coworkers have investigated the effect of branching on transfection of plasmid DNA coding for G-luciferase and also green fluorescent protein (GFP).[68] Variation of

primary chain length and density of branching between individual polymer chains was achieved using ATRP with redox responsive divinyl commonomer. The authors found that the most highly branched polymer had the least adverse cytotoxic effects, whilst having higher transfection efficiencies than the linear pDMAEMA control.

1.2.2.2. Self-condensing vinyl polymerisation

In 1995, Frechet *et al*. showed that polymerisation of a vinyl monomer bearing an initiating group allowed polymerisation through the vinyl group and also through the initiating site, leading to the formation of highly branched polymers.[57] The authors termed this self-condensing vinyl polymerisation (SCVP). The SCVP process has been extended to various chain growth polymerisation methods, such as, nitroxide mediated polymerisation (NMP),[116] reversible addition chain transfer polymerisation (RAFT),[117] atom transfer radical polymerisation (ATRP),[118] and ring opening polymerisation (ROP).[119,120] Chain growth methods to highly branched polymers, such as divinyl commoner method, and SCVP, allow for facile incorporation of stimuli responsive groups, prodrug monomers, and imaging moieties for theranostic applications.[121]

The group of Gao has investigated branched polymers by SCVP for breast cancer therapies. The researchers used ATRP of inimers in microemulsion, and were able to load a drug combination of DNA damage repair agents and also STAT-3 inhibitors (amonafide and niclosamide respectively).[69] Selective growth inhibition of triple negative breast cancers was seen with the synergistic combination of drugs encapsulated in the branched polymer delivery system. Luo *et al.*, synthesised branched hydroxypropyl methacrylamide copolymers by a RAFT SCVP method, incorporating a DOX prodrug monomer and cathepsin-B enzyme cleavable branching units.[122] The high molecular weight and large (102 nm diameter) branched polymers could be degraded into lower molecular weight and smaller (8.2 nm diameter) species. These branched drug conjugates were investigated for breast cancer therapy both in vitro and with a mouse model. Enhanced antitumour efficacies in a 4T1 tumour model was observed by TG1,

immunohistochemical results, and the in vivo toxicity assays, highlighting potential benefits of designing polymer drug delivery systems with stimuli responsive and degradable properties compared to the non formulated free drug. Recently RAFT SCVP was also employed by Wei and colleagues, to form highly branched polymer prodrug conjugates with both redox sensitive disulphide groups and acid sensitive groups carbonate groups.[71] The presence of acidic pH conditions or glutathione environments enhances the release of captothecin, with the polymer system having IC50 values of 365.1 ug/ml, to HeLa cell-line with an MTS cell viablilty assay.

1.2.3. Hyperbranched polymers

Hyperbranched polymers have a more defined branching pattern than highly branched polymers, as branch points are introduced at high proportion of monomer units, compared to randomly along a chain growth polymer chain with highly branched polymers.[41] This feature makes hyperbranched polymers interesting for therapeutic delivery applications as the degree of branching in terms of branching units, linear units, and terminal units is much more easily defined and characterised.[42]

1.2.3.1. Step growth polymerisation of AB_n monomers

Much of the theory of branched and hyperbranched polymers was outlined by Flory in the mid-20th century, based on polycondensation reactions.[55] In order for AB_n hyperbranched polymers to be formed, a number of requirements were outlined by Flory: the A moiety must react selectively with B groups, B groups must have equal reactivity, and no cyclisation reactions should occur. These reactions proceed in a manner similar to most step growth polymerisations with rapid loss of monomer early in the reaction, high conversions required for high molecular weights, and the case of AB_n polymerisations there is no possibility of crosslinking (in theory). The resulting polymers contain dendritic units (fully reacted B moieties), linear units (singly reacted B moieties), terminal units (unreacted B moieties), and one focal A group. One of the most well-known examples of

a hyperbranched polymer formed from AB_n polycondensation is the commercial polymer Boltron, synthesised from the monomer bis(methylol)propionic acid (bis-MPA).[123] Boltron hyperbranched polymers with multiple surface hydroxyl functional groups have been synthesised, which have been used in a large number of applications, both as the native polymer and also post-polymerisation modified *via* the hydroxyl groups to impart further functionality or different solubility properties.[124] In this case control over the reaction (resulting molecular weight, molecular weight distribution, and degree of branching) can be achieved by addition of monomer in discrete portions, later developed into the 'slow monomer addition' method.[125,126]

Klok and coworkers have investigated the effect of degree of branching of polylysine on DNA complexation and delivery.[84] Transfection efficiency was affected by both polymer architecture and molecular weight. At similar molecular weights the hyperbranched polylysines showed greater transfection and gene knockdown compared to their linear and dendrimer analogues. In the 1990's, Mulhaupt and Frey developed the chemistry of hyperbranched polyglycerols which are formed from the step growth polymerisation of glycidol, a latent AB_2 monomer.[127] The polymers have very high biocompatibility similarly to the established linear polyethylene glycol, however great control over the branching and architecture can be achieved, opening up the application of these materials as nanocarriers for therapeutic purposes. In 2014, the Frey group showed that conjugating the MUC1 glycopeptide B-cell epitope and the tetanus toxoid T-cell epitope to the surface of hyperbranched polygycerol, enabled optimal presentation of antibodies due to the 3d topology of the branched structure.[128] This synthetic vaccine led to significant immune responses in a mouse study, highlighting the potential of these systems to be used in anticancer immunotherapy. Haag and colleagues have further expanded these hyperbranched polyglycerols as drug delivery systems, by attaching enzymatically cleavable therapeutics to the surface of these nanocarriers.[75] Further work by the group has shown that conjugating doxorubicin via an acid cleavable hydrazine linker had high drug loadings and an improved antitumour efficiency compared to free doxorubicin in a mouse tumour model.[129]

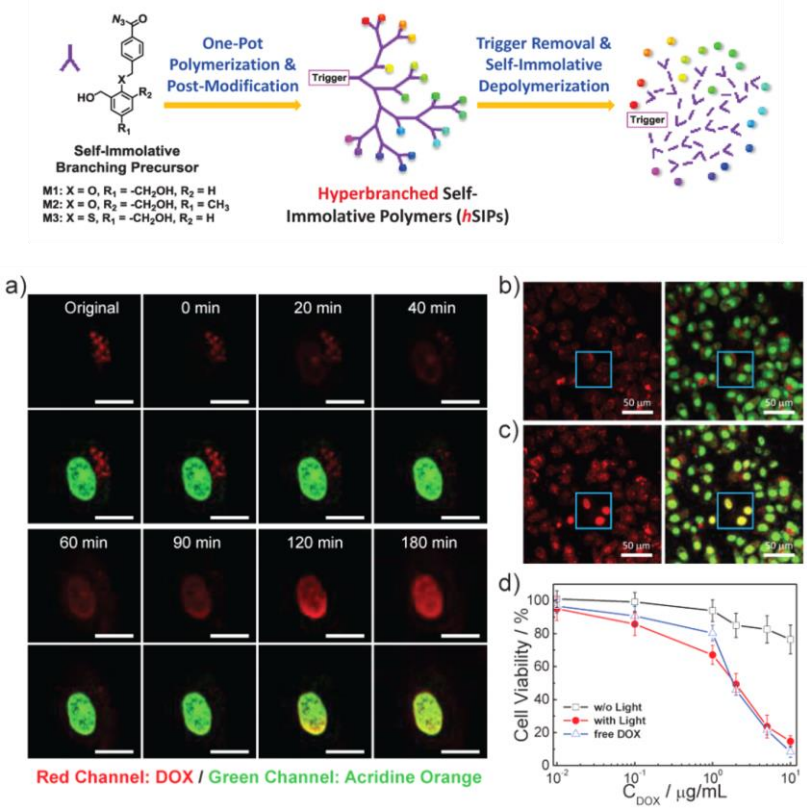

Figure 1.5. Synthetic scheme and confocal laser scanning microscopy images of HeLa cells incubated with hyperbranched and self-immolative polymers conjugated with doxorubicin and cRGD peptide. Figure adapted from reference [73].

Hyperbranched and self-immolative polymers undergo a cascade depolymerisation process after stimuli responsive removal of a trigger at the focal point of the hyperbranched polymer. Liu and coworkers synthesisd hyperbranched self immolative polymers in a onepot AB_2 polycondensation method, after which, the polymer were funtionalised with various imaging, targeting, and therapeutic groups including, cRGD peptides, Doxorubicin, coumarin, choline, and DMAEMA for nucleic acid complexation.[73] Depolymerisation triggered by blue light was investigated, and the polymer was determined to be completely degraded after 6 hours. Additionally intracellular release (HeLa cell-line) of doxorubicin conjugated to the exterior of the hyperbranched polymer was followed with confocal microscopy (**Figure 5**). Colocalisation studies indicated polymer cellular uptake via endocytosis and release of

doxorubicin into the cytosol, which overtime was seen to enter the nucleus with use of acridine orange stain.

Step growth polymerisation of AB_n monomers, where $n \geq 3$, has also been used to synthesise hyperbranched polymers for therapeutic delivery. For example, Zhu et al. synthesised biodegradable hyperbranched polyglycerol by *in situ* formation of an AB_3 monomer, to which they then conjugated the anticancer drug methotrexate (MTX) and fluorescent dye rhodamine.[76] The polymers showed good biocompatibility and biodegradability through the polymer ester bonds, and MTT assay against a cancerous cell line suggested high anticancer efficiency of the hyperbranched polymer drug delivery system.

1.2.3.2. Step growth polymerisation of A_2+B_m monomers

Synthesis of branched polymers *via* a double monomer methodology, $A_2 + B_m$, is attractive due to the range of much more readily available monomers, however the approach can lead to gelation at high conversions and critical concentrations.[42] These syntheses also require careful optimisation of the ratio of functional groups, monomer concentrations, purity of reagents, reaction time and temperature, in order to achieve controlled and reproducible reactions of high molecular weights without purification methods.[130,131] The growth and final structure profile of $A_2 + B_m$ systems is also not fully comparable to AB_n systems with their cascade type of branching patterns, leading to some in the community not considering them true hyperbranched polymers.[39]

A particularly simple but elegant step growth polymerisation method was developed by Lynn, Anderson, and Langer in the early 2000's, involving Michael additions of amines to multifunctional acrylate groups to form poly(β-aminoesters).[132,133] This was further developed to hyperbranched poly(β-aminoesters) by $A_2 + B_m$ routes more recently by a number of research groups. In 2016, Wang *et al*, investigated highly branched poly(β-aminoesters) for gene therapy, synthesised by the Michael addition polymerisation of an A_2 amine monomer with B_3 and B_2 triacrylates and diacrylates.[79] The authors found that the branched polymer topology imparts favourable properties of improved transfection

efficiencies and reduced toxicities *in vitro*. Additionally, the highly branched poly(β-aminoesters) effectively delivered genetic material *in vivo*, and resulted in the expression of significant functional proteins in the skin. A similar strategy was employed by Oupicky and colleagues, who prepared hyperbranched poly(β-amido amines) through the michael addition polymerisation of and A_2 diacrylamide monomer and a B_3 amine monomer (**Figure 6**).[77] The polymers were degradable with a glutathione redox stimuli through use of a disulphide containing diacrylamide, and were also functionalised with fluorine moieties. Good ability to bind siRNA by the polymers was confirmed, and gene silencing was successfully demonstrated with an *in vivo* luciferase expressing tumor model.

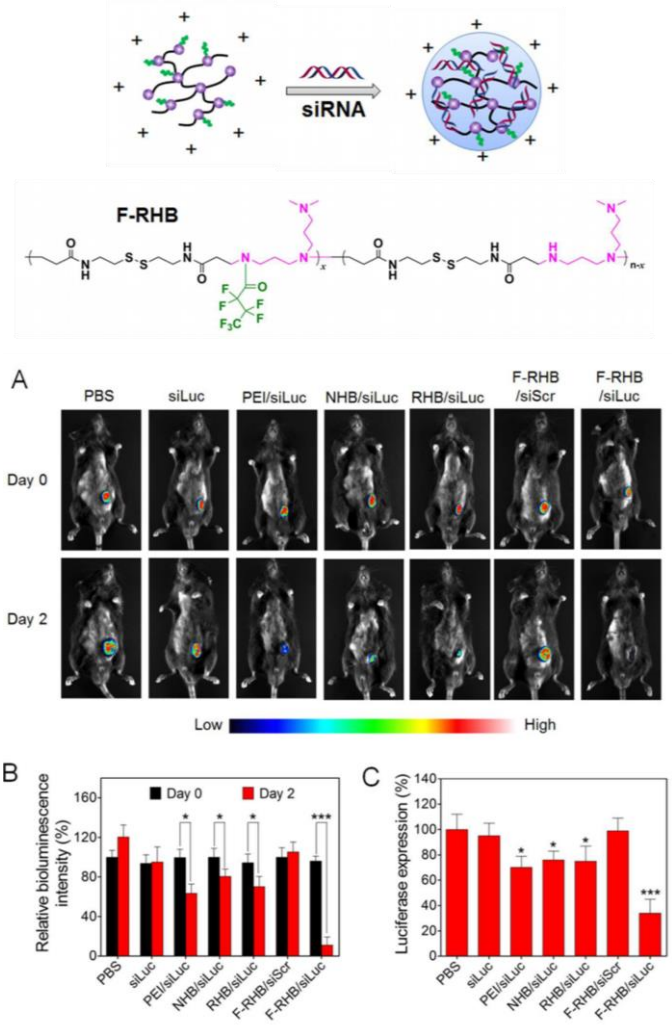

Figure 1.6. Hyperbranched poly(amido amines) and in vivo luc gene silencing, **a)** bioluminescence images of mice with B16F10-luc tumours, **b)** quantification of whole-body images, **c)** ex vivo anaylsis of luc activity in isolated tumour samples. Figure adapted from reference [77].

In a different example, the $A_2 + B_m$ system has also been recently employed to synthesise hyperbranched lysine based polymers that mimic cell-penetrating peptides. Chen *et al*. used a polycondensation reaction involving $A_2 + B_3 + B_2$ monomers, and showed that the resulting hyperbranched polymers had high cellular internalisation rates which were dependent on pH.[78] The branched architectures enhanced the membrane lytic properties of the polymers compared to the linear version, and thus showed potential for cytoplasmic delivery of therapeutic molecules.

1.2.3.3. Long chain hyperbranched polymers

Hyperbranched polymers from macromolecular units are a particularly interesting class of dendritic polymer architecture due to the ability to introduce additional functionality along the macromonomer chain, and the control over distance between branch points by tuning the degree of polymerisation of the linear macromonomer.[50] Synthetic strategies involve combination of chain growth polymerisation methods to gain well defined AB_2 macromonomers which can be further polymerised in an AB_2 step growth method.

Long chain hyperbranched PEG materials have been synthesised in this manner by Zhu and coworkers, and used for anticancer drug molecule delivery and plasmid DNA delivery.[80] The researchers were able to combine the advantages of a long chain hyperbranched architecture with the favourable biological properties of PEG to produce promising branched materials for use as drug delivery systems. An alternative route to hyperbranched polymers has been developed by our group, utilising thiol-yne radical chemistry.[56,93,134-136] This reaction involves the addition of a thiol to a reactive alkyne followed by the addition of another thiol to the resulting vinylthioether at a faster rate. This leads to hyperbranched polymers with very high degrees of branching. This approach can be used for both small molecules and polymers with thiol and alkyne end groups.[137,138] The AB_2 thiol-yne step growth approach to long chain hyperbranched polymers has also been employed by Dong *et al*., who synthesised hyperbranched polypeptide with a PEG shell for encapsulation and delivery of doxorubicin.[82] The researchers produced poly(e-benzyloxycarbonyl-L-lysine) with thiol and alkyne end

groups which formed hyperbranched polylysine under UV irradiation, to which a linear PEG shell was attached. The hyperbranched polymer gave a higher drug loading than the linear counterpart block copolymer, and a slower drug release rate.

1.2.4. Dendrimers

Dendrimers are possibly the most studied of branched polymers for therapeutic delivery applications. This is due, in part, to their structurally perfect branching patterns and also to being very well defined unimolecular species.[139] Poly(amido amine) (PAMAM) dendrimers were the first dendrimers to be widely studied and are now commercially available, in addition to the large variety in backbone structures and coupling chemistries that have since been developed.[54] The dendrimer architecture offers the attractive property of multivalent surface functionality for increased interaction with biointerfaces, while also allowing efficient drug conjugation to the surface or encapsulation in the unimolecular micelle-like core.

Anderson *et al*., employed a combinatorial approach to obtain a library of modified dendrimers of varying generation PAMAM and p(propylenimine) (PPI), with different alkyl chain substituents (C10 – C16).[140] SiRNA formulated dendrimers were found to preferentially accumulate in Tie2-positive endothelial cells in the lung, when studied with an in vivo mouse model. The materials showed promise for the delivery of nucleic acid therapeutics in diseases or injuries involving dysfunctional endothelium, whilst having clinical translation advatages relating to molecularly defined dendrimer cores. Glutathione responsive PAMAM dendrimers have been developed by Kannan *et al*., and recently been investigated in a large animal model of hypothermic circulatory arrest induced brain injury.[87] Systemically injected dendrimer drug conjugates were able to deliver the antineuroinflamitory therapeutic N-acetyl cysteine, and the antiexcitotoxicity therapeutic valproic acid. The dendrimer delivery system produced 24 hr neurological score improvements of similar values to a 10 fold higher dose of free drug, and with much reduced adverse side effects.

In 2016, the group of Siegwart, reported modular and degradable dendrimers that had low toxicities and high antitumor efficiencies, and gave a significant survival benefit in the *in vivo* cancer model studied.[141] The ester based dendrimers were synthesised using sequential thiol or amine Michael additions, which allowed a large library of dendrimers to be produced with differing functionalities and generations. Initial *in vitro* and *in vivo* siRNA luciferase gene silencing screens were performed to evaluate dendrimer candidates to be taken forward to a further aggressive liver cancer model. An optimal degradable dendrimer was identified that was able to inhibit growth in the studied cancerous tumour model, while having low toxicity and biodegradability.

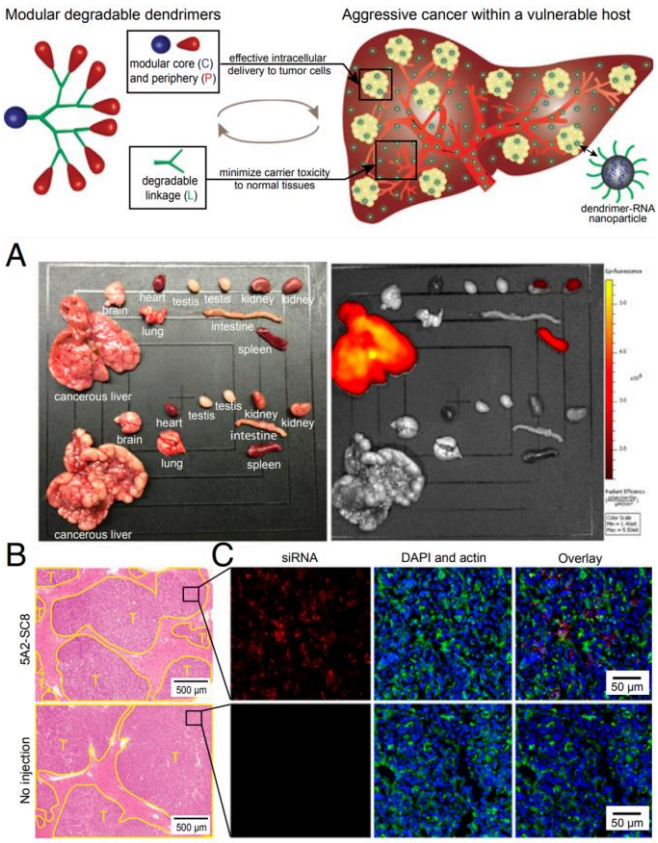

Figure 1.7. Modular degradable dendrimers for therapeutic delivery to liver cancer, **a)** fluorescent imaging showing cancerous liver accumulation of siRNA, **b)** histology staining comnfirmed livers contained tumours, **c)** confocal imaging confirmed siRNA intracellular location. Figure adapted from reference [141].

1.2.5. Branched-linear hybrid polymers

As the field of branched and dendritic polymers has rapidly developed, new classes of hybrid polymers have emerged.[51,142] These branched-linear hybrid polymer architectures can contain either dendrimers or hyperbanched polymers and include block copolymers, branched core star polymers, and dendronised polymers.

1.2.5.1. Branched-linear block copolymers

Hybrid block copolymer structures of branched polymers can be synthesised by either a chain first strategy, dendron/branched polymer first strategy, or a coupling strategy. A particular advantage of hybrid branched-linear block copolymers is the combination of branched topology traits with the self-assembly possibilities of block copolymers, which enables further development of drug delivery systems based on micelle like structures. This is illustrated by Hammond *et al*., who synthesised amphiphilic Dendron-linear block copolymers with poly(β-benzyl-L-aspartate) linear hydrophobic chain and hydrophilic polyester dendron unit functionalised with folate groups.[89,143] The anticancer therapeutic paclitaxel was encapsulated in the micelle core with loading efficiencies of up to 40%, while the exterior of the drug carrier presents a multivalent targeting by the folate groups. Both targeted and non-targeted micelles accumulated in tumour sites by the EPR effect after injection in mice, however the folate system was able to enter tumour cells from the extracellular environment by receptor mediated endocytosis, and had a 4 fold improved anticancer efficiency compared to the non-targeted system.

The Luo group has investigated amphiphilic dendritic-linear copolymers for anticancer drug delivery (**Figure 9**).[88,144] The synthesised polymers form micelles having a hydrophilic linear PEG shell and hydrophobic dendron core functionalised with rhein, or cholic acid, or riboflavin, which are able to bind to the drug doxorubicin thus forming stable nanoparticles. The strong doxorubicin dendron interactions leads to very high drug loadings. The dendritic-linear polymer systems investigated formed particles with high stabilities, long circulation times, reduced toxicities, whilst also showing favourable

anticancer efficiencies in the particular subcutaneous Raji lymphoma xenograft mouse model that was employed.

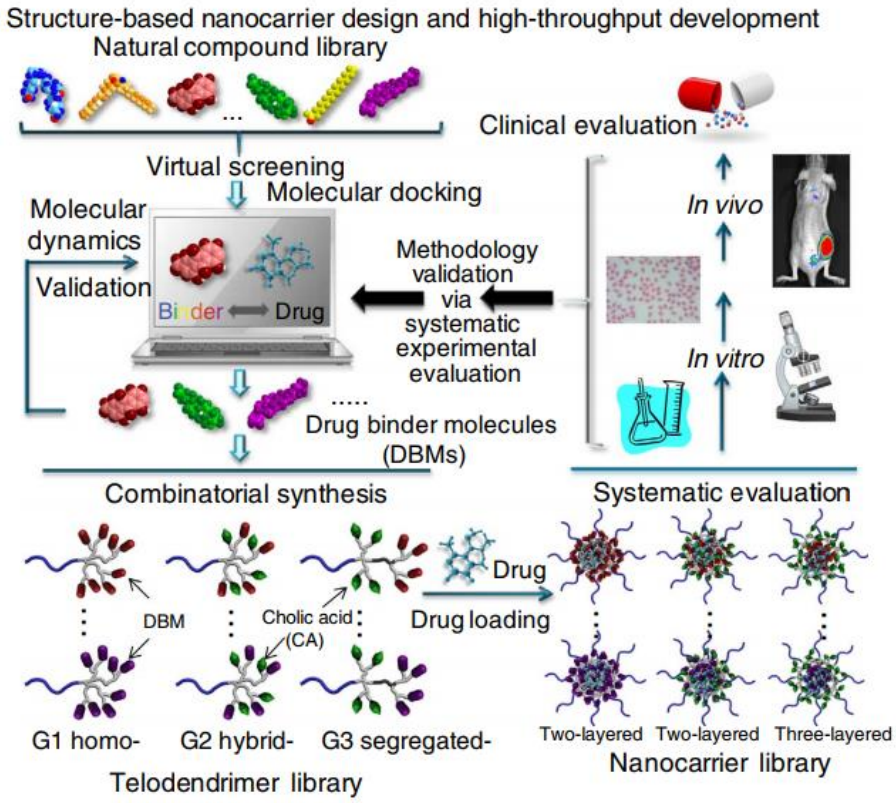

Figure 1.8. Dendritic-linear hybrid block copolymers for doxorubicin delivery, synthesised by a rational design and high throughput development process. Figure from reference [88].

Shen *et al*., studied dendritic-linear block copolymers for delivery of camptothecin.[90] The therapeutic agents were conjugated to the hydrophobic dendron segment of the polymer *via* a redox responsive disulphide bridge, while the linear PEG segment provided solubility and biocompatibility. Due to the active ingredient being convalently attached to the multivalent dendron, high drug loadings were achieved. The polymer drug conjugate self-assembled into micelles of different morphologies depending on the number of conjugated drugs and thus the hydrophobicity of the core forming block. It was found that medium length rod-like micelles of these branched-linear block copolymers had long circulation times, and released camptothecin intracellularly,

demonstrating the advantages of branched-linear block copolymers for therapeutic delivery to tumours.

1.2.5.2. Branched-core star polymers

Star polymers involving linear polymer chains extending radially from a globlular three dimensional branched polymer, are another interesting class of branched-linear hybrid polymers. This polymer architecture can be rationally designed for use as efficient encapsulation devices for various guest molecules, as well as direct conjugation to the star exterior. In cases where a high number of polymer arms can be attached to the branched polymer core, the star polymer can act as a unimolecular nanocarrier.[64,145] When considering amphiphilic core shell systems with high number of arms, the architecture can offer the advantage of not dissembling into individual polymer chains upon dilution, as would be the case for micelle systems. However, there are also studies looking at the self-assembly of star polymers with low number of arms.

Branched core star polymers have been investigated as nucleic acid delivery vehicles by a number of research groups, either utilising cationic branched cores or cationic linear polymer shells for electrostatic complexation of the therapeutic payload. Gong and colleagues utilised a hyperbranched polyester core (Boltron H40) coupled with linear cationic polymer arms through pH sensitive imine bonds, to complex and deliver siRNA to GFP expressing triple negative breast cancer cells *in vitro*.[92] The linear polymer arms consisted of poly(aspartic acid) with disulphide linked 2-aminoethyl groups for nucleic acid complexation and also disulphide linked imidazole groups to promote enosomal escape. This RNA delivery system showed GFP down regulation capabilities comparable to commercial transfection reagents but with lower toxicity, particularly when further functionalised with GE11 targeting peptide and tested on EFGR overexpressing cell-lines. In contrast, Matyjaszewski *et al*. investigated cationic core star polymers, synthesised in an onepot ATRP approach, for siRNA complexation and cellular uptake.[96,146] While Wang and coworkers synthesied star polymers combining a branced PEI core and linear poly(β-amino ester) arms.[95] This star poly(β-amino ester) showed excellent gene transfection efficiencies of primary rat adipose derived mesenchymal stem

cells, of between 200 and 15000 times higher than either the PEI core, or the poly(β-amino ester) arms on their own.

Similar bPEI core star polymers have been synthesised by the Voit group for small molecule encapsulation, who employed an oligosaccharide shell to stabablise the PEI structures.[147] The researchers studied encapsulation efficiencies of the branched core star polymers with various small molecules, including vitamin-B, an estradiol derivative, and pantoprazole. Interestingly, the core shell glycopolymer architecture was found to be necessary for stable complexes with high encapsulation efficiencies, and the maltriose polymer in particular showed good potential for use as a drug delivery system. Cationic core star polymers have been used to deliver platinum based anticancer drugs with high efficiencies, by Nie, Wang, and colleagues.[148] PAMAM dendrimers were conjugated with platinum prodrug, and poly(ethylene glycol)-block-(2-azepane ethyl methacrylate) linear polymer arms, which had pH based size switching behaviour for enhanced tumour penetration and drug delivery *in vivo*.

Another option for small molecule drug delivery with branched core star polymers, is to employ an amphiphilic system to either conjugate or encapsulate hydrophobic molecules. Amphiphillic star based hyperbranched Boltron H40 has been used by a number of research groups for both encapsulation and drug conjugation.[94,149] A hydrophilic linear polymer such as PEG is typically used as the hydrophilic shell. Our group has recently utilised amphiphilic branched core star polymers for hydrophobic molecule encapsulation and cellular internalisation.[93] A hydrophilic and biocompatible poly(2-ethyl oxazoline) shell was conjugated to a hyperbanched and hydrophobic polyester core polymer that was based on a thiol-yne polymerisation system. The core shell architecture allowed encapsulation of hydrophobic Nile Red as a model drug, and the polymers were readily uptaken by A2780 ovarian cancer cells *via* an energy dependent mechanism, suggesting endocytosis.

1.2.5.3. Dendronised polymers

Dendronised polymers (linear polymers grafted with dendrons), and hypergrafted polymers (linear polymers grafted with hyperbranched polymers) are hybrid polymer architectures which have only more recently been established for use in therapeutic delivery.[142] The first study evaluating rigid-rod dendronised polymer toxicity, biodistribution, and pharmacokinetics *in vivo*, was undertaken by Fréchet and Szoka.[98] The poly materials comprising a poly(4-hydroxystyrene) backbone with 4 generation polyester dendrons were evaluated for cytotoxicity against MDA breast cancer cells *in vitro*, which displayed 70% viablilty at a polymer concentration of 3 mg/mL. In vivo biodistribution studies were performed with tumoured and non tumoured mice. The smaller molecular weight dendronised polymers (67 kDa) exhibited urinary excretion, the largest polymer (1740 kDa) was cleared by the reticuloendothelial organs, while the medium molecular weight system (251 kDa) accumulated the most in tumour environments. The long blood circulation times of the dendronised polymers was attributed to their large molecular weights and rigid-rod shapes.

Dendronised amphiphilic polymers have been synthesised using an alkyne azide click reaction to graft polyglycerol dendrons to a PEG based linear backbone.[99] The systems formed supramolecular aggregates able to efficiently encapsulate hydrophobic guest moelcules, and then be internalised by cells as followed by flow cytometry and confocal microscopy. In addition, the polyglycerol shell imparted non cytotoxic properties to the nanocarriers over a range of concentrations, and the dendronised polymers performed better than similar linear-dendron block copolymers which could be destabalised at lower concentrations.

Gu *et al*. investigated *in vivo* doxorubicin delivery using a dendronised heparin based polymer system.[97] The researchers utilised a pH sensitive hydrazine bond to conjugate doxorubicin to a lysine based Dendron, which was then attached to a linear heparin chain with the use of azide alkyne cycloaddition chemistry. Drug loadings of 9 wt% could be achieved and the polymer architecture further self assemebled into nanoparticles of around 100 nm. In a mice 4T1 breast tumour model the polymer delivery system produced strong antitumour results, high antiangiogenisis effects, and apoptosis compared to the

free drug as observed by a variety of mice and tumour weight analysis, immunohistochemical analysis, and histology.

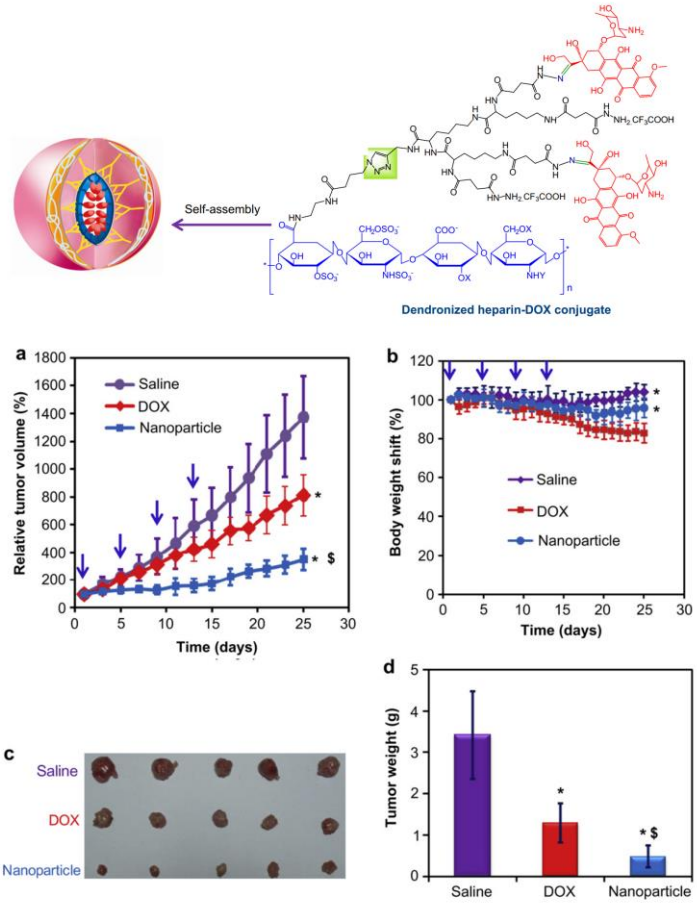

Figure 1.9. Dendronised heparin-doxorubicin conjugates as a pH responsive therapeutic delivery system, including in vivo studies showing **a)** relative tumour volumes, **b)** mouse body weights, **c)** tumour size analysis, and **d)** tumour weight analysis. Figure adapted from reference [97].

Dendronised polymers have also been used for gene delivery applications. Guon *et al.* synthesised a range of biodegradable dendronised polypeptides with variations in structure that were tuned in order to identify superior delivery vectors.[150] A dendronised polymer based on a second generation lysine dendron functionalised with 75% histidine and 25% tryptophan, was found to have the optimal combination of charged and aromatic residues required for successful delivery. The polymers showed good efficiencies when

complexed with siRNA to eGFP expressing NIH-3T3 cells *in vitro*, while also exhibiting minimal toxicity.

1.2.6. Architecture property relationships

With increased access to complex polymer architectures through new chemical technologies, researchers have been able to start hypothesising relationships between polymer architecture and subsequent properties as therapeutic delivery systems as well as physiochemical properties. The physiochemical properties of linear polymers are largely determined by the monomer repeat unit, however the properties of branched polymers result mainly from the polymer end groups at the surface of the polymer.[39] The biocompatibility of polymers is a complex assessment and is mainly affected by non-architecture related factors such as polymer functionality, however branched structures can offer ability to modulate biocompatibility. Known toxic molecules or functionalities can be embedded within the core of branched topologies, and new polymer architectures could be used to alter the protein corona by recruiting or repelling specific endogenous biomolecules to polymer surfaces by variation branching densities.[151] Polymer toxicity is also known to be affected by polymer flexibility with a number of studies reporting reduced toxicity for branched polymer systems.[152] The globular and approximately spherical conformation of branched polymers in solution is a significant attraction for drug delivery applications. This size and shape of polymers is an important parameter and can alter significantly the final properties of the delivery system, in particular, whether the polymer forms unimolecular and stable objects, or forms larger self-assembled structures, which in turn impacts the circulation times and biodistribution of the polymer systems.[153,154] The tunablity of polymer architecture and shape offers opportunities to increase drug loading either through manipulating the polymer core or self-assembled structure, or by the increased number of functionalisable groups on the exterior of a branched polymer.[64] When considering *in vivo* therapeutic delivery barriers, branched polymers offer opportunities for stimuli responsive endosome escape by proton sponge/osomotic pressure changes and subsequent polymer swelling of charge alteration.[29] Cell uptake has also been reported to depend on polymer architecture, with

increased branching potentially resulting in a higher number of multivalent interactions with cell surface receptors, thereby increasing internalisation.

1.3 Motivation for this work

Recent advances in synthetic polymer chemistry have led to the design and development of a variety of cationic gene delivery systems with different polymer architectures. In particular, branched polymers have received significant attention due to their interesting properties such as, globular three dimensional conformations, low intrinsic viscosities, and high surface functionality. However, there is still need for further understanding of structure-function relationships of well controlled polymer architectures in nucleic acid delivery applications. The aim of this work is to utilise advanced polymer synthesis methods to create and characterise various new cationic polymers with well controlled branched architectures and varying charged moieties; with the additional aims of investigating polymer toxicity, nucleic acid complexation, polyplex morphology, and gene transfection efficiency.

Initially, the synthesis of AB_2 hyperbranched polymers using thiol-yne chemistry will be explored in a systematic study involving a semi-batch process to form hyperbranched polymers with well-defined molecular weights and dispersities. Subsequently, the focus will shift to introducing cationic moieties on thiol-yne hyperbranched polymers. This is will be achieved by the ring opening polymerisation of 2-ethyloxazoline to form a polyoxazoline thiol-yne macromonomer. The macromonomer will then by polymerised by irradiation with UV light in the presence of a photoinitiator, with an additionally hydrolysis step to form PEI-POx copolymers with hyperbranched architectures. An investigation of plasmid DNA complexation, and *in vitro* toxicity and gene transfection will then be undertaken.

RAFT polymerisation will be utilised to form another type of branched polymer architecture, but with the advantage of being able to introduce tuneable degradation and nucleic acid release. The hypothesis was that rates of polymer hydrolysis and subsequent nucleic acid release due to polymer charge alteration from cationic to anionic, could be

tuned by incorporating a non hydrolysable monomer. Finally, the possibility of using RAFT to synthesis branched polymers with phosphonium cationic moieties will also be investigated, and their DNA complexation, toxicity, and gene transfection efficiency compared to the equivalent cationic polyammoniums. The aim of this chapter was to investigate potential cationic species as alternatives to the commonly employed ammonium moieties.

Overall, this thesis will describe advanced polymer synthesis methods to create hyperbranched and highly branched cationic polymers suitable for nucleic acid complexation, and investigate their associated structure-function characteristics.

1.4 References

(1) Karvinen, H.; Yla-Herttuala, S., New aspects in vascular gene therapy, *Curr. Opin. Pharmacol.* **2010**, *10*, 208.

(2) Somia, N.; Verma, I. M., Gene therapy: Trials and tribulations, *Nature Reviews Genetics* **2000**, *1*, 91.

(3) Bowles, D. E.; McPhee, S. W. J.; Li, C. W.; Gray, S. J.; Samulski, J. J.; Camp, A. S.; Li, J.; Wang, B.; Monahan, P. E.; Rabinowitz, J. E.; Grieger, J. C.; Govindasamy, L.; Agbandje-McKenna, M.; Xiao, X.; Samulski, R. J., Phase 1 Gene Therapy for Duchenne Muscular Dystrophy Using a Translational Optimized AAV Vector, *Mol. Ther.* **2012**, *20*, 443.

(4) Davis, M. E.; Zuckerman, J. E.; Choi, C. H. J.; Seligson, D.; Tolcher, A.; Alabi, C. A.; Yen, Y.; Heidel, J. D.; Ribas, A., Evidence of RNAi in humans from systemically administered siRNA via targeted nanoparticles, *Nature* **2010**, *464*, 1067.

(5) Griesenbach, U.; Alton, E., Gene transfer to the lung: Lessons learned from more than 2 decades of CF gene therapy, *Adv. Drug Del. Rev.* **2009**, *61*, 128.

(6) Kaplitt, M. G.; Feigin, A.; Tang, C.; Fitzsimons, H. L.; Mattis, P.; Lawlor, P. A.; Bland, R. J.; Young, D.; Strybing, K.; Eidelberg, D.; During, M. J., Safety and tolerability of gene therapy with an adeno-associated virus (AAV) borne GAD gene for Parkinson's disease: an open label, phase I trial, *Lancet* **2007**, *369*, 2097.

(7) Maguire, A. M.; High, K. A.; Auricchio, A.; Wright, J. F.; Pierce, E. A.; Testa, F.; Mingozzi, F.; Bennicelli, J. L.; Ying, G. S.; Rossi, S.; Fulton, A.; Marshall, K. A.; Banfi, S.; Chung, D. C.; Morgan, J. I. W.; Hauck, B.; Zelenaia, O.; Zhu, X. S.; Raffini, L.; Coppieters, F.; De Baere, E.; Shindler, K. S.; Volpe, N. J.; Surace, E. M.; Acerra, C.; Lyubarsky, A.; Redmond, T. M.; Stone, E.; Sun, J. W.; McDonnell, J. W.; Leroy, B. P.; Simonelli, F.; Bennett, J., Age-dependent effects of RPE65 gene therapy for Leber's congenital amaurosis: a phase 1 dose-escalation trial, *Lancet* **2009**, *374*, 1597.

(8) Jinek, M.; Chylinski, K.; Fonfara, I.; Hauer, M.; Doudna, J. A.; Charpentier, E., A Programmable Dual-RNA-Guided DNA Endonuclease in Adaptive Bacterial Immunity, *Science* **2012**, *337*, 816.

(9) Cong, L.; Ran, F. A.; Cox, D.; Lin, S. L.; Barretto, R.; Habib, N.; Hsu, P. D.; Wu, X. B.; Jiang, W. Y.; Marraffini, L. A.; Zhang, F., Multiplex Genome Engineering Using CRISPR/Cas Systems, *Science* **2013**, *339*, 819.

(10) Dykxhoorn, D. M.; Novina, C. D.; Sharp, P. A., Killing the messenger: Short RNAs that silence gene expression, *Nat. Rev. Mol. Cell Biol.* **2003**, *4*, 457.

(11) Fire, A.; Xu, S. Q.; Montgomery, M. K.; Kostas, S. A.; Driver, S. E.; Mello, C. C., Potent and specific genetic interference by double-stranded RNA in Caenorhabditis elegans, *Nature* **1998**, *391*, 806.

(12) Kanasty, R.; Dorkin, J. R.; Vegas, A.; Anderson, D., Delivery materials for siRNA therapeutics, *Nat. Mater.* **2013**, *12*, 967.

(13) Blanco, E.; Shen, H.; Ferrari, M., Principles of nanoparticle design for overcoming biological barriers to drug delivery, *Nat. Biotechnol.* **2015**, *33*, 941.

(14) Pecot, C. V.; Calin, G. A.; Coleman, R. L.; Lopez-Berestein, G.; Sood, A. K., RNA interference in the clinic: challenges and future directions, *Nature Reviews Cancer* **2011**, *11*, 59.

(15) Whitehead, K. A.; Langer, R.; Anderson, D. G., Knocking down barriers: advances in siRNA delivery, *Nat. Rev. Drug Discov.* **2009**, *8*, 129.

(16) Wolfram, J.; Shen, H.; Ferrari, M., Multistage vector (MSV) therapeutics, *J. Control. Release* **2015**, *219*, 406.

(17) Yin, H.; Kanasty, R. L.; Eltoukhy, A. A.; Vegas, A. J.; Dorkin, J. R.; Anderson, D. G., Non-viral vectors for gene-based therapy, *Nature Reviews Genetics* **2014**, *15*, 541.

(18) Katoch, R.; Sethi, A.; Thakur, N.; Murdock, L. L., RNAi for Insect Control: Current Perspective and Future Challenges, *Appl. Biochem. Biotechnol.* **2013**, *171*, 847.

(19) Dash, P. R.; Read, M. L.; Barrett, L. B.; Wolfert, M.; Seymour, L. W., Factors affecting blood clearance and in vivo distribution of polyelectrolyte complexes for gene delivery, *Gene Ther.* **1999**, *6*, 643.

(20) Nishikawa, M.; Takakura, Y.; Hashida, M., Theoretical considerations involving the pharmacokinetics of plasmid DNA, *Adv. Drug Del. Rev.* **2005**, *57*, 675.

(21) Voet, D.; Voet, J. G. *Biochemistry*; 4th ed.; John Wiley & Sons: New York, 2011.

(22) van der Aa, M.; Huth, U. S.; Hafele, S. Y.; Schubert, R.; Oosting, R. S.; Mastrobattista, E.; Hennink, W. E.; Peschka-Suss, R.; Koning, G. A.; Crommelin, D. J. A., Cellular uptake of cationic polymer-DNA complexes via caveolae plays a pivotal role in gene transfection in COS-7 cells, *Pharm. Res.* **2007**, *24*, 1590.

(23) Cho, Y. W.; Kim, J. D.; Park, K., Pollycation gene delivery systems: escape from endosomes to cytosol, *J. Pharm. Pharmacol.* **2003**, *55*, 721.

(24) Paine, P. L.; Moore, L. C.; Horowitz, S. B., Nuclear-envelope permeability, *Nature* **1975**, *254*, 109.

(25) van der Aa, M.; Mastrobattista, E.; Oosting, R. S.; Hennink, W. E.; Koning, G. A.; Crommelin, D. J. A., The nuclear pore complex: The gateway to successful nonviral gene delivery, *Pharm. Res.* **2006**, *23*, 447.

(26) Schaffer, D. V.; Fidelman, N. A.; Dan, N.; Lauffenburger, D. A., Vector unpacking as a potential barrier for receptor-mediated polyplex gene delivery, *Biotechnol. Bioeng.* **2000**, *67*, 598.

(27) Nayak, S.; Herzog, R. W., Progress and prospects: immune responses to viral vectors, *Gene Ther.* **2010**, *17*, 295.

(28) Zhou, H. S.; Liu, D. P.; Liang, C. C., Challenges and strategies: The immune responses in gene therapy, *Med. Res. Rev.* **2004**, *24*, 748.

(29) Pack, D. W.; Hoffman, A. S.; Pun, S.; Stayton, P. S., Design and development of polymers for gene delivery, *Nat. Rev. Drug Discov.* **2005**, *4*, 581.

(30) Zauner, W.; Ogris, M.; Wagner, E., Polylysine-based transfection systems utilizing receptor-mediated delivery, *Adv. Drug Del. Rev.* **1998**, *30*, 97.

(31) Boussif, O.; Lezoualch, F.; Zanta, M. A.; Mergny, M. D.; Scherman, D.; Demeneix, B.; Behr, J. P., A Versatile Vector for Gene and Oligonucleotide Transfer Into Cells in Culture and In-Vivo - Polyethylenimine, *Proc. Natl. Acad. Sci. U. S. A.* **1995**, *92*, 7297.

(32) Tan, P. H.; Yang, L. C.; Shih, H. C.; Lan, K. C.; Cheng, J. T., Gene knockdown with intrathecal siRNA of NMDA receptor NR2B subunit reduces formalin-induced nociception in the rat, *Gene Ther.* **2005**, *12*, 59.

(33) Katas, H.; Alpar, H. O., Development and characterisation of chitosan nanoparticles for siRNA delivery, *J. Control. Release* **2006**, *115*, 216.

(34) Duncan, R.; Vicent, M. J., Polymer therapeutics-prospects for 21st century: the end of the beginning, *Adv. Drug Del. Rev.* **2013**, *65*, 60.

(35) Polymeropoulos, G.; Zapsas, G.; Ntetsikas, K.; Bilalis, P.; Gnanou, Y.; Hadjichristidis, N., 50th Anniversary perspective: polymers with complex architectures, *Macromolecules* **2017**, *50*, 1253.

(36) Kakkar, A.; Traverso, G.; Farokhzad, O. C.; Weissleder, R.; Langer, R., Evolution of macromolecular complexity in drug delivery systems, *Nature Reviews Chemistry* **2017**, *1*, 0063.

(37) Blasco, E.; Sims, M. B.; Goldmann, A. S.; Sumerlin, B. S.; Barner-Kowollik, C., 50th Anniversary Perspective: Polymer Functionalization, *Macromolecules* **2017**, *50*, 5215.

(38) Perrier, S. b., 50th Anniversary Perspective: RAFT Polymerization · A User Guide, *Macromolecules* **2017**, *50*, 7433.

(39) Voit, B. I.; Lederer, A., Hyperbranched and Highly Branched Polymer Architectures-Synthetic Strategies and Major Characterization Aspects, *Chem. Rev.* **2009**, *109*, 5924.

(40) England, R. M.; Rimmer, S., Hyper/highly-branched polymers by radical polymerisations, *Polymer Chemistry* **2010**, *1*, 1533.

(41) Voit, B., New developments in hyperbranched polymers, *J. Polym. Sci., Part A: Polym. Chem.* **2000**, *38*, 2505.

(42) Gao, C.; Yan, D., Hyperbranched polymers: from synthesis to applications, *Prog. Polym. Sci.* **2004**, *29*, 183.

(43) Bruchmann, B., Dendritic polymers based on urethane chemistry - Syntheses and applications, *Macromolecular Materials and Engineering* **2007**, *292*, 981.
(44) Wang, Y.; Grayson, S. M., Approaches for the preparation of non-linear amphiphilic polymers and their applications to drug delivery, *Adv. Drug Del. Rev.* **2012**, *64*, 852.
(45) Tomalia, D. A.; Baker, H.; Dewald, J.; Hall, M.; Kallos, G.; Martin, S.; Roeck, J.; Ryder, J.; Smith, P., A NEW CLASS OF POLYMERS - STARBURST-DENDRITIC MACROMOLECULES, *Polym. J.* **1985**, *17*, 117.
(46) Buhleier, E.; Wehner, W.; Vogtle, F., "Cascade" and "Nonskid-Chain-like" Syntheses of Molecular Cavity Topologies, *Synthesis-Stuttgart* **1978**, 155.
(47) Hawker, C. J.; Frechet, J. M. J., Preparation of polymers with controlled molecular architecture. A new convergent approach to dendritic macromolecules, *J. Am. Chem. Soc.* **1990**, *112*, 7638.
(48) Hawker, C. J.; Lee, R.; Frechet, J. M. J., One-step synthesis of hyperbranched dendritic polyesters, *J. Am. Chem. Soc.* **1991**, *113*, 4583.
(49) Holter, D.; Burgath, A.; Frey, H., Degree of branching in hyperbranched polymers, *Acta Polym.* **1997**, *48*, 30.
(50) Konkolewicz, D.; Monteiro, M. J.; Perrier, S., Dendritic and hyperbranched polymers from macromolecular units: elegant approaches to the synthesis of functional polymers, *Macromolecules* **2011**, *44*, 7067.
(51) Wurm, F.; Frey, H., Linear–dendritic block copolymers: the state of the art and exciting perspectives, *Prog. Polym. Sci.* **2011**, *36*, 1.
(52) Tomalia, D. A.; Frechet, J. M. *Introduction to the dendritic state*; Wiley Online Library, 2002.
(53) Hawker, C. J.; Frechet, J. M., Preparation of polymers with controlled molecular architecture. A new convergent approach to dendritic macromolecules, *J. Am. Chem. Soc.* **1990**, *112*, 7638.
(54) Walter, M. V.; Malkoch, M., Simplifying the synthesis of dendrimers: accelerated approaches, *Chem. Soc. Rev.* **2012**, *41*, 4593.
(55) Flory, P. J., Molecular Size Distribution in Three Dimensional Polymers. VI. Branched Polymers Containing A—R—Bf-1 Type Units, *J. Am. Chem. Soc.* **1952**, *74*, 2718.

(56) Konkolewicz, D.; Gray-Weale, A.; Perrier, S., Hyperbranched Polymers by Thiol-Yne Chemistry: From Small Molecules to Functional Polymers, *J. Am. Chem. Soc.* **2009**, *131*, 18075.

(57) Fréchet, J. M.; Henmi, M.; Gitsov, I.; Aoshima, S.; Leduc, M. R.; Grubbs, R. B., Self-Condensing Vinyl Polymerization: An Approach to Dendritic Materials, *Science* **1995**, *269*, 1080.

(58) O'Brien, N.; McKee, A.; Sherrington, D. C.; Slark, A. T.; Titterton, A., Facile, versatile and cost effective route to branched vinyl polymers, *Polymer* **2000**, *41*, 6027.

(59) Szwarc, M., 'Living'polymers, *Nature* **1956**, *178*, 1168.

(60) Grubbs, R. B.; Grubbs, R. H., 50th Anniversary Perspective: Living Polymerization · Emphasizing the Molecule in Macromolecules, *Macromolecules* **2017**, *50*, 6979.

(61) Boyer, C.; Bulmus, V.; Davis, T. P.; Ladmiral, V.; Liu, J. Q.; Perrier, S., Bioapplications of RAFT Polymerization, *Chem. Rev.* **2009**, *109*, 5402.

(62) Kolb, H. C.; Finn, M.; Sharpless, K. B., Click chemistry: diverse chemical function from a few good reactions, *Angew. Chem. Int. Ed.* **2001**, *40*, 2004.

(63) Gody, G.; Rossner, C.; Moraes, J.; Vana, P.; Maschmeyer, T.; Perrier, S. b., One-pot RAFT/"click" chemistry via isocyanates: efficient synthesis of α-end-functionalized polymers, *J. Am. Chem. Soc.* **2012**, *134*, 12596.

(64) Kurniasih, I. N.; Keilitz, J.; Haag, R., Dendritic nanocarriers based on hyperbranched polymers, *Chem. Soc. Rev.* **2015**, *44*, 4145.

(65) Lu, Y.; Aimetti, A. A.; Langer, R.; Gu, Z., Bioresponsive materials, *Nature Reviews Materials* **2017**, *2*, 16075.

(66) Tan, J. H.; McMillan, N. A. J.; Payne, E.; Alexander, C.; Heath, F.; Whittaker, A. K.; Thurecht, K. J., Hyperbranched Polymers as Delivery Vectors for Oligonucleotides, *J. Polym. Sci., Part A: Polym. Chem.* **2012**, *50*, 2585.

(67) Giardiello, M.; Hatton, F. L.; Slater, R. A.; Chambon, P.; North, J.; Peacock, A. K.; He, T.; McDonald, T. O.; Owen, A.; Rannard, S. P., Stable, polymer-directed and SPION-nucleated magnetic amphiphilic block copolymer nanoprecipitates with readily reversible assembly in magnetic fields, *Nanoscale* **2016**, *8*, 7224.

(68) Zhao, T.; Zhang, H.; Newland, B.; Aied, A.; Zhou, D.; Wang, W., Significance of branching for transfection: synthesis of highly branched degradable functional poly

(dimethylaminoethyl methacrylate) by vinyl oligomer combination, *Angew. Chem. Int. Ed.* **2014**, *53*, 6095.

(69) Misra, S.; Wang, X.; Srivastava, I.; Imgruet, M.; Graff, R.; Ohoka, A.; Kampert, T.; Gao, H.; Pan, D., Combinatorial therapy for triple negative breast cancer using hyperstar polymer-based nanoparticles, *Chem. Commun.* **2015**, *51*, 16710.

(70) Zhuang, Y.; Deng, H.; Su, Y.; He, L.; Wang, R.; Tong, G.; He, D.; Zhu, X., Aptamer-functionalized and backbone redox-responsive hyperbranched polymer for targeted drug delivery in cancer therapy, *Biomacromolecules* **2016**, *17*, 2050.

(71) Zheng, L.; Wang, Y.; Zhang, X.; Ma, L.; Wang, B.; Ji, X.; Wei, H., Fabrication of Hyperbranched Block-Statistical Copolymer-Based Prodrug with Dual Sensitivities for Controlled Release, *Bioconjugate Chem.* **2017**.

(72) Hu, X.; Liu, G.; Li, Y.; Wang, X.; Liu, S., Cell-penetrating hyperbranched polyprodrug amphiphiles for synergistic reductive milieu-triggered drug release and enhanced magnetic resonance signals, *J. Am. Chem. Soc.* **2014**, *137*, 362.

(73) Liu, G.; Zhang, G.; Hu, J.; Wang, X.; Zhu, M.; Liu, S., Hyperbranched self-immolative polymers (h SIPs) for programmed payload delivery and ultrasensitive detection, *J. Am. Chem. Soc.* **2015**, *137*, 11645.

(74) Heckert, B.; Banerjee, T.; Sulthana, S.; Naz, S.; Alnasser, R.; Thompson, D.; Normand, G.; Grimm, J.; Perez, J. M.; Santra, S., Design and Synthesis of New Sulfur-Containing Hyperbranched Polymer and Theranostic Nanomaterials for Bimodal Imaging and Treatment of Cancer, *ACS Macro Lett.* **2017**, *6*, 235.

(75) Calderón, M.; Graeser, R.; Kratz, F.; Haag, R., Development of enzymatically cleavable prodrugs derived from dendritic polyglycerol, *Biorg. Med. Chem. Lett.* **2009**, *19*, 3725.

(76) Hu, M.; Chen, M.; Li, G.; Pang, Y.; Wang, D.; Wu, J.; Qiu, F.; Zhu, X.; Sun, J., Biodegradable hyperbranched polyglycerol with ester linkages for drug delivery, *Biomacromolecules* **2012**, *13*, 3552.

(77) Chen, G.; Wang, K.; Hu, Q.; Ding, L.; Yu, F.; Zhou, Z.; Zhou, Y.; Li, J.; Sun, M.; Oupický, D., Combining Fluorination and Bioreducibility for Improved siRNA Polyplex Delivery, *ACS Applied Materials & Interfaces* **2017**, *9*, 4457.

(78) Wang, S.; Chen, R., pH-Responsive, Lysine-Based, Hyperbranched Polymers Mimicking Endosomolytic Cell-Penetrating Peptides for Efficient Intracellular Delivery, *Chem. Mater.* **2017**, *29*, 5806.

(79) Zhou, D.; Gao, Y.; Aied, A.; Cutlar, L.; Igoucheva, O.; Newland, B.; Alexeeve, V.; Greiser, U.; Uitto, J.; Wang, W., Highly branched poly (β-amino ester) s for skin gene therapy, *J. Control. Release* **2016**, *244*, 336.

(80) Pang, Y.; Liu, J.; Wu, J.; Li, G.; Wang, R.; Su, Y.; He, P.; Zhu, X.; Yan, D.; Zhu, B., Synthesis, characterization, and in vitro evaluation of long-chain hyperbranched poly (ethylene glycol) as drug carrier, *Bioconjugate Chem.* **2010**, *21*, 2093.

(81) Tu, C.; Li, N.; Zhu, L.; Zhou, L.; Su, Y.; Li, P.; Zhu, X., Cationic long-chain hyperbranched poly (ethylene glycol) s with low charge density for gene delivery, *Polymer Chemistry* **2013**, *4*, 393.

(82) Chang, X.; Dong, C.-M., Synthesis of hyperbranched polypeptide and PEO block copolymer by consecutive thiol-yne chemistry, *Biomacromolecules* **2013**, *14*, 3329.

(83) Khan, O. F.; Zaia, E. W.; Jhunjhunwala, S.; Xue, W.; Cai, W.; Yun, D. S.; Barnes, C. M.; Dahlman, J. E.; Dong, Y.; Pelet, J. M., Dendrimer-inspired nanomaterials for the in vivo delivery of siRNA to lung vasculature, *Nano Lett.* **2015**, *15*, 3008.

(84) Kadlecova, Z.; Rajendra, Y.; Matasci, M.; Baldi, L.; Hacker, D. L.; Wurm, F. M.; Klok, H. A., DNA delivery with hyperbranched polylysine: A comparative study with linear and dendritic polylysine, *J. Control. Release* **2013**, *169*, 276.

(85) Kurtoglu, Y. E.; Navath, R. S.; Wang, B.; Kannan, S.; Romero, R.; Kannan, R. M., Poly (amidoamine) dendrimer–drug conjugates with disulfide linkages for intracellular drug delivery, *Biomaterials* **2009**, *30*, 2112.

(86) Gorzkiewicz, M.; Jatczak-Pawlik, I.; Studzian, M.; Pułaski, Ł.; Appelhans, D.; Voit, B.; Klajnert-Maculewicz, B., Glycodendrimer nanocarriers for direct delivery of fludarabine triphosphate to leukaemic cells: improved pharmacokinetics and pharmacodynamics of fludarabine, *Biomacromolecules* **2018**, *accepted*.

(87) Mishra, M. K.; Beaty, C. A.; Lesniak, W. G.; Kambhampati, S. P.; Zhang, F.; Wilson, M. A.; Blue, M. E.; Troncoso, J. C.; Kannan, S.; Johnston, M. V., Dendrimer brain uptake and targeted therapy for brain injury in a large animal model of hypothermic circulatory arrest, *ACS nano* **2014**, *8*, 2134.

(88) Shi, C.; Guo, D.; Xiao, K.; Wang, X.; Wang, L.; Luo, J., A drug-specific nanocarrier design for efficient anticancer therapy, *Nature communications* **2015**, *6*, 7449.

(89) Poon, Z.; Lee, J. A.; Huang, S.; Prevost, R. J.; Hammond, P. T., Highly stable, ligand-clustered "patchy" micelle nanocarriers for systemic tumor targeting, *Nanomed. Nanotechnol. Biol. Med.* **2011**, *7*, 201.

(90) Zhou, Z.; Ma, X.; Jin, E.; Tang, J.; Sui, M.; Shen, Y.; Van Kirk, E. A.; Murdoch, W. J.; Radosz, M., Linear-dendritic drug conjugates forming long-circulating nanorods for cancer-drug delivery, *Biomaterials* **2013**, *34*, 5722.

(91) Yang, Y.; Hua, C.; Dong, C.-M., Synthesis, self-assembly, and in vitro doxorubicin release behavior of dendron-like/linear/dendron-like poly (ε-caprolactone)-b-poly (ethylene glycol)-b-poly (ε-caprolactone) triblock copolymers, *Biomacromolecules* **2009**, *10*, 2310.

(92) Chen, G.; Wang, Y.; Xie, R.; Gong, S., Tumor-targeted pH/redox dual-sensitive unimolecular nanoparticles for efficient siRNA delivery, *J. Control. Release* **2017**, *259*, 105.

(93) Hartlieb, M.; Floyd, T.; Cook, A. B.; Sanchez-Cano, C.; Catrouillet, S.; Burns, J. A.; Perrier, S., Well-defined hyperstar copolymers based on a thiol-yne hyperbranched core and a poly(2-oxazoline) shell for biomedical applications, *Polymer Chemistry* **2017**, *8*, 2041.

(94) Chen, H.; Li, G.; Chi, H.; Wang, D.; Tu, C.; Pan, L.; Zhu, L.; Qiu, F.; Guo, F.; Zhu, X., Alendronate-conjugated amphiphilic hyperbranched polymer based on Boltorn H40 and poly (ethylene glycol) for bone-targeted drug delivery, *Bioconjugate Chem.* **2012**, *23*, 1915.

(95) Huang, X.; Zhou, D.; Zeng, M.; Alshehri, F.; Li, X.; O'Keeffe-Ahern, J.; Gao, Y.; Pierucci, L.; Greiser, U.; Yin, G.; Wang, W., Star Poly (β-amino esters) Obtained from the Combination of Linear Poly (β-amino esters) and Polyethylenimine, *ACS Macro Lett.* **2017**, *6*, 575.

(96) Cho, H. Y.; Srinivasan, A.; Hong, J.; Hsu, E.; Liu, S. G.; Shrivats, A.; Kwak, D.; Bohaty, A. K.; Paik, H. J.; Hollinger, J. O.; Matyjaszewski, K., Synthesis of Biocompatible PEG-Based Star Polymers with Cationic and Degradable Core for siRNA Delivery, *Biomacromolecules* **2011**, *12*, 3478.

(97) She, W.; Li, N.; Luo, K.; Guo, C.; Wang, G.; Geng, Y.; Gu, Z., Dendronized heparin−doxorubicin conjugate based nanoparticle as pH-responsive drug delivery system for cancer therapy, *Biomaterials* **2013**, *34*, 2252.

(98) Lee, C. C.; Yoshida, M.; Fréchet, J. M.; Dy, E. E.; Szoka, F. C., In vitro and in vivo evaluation of hydrophilic dendronized linear polymers, *Bioconjugate Chem.* **2005**, *16*, 535.

(99) Kumari, M.; Gupta, S.; Achazi, K.; Böttcher, C.; Khandare, J.; Sharma, S. K.; Haag, R., Dendronized multifunctional amphiphilic polymers as efficient nanocarriers for biomedical applications, *Macromol. Rapid Commun.* **2015**, *36*, 254.

(100) Moad, G.; Solomon, D. H. *The Chemistry of Radical Polymerization*; Elsevier Science, 2005.

(101) Flory, P. J., Molecular Size Distribution in Three Dimensional Polymers. I. Gelation1, *J. Am. Chem. Soc.* **1941**, *63*, 3083.

(102) Flory, P. J., Kinetics of Polyesterification: A Study of the Effects of Molecular Weight and Viscosity on Reaction Rate, *J. Am. Chem. Soc.* **1939**, *61*, 3334.

(103) Jacobson, H.; Beckmann, C. O.; Stockmayer, W. H., Intramolecular Reaction in Polycondensations. II. Ring-Chain Equilibrium in Polydecamethylene Adipate, *The Journal of Chemical Physics* **1950**, *18*, 1607.

(104) Stockmayer, W. H., Theory of molecular size distribution and gel formation in branched-chain polymers, *The Journal of chemical physics* **1943**, *11*, 45.

(105) Bannister, I.; Billingham, N. C.; Armes, S. P.; Rannard, S. P.; Findlay, P., Development of branching in living radical copolymerization of vinyl and divinyl monomers, *Macromolecules* **2006**, *39*, 7483.

(106) Ide, N.; Fukuda, T., Nitroxide-controlled free-radical copolymerization of vinyl and divinyl monomers. 2. Gelation, *Macromolecules* **1999**, *32*, 95.

(107) Gao, H.; Polanowski, P.; Matyjaszewski, K., Gelation in living copolymerization of monomer and divinyl cross-linker: Comparison of ATRP experiments with Monte Carlo simulations, *Macromolecules* **2009**, *42*, 5925.

(108) Isaure, F.; Cormack, P. A. G.; Graham, S.; Sherrington, D. C.; Armes, S. P.; Butun, V., Synthesis of branched poly(methyl methacrylate)s via controlled/living

polymerisations exploiting ethylene glycol dimethacrylate as branching agent, *Chem. Commun.* **2004**, 1138.

(109) Isaure, F.; Cormack, P. A. G.; Sherrington, D. C., Synthesis of branched poly(methyl methacrylate)s: Effect of the branching comonomer structure, *Macromolecules* **2004**, *37*, 2096.

(110) Liu, B. L.; Kazlauciunas, A.; Guthrie, J. T.; Perrier, S., Influence of reaction parameters on the synthesis of hyperbranched polymers via reversible addition fragmentation chain transfer (RAFT) polymerization, *Polymer* **2005**, *46*, 6293.

(111) Liu, B. L.; Kazlauciunas, A.; Guthrie, J. T.; Perrier, S., One-pot hyperbranched polymer synthesis mediated by reversible addition fragmentation chain transfer (RAFT) polymerization, *Macromolecules* **2005**, *38*, 2131.

(112) Tao, L.; Chou, W. C.; Tan, B. H.; Davis, T. P., DNA Polyplexes Formed Using PEGylated Biodegradable Hyperbranched Polymers, *Macromol. Biosci.* **2010**, *10*, 632.

(113) Tao, L.; Liu, J.; Tan, B. H.; Davis, T. P., RAFT Synthesis and DNA Binding of Biodegradable, Hyperbranched Poly(2-(dimethylamino)ethyl Methacrylate, *Macromolecules* **2009**, *42*, 4960.

(114) Ardana, A.; Whittaker, A. K.; Thurecht, K. J., PEG-Based Hyperbranched Polymer Theranostics: Optimizing Chemistries for Improved Bioconjugation, *Macromolecules* **2014**, *47*, 5211.

(115) Hatton, F. L.; Tatham, L. M.; Tidbury, L. R.; Chambon, P.; He, T.; Owen, A.; Rannard, S. P., Hyperbranched polydendrons: a new nanomaterials platform with tuneable permeation through model gut epithelium, *Chemical science* **2015**, *6*, 326.

(116) Hawker, C. J.; Frechet, J. M.; Grubbs, R. B.; Dao, J., Preparation of hyperbranched and star polymers by a" living", self-condensing free radical polymerization, *J. Am. Chem. Soc.* **1995**, *117*, 10763.

(117) Wang, Z.; He, J.; Tao, Y.; Yang, L.; Jiang, H.; Yang, Y., Controlled chain branching by RAFT-based radical polymerization, *Macromolecules* **2003**, *36*, 7446.

(118) Gaynor, S. G.; Edelman, S.; Matyjaszewski, K., Synthesis of branched and hyperbranched polystyrenes, *Macromolecules* **1996**, *29*, 1079.

(119) Liu, M.; Vladimirov, N.; Fréchet, J. M., A new approach to hyperbranched polymers by ring-opening polymerization of an AB monomer: 4-(2-hydroxyethyl)-ε-caprolactone, *Macromolecules* **1999**, *32*, 6881.

(120) Chang, H.-T.; Fréchet, J. M., Proton-transfer polymerization: a new approach to hyperbranched polymers, *J. Am. Chem. Soc.* **1999**, *121*, 2313.

(121) Wang, K.; Peng, H.; Thurecht, K. J.; Puttick, S.; Whittaker, A. K., Segmented Highly Branched Copolymers: Rationally Designed Macromolecules for Improved and Tunable 19F MRI, *Biomacromolecules* **2015**, *16*, 2827.

(122) Wei, X.; Luo, Q.; Sun, L.; Li, X.; Zhu, H.; Guan, P.; Wu, M.; Luo, K.; Gong, Q., Enzyme-and pH-sensitive branched polymer–doxorubicin conjugate-based nanoscale drug delivery system for cancer therapy, *ACS applied materials & interfaces* **2016**, *8*, 11765.

(123) Hult, A.; Johansson, M.; Malmstrom, E., Hyperbranched polymers, *Adv. Polym. Sci.* **1999**, *143*, 1.

(124) Claesson, H.; Malmstrom, E.; Johansson, M.; Hult, A., Synthesis and characterisation of star branched polyesters with dendritic cores and the effect of structural variations on zero shear rate viscosity, *Polymer* **2002**, *43*, 3511.

(125) Holter, D.; Frey, H., Degree of branching in hyperbranched polymers .2. Enhancement of the DB: Scope and limitations, *Acta Polym.* **1997**, *48*, 298.

(126) Hanselmann, R.; Holter, D.; Frey, H., Hyperbranched polymers prepared via the core-dilution/slow addition technique: Computer simulation of molecular weight distribution and degree of branching, *Macromolecules* **1998**, *31*, 3790.

(127) Sunder, A.; Hanselmann, R.; Frey, H.; Mulhaupt, R., Controlled synthesis of hyperbranched polyglycerols by ring-opening multibranching polymerization, *Macromolecules* **1999**, *32*, 4240.

(128) Glaffig, M.; Palitzsch, B.; Hartmann, S.; Schüll, C.; Nuhn, L.; Gerlitzki, B.; Schmitt, E.; Frey, H.; Kunz, H., A fully synthetic glycopeptide antitumor vaccine based on multiple antigen presentation on a hyperbranched polymer, *Chemistry-A European Journal* **2014**, *20*, 4232.

(129) Calderón, M.; Welker, P.; Licha, K.; Fichtner, I.; Graeser, R.; Haag, R.; Kratz, F., Development of efficient acid cleavable multifunctional prodrugs derived from dendritic polyglycerol with a poly (ethylene glycol) shell, *J. Control. Release* **2011**, *151*, 295.

(130) Emrick, T.; Chang, H. T.; Frechet, J. M. J., An A(2)+B-3 approach to hyperbranched aliphatic polyethers containing chain end epoxy substituents, *Macromolecules* **1999**, *32*, 6380.

(131) Russo, S.; Boulares, A.; da Rin, A.; Mariani, A.; Cosulich, M. E., Hyperbranched aramids by direct polyamidation of two reactant sytems: Synthesis and properties, *Macromolecular Symposia* **1999**, *143*, 309.

(132) Lynn, D. M.; Anderson, D. G.; Putnam, D.; Langer, R., Accelerated discovery of synthetic transfection vectors: Parallel synthesis and screening of degradable polymer library, *J. Am. Chem. Soc.* **2001**, *123*, 8155.

(133) Lynn, D. M.; Langer, R., Degradable poly(beta-amino esters): Synthesis, characterization, and self-assembly with plasmid DNA, *J. Am. Chem. Soc.* **2000**, *122*, 10761.

(134) Konkolewicz, D.; Gaillard, S.; West, A. G.; Cheng, Y. Y.; Gray-Weale, A.; Schmidt, T. W.; Nolan, S. P.; Perrier, S., Luminescent Hyperbranched Polymers: Combining Thiol-Yne Chemistry with Gold-Mediated C-H Bond Activation, *Organometallics* **2011**, *30*, 1315.

(135) Konkolewicz, D.; Poon, C. K.; Gray-Weale, A.; Perrier, S., Hyperbranched alternating block copolymers using thiol-yne chemistry: materials with tuneable properties, *Chem. Commun.* **2011**, *47*, 239.

(136) Cook, A. B.; Barbey, R.; Burns, J. A.; Perrier, S., Hyperbranched Polymers with High Degrees of Branching and Low Dispersity Values: Pushing the Limits of Thiol–Yne Chemistry, *Macromolecules* **2016**, *49*, 1296.

(137) Barbey, R.; Perrier, S., Synthesis of Polystyrene-Based Hyperbranched Polymers by Thiol-Yne Chemistry: A Detailed Investigation, *Macromolecules* **2014**, *47*, 6697.

(138) Barbey, R.; Perrier, S., A Facile Route to Functional Hyperbranched Polymers by Combining Reversible Addition-Fragmentation Chain Transfer Polymerization, Thiol-Yne Chemistry, and Postpolymerization Modification Strategies, *ACS Macro Lett.* **2013**, *2*, 366.

(139) Gillies, E. R.; Frechet, J. M., Dendrimers and dendritic polymers in drug delivery, *Drug Discovery Today* **2005**, *10*, 35.
(140) Khan, O. F.; Zaia, E. W.; Jhunjhunwala, S.; Xue, W.; Cai, W.; Yun, D. S.; Barnes, C. M.; Dahlman, J. E.; Dong, Y.; Pelet, J. M.; Webber, M. J.; Tsosie, J. K.; Jacks, T. E.; Langer, R.; Anderson, D. G., Dendrimer-Inspired Nanomaterials for the in Vivo Delivery of siRNA to Lung Vasculature, *Nano Lett.* **2015**, *15*, 3008.
(141) Zhou, K.; Nguyen, L. H.; Miller, J. B.; Yan, Y.; Kos, P.; Xiong, H.; Li, L.; Hao, J.; Minnig, J. T.; Zhu, H.; Siegwart, D. J., Modular degradable dendrimers enable small RNAs to extend survival in an aggressive liver cancer model, *Proceedings of the National Academy of Sciences* **2016**, *113*, 520.
(142) Frauenrath, H., Dendronized polymers—building a new bridge from molecules to nanoscopic objects, *Prog. Polym. Sci.* **2005**, *30*, 325.
(143) Poon, Z.; Chen, S.; Engler, A. C.; Lee, H. i.; Atas, E.; von Maltzahn, G.; Bhatia, S. N.; Hammond, P. T., Ligand-Clustered "Patchy" Nanoparticles for Modulated Cellular Uptake and In Vivo Tumor Targeting, *Angew. Chem. Int. Ed.* **2010**, *49*, 7266.
(144) Guo, D.; Shi, C.; Wang, X.; Wang, L.; Zhang, S.; Luo, J., Riboflavin-containing telodendrimer nanocarriers for efficient doxorubicin delivery: High loading capacity, increased stability, and improved anticancer efficacy, *Biomaterials* **2017**, *141*, 161.
(145) Ren, J. M.; McKenzie, T. G.; Fu, Q.; Wong, E. H.; Xu, J.; An, Z.; Shanmugam, S.; Davis, T. P.; Boyer, C.; Qiao, G. G., Star polymers, *Chem. Rev.* **2016**, *116*, 6743.
(146) Cho, H. Y.; Averick, S. E.; Paredes, E.; Wegner, K.; Averick, A.; Jurga, S.; Das, S. R.; Matyjaszewski, K., Star Polymers with a Cationic Core Prepared by ATRP for Cellular Nucleic Acids Delivery, *Biomacromolecules* **2013**, *14*, 1262.
(147) Tripp, S.; Appelhans, D.; Striegler, C.; Voit, B., Oligosaccharide shells as a decisive factor for moderate and strong ionic interactions of dendritic poly (ethylene imine) scaffolds under shear forces, *Chemistry-A European Journal* **2014**, *20*, 8314.
(148) Li, H.-J.; Du, J.-Z.; Liu, J.; Du, X.-J.; Shen, S.; Zhu, Y.-H.; Wang, X.; Ye, X.; Nie, S.; Wang, J., Smart superstructures with ultrahigh pH-sensitivity for targeting acidic tumor microenvironment: instantaneous size switching and improved tumor penetration, *ACS nano* **2016**, *10*, 6753.

(149) Prabaharan, M.; Grailer, J. J.; Pilla, S.; Steeber, D. A.; Gong, S., Amphiphilic multi-arm-block copolymer conjugated with doxorubicin via pH-sensitive hydrazone bond for tumor-targeted drug delivery, *Biomaterials* **2009**, *30*, 5757.

(150) Zeng, H.; Little, H. C.; Tiambeng, T. N.; Williams, G. A.; Guan, Z., Multifunctional dendronized peptide polymer platform for safe and effective siRNA delivery, *J. Am. Chem. Soc.* **2013**, *135*, 4962.

(151) Nelson, C. E.; Kintzing, J. R.; Hanna, A.; Shannon, J. M.; Gupta, M. K.; Duvall, C. L., Balancing Cationic and Hydrophobic Content of PEGylated siRNA Polyplexes Enhances Endosome Escape, Stability, Blood Circulation Time, and Bioactivity in Vivo, *Acs Nano* **2013**, *7*, 8870.

(152) Synatschke, C. V.; Schallon, A.; Jerome, V.; Freitag, R.; Muller, A. H. E., Influence of Polymer Architecture and Molecular Weight of Poly(2-(dimethylamino)ethyl methacrylate) Polycations on Transfection Efficiency and Cell Viability in Gene Delivery, *Biomacromolecules* **2011**, *12*, 4247.

(153) Decuzzi, P.; Godin, B.; Tanaka, T.; Lee, S. Y.; Chiappini, C.; Liu, X.; Ferrari, M., Size and shape effects in the biodistribution of intravascularly injected particles, *J. Control. Release* **2010**, *141*, 320.

(154) Doncom, K. E.; Blackman, L. D.; Wright, D. B.; Gibson, M. I.; O'Reilly, R. K., Dispersity effects in polymer self-assemblies: a matter of hierarchical control, *Chem. Soc. Rev.* **2017**, *46*, 4119.

2.

Hyperbranched polymers with high degrees of branching and low dispersity values: Pushing the limits of thiol–yne chemistry

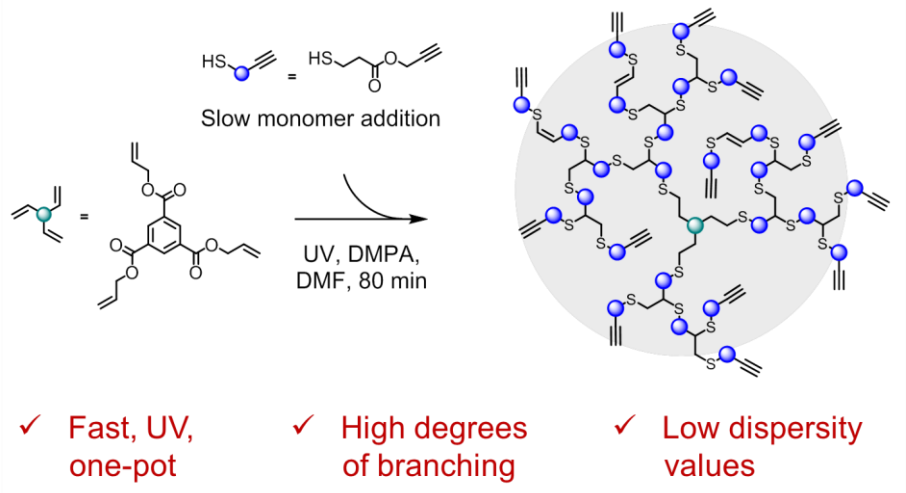

Abstract

Described here is a versatile approach to the production of hyperbranched polymers with high degrees of branching and low dispersity values (*Đ*), involving slow monomer addition of a thiol/yne monomer to multifunctional core molecules in the presence of photoinitiator and under UV irradiation. The small thiol/yne monomer was synthesized via 1-ethyl-3-(3-dimethylaminopropyl)carbodiimide hydrochloride (EDC.HCl) esterification and batch polymerizations were performed at varying concentrations. The batch thiol–yne polymerizations had fast reaction kinetics and large dispersity values that increased with increasing concentration. Introduction of monomer by slow addition to a multifunctional alkyne core (tri(prop-2-yn-1-yl) 1,3,5-benzenetricarboxylate) or alkene core (triallyl 1,3,5-benzenetricarboxylate) was found to lower dispersity at monomer concentrations of 0.5 M to 2.0 M. Degrees of branching were determined by ^{1}H NMR spectroscopy to be greater than 0.8 in most cases. Increasing the fraction of core molecule was found to decrease dispersity to values as low as 1.26 and 1.38 for the alkene core and alkyne core respectively, for monomer concentrations of 0.5 M with 10 mol% core molecule. Molecular weights of the hyperbranched structures were also determined by light scattering size exclusion chromatography (SEC) detection, and intrinsic viscosities determined by viscometry SEC detection. The Kuhn-Mark-Houwink-Sakurada α parameter decreased from 0.35 for the batch process to values as low as 0.21 (10 mol% alkene core) or 0.16 (10 mol% alkyne core), indicating that the thiol–yne structures became more globular and dense with the slow monomer addition strategy. This simple and versatile approach is a promising new development for the design of hyperbranched polymers of well-controlled molecular weight and molecular weight distributions, with very high degrees of branching.

2.1 Introduction

Highly branched and three dimensional macromolecular structures, or dendritic polymers, have become an important class of materials over recent decades.[1,2] These structures, including dendrimers and hyperbranched polymers, have received increasing interest due to their unique properties including large number of terminal functional groups, globular three dimensional structures, and low intrinsic viscosities.[3,4] Dendrimers were first reported in the late 1970's and early 1980's, and were synthesized *via* a divergent approach which involves many synthetic steps and tends to lead to branching irregularities at higher generations.[5,6] The convergent approach to dendrimer synthesis was introduced in pioneering work by Fréchet and Hawker in the early 1990's and can lead to higher purity.[7] While perfectly branched dendrimers with degrees of branching (DB) of 1 are very promising structures, the sometimes complicated synthetic and purification steps have led to attempts to replicate their structural properties *via* synthesis of hyperbranched polymers with high degrees of branching in one pot processes.

Flory established the theory of AB_2 hyperbranched polymers that could be prepared without gelation in 1952,[8] but it wasn't until 1988 that AB_2 hyperbranched polymers were synthesized for the first time in practice.[9-11] Traditional AB_2 hyperbranched polymers where both B groups have the same reactivity have a maximum degree of branching of 0.5 due to the statistical nature of the reaction.[12] But by designing monomers where the second B group reacts at a faster rate, DB can be dramatically increased producing hyperbranched polymers with degrees of branching in the region of dendrimers.[13] An interesting chemistry that shows this enhanced reactivity are radical-mediated thiol–yne additions, which were re-introduced by the group of Bowman in 2009,[14] and applied in the synthesis of hyperbranched polymers with high degrees of branching by our group.[15-18] Another recent example involves copper-catalyzed azide–alkyne click chemistry, where the second B group reacts at a faster rate, due to the first triazole formed complexing the copper catalyst and causing faster reaction of the second moiety.[19]

Accelerated strategies to dendrimer synthesis using orthogonal click chemistry have greatly improved applications of dendrimers and increased their availability to the scientific community, by reducing number of reaction steps and need for demanding

purifications.[20-23] Further to this, the development of methods to produce hyperbranched polymers with narrow molecular weight distributions is an important target as it would allow the preparation of materials with greater control and more similarities to dendrimers, in a convenient manner. This could improve the application of hyperbranched polymers in a number of areas including biological systems, and as rheology additives. A number of strategies have been employed to control the molecular weight and dispersity of hyperbranched polymers including polymerization of inimers in confined space;[24,25] however this has yet to be used to produce polymers with degrees of branching higher than 0.5. Slow feeding of AB_2 monomer to multifunctional core has been described previously theoretically,[26,27] and in practice,[28] as another method to control molecular weight and dispersity of hyperbranched polymers. Further to this, increasing the reactivity of the core molecule has been shown to have a greater effect on the narrowing of hyperbranched polymer dispersity.[29-31]

In this chapter, a new strategy to generate hyperbranched polymers via radical thiol–yne chemistry is reported. The method dramatically improves previously published procedures by producing hyperbranched polymers with high degrees of branching and remarkably low dispersity values, *via* slow addition of the thiol/yne monomer to a trifunctional alkyne core and a trifunctional alkene core, tri(prop-2-yn-1-yl) 1,3,5-benzenetricarboxylate and triallyl 1,3,5-benzenetricarboxylate, respectively. The first part of this chapter involves the investigation of the effect of concentration and reactivity of the core molecule on the hyperbranched structure formed with slow monomer addition. The degree of branching for this system and also the kinetics of the thiol–yne batch polymerization were studied in order to establish appropriate slow monomer addition parameters. The second part of this chapter discusses the effect of the type and amount of core molecules on the production of hyperbranched structures. The molecular weight distributions of the hyperbranched polymers, their molecular weight and dendritic conformation in solution were determined by multidetector SEC, and the degrees of branching by nuclear magnetic resonance (NMR) spectroscopy.

2.2 Results and Discussion

2.2.1 Preparation of thiol/yne monomer and batch thiol–yne photopolymerization

The traditional batch polymerization of AB_2 monomers typically gives hyperbranched polymers with poor control and broad molecular weight distributions. Batch copolymerization of AB_2 and B_f (core molecule with f number of B functionalities) monomers in the molten state was first shown to decrease dispersity in 1995, with a degree of control over molecular weight achieved by varying the core to monomer ratio.[32-37] In 1998, the theory and computational studies of slow monomer addition to multifunctional core were developed by Frey and Müller,[26,27] which showed that the slow monomer addition method could be used to lower dispersity further. The slow monomer addition to multifunctional core strategy was employed to control the synthesis of hyperbranched polymers by Moore *et al.* for the preparation of hyperbranched phenylacetylenes with low dispersity values, however the degree of branching was not determined.[28] Frey *et al.* used slow monomer addition to a core initiator in the synthesis of polyglycerols by ring-opening polymerization, to give hyperbranched polymers with low dispersity values and DB's of ~0.55.[38] Thus, in order to determine appropriate slow addition parameters for the thiol–yne system, an initial set of experiments was conducted in which thiol/yne monomer was polymerized in a batch system allowing characterization of the kinetics of the reaction and degree of branching.

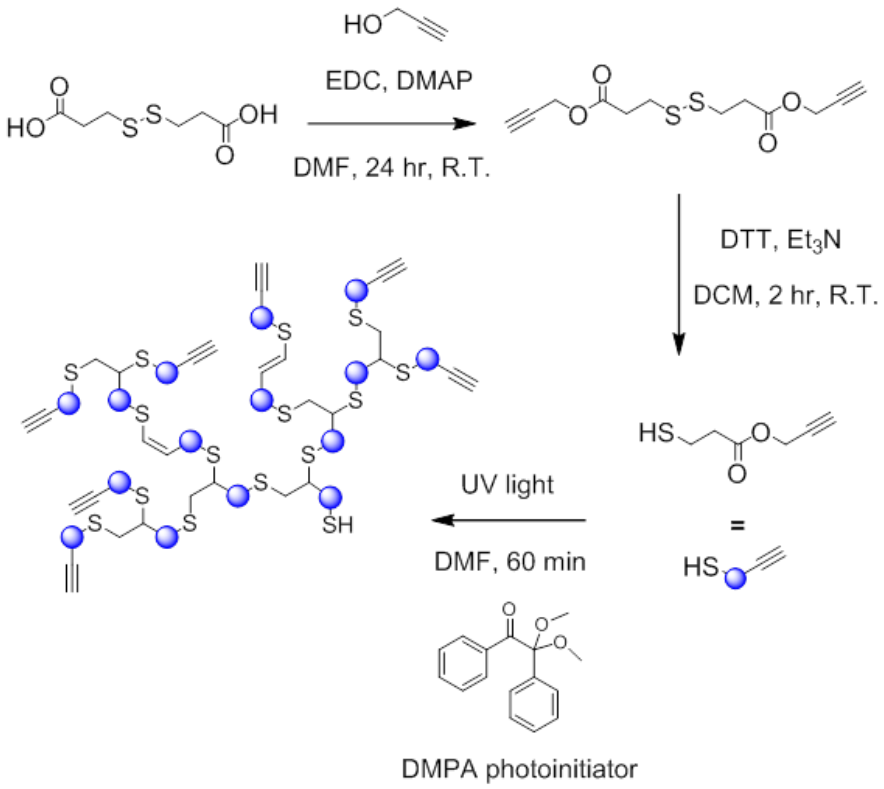

Scheme 10.1. Preparation of thiol/yne monomer and batch photopolymerization to form hyperbranched thiol–yne polymers.

The thiol/yne monomer used in this study was synthesized via a two-step procedure, as shown in **Scheme 10.1**. The first step involved the esterification of propargyl alcohol with 3,3-dithiodipropionic acid. This reaction procedure allows large scale synthesis and convenient storage of thiols in their disulfide form, compared to the reduced form, which is subject to reasonably fast oxidation under air. However, storage of the reduced thiol form of the monomer under inert atmosphere is also possible for periods of up to a week (longer storage not tested), and subsequent polymerisations showing no effect on polymer characteristics. Facile reduction of the disulfide (i.e., thiol-protected) monomer was achieved using dithiothreitol (DTT) over 2 hours, and extraction of the DTT with water, to give the pure thiol/yne monomer, prop-2-ynyl 3-mercaptopropanoate, in good yields. The monomer was polymerized under UV light (365 nm) with the radical photoinitiator 2,2-dimethoxy-2-phenylacetophenone (DMPA) in a 1.1 M solution in DMF, following a method similar to that previously published by our group.[15,17,18] A summary of the results

is shown in **Table 2.1**. The reaction proceeds through the radical-mediated addition of a thiol to an alkyne followed by the addition of a second thiol to the formed vinylthioether to give a dendritic unit. The rate of the second addition is much faster than the first addition, which leads to hyperbranched polymers with very high degrees of branching.

Table 10.1. Conversions, molecular weights, dispersity, and degree of branching values for hyperbranched thiol–yne polymers prepared by batch process.

Time (min)	Conv. [a]	$M_{n,SEC}$ (g/mol) [b]	$M_{w,SEC}$ (g/mol) [b]	$Đ$ [b]	DB [c]
2	35%	1600	2400	1.50	0.84
5	61%	2300	3900	1.66	0.89
10	86%	3400	6500	1.89	0.87
20	98%	4700	10900	2.30	0.84
30	> 99%	5400	14400	2.67	0.83
60	> 99%	5600	16100	2.88	0.84
60 (ppt)	-	9500	19900	2.09	0.85

[a] Determined by ^{1}H NMR spectroscopy, from disappearance of thiol triplet at 1.7 ppm. [b] From DMF SEC with DRI detector and PMMA standard, [c] DB = degree of branching, following equation DB = (D+T)/(D+T+L).[39]

Figure 2.1a shows the conversion of the thiol/yne monomer over time. Conversion was monitored by ^{1}H NMR spectroscopy, by comparing the integral of the thiol triplet at 1.7 ppm to the integrals corresponding to the dendritic monomer units at 4.3 ppm, the terminal monomer units at 4.7 ppm, and the linear monomer units at 6.4 ppm (see **Figure A2.9**). The reaction proceeds very rapidly and reaches 98% conversion after 20 minutes, with no observable monomer peaks remaining in the ^{1}H NMR spectrum after 60 minutes. The molecular weight increases in a linear fashion until high conversion, where above 90% conversion, polymer–polymer coupling is observed as expected from a step growth hyperbranched polymer synthesis (**Figure 2.1b**). The step growth nature of the thiol–yne hyperbranched system also leads to broadening of the molecular weight distribution as

conversion increases, as seen in **Figure 2.1c**. Note that purification by precipitation removes the smallest hyperbranched oligomers thus leading to a small decrease in the dispersity (**Figure 2.1c**).

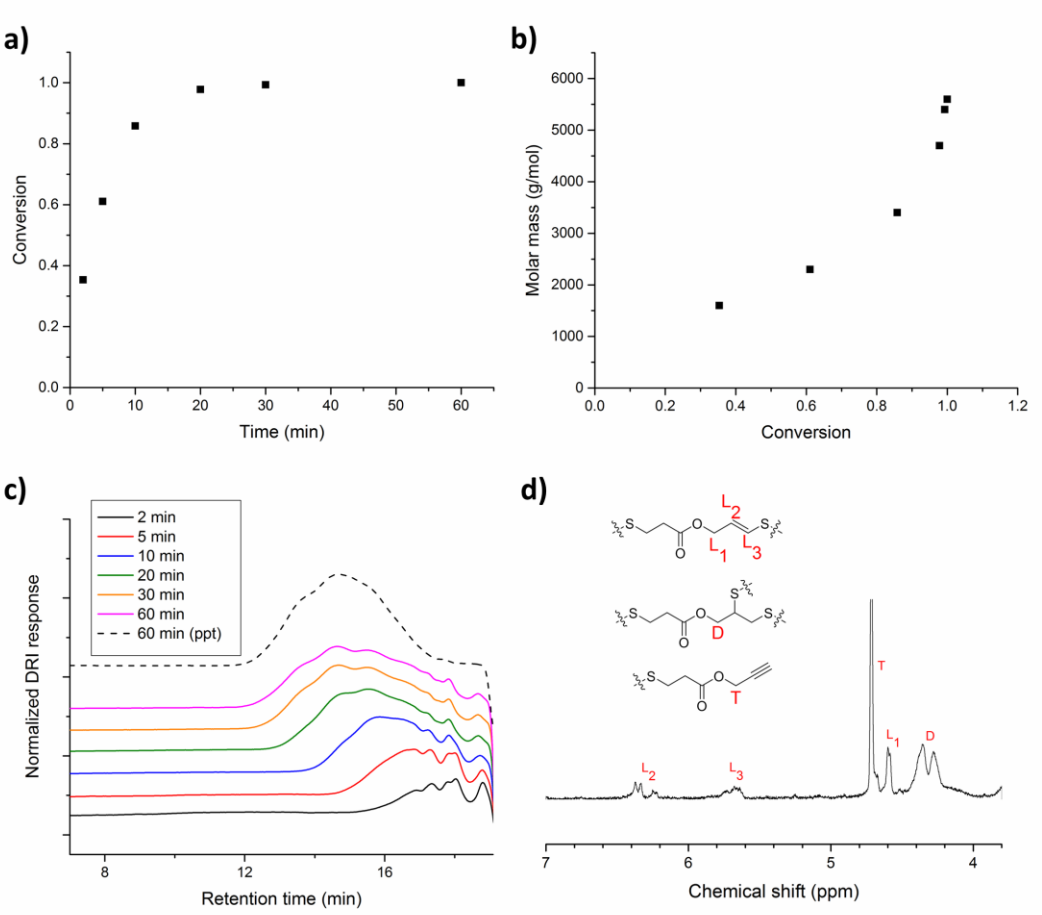

Figure 2.1. a) Conversion of thiol/yne monomer as a function of time, **b)** Number average molecular weight as a function of conversion, **c)** SEC chromatograms of polymer samples at different times during the polymerization, **d)** 1H NMR spectrum of the precipitated hyperbranched thiol–yne polymer showing peaks corresponding to dendritic, linear, and terminal units for calculation of degree of branching (see appen.).

The concept of 'degree of branching' (DB) was introduced by Flory in the 1940's with polymers in the state of gelation,[40] and expanded to highly-branched polymers in solution with the theory of AB_2 polymerizations in 1952.[8] An important associated equation for the characterization degree of branching in hyperbranched polymers was proposed by Hawker and Fréchet in 1991.[39] The polymerization of the thiol/yne monomer allows for

easy determination of the degree of branching by ^{1}H NMR spectroscopy, as the peaks for terminal, dendritic, and linear units appear at distinct chemical shifts.[41] For batch polymerization of thiol/yne monomer at 1.1 M concentration, the precipitated polymer had a degree of branching of 0.85 (**Figure A2.11**), which corresponds to 15% linear units. It is remarkable to achieve such a high degree of branching for hyperbranched polymers, especially considering the simplicity and versatility of the process, although the final materials exhibit relatively high dispersity.

2.2.2 Slow addition of thiol/yne monomer to multifunctional core

In order to lower this dispersity, the thiol/yne monomer was fed to a trifunctional alkyne core, tri(prop-2-yn-1-yl) 1,3,5-benzenetricarboxylate, at varying concentrations (**Scheme 2.2**). The proportion of core molecule was chosen to be 10 mol% core for an initial series of feeding experiments. Thiol/yne monomer was introduced gradually into the reaction vessel at a rate that allows the majority of monomer to react with the core before more monomer is added, thus limiting monomer–monomer reactions and promoting monomer–polymer reactions, ie. polymerization from core. This process creates a core region of the hyperbranched polymers analogous to dendrimers, and indicates that there are no thiol focal points which could cause polymer–polymer coupling at high conversions and broaden the molecular weight distribution. Based on the initial thiol–yne batch polymerization kinetic experiments (with 98% conversion after 20 minutes) and previous studies,[15,17] slow monomer addition conditions were employed with the monomer fed over 20 minutes. The matching of the rate of feeding to rate of polymerization means there is always a low concentration of unreacted AB_2 in the reaction vessel.

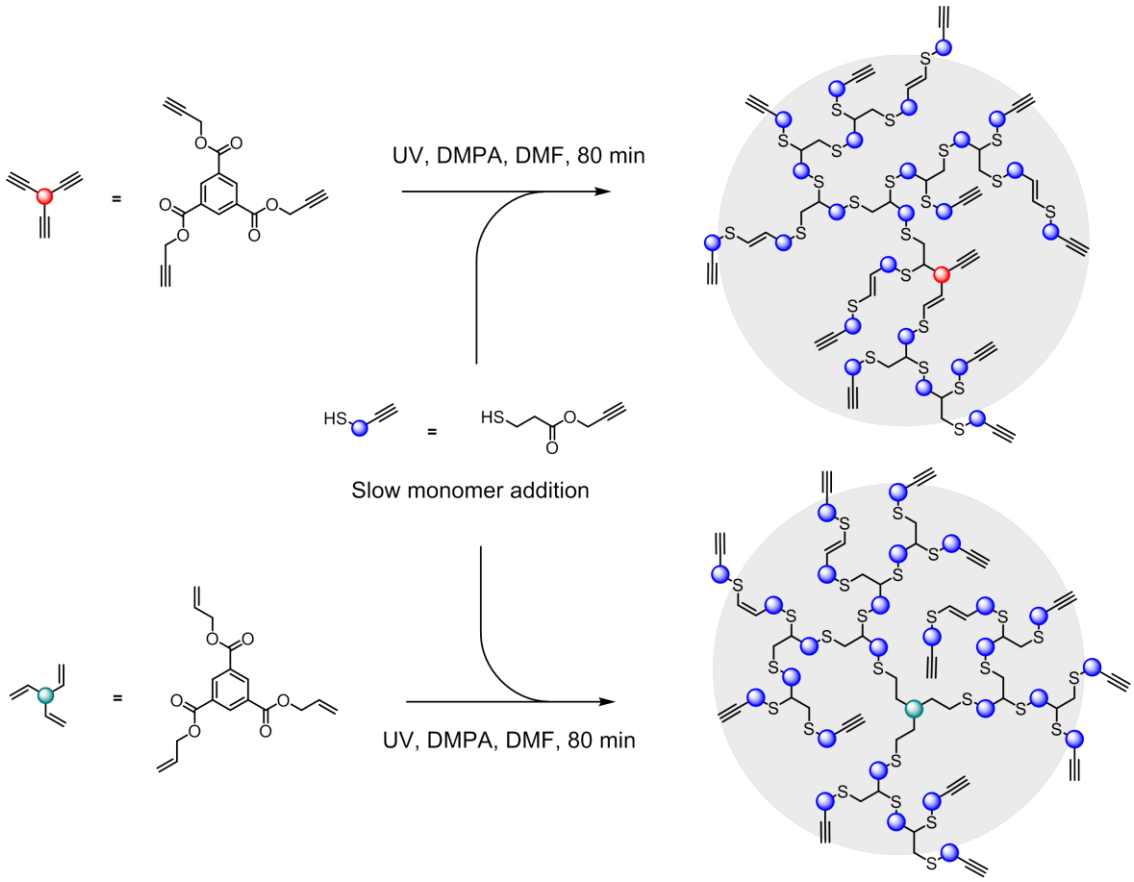

Scheme 10.2. Preparation of hyperbranched thiol–yne polymers by slow monomer addition to multifunctional core molecules, tri(prop-2-yn-1-yl) 1,3,5-benzenetricarboxylate or triallyl 1,3,5-benzenetricarboxylate.

Figure 2.2 shows the SEC chromatograms of hyperbranched thiol–yne polymers prepared at varying concentrations either by slow monomer addition or in a batch process. Molecular weights and dispersity values are shown in **Table 2.2**, and were determined using a conventional calibration with PMMA standards and also multi angle light scattering (MALLS) SEC detection. With increasing concentration the batch thiol–yne hyperbranched polymers have higher molecular weights and broader molecular weight distributions, with the batch polymerization at 2.0 M having a very high apparent molecular weight and large dispersity values. At 0.5 M the use of slow monomer addition to multifunctional alkyne core allows the reduction of the molecular weight to $M_{w,MALLS}$ = 13,300 g/mol and the molecular weight distribution is narrowed to 1.38. Using the slow

monomer addition strategy with the alkyne core, and with careful choice of monomer concentration, the molecular weight can be targeted to between 13,300 g/mol and 77,700 g/mol with considerably lower dispersity values than the equivalent batch polymerization.

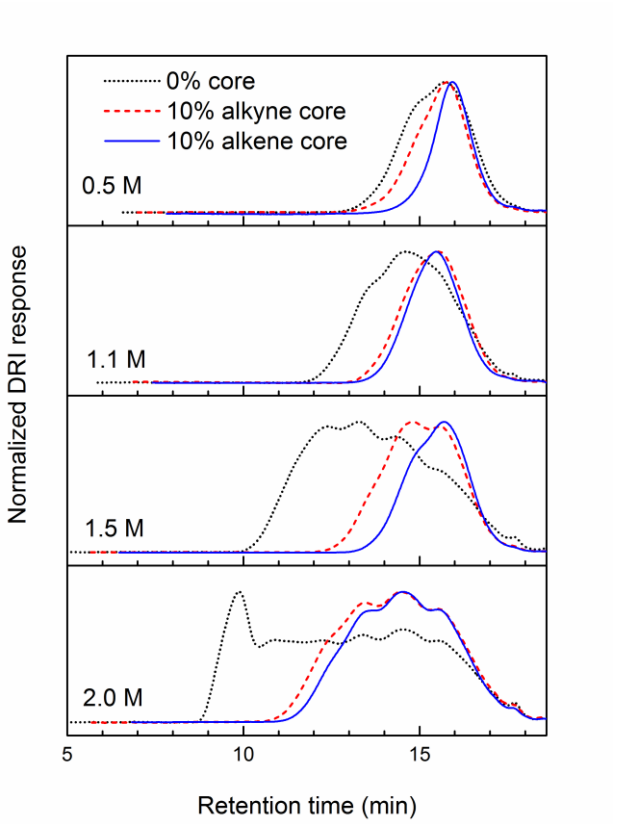

Figure 2.2. Normalized DRI response SEC chromatograms of hyperbranched thiol–yne polymers prepared by both batch and slow monomer addition process to multifunctional alkyne and alkene core molecules at varying concentrations.

With respect to the monomer concentrations discussed above, the semi-batch methods were designed to have the same concentration of monomer after the initial feeding period. This does lead to differences in concentrations of various reaction components in the two polymerisation processes. In the feeding polymerisations, the total amount of initiator and solvent were kept the same for the batch and semi-batch after the initial feeding period. For the feeding period, equal volumes of solvent and initiator were used in both the reaction vessel and the feed syringe (see experimental).

Increasing the reactivity of the core functional groups compared to the monomer can further enhance control and lower dispersity.[42-45] This approach has been used in batch polymerizations to reasonable effect. Fossum *et al*. have shown that copolymerization of an AB_2 monomer with multifunctional C_f cores, where the reactivity towards A of the C group is higher than that of the B group, permits to reduce dispersity of the resulting hyperbranched polymers.[29] Similar results were obtained by Ramakrishnan *et al.* for the copolymerization of AB_2 with a higher reactivity core molecule.[30] In an attempt to reduce dispersity further, use of slow feeding combined with higher reactivity core can be used.[31] Since alkenes are usually more reactive in radical thiol yne/ene reactions,[46] thiol/yne monomer was fed to a trifunctional alkene core, triallyl 1,3,5-benzenetricarboxylate, at varying concentrations.

Use of the alkene core gave narrower molecular weight distributions compared to the same polymerization protocols using the alkyne core. The most remarkable results were obtained with reducing monomer concentration, leading to dispersity as low as 1.26 – a value close to that expected from controlled polymer synthesis techniques such as controlled radical polymerizations – whilst keeping very high degrees of branching (above 0.8).

Molecular weights can also be relatively well-controlled, with lower M_w obtained at lower monomer concentrations. Note that increasing molecular weight by increasing monomer concentration leads to higher $Đ$, as expected from theory and previous reports in the literature.[17,28,29,38] A monomer concentration of 1.1 M was found to give a good combination of control over molecular weight and molecular weight distribution, with very high degree of branching. These conditions were used to investigate the effect of mole fraction core molecule, and conduct a more detailed study of polymer conformation and molecular weight using multidetector SEC.

Table 10.2. Conversions, molecular weights, dispersity, and degree of branching values for hyperbranched thiol–yne polymers prepared by batch polymerization or by slow monomer addition process to multifunctional alkyne and alkene core molecules at varying concentrations.

Conc. (M)	Core mol%	Conv. [a]	$M_{n,SEC}$ (g/mol) [b]	$M_{w,SEC}$ (g/mol) [b]	$Đ$ [b]	$M_{w,MALLS}$ (g/mol) [c]	DB [d]
0.5	0%	> 99%	6700	10300	1.53	17100	0.80
	10% yne	> 99%	6700	9200	1.38	13300	0.79
	10% ene	> 99%	5400	6800	1.26	12100	0.82
1.1	0%	> 99%	9500	19900	2.09	46800	0.85
	10% yne	> 99%	7200	10400	1.44	19600	0.82
	10% ene	> 99%	7200	9700	1.35	13600	0.82
1.5	0%	> 99%	13800	73400	5.30	175400	0.86
	10% yne	> 99%	8100	16800	2.07	25700	0.83
	10% ene	> 99%	6300	10300	1.62	16500	0.84
2.0	0%	> 99%	13900	291600	21.0	1698000	0.87
	10% yne	> 99%	9600	42600	4.44	77700	0.88
	10% ene	> 99%	9400	33500	3.55	54000	0.86

[a] Determined by ^{1}H NMR spectroscopy, from disappearance of thiol triplet at 1.7 ppm. [b] From DMF SEC with DRI detector and PMMA standard. [c] Absolute MW from DMF SEC, MALLS detector. [d] DB = degree of branching, following equation DB = (D+T)/(D+T+L).[39]

2.2.3. Variation of amounts of multifunctional core

The thiol/yne monomer was slowly fed to multifunctional core alkyne and core alkene at 1.1 M final monomer concentrations, with the fraction of core molecule ranging from 2 mol% to 20 mol% (**Table 2.3**). The molecular weights of the resulting hyperbranched structures were determined by SEC using a DRI detector and comparing retention time to retention time of PMMA. As retention time is based on hydrodynamic volume, the molecular weight determined by this conventional calibration is significantly underestimated, hyperbranched polymers having a smaller hydrodynamic volume than their linear counterparts, at equivalent molecular weight.[47] For this reason molecular weight was also determined by MALLS SEC detection which determines molecular weight based on scattered light of the polymer.

Figures 2.3a and **2.3b** show the ^{1}H NMR spectra of the hyperbranched polymers synthesized by both batch and slow monomer addition to core molecules. The degrees of branching and also the extent to which the core molecule functional groups have reacted were calculated. For the polymers synthesized with slow monomer addition, the degrees of branching are all ~0.82 (**Table 2.3**), which corresponds to ~18% linear units in the main structure of the hyperbranched polymers. For the hyperbranched polymers specifically with trifunctional alkyne core, the fraction of core alkyne functional groups and core thiovinylether groups remaining after polymerization is the same for all initial core ratios. These remaining core functionalities are ~19% vinylthioether groups, and 40% alkyne groups. In the case of slow monomer addition to alkene core the polymers have 30% alkene functionality remaining on the core after polymerization, with very similar degrees of branching for the main thiol–yne polymer structure as expected. This fraction of residual functionality located on the core molecule after polymerization is the same for all initial core ratios, and is most likely due to steric hindrance around the core as the hyperbranched polymer grows.

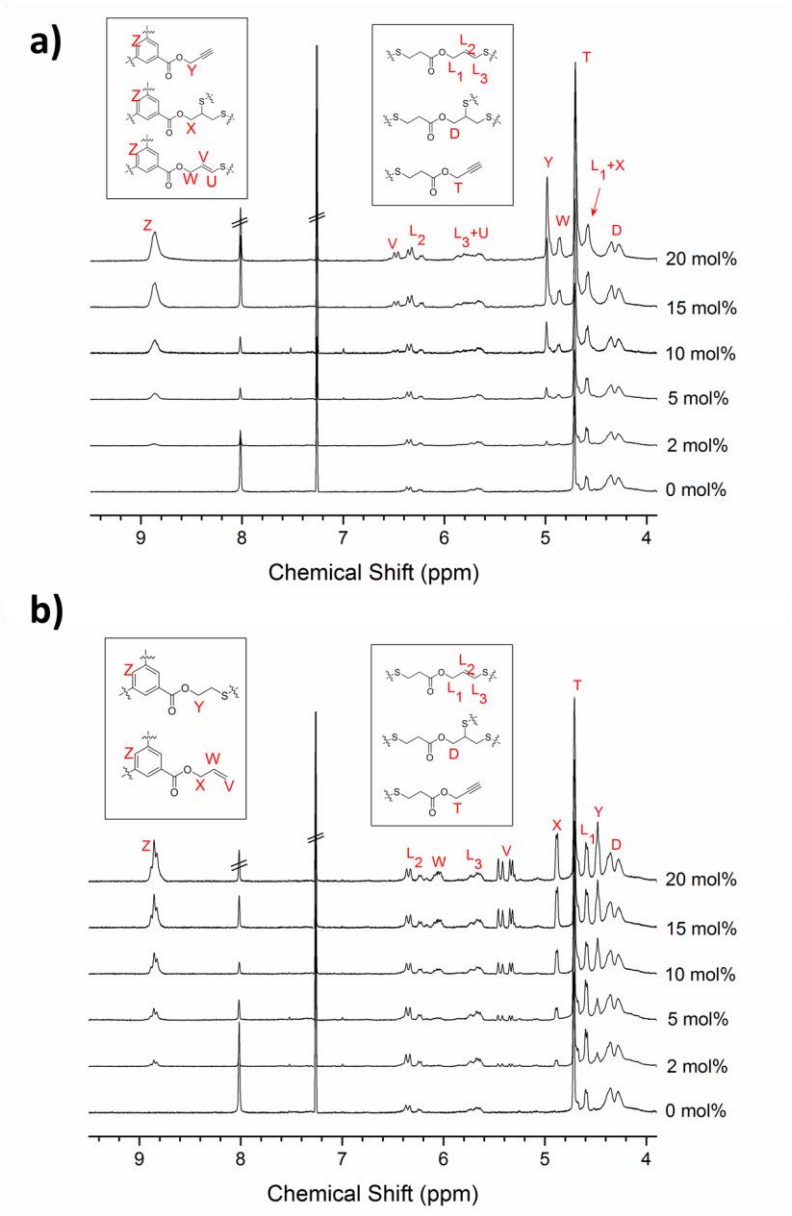

Figure 2.3. ^{1}H NMR spectra of hyperbranched thiol–yne polymers prepared by both batch and slow monomer addition process to varying amounts of multifunctional **a)** alkyne and **b)** alkene core molecules at 1.1 M concentration.

Table 10.3. Conversions, molecular weights, dispersity, degree of branching values, and KMHS parameter α, for hyperbranched thiol–yne polymers prepared by slow monomer addition process to varying amounts of multifunctional alkyne and alkene core molecules at 1.1 M concentration.

	Core mol%	Conv. [a]	$M_{n,SEC}$ (g/mol) [b]	$M_{w,SEC}$ (g/mol) [b]	$Đ$ [b]	$M_{w,MALLS}$ (g/mol) [c]	DB [d]	α [e]
	0%	> 99%	9500	19900	2.09	46800	0.85	0.35
Alkyne Core	2%	> 99%	8500	15100	1.79	34200	0.81	0.32
	5%	> 99%	8200	12800	1.56	24600	0.81	0.27
	10%	> 99%	7200	10400	1.44	19600	0.82	0.21
	15%	98%	6300	9000	1.42	14200	0.79	0.35
	20%	97%	6100	8600	1.43	12600	0.73	0.40
Alkene Core	2%	> 99%	9400	16200	1.72	29400	0.82	0.34
	5%	> 99%	7900	11900	1.52	23000	0.81	0.20
	10%	> 99%	7200	9700	1.35	13600	0.82	0.16
	15%	99%	6500	8800	1.36	13400	0.82	0.31
	20%	97%	6300	8300	1.31	12400	0.82	0.34

[a] Determined by ^{1}H NMR spectroscopy, from disappearance of thiol triplet at 1.7 ppm. [b] From DMF SEC, DRI detector, PMMA standard. [c] Absolute MW from DMF SEC, MALLS detector. [d] DB = degree of branching, following equation DB = (D+T)/(D+T+L)[39]. [e] α = Kuhn-Mark-Houwink-Sakurada parameter, from DMF SEC viscometry detector.

Figures 2.4a and **2.4b** show that as the proportion of multifunctional alkyne core is increased the molecular weight distribution becomes narrower. As previously discussed the batch polymerization has a broad dispersity of over 2, with 2 mol% core this decreases to 1.7-1.8 for both core molecules. For 5 mol% this is reduced further to around 1.5 for both core molecules. At 10 mol% the dispersity reaches 1.35 for alkene core and 1.44 for the alkyne core, with higher core ratios not having a significant further effect on the dispersity. High molar ratios of 20% core did however reduce the molecular weight further, and cause a reduction in the degree of branching most notable for the alkyne core. The distributions also become monomodal due to reduction in polymer–polymer coupling with higher amounts of core.

Lack of entanglements in hyperbranched polymers leads to lower solution viscosities compared to their linear analogues.[47] **Figure 2.4c** and **2.4d** show the Kuhn-Mark-Houwink-Sakurada (KMHS) plots of intrinsic viscosity as a function of molecular weight, which describe polymer conformation in solution, obtained using a viscometry detector on the SEC. KMHS α values, which correspond to the gradient of these plots, are 0 for a hard sphere, 2 for a rigid rod and ~0.7 for linear polymers.[48] An α of between 0.2 – 0.4 corresponds to globular structures with a high degree of branching, consistent with hyperbranched polymers.[2,49] For the batch polymerization of thiol–yne hyperbranched structures the α value was 0.35, indicating globular hyperbranched polymer structures. With increasing core fraction the α value decreases to 0.21 for the 10% alkyne core hyperbranched polymer and 0.16 for the 10% alkene core hyperbranched polymer, as the structures become more uniform in size and more dense, consistent with the molecular weight distribution traces. Intrinsic viscosity decreases for the alkene core compared to the alkyne core as seen in **Figure 2.4c** and **2.4d**, which also indicates a more uniform structure with fewer entanglements, as expected from a more reactive core.

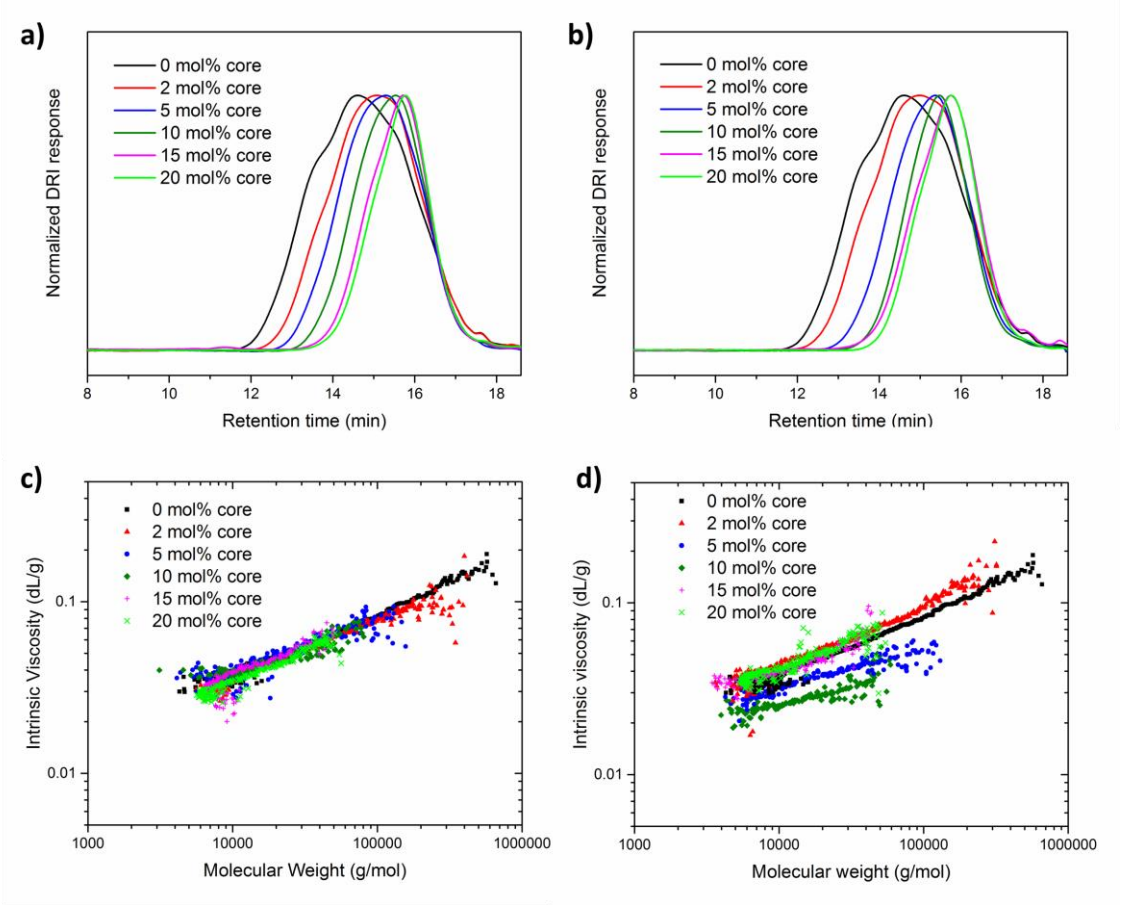

Figure 2.4. Normalized DRI response SEC chromatograms of hyperbranched thiol–yne polymers prepared by both batch and slow monomer addition process to varying amounts of multifunctional **a)** alkyne and **b)** alkene core molecules at 1.1 M concentration. Kuhn-Mark-Houwink-Sakurada plots of intrinsic viscosity as a function of molecular weight, determined by viscometry detector on DMF SEC, for hyperbranched thiol–yne polymers prepared by both batch and slow monomer addition process to varying amounts of multifunctional **c)** alkyne and **d)** alkene core molecules at 1.1 M concentration.

2.3. Conclusions

A method for the preparation of hyperbranched polymers with high degrees of branching, predictable molecular weights and narrow molecular weight distributions has been described, involving slow monomer addition of a thiol/yne monomer to multifunctional core molecules in the presence of photoinitiator and UV irradiation. A small thiol/yne monomer was synthesized via simple esterification, giving a route to high purity monomers. Addition of the thiol/yne monomer to multifunctional alkyne and alkene cores was found to lower dispersity of the resulting hyperbranched polymers, whilst maintaining very high degrees of branching. Increasing the fraction of core molecule was found to decrease dispersity, with the ideal value being approximately 10 mol% core molecule. Molecular weights of the hyperbranched structures were determined by conventional calibration SEC and also light scattering SEC detection, and intrinsic viscosities determined by viscometry SEC detection. The KMHS α parameter was found to be below 0.4 in all cases indicating dense and highly branched structures. Using the slow monomer addition strategy reduced the α value to 0.16 in the case of 10% the alkene core molecule, and 0.21 when using 10% alkyne core. In summary, this approach proves to be a simple and versatile process for the synthesis of hyperbranched polymers of remarkably well-controlled molecular weight and molecular weight distributions, with very high degrees of branching.

2.4. Experimental

2.4.1. Materials

Propargyl alcohol, 1,3,5-benzenetricarboxylic acid, 3,3-dithiodipropionic acid, dithiothreitol (DTT), 4-dimethylaminopyridine (DMAP), and 2,2-dimethoxy-2-phenylacetophenone (DMPA) were all purchased from Sigma Aldrich. 1-ethyl-3-(3-dimethylaminopropyl)carbodiimide hydrochloride (EDC.HCl) was purchased from Iris Biotech. Triethylamine was purchased from Fischer Scientific. Triallyl 1,3,5-benzenetricarboxylate was purchased from Acros. All other materials were purchased from Fisher Scientific or Sigma Aldrich.

2.4.2. Characterization

Size Exclusion Chromatography (SEC) was performed in DMF, using an Agilent 390-LC MDS instrument equipped with differential refractive index (DRI), viscometry, dual angle light scattering, and dual wavelength UV detectors. The system was equipped with 2 x PLgel Mixed D columns (300 x 7.5 mm) and a PLgel 5 μm guard column. The eluent was DMF with 5 mmol NH_4BF_4 additive, and samples were run at 1 mL/min at 50 °C. Analyte samples were filtered through a nylon membrane with 0.22 μm pore size before injection. Apparent molar mass values ($M_{n,SEC}$ and $M_{w,SEC}$) and dispersity ($Đ$) of synthesized polymers were determined by DRI detector and conventional calibration using Agilent SEC software. Poly(methyl methacrylate) (PMMA) standards (Agilent EasyVials) were used for calibration. Molar mass ($M_{w,MALLS}$) was determined on Agilent SEC software using a dual angle light scattering detector, and also DRI detector to determine the incremental refractive index dn/dc. The Kuhn-Mark-Houwink-Sakurada parameter α, relating to polymer conformation in solution was determined from the gradient of the double logarithmic plot of intrinsic viscosity as a function of molecular weight, using the SEC viscometry detector and Agilent SEC software. Proton nuclear magnetic resonance spectra (^{1}H NMR) were recorded on a Bruker Advance 400 or 500 spectrometer (400 MHz or 500 MHz) at 27 °C in $CDCl_3$, with chemical shift values (δ) reported in ppm, and the residual proton signal of the solvent used as internal standard

(δH 7.26). Proton-decoupled carbon nuclear magnetic resonance spectra (^{13}C NMR) were recorded on a Bruker Advance 400 or 500 spectrometer (100 MHz or 125 MHz) at 27 °C in $CDCl_3$, with chemical shift values (δ) reported in ppm, and the residual proton signal of the solvent used as internal standard (δC 77.16). Fourier transform infrared spectra (FTIR) were recorded on a Bruker Vector 22 FTIR spectrometer. Electrospray ionisation mass spectra (ESI-MS) were recorded using an Agilent 6130B single Quad mass spectrometer or an Apex Ultra 7T Fourier transform ion cyclotron resonance (FTICR) from Bruker Daltonics.

2.4.3. Preparation of tri(prop-2-yn-1-yl) 1,3,5-benzenetricarboxylate (trialkyne core)

1,3,5-benzenetricarboxylic acid (5.00 g, 23.8 mmol) in 100 mL of DCM, in a round bottomed flask was cooled to 0 ˚C. 1-ethyl-3-(3-dimethylaminopropyl)carbodiimide hydrochloride (EDC.HCl) (16.47 g, 85.9 mmol) and 4-dimethylaminopyridine (DMAP) (1.08 g, 8.8 mmol) were dissolved in 100 mL DCM and added to the round bottomed flask under vigorous stirring. Propargyl alcohol (5.30 g, 94.5 mmol) was then added over 1 minute; the reaction mixture was allowed to reach room temperature and stirred for 24 hours. The DCM phase was washed with MilliQ water (2 × 150 mL, 2 × 100 mL), dried with $MgSO_4$, filtered, and the solvent was removed by rotary evaporation. The light brown solid was purified over a short silica column with DCM as the eluent, and the solvent removed by rotary evaporation to give a white powder (5.83 g, 76% yield). ^{1}H NMR ($CDCl_3$, 500 MHz), δ ppm: 8.93 (s, 3H, C**H** phenyl) 4.99 (s, 6H, O-C**H**$_2$-C≡), 2.56 (s, 3H, C≡C**H**). ^{13}C NMR ($CDCl_3$, 125 MHz), δ ppm: 164.06 (**C**=O), 135.36 (**C**H phenyl), 130.87 (**C** phenyl), 77.24 (CH_2-**C**≡CH), 75.76 (C≡**C**H), 53.24 (O-**C**H_2-C≡). High resolution ESI-MS, expected: *m/z* 347.05 $[M+Na]^+$, found: *m/z* 347.0526 $[M+Na]^+$. ^{1}H and ^{13}C NMR spectra can be found in the Supporting Information (**Figure A2.1** and **A2.2**).

2.4.4. Preparation of di(prop-2-yn-1-yl) 3,3'-disulfanediyldipropionate (protected thiol/yne monomer)

1-ethyl-3-(3-dimethylaminopropyl)carbodiimide hydrochloride (EDC.HCl) (21.88 g, 114.14 mol), 3,3-dithiodipropionic acid (10.0 g, 47.56 mol), and 4-dimethylaminopyridine (DMAP) (1.14 g, 9.52 mol) were dissolved in 250 mL of DMF and cooled in an ice bath under stirring. Propargyl alcohol (6.4 g, 114.14 mol) was added; the reaction was allowed to reach room temperature and stirred for 24 hours. The reaction mixture was concentrated via rotary evaporation to yield a yellow oil which was redissolved in DCM, and washed with water (3 × 100 mL) to remove trace DMF. The DCM phase was then washed with HCl (1 M, 1 × 100 mL), NaOH (1 M, 1 × 100 mL), and water (1 × 100 mL), then dried with Na_2SO_4, filtered and the solvent removed by rotary evaporation. The product was purified by column chromatography (eluent: DCM with 2.5% MeOH), and the resulting viscous liquid (10.3 g, 87% yield) crystallized at 4 °C. ^{1}H-NMR ($CDCl_3$, 400 MHz) δ ppm: 4.71 (s, 2H, O-C**H**$_2$-C≡), 2.94 (t, 2H, C(O)-C**H**$_2$-CH_2), 2.80 (t, 2H, CH_2-C**H**$_2$-S), 2.49 (s, 1H, C≡C**H**). ^{13}C-NMR ($CDCl_3$, 100 MHz) δ ppm: 170.91 (**C**=O), 76.84 (CH_2-**C**≡CH), 75.25 (C≡**C**H), 52.32 (O-**C**H$_2$-C≡), 33.86 (C(O)-**C**H$_2$-CH_2), 32.79 (CH_2-**C**H$_2$-S). FTIR ν cm^{-1}: 3240-3270 (≡C-H), 2125 (C≡C), 1732 (C(O)=O), 561 (S-S). ESI-MS, expected: *m/z* 309.02 $[M+Na]^+$, found: *m/z* 309.0 $[M+Na]^+$. Characterisation data agree with literature.[50] The different spectra are available in the Supporting Information (**Figure A2.3**–**A2.5**).

2.4.5. Preparation of prop-2-yn-1-yl 3-mercaptopropanoate (monomer deprotection)

Disulfide protected thiol/yne monomer (0.79 g, 5.5 mmol) was dissolved in DCM (10 mL), DTT (1.85 g, 12.1 mmol) and triethylamine (1.75 mL, 12.5 mmol) were added and solution deoxygenated with nitrogen bubbling for 10 min. The solution was stirred at room temperature for 2 hours. The organic layer was washed with 1 M HCl (1 × 20 mL) and water (2 × 20 mL), dried with Na_2SO_4, and solvent removed by rotary evaporation. The resulting viscous liquid (0.73 g, 92% yield) was stored under nitrogen, to prevent

disulfide formation. Characterization data agrees with previously published synthetic method.[15] ^{1}H-NMR ($CDCl_3$, 400 MHz) δ ppm: 4.71 (s, 2H, O-C**H**$_2$-C≡), 2.79 (m, 2H, C(O)-C**H**$_2$-CH_2), 2.71 (m, 2H, CH_2-C**H**$_2$-SH), 2.49 (s, 1H, C≡C**H**), 1.66 (t, 1H, CH_2-S**H**). ^{13}C-NMR ($CDCl_3$, 100 MHz) δ ppm: 170.81 (**C**=O), 76.84 (CH_2-**C**≡CH), 75.20 (C≡**C**H), 52.15 (O-**C**H_2-C≡), 38.16 (C(O)-**C**H_2-CH_2), 19.56 (CH_2-**C**H_2-SH). FTIR ν cm^{-1}: 3270-3290 (≡C-H), 2565-2570 (S-H), 2127 (C≡C), 1732 (C(O)=O). ESI-MS, expected: *m/z* 311.04 $[2M+Na]^+$, found: *m/z* 311.0 $[2M+Na]^+$. The spectra are reported in the Supporting Information as Figures S6–S8.

2.4.6. Typical thiol–yne batch polymerization procedure

A typical polymerization is as follows: deprotected thiol/yne monomer (50 mg, 0.347 mmol) was dissolved with DMPA (2 mg, 0.195 mmol) in DMF (300 mg) in a 1.5 mL vial equipped with a small stirrer bar and a rubber septum screw cap. Monomer to initiator ratio was kept the same for all polymerizations. The vial was wrapped in aluminium foil and deoxygenated with nitrogen for 5 min. The vial was placed under a 365 nm UV lamp (UVP, UVGL-55, 6 watt, 365 nm) in an aluminium foil lined dark box over a magnetic stirrer plate. For the kinetic samples, each time point corresponds to a separate vial removed after the allocated polymerization time. After the predetermined reaction time the vial was removed and analyzed by NMR spectroscopy and SEC. Polymer reaction mixture was precipitated in diethyl ether and the polymer recovered by centrifugation. Conversion was determined by disappearance of thiol peak at ~1.7 ppm, compared to total polymer. The monomer contribution to the integral of the terminal polymer CH_2 next to the alkyne (4.7 ppm) was subtracted.

2.4.7. Typical thiol–yne polymerization procedure with slow monomer addition

A typical polymerization is as follows: a solution of deprotected thiol/yne monomer (50 mg, 0.347 mmol) was dissolved with DMPA (1 mg, 0.0975 mmol) in DMF (150 mg) and deoxygenated by bubbling with nitrogen. This was then added to a 250 μL Hamilton gastight glass syringe fitted with stainless steel cannula, and wrapped in aluminium foil

and placed on syringe pump. Trialkyne core molecule (11.25 mg, 0.0347 mmol) and DMPA (1 mg, 0.0975 mmol) were dissolved in DMF (150 mg) with a small stirrer in a 1.5 mL vial with a rubber septum screw cap. The vial was wrapped in aluminium foil and deoxygenated with nitrogen for 5 min. Initiator was split between feed syringe and reaction vessel to keep rate of radical formation high and approximately constant, after preliminary experiments showed having all the initiator in the syringe led to slower polymerization due to low concentration of radicals in the reaction vessel. Monomer and initiator concentrations were chosen to keep final concentrations after feeding period the same as the batch polymerizations to enable comparison of results. The vial was placed under a 365nm UV lamp (UVP, UVGL-55, 6 watt) in an aluminium foil lined dark box over a magnetic stirrer plate and feeding started at the same time as irradiation. The feeding was performed over a period of 20 min. For thiol/yne monomer feeding to trialkene core the procedure was the same. After the predetermined reaction time the vial was removed, exposed to air, and analyzed by NMR spectroscopy and SEC. Polymer reaction mixture was precipitated in diethyl ether and the polymer recovered by centrifugation. After a maximum of 80 min, the reaction was stopped.

Appendix to Chapter 2

FTIR spectroscopy spectra, ^{1}H and ^{13}C NMR spectroscopy spectra, representative conversion and degree of branching calculations, representative multidetector SEC chromatograms, and polymerisation kinetics of slow monomer addition.

2.5. References

(1) Gao, C.; Yan, D., Hyperbranched polymers: from synthesis to applications, *Prog. Polym. Sci.* **2004**, *29*, 183.

(2) Jikei, M.; Kakimoto, M., Hyperbranched polymers: a promising new class of materials, *Prog. Polym. Sci.* **2001**, *26*, 1233.

(3) Frechet, J. M. J.; Hawker, C. J.; Gitsov, I.; Leon, J. W., Dendrimers and hyperbranched polymers: Two families of three-dimensional macromolecules with similar but clearly distinct properties, *J. Macromol. Sci., Pure Appl. Chem.* **1996**, *A33*, 1399.

(4) Voit, B., New developments in hyperbranched polymers, *J. Polym. Sci., Part A: Polym. Chem.* **2000**, *38*, 2505.

(5) Tomalia, D. A.; Baker, H.; Dewald, J.; Hall, M.; Kallos, G.; Martin, S.; Roeck, J.; Ryder, J.; Smith, P., A new class of polymers: starburst-dendritic macromolecules, *Polym. J.* **1985**, *17*, 117.

(6) Buhleier, E.; Wehner, W.; Vogtle, F., "Cascade" and "Nonskid-Chain-like" Syntheses of Molecular Cavity Topologies, *Synthesis-Stuttgart* **1978**, 155.

(7) Hawker, C. J.; Frechet, J. M., Preparation of polymers with controlled molecular architecture. A new convergent approach to dendritic macromolecules, *J. Am. Chem. Soc.* **1990**, *112*, 7638.

(8) Flory, P. J., Molecular Size Distribution in Three Dimensional Polymers. VI. Branched Polymers Containing A—R—Bf-1 Type Units, *J. Am. Chem. Soc.* **1952**, *74*, 2718.

(9) Kim, Y. H.; Webster, O. W., Hyperbranched polyphenylenes, *Polym. Prepr. (Am. Chem. Soc., Div. Polym. Chem.)* **1988**, *29*, 310.

(10) Kim, Y. H.; Webster, O. W., Hyperbranched Polyphenylenes, *Macromolecules* **1992**, *25*, 5561.

(11) Kim, Y. H.; Webster, O. W., Water-Soluble Hyperbranched Polyphenylene - A Unimolecular Micelle, *J. Am. Chem. Soc.* **1990**, *112*, 4592.

(12) Holter, D.; Burgath, A.; Frey, H., Degree of branching in hyperbranched polymers, *Acta Polym.* **1997**, *48*, 30.

(13) Holter, D.; Frey, H., Degree of branching in hyperbranched polymers .2. Enhancement of the DB: Scope and limitations, *Acta Polym.* **1997**, *48*, 298.

(14) Fairbanks, B. D.; Scott, T. F.; Kloxin, C. J.; Anseth, K. S.; Bowman, C. N., Thiol-Yne Photopolymerizations: Novel Mechanism, Kinetics, and Step-Growth Formation of Highly Cross-Linked Networks, *Macromolecules* **2009**, *42*, 211.

(15) Konkolewicz, D.; Gray-Weale, A.; Perrier, S., Hyperbranched Polymers by Thiol-Yne Chemistry: From Small Molecules to Functional Polymers, *J. Am. Chem. Soc.* **2009**, *131*, 18075.

(16) Konkolewicz, D.; Poon, C. K.; Gray-Weale, A.; Perrier, S., Hyperbranched alternating block copolymers using thiol-yne chemistry: materials with tuneable properties, *Chem. Commun.* **2011**, *47*, 239.

(17) Barbey, R.; Perrier, S., Synthesis of Polystyrene-Based Hyperbranched Polymers by Thiol-Yne Chemistry: A Detailed Investigation, *Macromolecules* **2014**, *47*, 6697.

(18) Barbey, R.; Perrier, S., A Facile Route to Functional Hyperbranched Polymers by Combining Reversible Addition-Fragmentation Chain Transfer Polymerization, Thiol-Yne Chemistry, and Postpolymerization Modification Strategies, *ACS Macro Lett.* **2013**, *2*, 366.

(19) Shi, Y.; Graff, R. W.; Cao, X.; Wang, X.; Gao, H., Chain-Growth Click Polymerization of AB(2) Monomers for the Formation of Hyperbranched Polymers with Low Polydispersities in a One-Pot Process, *Angew. Chem. Int. Ed.* **2015**, *54*, 7631.

(20) Killops, K. L.; Campos, L. M.; Hawker, C. J., Robust, efficient, and orthogonal synthesis of dendrimers via thiol-ene "Click" chemistry, *J. Am. Chem. Soc.* **2008**, *130*, 5062.

(21) Malkoch, M.; Schleicher, K.; Drockenmuller, E.; Hawker, C. J.; Russell, T. P.; Wu, P.; Fokin, V. V., Structurally diverse dendritic libraries: A highly efficient functionalization approach using Click chemistry, *Macromolecules* **2005**, *38*, 3663.

(22) Wu, P.; Feldman, A. K.; Nugent, A. K.; Hawker, C. J.; Scheel, A.; Voit, B.; Pyun, J.; Frechet, J. M. J.; Sharpless, K. B.; Fokin, V. V., Efficiency and fidelity in a click-chemistry route to triazole dendrimers by the copper(I)-catalyzed ligation of azides and alkynes, *Angew. Chem. Int. Ed.* **2004**, *43*, 3928.

(23) Walter, M. V.; Malkoch, M., Simplifying the synthesis of dendrimers: accelerated approaches, *Chem. Soc. Rev.* **2012**, *41*, 4593.

(24) Graff, R. W.; Wang, X.; Gao, H., Exploring Self-Condensing Vinyl Polymerization of Inimers in Microemulsion To Regulate the Structures of Hyperbranched Polymers, *Macromolecules* **2015**, *48*, 2118.

(25) Min, K.; Gao, H., New Method To Access Hyperbranched Polymers with Uniform Structure via One-Pot Polymerization of Inimer in Microemulsion, *J. Am. Chem. Soc.* **2012**, *134*, 15680.

(26) Hanselmann, R.; Holter, D.; Frey, H., Hyperbranched polymers prepared via the core-dilution/slow addition technique: Computer simulation of molecular weight distribution and degree of branching, *Macromolecules* **1998**, *31*, 3790.

(27) Radke, W.; Litvinenko, G.; Muller, A. H. E., Effect of core-forming molecules on molecular weight distribution and degree of branching in the synthesis of hyperbranched polymers, *Macromolecules* **1998**, *31*, 239.

(28) Bharathi, P.; Moore, J. S., Controlled synthesis of hyperbranched polymers by slow monomer addition to a core, *Macromolecules* **2000**, *33*, 3212.

(29) Bernal, D. P.; Bedrossian, L.; Collins, K.; Fossum, E., Effect of core reactivity on the molecular weight, polydispersity, and degree of branching of hyperbranched poly(arylene ether phosphine oxide)s, *Macromolecules* **2003**, *36*, 333.

(30) Roy, R. K.; Ramakrishnan, S., Control of Molecular Weight and Polydispersity of Hyperbranched Polymers Using a Reactive B-3 Core: A Single-Step Route to Orthogonally Functionalizable Hyperbranched Polymers, *Macromolecules* **2011**, *44*, 8398.

(31) Chen, J.-Y.; Smet, M.; Zhang, J.-C.; Shao, W.-K.; Li, X.; Zhang, K.; Fu, Y.; Jiao, Y.-H.; Sun, T.; Dehaen, W.; Liu, F.-C.; Han, E.-H., Fully branched hyperbranched polymers with a focal point: analogous to dendrimers, *Polymer Chemistry* **2014**, *5*, 2401.

(32) Malmstrom, E.; Johansson, M.; Hult, A., Hyperbranched Aliphatic Polyesters, *Macromolecules* **1995**, *28*, 1698.

(33) Feast, W. J.; Stainton, N. M., Synthesis, Structure and Properties of Some Hyperbranched Polyesters, *J. Mater. Chem.* **1995**, *5*, 405.

(34) Lach, C.; Muller, P.; Frey, H.; Mulhaupt, R., Hyperbranched polycarbosilane macromonomers bearing oxazoline functionalities, *Macromol. Rapid Commun.* **1997**, *18*, 253.

(35) Parker, D.; Feast, W. J., Synthesis, structure, and properties of core-terminated hyperbranched polyesters based on dimethyl 5-(2-hydroxyethoxy)isophthalate, *Macromolecules* **2001**, *34*, 5792.

(36) Hobson, L. J.; Feast, W. J., Poly(amidoamine) hyperbranched systems: synthesis, structure and characterization, *Polymer* **1999**, *40*, 1279.

(37) Hobson, L. J.; Feast, W. J., Dendritic solution viscosity behaviour in core terminated hyperbranched poly(amidoamine)s, *Chem. Commun.* **1997**, 2067.

(38) Sunder, A.; Hanselmann, R.; Frey, H.; Mulhaupt, R., Controlled synthesis of hyperbranched polyglycerols by ring-opening multibranching polymerization, *Macromolecules* **1999**, *32*, 4240.

(39) Hawker, C. J.; Lee, R.; Frechet, J. M. J., One-step synthesis of hyperbranched dendritic polyesters, *J. Am. Chem. Soc.* **1991**, *113*, 4583.

(40) Flory, P. J., Molecular Size Distribution in Three Dimensional Polymers. I. Gelation1, *J. Am. Chem. Soc.* **1941**, *63*, 3083.

(41) Han, J.; Zhao, B.; Gao, Y. Q.; Tang, A. J.; Gao, C., Sequential click synthesis of hyperbranched polymers via the A(2) + CB2 approach, *Polymer Chemistry* **2011**, *2*, 2175.

(42) Cheng, K. C.; Wang, L. Y., Kinetic model of hyperbranched polymers formed in copolymerization of AB(2) monomers and multifunctional core molecules with various reactivities, *Macromolecules* **2002**, *35*, 5657.

(43) Zhou, Z.; Jia, Z.; Yan, D., Kinetic analysis of AB(2) polycondensation in the presence of multifunctional cores with various reactivities, *Polymer* **2012**, *53*, 3386.

(44) Ohta, Y.; Kamijyo, Y.; Fujii, S.; Yokoyama, A.; Yokozawa, T., Synthesis and Properties of a Variety of Well-Defined Hyperbranched N-Alkyl and N-H Polyamides by Chain-Growth Condensation Polymerization of AB(2) Monomers, *Macromolecules* **2011**, *44*, 5112.

(45) Ohta, Y.; Fujii, S.; Yokoyama, A.; Furuyama, T.; Uchiyama, M.; Yokozawa, T., Synthesis of Well-Defined Hyperbranched Polyamides by Condensation Polymerization

of AB(2) Monomer through Changed Substituent Effects, *Angew. Chem. Int. Ed.* **2009**, *48*, 5942.

(46) Lowe, A. B.; Hoyle, C. E.; Bowman, C. N., Thiol-yne click chemistry: A powerful and versatile methodology for materials synthesis, *J. Mater. Chem.* **2010**, *20*, 4745.

(47) Voit, B. I.; Lederer, A., Hyperbranched and Highly Branched Polymer Architectures-Synthetic Strategies and Major Characterization Aspects, *Chem. Rev.* **2009**, *109*, 5924.

(48) Hiemenz, P. C.; Lodge, T. P. *Polymer Chemistry, Second Edition*; Taylor & Francis, 2007.

(49) Striegel, A. M., Multiple detection in size-exclusion chromatography of macromolecules, *Anal. Chem.* **2005**, *77*, 104 A.

(50) Willenbacher, J.; Schmidt, B.; Schulze-Suenninghausen, D.; Altintas, O.; Luy, B.; Delaittre, G.; Barner-Kowollik, C., Reversible single-chain selective point folding via cyclodextrin driven host-guest chemistry in water, *Chem. Commun.* **2014**, *50*, 7056.

Appendix to Chapter 2

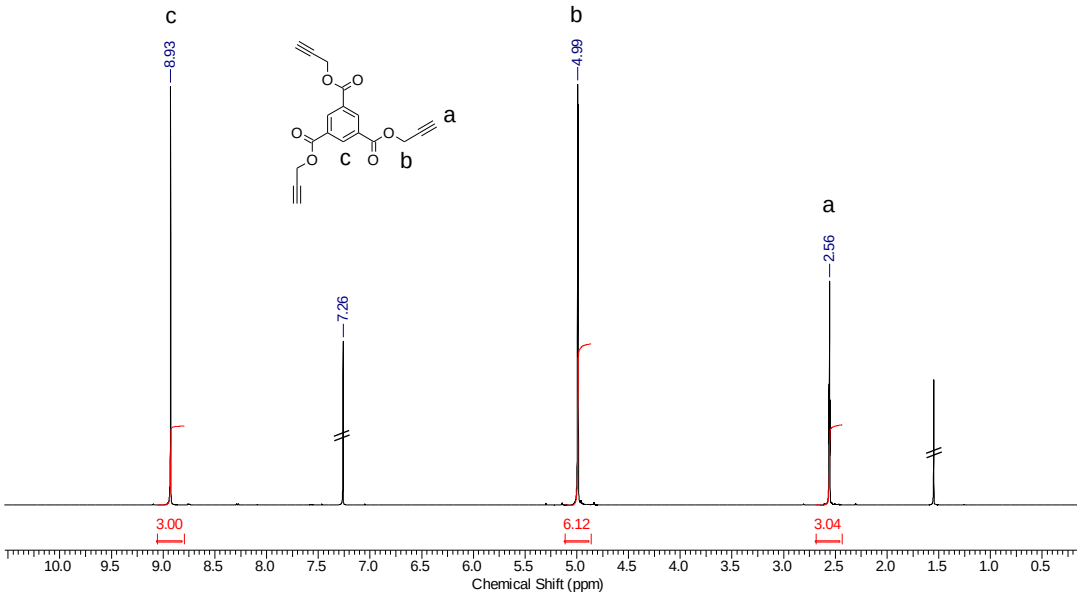

Figure A2.1. ^{1}H NMR spectrum (500 MHz, $CDCl_3$) of tri(prop-2-yn-1-yl) 1,3,5-benzenetricarboxylate (trialkyne core) synthesized by EDC/DMAP esterification.

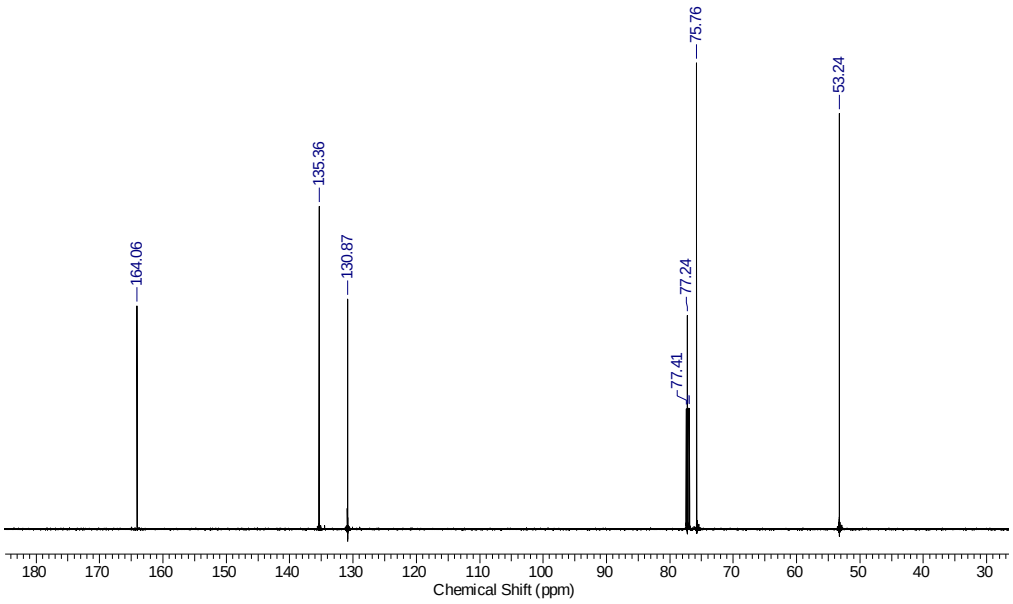

Figure A2.2. ^{13}C NMR spectrum (125 MHz, $CDCl_3$) of tri(prop-2-yn-1-yl) 1,3,5-benzenetricarboxylate (trialkyne core) synthesized by EDC/DMAP esterification.

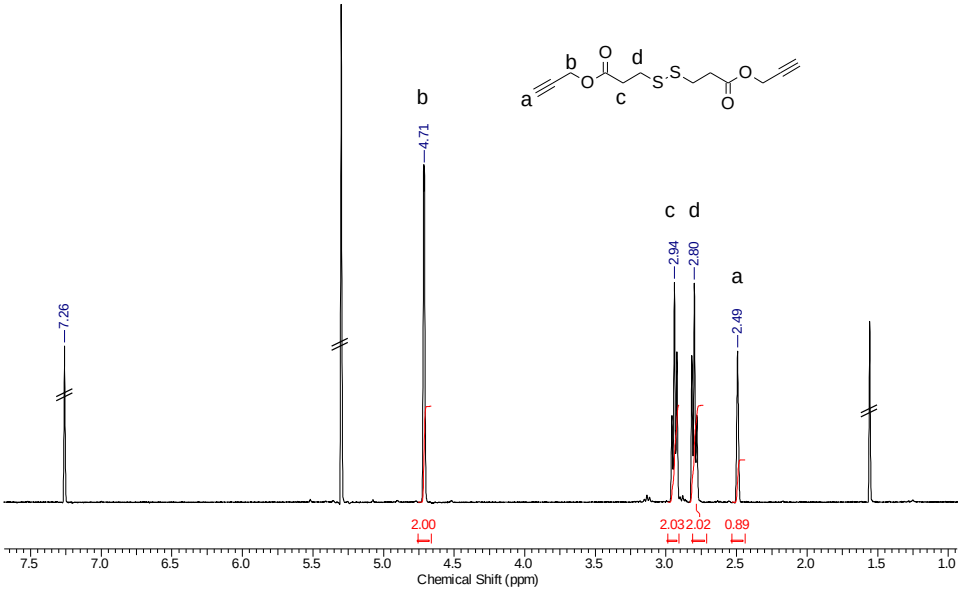

Figure A2.3. ^{1}H NMR spectrum (400 MHz, $CDCl_3$) of di(prop-2-yn-1-yl) 3,3'-disulfanediyldipropionate (protected thiol/yne monomer) synthesized by EDC/DMAP esterification.

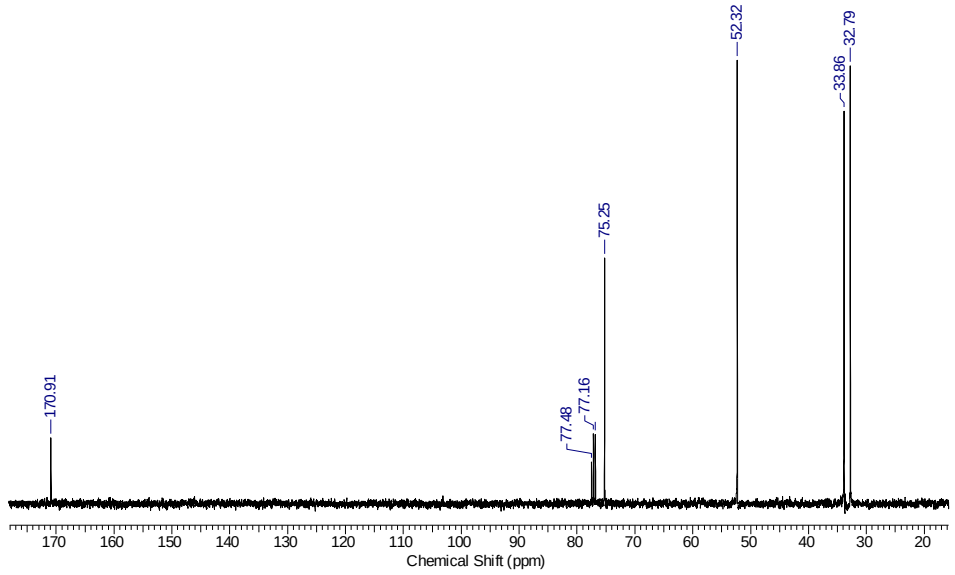

Figure A2.4. ^{13}C NMR spectrum (100 MHz, $CDCl_3$) of di(prop-2-yn-1-yl) 3,3'-disulfanediyldipropionate (protected thiol/yne monomer) synthesized by EDC/DMAP esterification.

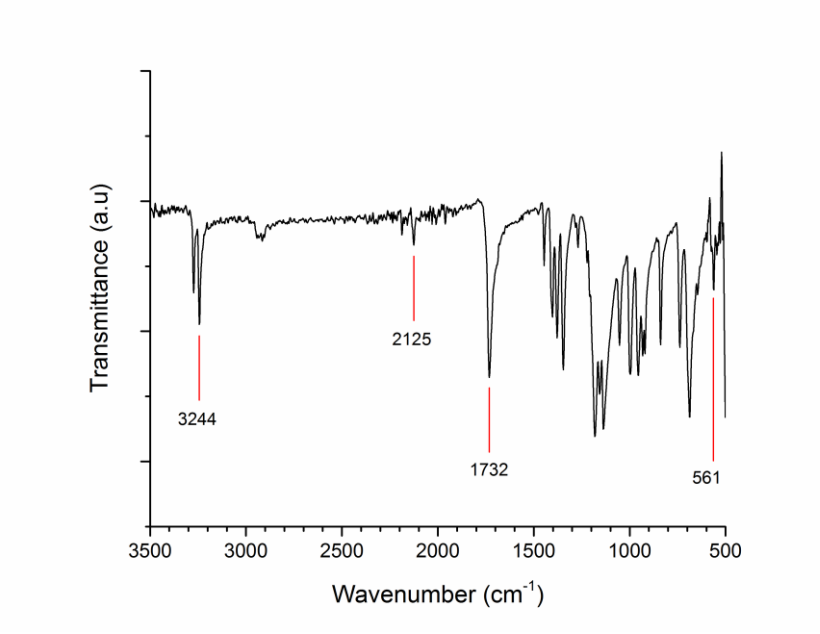

Figure A2.5. FTIR spectrum of di(prop-2-yn-1-yl) 3,3'-disulfanediyldipropionate (protected thiol/yne monomer) synthesized by EDC/DMAP esterification.

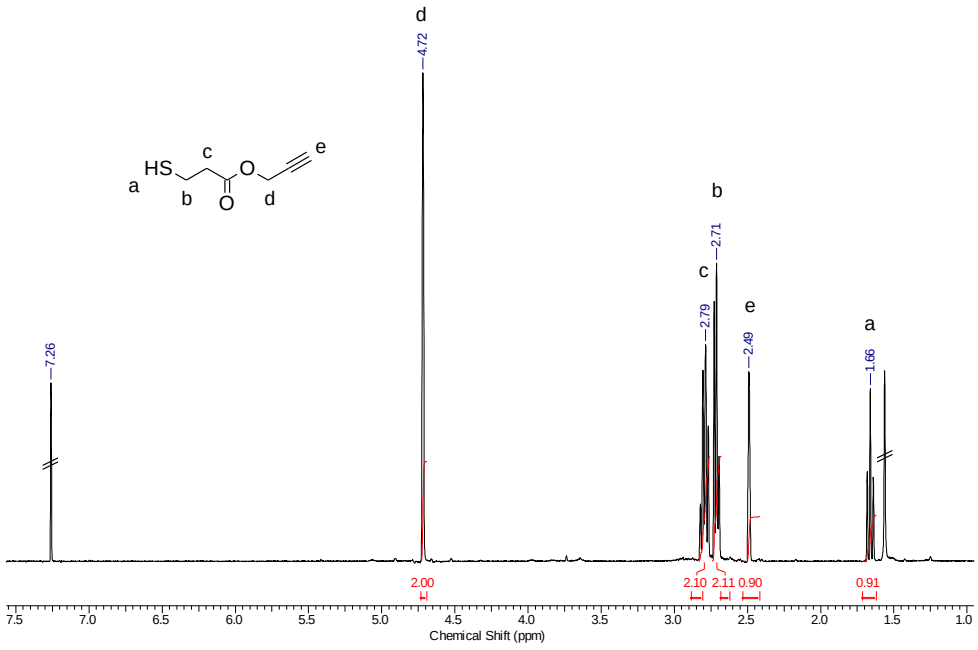

Figure A2.6. ^{1}H NMR spectrum (400 MHz, $CDCl_3$) of prop-2-yn-1-yl 3-mercaptopropanoate (deprotected monomer).

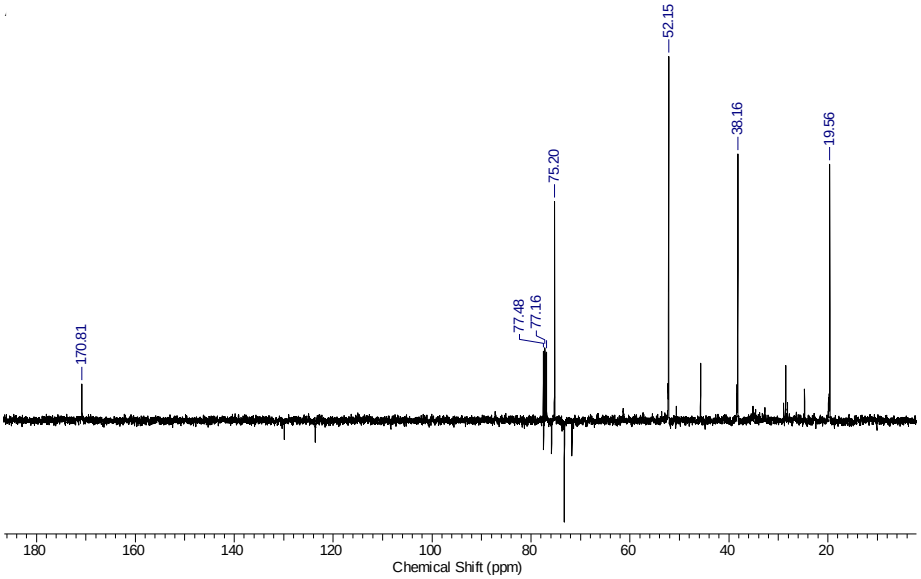

Figure A2.7. ^{13}C NMR spectrum (100 MHz, $CDCl_3$) of prop-2-yn-1-yl 3-mercaptopropanoate (deprotected monomer).

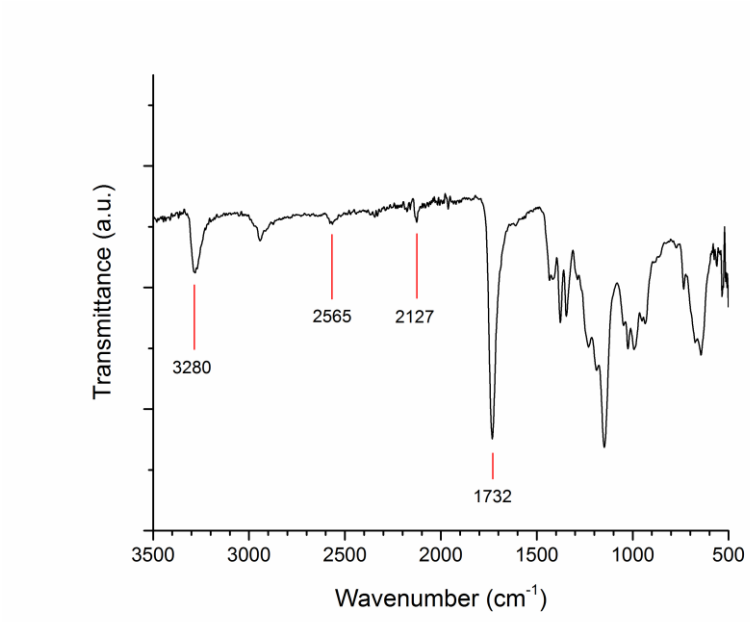

Figure A2.8. FTIR spectrum of prop-2-yn-1-yl 3-mercaptopropanoate (deprotected monomer).

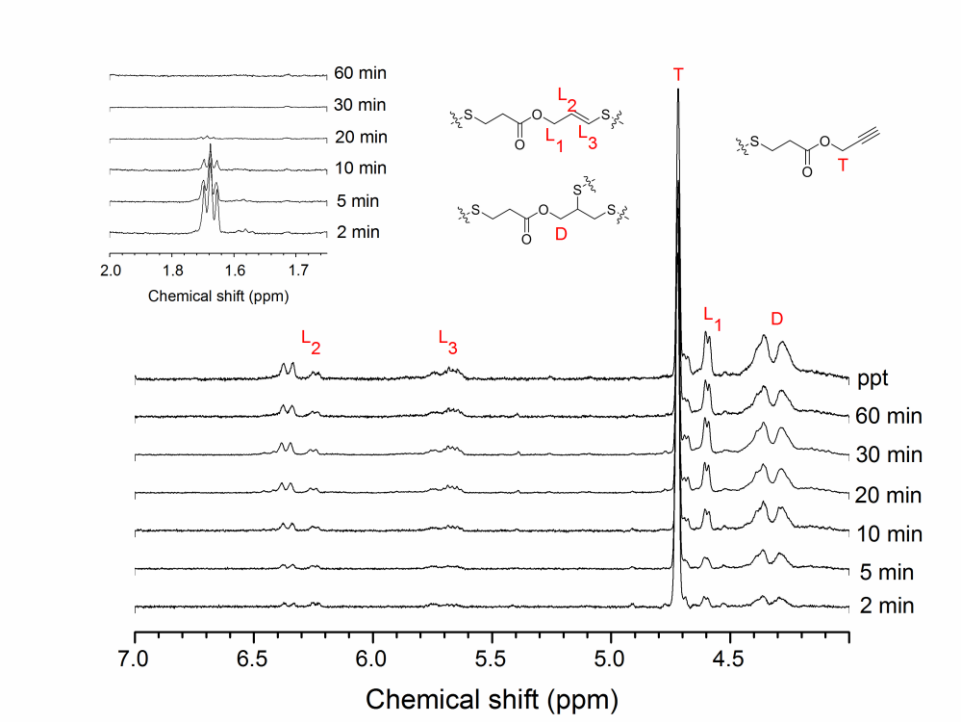

Figure A2.9. Kinetic ^{1}H NMR spectra of hyperbranched polymers by batch thiol–yne polymerization at 1.1 M. Inset shows thiol triplet from monomer as reaction proceeds.

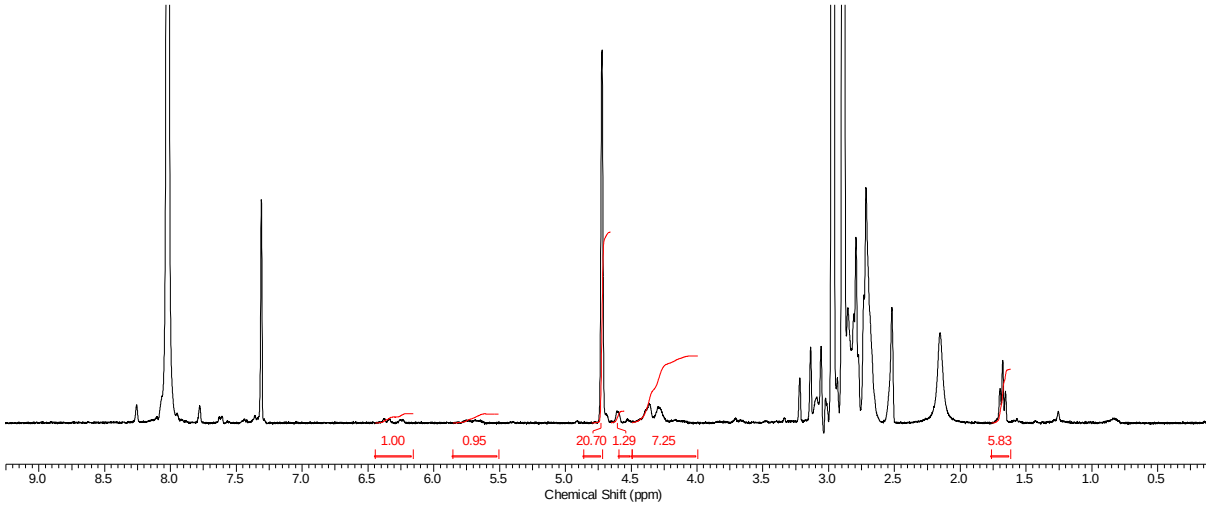

$$Conv. = \frac{Polymer}{Polymer + Monomer}$$

$$Conv. = \frac{D + T + L}{D + T + L + Monomer}$$

$$Conv. = \frac{\frac{7.25}{2} + \frac{20.70 - (5.83 \times 2)}{2} + 1}{\frac{7.25}{2} + \frac{20.70 - (5.83 \times 2)}{2} + 1 + 5.83}$$

$$Conv. = \frac{9.15}{9.51 + 5.83} = 61\%$$

Figure A2.10. Example conversion calculation of hyperbranched polymers by batch thiol–yne polymerization at 1.1 M (t = 5 min). The monomer contribution to the integral of the terminal polymer CH_2 next to the alkyne (4.7 ppm) was subtracted. Calculation is the same for polymers by slow monomer addition but accounting for proportion of monomer fed.

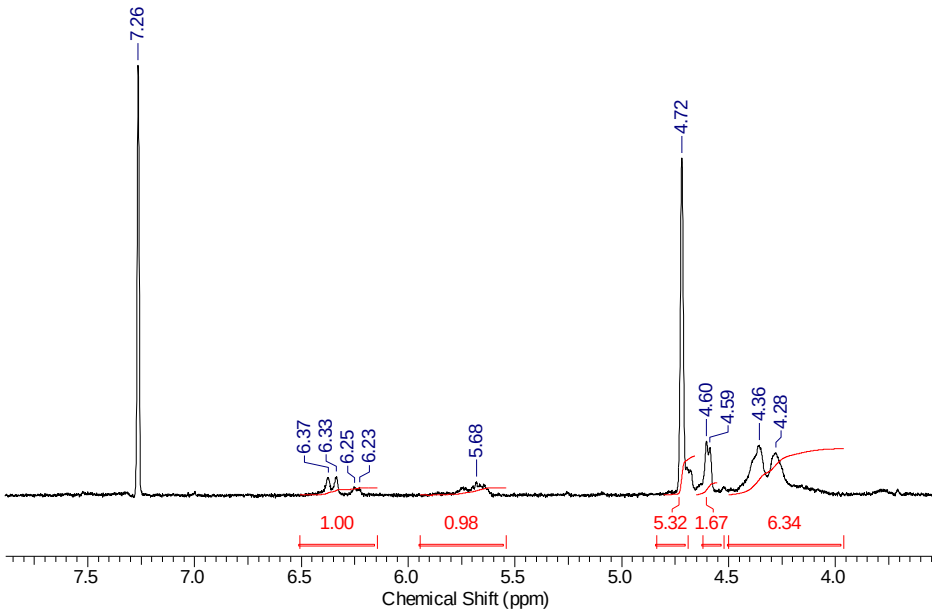

$$Degree\ of\ Branching\ (DB) = \frac{No.of\ dendritic\ units + No.of\ terminal\ units}{Total\ no.of\ units}$$

$$DB = \frac{D + T}{D + T + L}$$

$$DB = \frac{6.34/2 + 5.32/2}{6.34/2 + 5.32/2 + 1}$$

$$DB = 0.85$$

Figure A2.11. Example degree of branching calculation for hyperbranched polymer by batch thiol–yne polymerization at 1.1 M (final precipitated sample). Calculation is the same for polymers by slow monomer addition. For DB calculation of unprecipitated kinetic samples the monomer contribution to the integral of the terminal polymer CH_2 next to the alkyne (4.7 ppm) was subtracted.

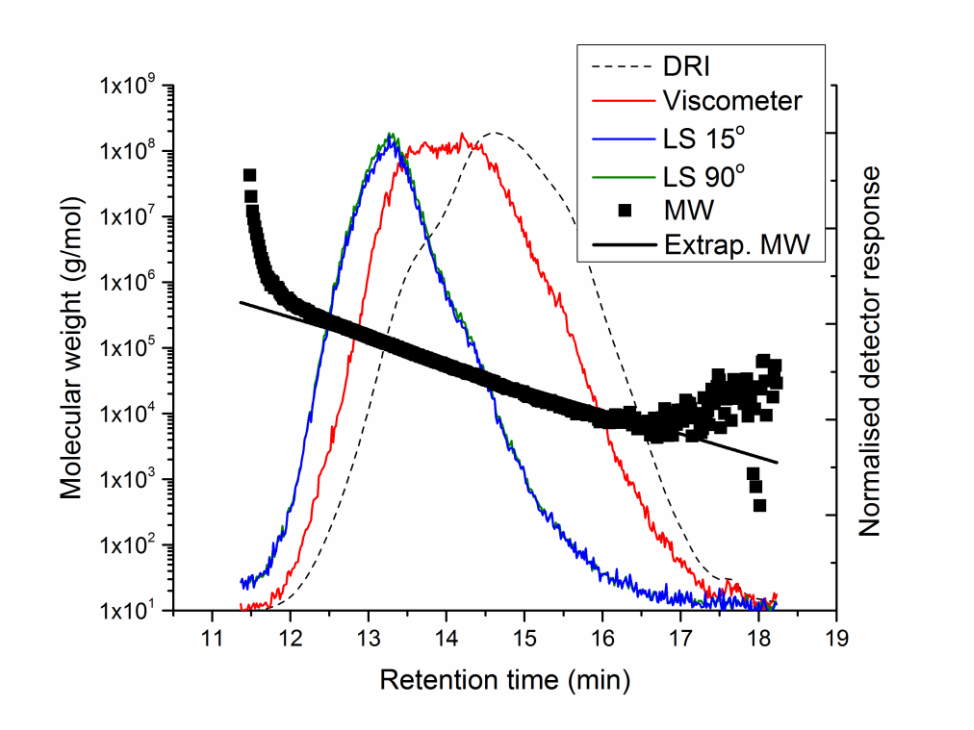

Figure A2.12. Multi-detector SEC chromatograms for hyperbranched polymer by batch thiol–yne polymerization at 1.1 M (final precipitated sample).

Table A2.1. Kinetic data for hyperbranched thiol–yne polymerization with slow monomer addition to 10 mol% alkene core at 1.1 M.

Time (min)	Monomer fed	Thiol/yne mon. conv. [a]	Core alkene conv. [b]	$M_{n,SEC}$ (g/mol) [c]	$M_{w,SEC}$ (g/mol) [c]	$Đ$ [c]	DB [d]
2	10%	60%	10%	1200	1300	1.06	0.32
10	50%	63%	37%	1600	2000	1.22	0.43
20	100%	63%	51%	2400	3500	1.43	0.84
30	-	75%	59%	2500	4200	1.68	0.92
50	-	89%	69%	2800	4900	1.74	0.88
80	-	99%	71%	3200	5900	1.88	0.86
ppt	-	-	-	6700	9300	1.38	0.82

[a] From disappearance of thiol triplet at 1.7 ppm. [b] From comparison of unreacted core alkene peak at 5.4 ppm and total core peak at 8.9 ppm. [c] From DMF SEC, with DRI detector and PMMA standard. [d] DB = degree of branching, following equation DB = (D+T)/(D+T+L).

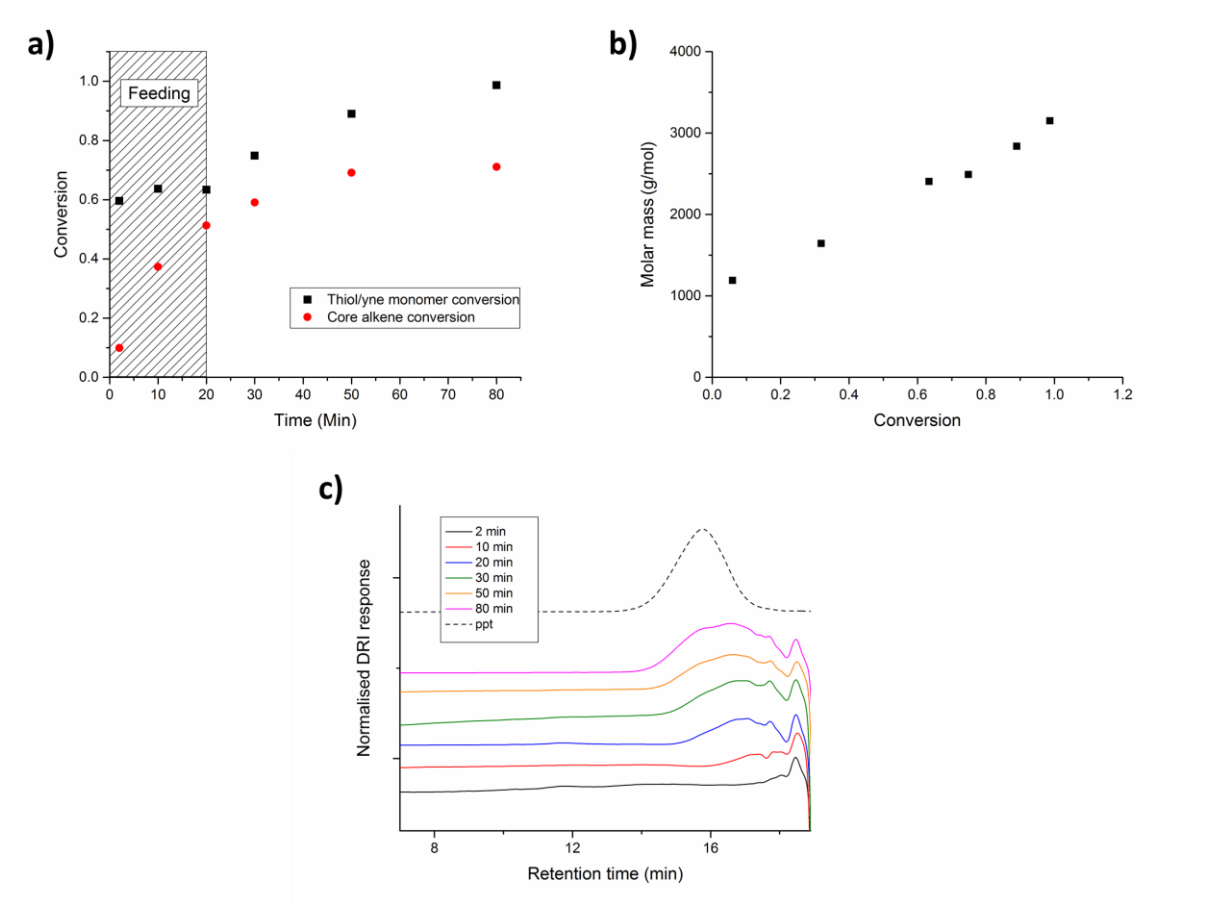

Figure A2.13. Kinetic plots for hyperbranched thiol–yne polymerization with slow monomer addition to 10 mol% alkene core at 1.1 M, **a)** Conversion of thiol-yne monomer, and alkene core as a function of time, **b)** Number average molecular weight as a function of conversion, **c)** SEC chromatograms of polymer samples at different times during the polymerization.

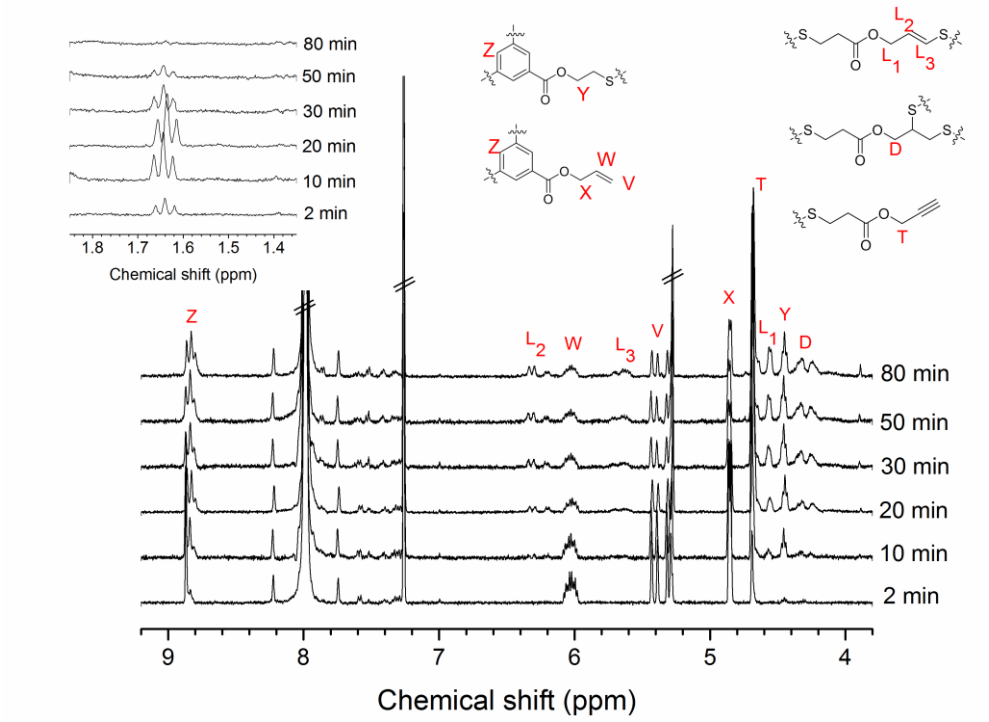

Figure A2.14. Kinetic ^{1}H NMR spectra of hyperbranched thiol–yne polymerization by slow monomer addition to 10 mol% alkene core at 1.1 M. Inset shows thiol triplet from monomer as reaction proceeds.

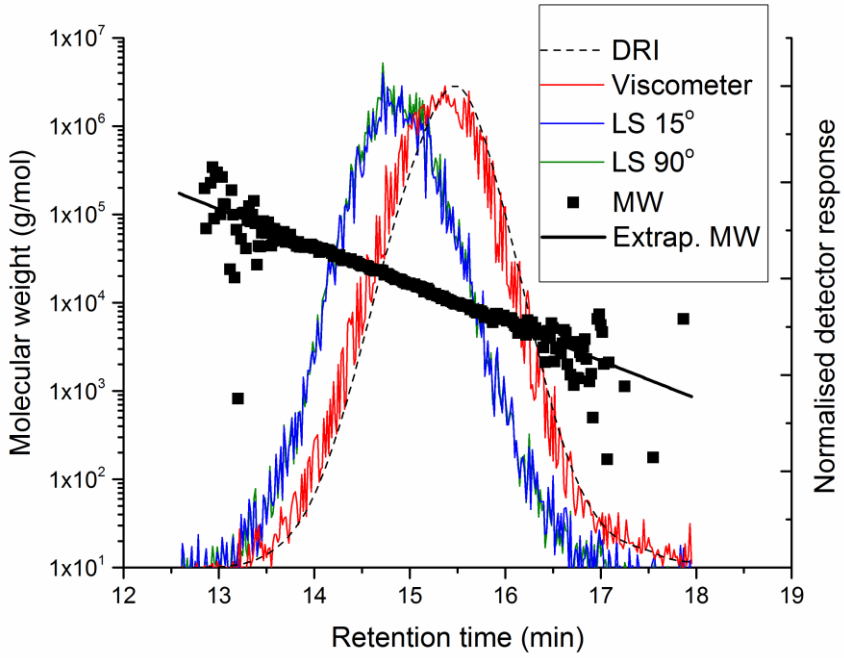

Figure A2.15. Multi-detector SEC chromatograms for thiol–yne hyperbranched polymer by slow monomer addition to 10 mol% multifunctional alkene core at 1.1 M (final precipitated sample).

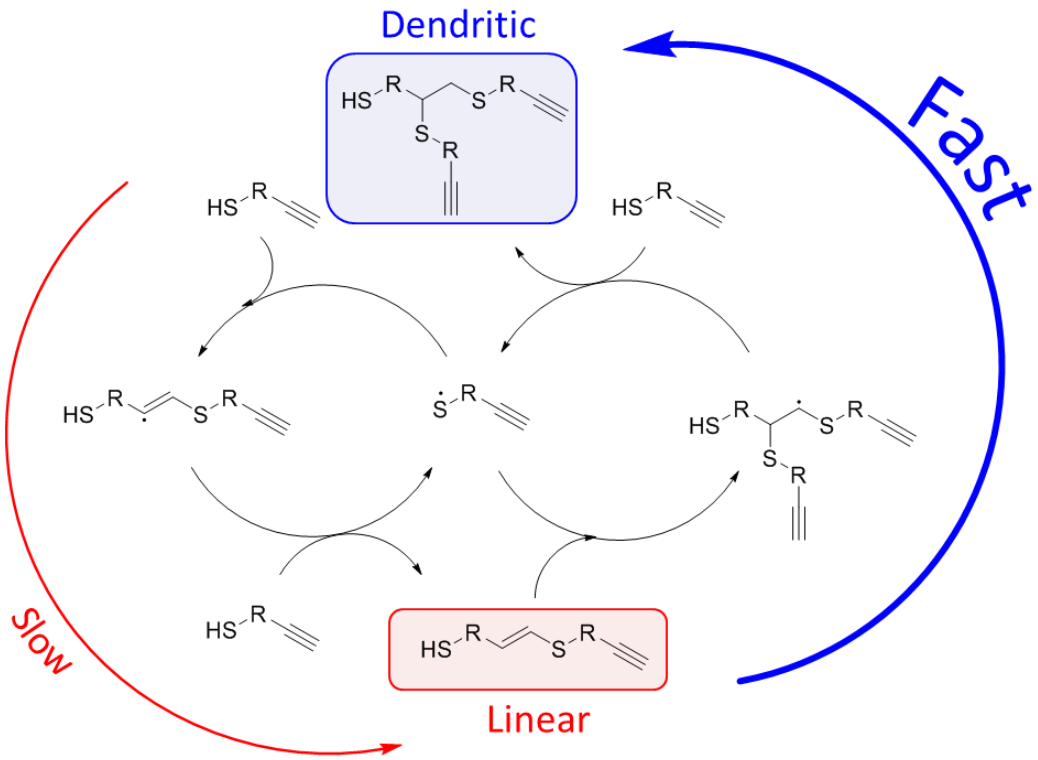

Figure A2.16. Radical mediated thiol-yne addition mechanism.

3.

Hyperbranched poly(ethylenimine-*co*-oxazoline) by thiol-yne chemistry for non-viral gene delivery: investigating the role of polymer architecture

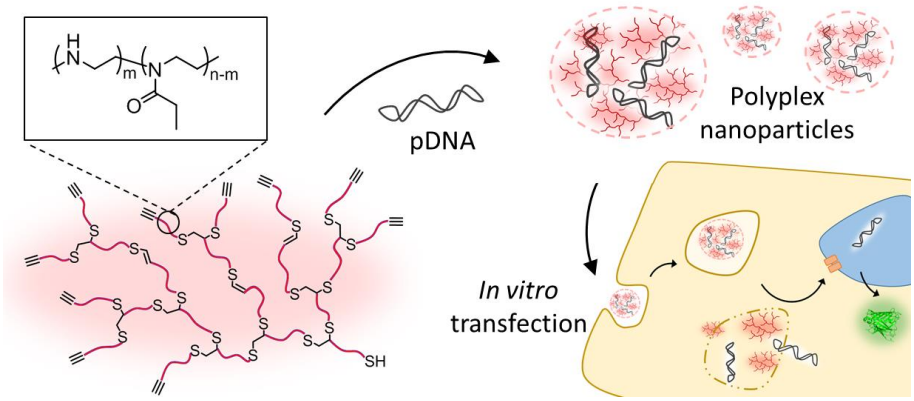

Abstract

Cationic polymers have been widely employed as gene delivery vectors to help circumvent extracellular and intracellular delivery barriers. Among them, polyethyleneimine (PEI) is the most commonly used despite its associated high cytotoxicity. PEI is typically obtained by uncontrolled ring opening polymerisation of aziridine, leading to either linear polymer architectures with only secondary amines, or branched architectures containing primary, secondary, and tertiary amines. In contrast, this chapter describes the preparation of hyperbranched poly(ethyleneimine-co-oxazoline)s that contains only secondary amines, *via* a fast thiol-yne based one pot reaction. A small library of these compounds with varying PEI contents was then used to study the effect of polymer architecture on pDNA polyplex formation, cytotoxicity, and *in vitro* transfection studies with GFP plasmid DNA reporter gene. Hyperbranched poly(ethyleneimine-*co*-oxazoline) was found to have reduced toxicity compared to the commercial standard 25K branched PEI (bPEI), with transfection efficiencies only slightly lower than its bPEI counterpart. The synthesised hyperbranched PEI copolymers represent alternatives to the long standing favourite bPEI, with similar transfection efficiencies and reduced toxicity, whilst also highlighting the importance of understanding polymer architecture in gene delivery systems.

3.1. Introduction

Gene therapy is an important and hugely promising pharmaceutical development that aims to treat diseases by delivering genes or recombinant DNA to target cells.[1,2] In the clinic, this can take the form of replacing, adding, or editing a gene that is absent or abnormal and which is responsible for a disease. This technique opens the door for treatment of a number of previously undruggable targets. The versatility of gene therapy makes it relevant for a wide variety of disease, including different type of cancers, Parkinson's disease, cystic fibrosis, macular degeneration, and muscular dystrophy among others.[3-7] In recent years, the potential impact of gene therapy has been expanded even further by the development of CRISPR/Cas9 gene editing technology.[8,9]

Since the early genetic engineering studies in the 1970s, the major hurdle associated with gene delivery lies in effectively delivering the genetic material inside target cells.[2] This is typically achieved using either viral vectors or synthetic non-viral vectors. Viral vectors, such as retroviruses, adenoviruses, or adeno-associated viruses (AAV) have the advantage of providing higher transgene expression but are typically limited by immunogenicity and safety-related issues, packaging constraints, as well as the requirement of cell mitosis.[10] Comparatively, non-viral gene delivery vectors offer access to large scale production, low host immunogenicity, easily tuneable architecture/functionality, long term storage stability, and batch to batch reproducibility of materials. Commonly used synthetic vectors include cationic polymers, liposomes, and covalent polymer conjugates. Cationic polymers such as poly-L-lysine (PLL), polyethylenimine (PEI), poly(2-(dimethylamino)ethyl methacrylate) (PDMAEMA), and polyamidoamine dendrimers (PAMAM) are promising systems for the non-viral trafficking of genetic material. Despite their popularity, high cytotoxicity associated with their polycationic nature, which tends to cause disruption of cellular membranes, remains a major limitation.[10]

The current gold-standard when referring to polymeric non-viral gene delivery systems is bPEI. Reports indicate that polymer molecular weight plays an important role in achieving optimal gene transfection.[11] However, these systems are notoriously difficult to characterise and there is still much debate about the individual influence of polymer

molecular weight and architecture on the transfection efficiency and toxicity of the resulting polyplexes.[12-15] Problems arise from difficulties in synthesising comparable polymer systems with differing architectures, without affecting several properties of the polymers at once. The importance of controlling branching in polyplex formation was demonstrated by Tang *et al.*, who showed that semi-degraded PAMAM dendrimers provide better transfection efficiency in comparison with whole PAMAM dendrimers.[16] In the case of bPEI, which is commonly prepared via uncontrolled ring-opening polymerisation of aziridine, the nature and frequency of the branching points are uncontrolled and highly dependent on the reaction conditions. In addition, the resulting polymer consists of a mixture of primary, secondary, and tertiary amines, whose pK_a values, and hence ability to interact with genetic material or membranes differ significantly.[17]

An alternative route to preparing PEI uses cationic ring-opening-polymerisation of oxazolines, followed by a hydrolysis step. The method allows preparation of polymers containing only secondary amines, with a defined molecular weight and well-controlled molecular weight distribution. This approach was used by Wightman *et al.* to demonstrate that branched and linear PEI differed in their ability to transfect cells, both *in vitro* and *in vivo*.[15] In 2015, the Grayson group prepared cyclic PEI and the exact linear equivalent and studied the effect of cyclic architecture on transfection efficiency and cytotoxicity.[18]

Over the past few years, our group has developed thiol-yne chemistry as a strategy to synthesise hyperbranched polymers with remarkably high degrees of branching and tuneable functionality.[19-22] Hyperbranched polymers from AB_2 monomers have received increasing interest due to a number of unique features including globular three dimensional conformations and high number of surface functionalities. The thiol-yne chemistry allows fast one pot synthesis of hyperbranched polymers with degrees of branching similar to that of perfectly branched dendrimers. Such control over the branching process is attributed to the reactive nature of pi bonds to thiyl radical additions. Recently, the Schubert group has reported the synthesis of poly(ethylenimine-*co*-oxazoline) copolymers and their application as gene delivery vectors.[23,24] The copolymers show reduced toxicity as compared to linear PEI homopolymers and incorporation of

'stealth' properties including reduced non-specific interactions with serum and other biological compounds.[25] However, the lack of access to more complex architectures, such as branched structures, has so far limited the potential application of these copolymers.

This chapter describes the combination of thiol-yne chemistry with well-defined poly(ethylenimine-*co*-oxazoline) copolymers, which allows synthesis of hyperbranched PEI containing only secondary amines for the first time. The study then moves onto a systematic study of this novel polymer architecture, including comparison with a precise linear equivalent, as well as comparison with commercially available bPEI. The polymers were then evaluated for their performance as non-viral gene delivery vectors. Results include plasmid DNA complexation ability, polyplex morphology, buffering capacity, polymer cytotoxicity, and gene transfection efficiency *in vitro* using green fluorescent protein encoding reporter plasmid.

3.2. Results and Discussion

3.2.1. Hyperbranched poly(ethylenimine-*co*-oxazoline) copolymers

The thiol-yne macromonomer used for the formation of hyperbranched poly(2-ethyl-2-oxazoline) (PEtOx) was prepared following a two-step process (**Scheme 3.1**). Firstly, cationic ring opening polymerisation (CROP) was employed to polymerise 2-ethyl-2-oxazoline (EtOx) in acetonitrile at 80 °C, using propargyl tosylate as an initiator and potassium ethyl xanthate as nucleophilic end-capping agent. This afforded separate functionalities at both ends of the polymer chains, an alkyne functional α-chain end and a protected thiol functional ω-chain end, whilst maintaining well-defined molecular weights and low dispersity values. To ensure a high end group fidelity, a degree of polymerisation (DP) of 10 was targeted for the PEtOx precursor.

From the ^{1}H NMR spectrum of the polymerisation mixture, a DP of 8 was determined by comparing the aromatic signals of the propargyl group with the signal of the polymer backbone (**Figure A3.1**). This value compares well with the value obtained by SEC (M_n = 1200 g/mol, $Đ$ = 1.19). After purification, ^{1}H-NMR spectroscopy was used to

determine the degree of functionalisation for both end groups. In both cases the degree of functionalisation was found to be higher than 95%, as expected when using a cationic polymerisation technique. In order to generate the thiol end group on the PEtOx chains, aminolysis of the xanthate group was carried out in the presence of dimethylamine. ^{1}H-NMR spectroscopy shows the complete disappearance of the peaks associated with the xanthate group. The presence of the thiol end group was confirmed using electrospray ionisation mass spectrometry (ESI-MS) of the macromonomer, which showed a single distribution corresponding to PEtOx with alkyne and thiol chain-ends (**Figure 3.1a**).

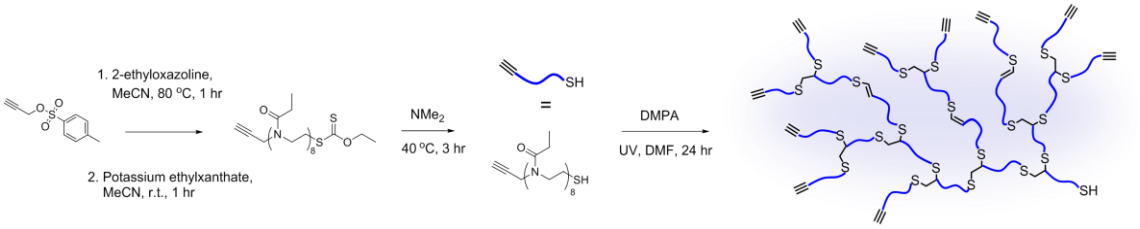

Scheme 3.3. Preparation of AB_2 poly(2-ethyl-2-oxazoline) thiol-yne macromonomer and subsequent batch photopolymerisation to from hyperbranched poly(2-ethyl-2-oxazoline).

Telechelic thiol-yne PEtOx macromonomers were then polymerised following a procedure depicted in **Scheme 3.1**. The polymerisation proceeded under UV light irradiation using 0.5 equivalents of photoinitiator DMPA per macromonomer chain, the mechanism of the radical mediated thiol-yne addition can be seen in the previous chapter. A macromonomer concentration of 0.3 M in DMF was chosen according to an initial polymerisation optimisation study (**Figure A3.5**). The inherent reactivity of pi bonds to thiyl radicals, which proceeds *via* a two-step mechanism, is expected to result in very high degrees of branching in the final compounds. Bowman *et al.* showed that the second addition of a thiyl radical to a vinylthioether species proceeds much faster that the first addition of a thiyl radical to an alkyne.[26] Therefore, most thiol-yne photo-additions proceed to the fully branched dendritic species. It is worth noting that the thioether units in both the polymers in this chapter, and the previous, could play a role in the final properties of the polymer, including possible sensitivity to oxidation.

The formation of hyperbranched PEtOx was followed *via* SEC, as shown in **Figure 3.1b**. Upon UV irradiation, the chromatogram peak associated with the macromonomer decreases while the DRI trace shifts to shorter retention times and thus higher molecular weights. In addition, a broadening of the chromatograms with increasing reaction time, due to the step growth nature of the thiol-yne polymerisation, was detected. Values for molecular weight and dispersity of the polymerisation kinetic study are summarised in **Table A3.1**. The M_n values reported correspond to SEC measurements compared to linear polymer calibration standards, which is expected to significantly underestimate the value as hyperbranched polymers have smaller hydrodynamic radii than their equivalent linear polymers. **Figure 3.1c** shows the Kuhn-Mark-Houwink-Sakurada plots of intrinsic viscosity against molecular weight for both the macromonomer and the final hyperbranched PEtOx after purification. The degree of branching, as described by Hawker,[27] can be calculated from the integral of the linear units in the ^{1}H NMR spectra which can be identified at around 6-6.5 ppm (**Figure 3.1d** and **A3.6**).

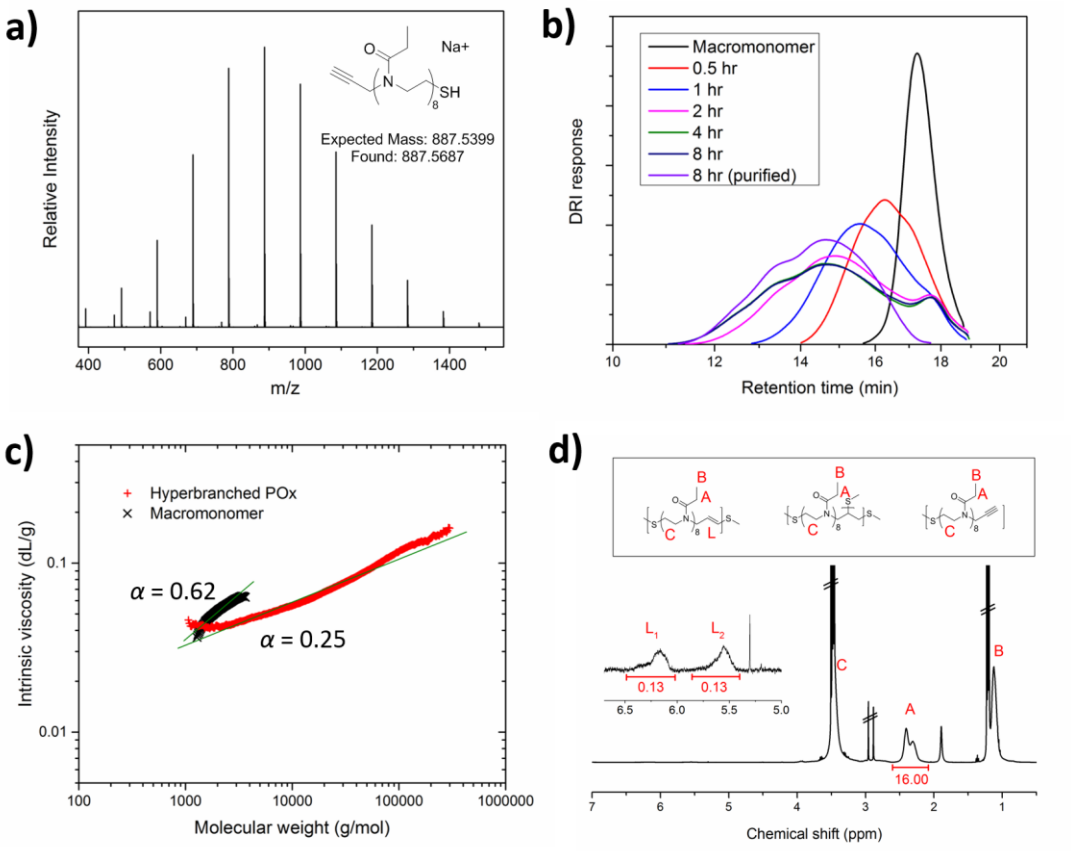

Figure 3.5. a) Size-exclusion chromatograms (normalised DRI detector response vs retention time) of the photopolymerisation of PEtOx thiol-yne macromonomer following various irradiation time; **b)** ESI mass spectra of telechelic PEtOx thiol-yne macromonomer; **c)** Kuhn-Mark-Houwink-Sakurada (KMHS) plots of log intrinsic viscosity against log molecular weight from SEC viscosity detector in DMF eluent of PEtOx thiol-yne macromonomer and hyperbranched PEtOx; **d)** ^{1}H NMR spectrum of hyperbranched PEtOx showing peak assignments, inset showing zoomed view of vinyl region.

Table 3.4. Polymer compositions, molecular weights, dispersity, and hydrodynamic radius values for both linear PEtOx and hyperbranched thiol–yne polymers prepared by photopolymerisation of PEtOx thiol-yne macromonomers.

	Sample	% PEI [a]	% PEtOx [a]	$M_{n\ NMR}$ (g/mol) [a]	$M_{n\ GPC}$ (g/mol) [b]	$Đ$ [b]	$M_{w\ SLS}$ (g/mol) [c]
	PEtOx macromonomer	0	100	800	1,200	1.19	-
	Hyperbranched PEtOx	0	100	17,100	14,000	1.5	20,400
HB 32%	Hyperbranched $P(EI_{0.32}$-*co*-$EtOx_{0.68})$	32	68	14,100	-	-	21,900
HB 58%	Hyperbranched $P(EI_{0.58}$-*co*-$EtOx_{0.42})$	58	42	12,500	-	-	65,300
HB 76%	Hyperbranched $P(EI_{0.76}$-*co*-$EtOx_{0.24})$	76	24	10,900	-	-	106,200
	Linear PEtOx	0	100	15,800	13,700	1.25	19,100
L 81%	Linear $P(EI_{0.81}$-*co*-$EtOx_{0.19})$	81	19	9,200	-	-	12,400

[a] Determined by ^{1}H NMR spectroscopy. [b] From DMF SEC with DRI detector and PMMA standard. [c] From SLS in water (further SLS details in Supplementary Info).

To create polymers able to interact with genetic material, cationic charges have to be introduced into the structure. In the present case, this is done using partial hydrolysis of the repeating unit of PEtOx, creating poly(ethylenimine) units along the polymer backbone. Hydrolysis of hyperbranched PEtOx was carried out in 1M aqueous solution of HCl at 120 °C. Microwave irradiation was chosen as the heating method of choice as it allows for increased pressure, thus reducing reaction times.[28] These hydrolysis conditions allow control over the rate and degree of hydrolysis. A kinetic study, in which the hydrolysis is determined from analysing the increase of the integral of the hydrolysed propionic acid small molecule over time in ^{1}H-NMR spectra, was undertaken with both hyperbranched PEtOx and linear PEtOx (**Figure A3.8**). Interestingly, the branched structure does not appear to affect the hydrolysis rate of the EtOx side chains. Using this method, three hyperbranched poly(ethylenimine-*co*-oxazoline) copolymers were produced. The final composition of the three hyperbranched copolymers was calculated

from the integrals of CH_2 groups from the polyethylenimine backbone and the CH_2 groups from the polyoxazoline backbone, between 2.5 ppm and 3.5 ppm (**Figure 3.2b**).

Copolymers were analysed by SEC (**Table 3.1**). Resulting chromatograms show a monomodal size distribution for all polymers (**Figure A3.9**) with varying values for M_n. SEC characterisation of highly charged polymers is often complicated by non-size exclusion interferences, such as intramolecular electrostatic interactions, column adsorption, or ion exchange effects, which are known to cause increased retention times and poor chromatographic peak shape, resulting in large errors in molecular weight estimation.[29-31] Therefore, static light scattering was employed to further investigate the molecular weight of the synthesized poly(ethylenimine-*co*-oxazoline) copolymers, as well as poly(2-ethyl-2-oxazoline) precursor materials. SLS is generally a good complementary method of molecular weight determination for hyperbranched polymers as it does not rely on calibration. However, the molecular weights obtained from SLS measurement show an unexpected increase with increasing degree of hydrolysis. This can be attributed to the presence of a combination of closely-spaced protonated amines and a hydrophobic backbone, which can lead to solution polyelectrolyte states that shift between aggregated and free forms.[32] For comparison, a linear polymer control of equivalent molecular weight was synthesised by CROP of EtOx ($M_{n,SEC}$ 14,000 g/mol, $Đ$ 1.25). The linear control was hydrolysed using the previously described methodology to yield poly(ethylenimine-*co*-oxazoline) with a degree of hydrolysis similar to that of the hyperbranched copolymer with the highest PEI content.

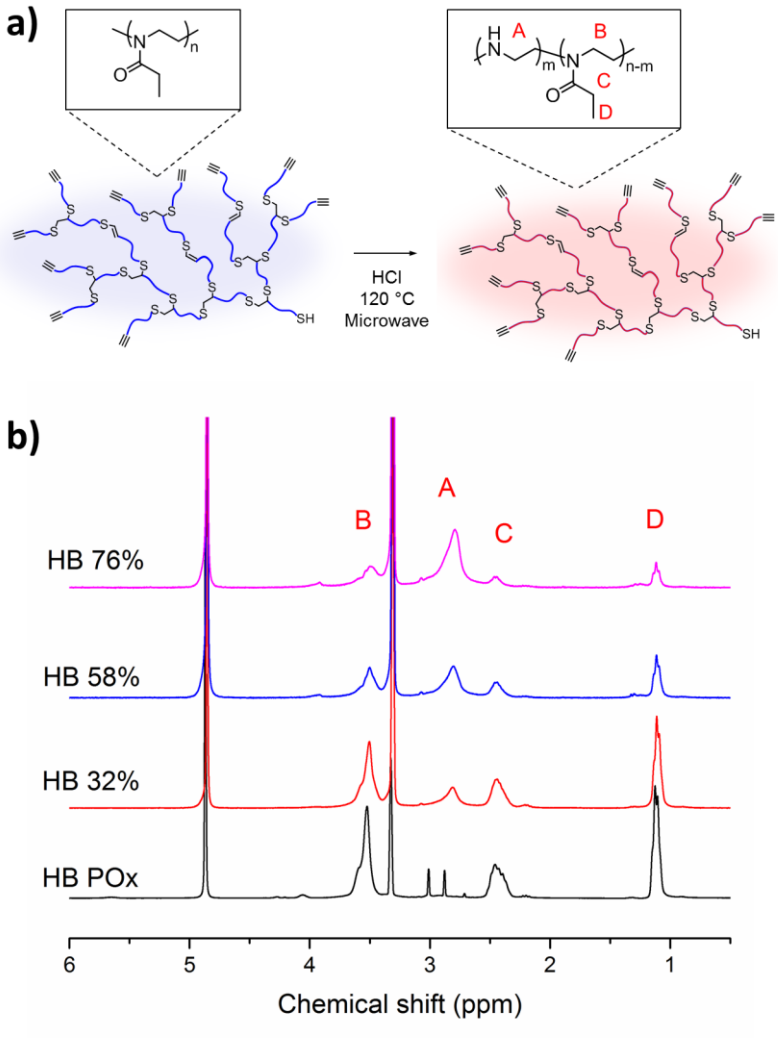

Figure 3.2. a) Schematic representation of the acid-catalysed hydrolysis of hyperbranched poly(2-ethyl-2-oxazoline) polymer into hyperbranched poly(ethylenimine-co-oxazoline) copolymers; **b)** ^{1}H NMR spectra of final hyperbranched poly(ethylenimine-co-oxazoline) copolymers, showing peaks used for calculation of the composition.

3.2.2. Effect of type of amine and branching on polymer buffering capacity

Successful gene expression in target cells requires escape of polyplexes from the endosomal/lysosomal pathway after cell internalisation.[33] For PEI polyplexes, this is assumed to occur *via* the 'proton sponge' effect, although this still receives considerable debate.[34-36] In brief, the abundance of amines groups in PEI results in a high buffering

capacity of the polymers, which is thought to cause an increase in lysosomal pH as protons are pumped into the lysosome from the cytosol. A combination of PEI swelling due to electrostatic repulsion of protonated amine groups, and osmotic pressure change in the vesicles is expected to cause interruption and rupture of the lysosomal membrane, releasing the polyplex into the cytosol. In the present study, for the first time hyperbranched PEI structures containing only secondary amines are used, allowing observation of the influence of architecture on the performance of the polymers isolated from the nature of the amines. To evaluate the buffering effect of hyperbranched poly(ethylenimine-*co*-oxazoline) and compare it to that of PEI, pH titrations were carried out by addition of NaOH solution into solutions of the acidified polymers. The titration of bPEI shows a very broad change in pH transition (between 0.2 - 1 mmol/dm^3 of NaOH added), which is expected from a polymer containing amine groups with the three different pK_a values. In contrast, ethylenimine oxazoline copolymers showed a sharper titration curve, with a pH transition occurring between 0.3 – 0.5 mmol/dm^3 of NaOH added, which can be attributed to the presence of secondary amine groups only. Most importantly, the negligible difference between the titration curves of linear and hyperbranched PEI structures shows that, indeed the polymer architecture has only a low influence on the overall pK_a values,which makes the presented polymers an ideal platform to study the impact of polymer architecture on transfection. These results support the hypothesis that hyperbranched poly(ethylenimine-*co*-oxazoline) could be an interesting candidate for non-viral gene delivery applications as it shows characteristics of linear PEI but with an globular hyperbranched polymer architecture.

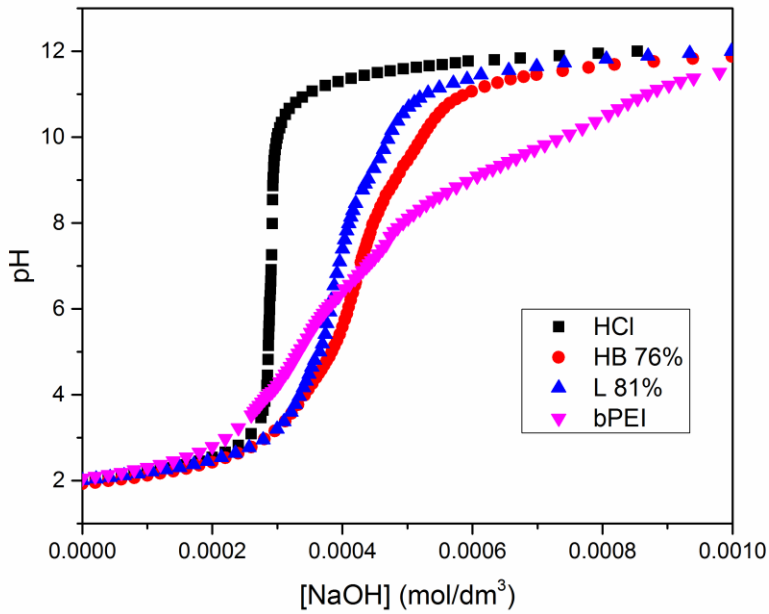

Figure 3.3. pH titration experiments for hyperbranched poly(ethyleneimine-co-oxazoline) copolymer (76% hydrolysed), linear equivalent (81% hydrolysed) as well as commercial branched PEI. A control of NaOH titration into HCl acid is shown for reference.

3.2.3. Polymer-pDNA complexation and resulting particle morphology

The ability of hyperbranched and linear poly(ethylenimine-*co*-oxazoline) to bind GFP plasmid DNA was first assessed using agaraose gel electrophoresis. Polymers were complexed with pDNA at varying N/P ratios (ratio of positively charged nitrogen groups on polymer to negatively charged phosphate groups on DNA). Images of the resulting agarose gels are shown in **Figure 3.4a**. As expected, hyperbranched poly(ethylenimine-*co*-oxazoline) with a degree of hydrolysis of 32% shows moderate ability to bind nucleic acids, with free pDNA still detectable at N/P ratio as high as 20. With a degree of hydrolysis of 58%, the polymer is able to fully complex pDNA at an N/P ratio of 10 to 20. Hyperbranched poly(ethylenimine-*co*-oxazoline) with a degree of hydrolysis of 76%, its linear equivalent, and the commercial bPEI all show formation of polyplexes and full binding of free pDNA at an N/P ratio of 5 to 10.

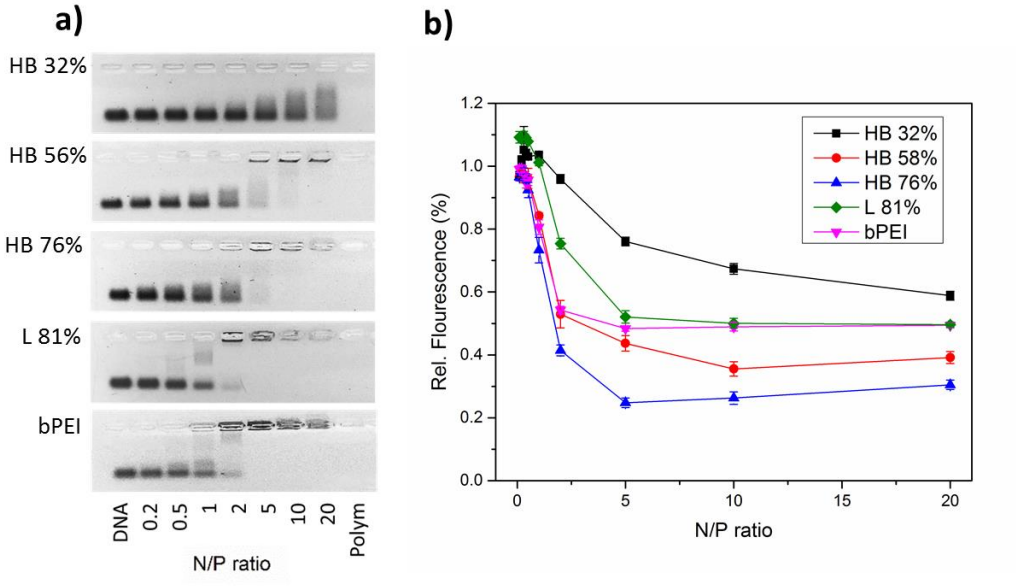

Figure 3.4. a) Polyplex formation with pDNA, as characterised by agarose gel electrophoresis using the various PEI polymers; **b)** Ethidium bromide displacement assay, as a complimentary technique to characterise polymer ability to complex pDNA.

A complimentary method to characterise DNA/RNA binding relies on competitive displacement of ethidium bromide, bound to DNA, by cationic polymers. A reduced fluorescence is observed when ethidium bromide is excluded from binding sites located in the groove of the oligonucleotides, due to addition of polymer.[37] The results, shown in **Figure 3.4B**, show a decrease in fluorescence intensity with increasing N/P ratio, typical of polyplex formation. A number of trends can be observed in this data: (i) For hyperbranched poly(ethylenimine-*co*-oxazoline), pDNA binding ability increases with increasing amine content from 32% to 58% and to 76%, which is in agreement with the results of the gel electrophoresis, (ii) linear poly(ethylenimine-*co*-oxazoline) binds to pDNA less strongly than the equivalent hyperbranched polymer, (iii) hyperbranched poly(ethylenimine-*co*-oxazoline) 76% binds more strongly than bPEI.

In addition, the presence of a plateau of residual fluorescence indicates the presence of remaining intercalated ethidium bromide which cannot be displaced. This is especially apparent in the case of hyperbranched p($EI_{0.32}$-*co*-$EtOx_{0.68}$), linear p($EI_{0.81}$-*co*-$EtOx_{0.19}$), and commercial bPEI. This phenomenon is due to the polymers forming complexes in

which fewer amines are available to interact with pDNA, and displace ethidium bromide. In the case of the linear polymer, its extended conformation is expected to result in looser and larger complexes. In the case of bPEI, the presence of tertiary amines which are not protonated at pH ~7, is expected to weaken the complexation of pDNA. This result highlights the importance of precise understanding polymer and pDNA interactions, and prompt a more thorough characterisation of the polyplex formed.

Table 3.5. Size and surface charge (zetapotential) of polyplexes formed with pDNA at both N/P = 20 and N/P = 40, as determined by dynamic light scattering and electrophoretic light scattering.

	N/P ratio	Z-average size (d.nm)	PDI	Zetapotential (mV)
HB 32%	20	499.6	0.18	5.4 ±0.421
	40	419.7	0.14	7.3 ±0.572
HB 58%	20	64.6	0.27	22.3 ±1.75
	40	72.3	0.36	24.3 ±1.91
HB 76%	20	53.6	0.36	24.4 ±1.91
	40	71.9	0.41	25.5 ±2.00
bPEI	20	82.3	0.51	39.7 ±3.11
	40	85.6	0.54	39.4 ±3.09
L 81%	20	246.7	0.36	45.9 ±3.60
	40	514.3	0.51	45.6 ±3.78

To further investigate the influence of polymer architecture on pDNA binding, polyplex physical characteristics were determined using dynamic light scattering and zetapotential measurements, to elucidate size and surface charge properties. Previous studies indicate that efficient cellular uptake occur for particles typically between 50 to 200 nm in size. Excess positive charge was also demonstrated to enhance cellular uptake.[38] **Table 3.2** shows the size and surface charge of the various polyplexes formed. For hyperbranched poly(ethylenimine-*co*-oxazoline), diameters follow a trend similar to the ethidium bromide assay, with size of the particles decreasing as the amine content increases from 32% to 58% and to 76%. Linear poly(ethylenimine-*co*-oxazoline) polyplexes appear to

form slightly larger particles, which can be attributed to the weaker DNA binding strength of the polymer when compared to the hyperbranched equivalent, as well as potential intermolecular crosslinking of DNA molecules with the extended linear polymer.

AFM imaging of polymer pDNA complexes was carried out to complement the size measurements obtained using DLS. Uncomplexed plasmid DNA deposited on a mica surface is distributed in a network type of structure (**Figure 3.5**). This is consistent with previous reports of uncondensed DNA morphologies in the literature.[39,40] In samples where the pDNA was previously mixed with hyperbranched p($EI_{0.76}$-*co*-$EtOx_{0.24}$), polyplexes with a size of approximately 100 nm were observed. A similar structure was obtained using the commercial branched PEI. Similarly to DLS data, polyplexes formed with linear p($EI_{0.81}$-*co*-$EtOx_{0.19}$) showed a size of approximately 200 nm instead. Height profiles available in the appendix. Furthermore, branched PEI and small cyclic polycations have previously been reported to more effectively condense DNA.[17,41] For example, Li *et al.* found that linear polycations/DNA complexes form larger aggregates than the cyclic polymer equivalent, which was attributed to the stretched conformation being able to intermolecularly crosslink DNA molecules.[42] Taken together, these data demonstrate the fundamental influence of polymer architecture on DNA complexation and polyplexes formation.

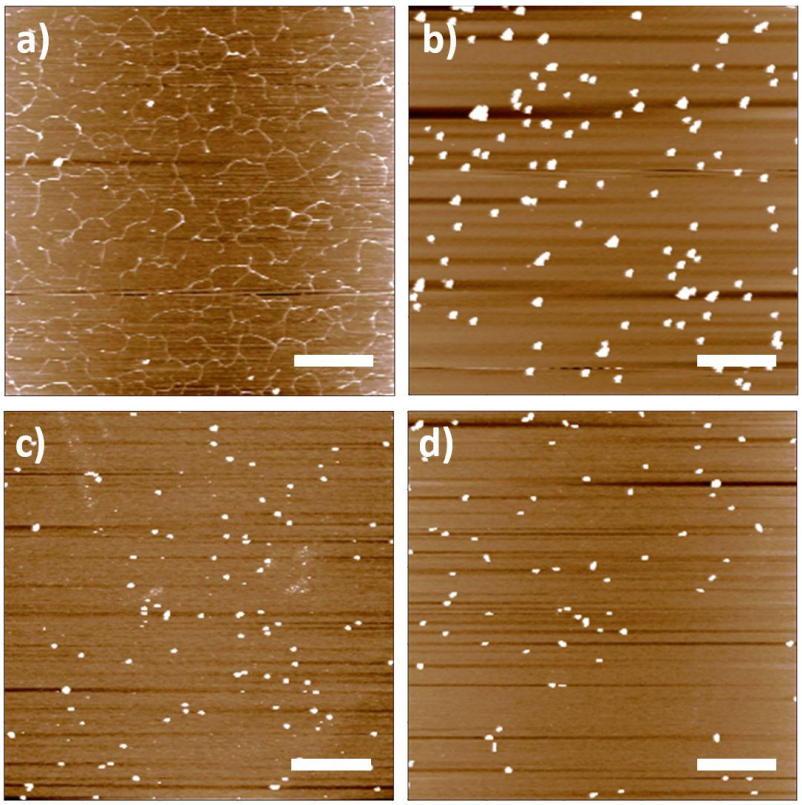

Figure 3.5. AFM images of polyplex morphology at N/P20, **a)** pDNA only, **b)** L 81% polyplex, **c)** HB 76% polyplex, **d)** bPEI polyplex. Each scan represents an area of 10 µm by 10 µm. Scale bars all 2 µm.

3.2.4. Effect of polymer architecture on toxicity and pDNA transfection *in vitro*

A common limitation of cationic polymers is their ability to permeabilise phospholipid cellular membranes.[43,44] Here, toxicity of the polymers was assessed using the XTT assay on human embryo kidney cells HEK293T as model (**Figure 3.6a**). Viability studies confirmed that commercial bPEI is toxic at concentrations as low as 0.2 mg/mL. In contrast, cells treated with poly(ethylenimine-*co*-oxazoline) polymers were found to have viability of over 80 % at concentration up to 0.8 mg/mL, which is far above the relevant concentrations used both *in vitro* and *in vivo*.[45] At higher polymer concentrations (>2 mg/mL), hyperbranched p($EI_{0.76}$-*co*-$EtOx_{0.24}$) becomes slightly toxic, whereas the linear equivalent polymer causes complete cell death at the same concentration. The reduced

toxicity of the hyperbranched architecture compared to the linear architecture follows similar observations made for branched/linear polymers of alternative monomers.[46,47] This can be attributed to differences in the 3D structure and flexibility of the polymers, resulting in different interaction of the polymers with the cell surface. It was previously shown that rigid polymers interact with lipid membranes with more difficulty than flexible equivalents.[48] Thus, it appears reasonable that the less flexible hyperbranched poly(ethylenimine-*co*-oxazoline) show decreased toxicity as compared to its flexible linear equivalent.

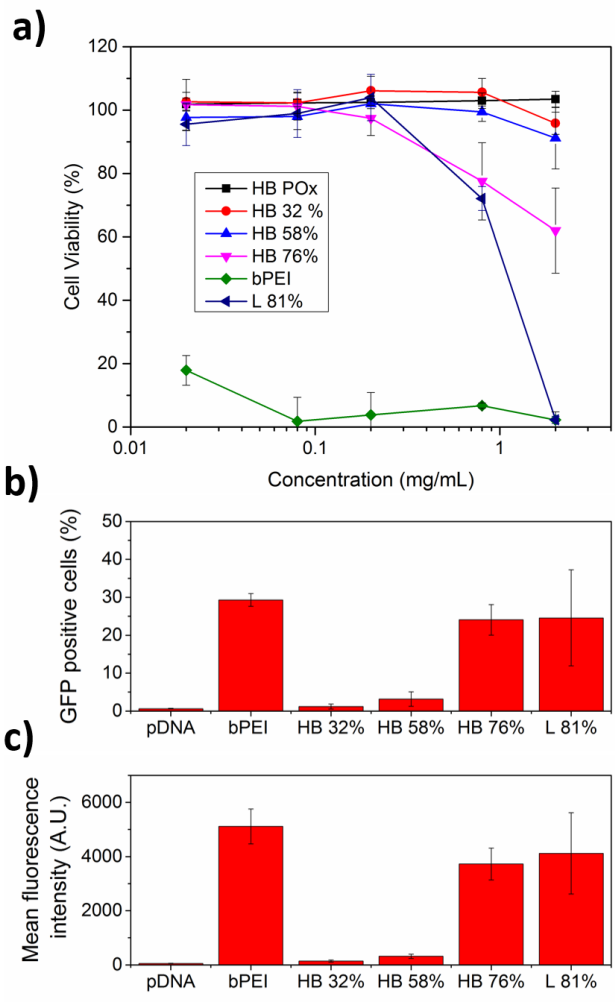

Figure 3.6. a) Cell viability as determined using XTT assay on human embryo kidney cells HEK293T treated with hyberbranched poly(ethyleneimine-co-oxazoline) copolymers, linear poly(ethyleneimine-co-oxazoline) copolymer, and bPEI for 24 hours at 37 °C; **b)** and **c)** GFP plasmid DNA transfection in HEK293T cell-line following 5 hours polyplex incubation (N/P 20, 10 µg/mL DNA concentration in well) and 24 hours subsequent growth. Intracellular fluorescence was determined by flow cytometry.

Finally, transfection of plasmid DNA containing GFP reporter gene using the polymers prepared in this study was evaluated on transfectable derivative of human embryonic kidney (HEK293T) cell line as model (**Figure 3.6b**) and reported relative to commercial bPEI. Cellular fluorescence histograms, obtained by flow cytometry following 5 hours of cell incubation with the polyplexes followed by 24 hours of subsequent growth, were used to determine transfection efficiencies (**Figure A3.21**). An N/P ratio of 20 was chosen for the transfection studies in order to have enough polymer to bind the plasmid even for copolymer samples with lower percentages of PEI. In the case of hyperbranched p($EI_{0.32}$-*co*-$EtOx_{0.68}$), transfection efficiencies only 2.5 fold better than naked pDNA were obtained, which can be attributed to incomplete complexation of the pDNA at this N/P ratio. Hyperbranched p($EI_{0.58}$-*co*-$EtOx_{0.42}$) showed a relatively similar transfection efficiency (around 6 fold better than naked pDNA). Accordingly, in the case of hyperbranched p($EI_{0.76}$-*co*-$EtOx_{0.24}$) and linear p($EI_{0.81}$-*co*-$EtOx_{0.19}$) copolymers where the degree of oxazoline hydrolysis is higher, transfection efficiencies reach values of 75% that of bPEI. This is a significant result when also taking into account the much reduced toxicity of the thiol-yne hyperbranched polymers, and suggests these materials are ideal candidates as lower toxicity alternatives to PEI.

3.3. Conclusions

Synthesis of hyperbranched poly(ethyleneimine-*co*-oxazoline) by AB_2 thiol-yne photo-addition chemistry is reported for the first time. This synthetic route allows for the preparation of hyperbranched polymers from macromolecular monomer units, with degrees of branching in the region of dendrimers. In contrast with the amine mixture and uncontrolled patterns typically obtained via the ring opening polymerisation of aziridine, the method presented here results in hyperbranched PEI structures containing only secondary amines and well defined branching patterns. Hyperbranched poly(ethyleneimine-*co*-oxazoline) and bPEI were found to complex GFP plasmid DNA to form positively charged particles. In comparison, linear forms were found to form larger aggregates. Differences were also found in polymer *in vitro* cytotoxicity, with

poly(ethyleneimine-*co*-oxazoline)s having reduced toxicity compared to bPEI, and the hyperbranched poly(ethyleneimine-*co*-oxazoline) having reduced toxicity compared to the linear equivalent. Delivery of pDNA encoding for GFP showed that poly(ethyleneimine-*co*-oxazoline) copolymers with high percentages of ethyleneimine units were have transfection efficiencies slightly lower than the commercial standard 25K branched PEI. When considering this in conjunction with the lower toxicities, the hyperbranched poly(ethyleneimine-*co*-oxazoline) represents an promising candidate for further non-viral gene delivery studies. In agreement with the literature, it is believed that the compact hyperbranched polymer conformation contributes, in some extent, to both the improved toxicity and also high transfection efficiencies. The synthesised hyperbranched PEI copolymers also highlight the importance of understanding polymer architecture when developing gene delivery systems

3.4. Experimental

3.4.1. Materials

Propargyl tosylate, methyl tosylate (MeTos), potassium ethyl xanthogenate, 2-ethyl-2-oxazoline (EtOx), dimethylamine (33% in ethanol), 2,2-dimethoxy-2-phenylacetophenone (DMPA), ethidium bromide (EtBr), polyethylenimine branched (bPEI, Mw ~25,000 by LS, Mn ~10,000 by SEC) were obtained from Sigma-Aldrich. All other materials were purchased from Fisher Scientific, or Sigma-Aldrich. Green fluorescent protein (GFP) expressing plasmid DNA (pWPI) was a gift from Didier Trono (Addgene plasmid # 12254). 2-Ethyl-2-oxazoline (EtOx) and methyl tosylate (MeTos) were distilled to dryness prior to use. EtOx was dried using CaH before distillation. 50X Tris-Acetate-EDTA (TAE) buffer for gel electrophoresis was made up at concentration of 2.0M Tris acetate (Sigma Aldrich) and 0.05M EDTA (Sigma Aldrich) in deionised water, pH 8.2 - 8.4 and stored at room temperature. Agarose loading buffer for samples (colourless) were made up at 30% (vol/vol) glycerol (Sigma Aldrich) in deionised water and stored at room temperature.

3.4.2. Characterisation

Size Exclusion Chromatography (SEC) was performed in DMF, using an Agilent 390-LC MDS instrument equipped with differential refractive index (DRI), viscometry, dual angle light scattering, and dual wavelength UV detectors. The system was equipped with 2 x PLgel Mixed D columns (300 x 7.5 mm) and a PLgel 5 μm guard column. The eluent was DMF with 5 mmol NH_4BF_4 additive, and samples were run at 1 mL/min at 50 °C. Analyte samples were filtered through a nylon membrane with 0.22 μm pore size before injection. Apparent molar mass values ($M_{n,SEC}$ and $M_{w,SEC}$) and dispersity ($Đ$) of synthesized polymers were determined by DRI detector and conventional calibration using Agilent SEC software. Poly(methyl methacrylate) (PMMA) standards (Agilent EasyVials) were used for calibration. The Kuhn-Mark-Houwink-Sakurada parameter α, relating to polymer conformation in solution was determined from the gradient of the double logarithmic plot of intrinsic viscosity as a function of molecular weight, using the

SEC viscometry detector and Agilent SEC software. Proton nuclear magnetic resonance spectra (^{1}H NMR) were recorded on a Bruker Advance 400 spectrometer (400 MHz) at 27 °C, with chemical shift values (δ) reported in ppm, and the residual proton signal of the solvent used as internal standard. Proton-decoupled carbon nuclear magnetic resonance spectra (^{13}C NMR) were recorded on a Bruker Advance 400 spectrometer (100 MHz) at 27 °C, with chemical shift values (δ) reported in ppm, and the residual proton signal of the solvent used as internal standard. Fourier transform infrared spectra (FTIR) were recorded on a Bruker Alpha FTIR ATR. Electrospray ionisation time-of-flight mass spectra (ESI-MS) were recorded using a Bruker MicroToF.

3.4.3. Oxazoline polymerisation

For a typical polymerisation, dry 2-ethyl-2-oxazoline (7.93 g, 80 mmol), porpargyl tosylate (1.68 g, 8 mmol), and acetonitrile (10.54 mL) were added to a Schlenk flask under nitrogen and left to stir in an oil bath at 80 °C. After a predetermined time, the solution was removed from the oil bath, a sample for the determination of the conversion was taken, and a solution of potassium ethyl xanthate (1.54 g, 9.6 mmol) was added to terminate the polymer chain. The product was left to stir for 1 h before being diluted with chloroform (100 mL). The organic layer was then washed with sat. Na_2CO_3 (3 × 100 mL) and brine (3 × 100 mL), and then dried over $MgSO_4$. The chloroform was removed to leave a colourless oil. The oil was re-dissolved in DCM (10 mL), precipitated into ether, the polymer was collected by gravity filtration as a white solid and then dried under vacuum. ^{1}H NMR spectrum shown in **Figure A3.1**. Propargyl-pEtOx-xanthate (1.1 g, 1.38 mmol) was dissolved in dimethylamine (33% in EtOH) (12 mL) deoxygenated with nitrogen bubbling and stirred at 40 °C for 3 h. The reaction mixture was then poured over a solution of sulphuric acid (H_2SO_4) (8 mL) and ice-water (80 mL). The polymer was extracted by washing with $CHCl_3$ (3 × 50 mL), followed by washing of the $CHCl_3$ layer with sat. Na_2CO_3 (2 × 50 mL) and brine (2 × 50 mL). The organic layer was then dried over $MgSO_4$ and filtered before the solvent was removed to yield the thiol-yne poly(oxazoline) macromonomer which was stored under nitrogen to reduced chance of disulfide formation. M_n = 1,200 g/mol, $Đ$ = 1.19 (DMF SEC, + NH_4BF_4 additive eluent,

PMMA calibration). Full functionalisation of both chain ends was confirmed using ESI-MS. ^{1}H NMR spectrum (400 MHz, $CDCl_3$, δ ppm): 4.12 (2H, -C**H$_2$**-C≡CH), 3.40-3.60 (4H, N-C**H$_2$**-C**H$_2$**-N), 2.25-2.45 (2H, NC(O)-C**H$_2$**-CH_3), 1.05-1.20 (3H, NC(O)-CH_2-C**H$_3$**). ^{13}C NMR spectrum (100 MHz, $CDCl_3$, δ ppm): 174.51 (N**C**(O)), 73.41 (-**C**≡CH), 70.46 (-C≡**C**H), 45.3 (N-**C**H_2-**C**H_2-N), 25.90 (NC(O)-**C**H_2-CH_3), 13.75 (-**C**H_2-SH), 9.39 (NC(O)-CH_2-**C**H_3). FTIR ν cm^{-1}: 3491 (broad, N-H amide), 3270-3290 (weak, ≡C-H alkyne), 2980 (medium, C-H alkane), 2835 (weak, N-CH_2- amine), 1624 (strong, C=O amide I), 1418 (medium, N-H amide II). The linear control poly(oxazoline) was synthesised in the same manner using methyl tosylate as the initiator and termination under ambient humid conditions. The ^{1}H NMR spectrum is shown in **Figure A3.3**, SEC chromatogram is shown in **Figure A3.2**, M_n = 13,700 g/mol, $Đ$ = 1.25 (DMF SEC, DRI detector).

3.4.4. Thiol-yne polymerisation

A typical polymerisation is as follows: thiol-yne macromonomer (600 mg, 0.75 mmol) was dissolved with DMPA (90 mg, 0.352 mmol) in DMF (2.5 mL) in a vial equipped with a small stirrer bar and a rubber septum screw cap. Monomer to initiator ratio was kept the same for all polymerisations. The vial was wrapped in aluminium foil and deoxygenated with nitrogen for 5 min. The vial was placed under a 365 nm UV lamp (UVP, UVGL-55, 6 watt, 365 nm) in an aluminium foil lined dark box over a magnetic stirrer plate. For the kinetic samples, each time point corresponds to a separate vial removed after the allocated polymerisation time. After the predetermined reaction time, the vial was removed and analysed by SEC. Polymer reaction mixture was precipitated in diethyl ether and the polymer recovered by centrifugation. M_w = 14,000 g/mol, $Đ$ = 1.5 (DMF SEC, DRI detector). ^{1}H NMR spectrum (400 MHz, $CDCl_3$, δ ppm): 5.60-6.20 (2H, -C**H**=C**H**-, weak), 3.95 (2H, -C**H$_2$**-C≡CH, weak), 3.40-3.55 (4H, N-C**H$_2$**-C**H$_2$**-N), 2.15-2.40 (2H, NC(O)-C**H$_2$**-CH_3), 0.90-1.20 (3H, NC(O)-CH_2-C**H$_3$**). ^{13}C NMR spectrum (100 MHz, $CDCl_3$, δ ppm): 174.59 (N**C**(O)), 45.41 (N-**C**H_2-**C**H_2-N), 25.90 (NC(O)-**C**H_2-CH_3), 9.30 (NC(O)-CH_2-**C**H_3). FTIR ν cm^{-1}: 3490 (broad, N-H amide), 3270-3290

(weak, ≡C-H alkyne), 2976 (medium, C-H alkane), 2830 (weak, N-CH_2- amine), 1621 (strong, C=O amide I), 1425 (medium, N-H amide II).

3.4.5. Poly(oxazoline) hydrolysis

The hydrolysis kinetics were performed in a microwave synthesiser (Biotage Initiator+ Eight). Hydrochloric acid (0.025 mL, 36 wt%) solution was mixed with 0.275 mL of PEtOx stock solution, giving a total volume in each vial (0.5 mL microwave vial) of 0.3 mL with a concentration of 1 M HCl. The vials were heated at 120 °C for varying reaction times. The reaction mixtures were cooled down by compressed air and made basic with 0.1 mL of a 4 M NaOH solution to a pH of 8-9, and freeze dried for ^{1}H NMR spectroscopy. The conversion was calculated from the ^{1}H NMR spectra signals of the hydrolysis products in deuterated methanol. Spectra can be found in **Figure A3.7-A3.8**. All signals described for PEtOx are present, together with the signals corresponding to the respective hydrolysis products. The dried crude polymer was then redissolved in water and dialysed against a 0.5 - 1 kDa membrane to remove propionic acid salts, and then freeze dried. Final poly(ethylenimine-*co*-2-ethyl-2-oxazoline) copolymer compositions were calculated from the appropriate backbone signals from the ^{1}H NMR spectra of the purified polymers. Once the kinetics of the hydrolysis had been established the hydrolysis was scaled up to 20 mL microwave vials, to obtain the appropriate polymers for the rest of the studies. For a typical ethylenimine oxazoline copolymer: ^{1}H NMR spectrum (400 MHz, $CDCl_3$, δ ppm): 3.45-3.71 (4H, N-C**H$_2$**-C**H$_2$**-N (POx)), 2.75-2.92 (4H, N-C**H$_2$**-C**H$_2$**-N (PEI)), 2.31-2.55 (2H, NC(O)-C**H$_2$**-CH_3), 1.04-1.20 (3H, NC(O)-CH_2-C**H$_3$**). ^{13}C NMR spectrum (100 MHz, $CDCl_3$, δ ppm): 175.97 (N**C**(O)), 48.33 (N-**C**H_2-**C**H_2-N), 26.20 (NC(O)-**C**H_2-CH_3), 9.30 (NC(O)-CH_2-**C**H_3). FTIR ν cm^{-1}: 3484 (broad, N-H amide), 3282 (broad, N-H amine secondary), 2987 (medium, C-H alkane), 2833 (weak, N-CH_2- amine), 1624 (strong, C=O amide I), 1420 (medium, N-H amide II).

3.4.6. pH titration

Potentiometric titration was performed manually at room temperature with a micropipette to control the added volume and a pH meter (HI2211 Hanna Instruments) to determine the pH. The pH of the polymer solutions (with 0.15 M NaCl) was set at 2.0 with concentrated HCl, and the solutions titrated with NaOH at 0.1 M or 0.2 M in various added volumes (from 0.01 mL to 0.2 mL) in order to obtain a constant increase of pH between each addition. 40 mL of polymer solution (1 mg/mL polymer) was used for each potentiometric titration experiment. For comparison, branched PEI (25 kDa) dissolved in 0.15 M NaCl aqueous solution adjusted to pH 2.0, was also titrated using the same method.

3.4.7. Static Light Scattering

The incremental refractive index, d*n*/d*C*, was determined by measuring the refractive index of the polymer over a range of concentrations. The RI was determined using a Shodex RI detector, operating at a wavelength of 632 nm. Multiplying the gradient, of the plot of RI vs conc., by the refractive index of the solvent (water = 1.3325) and dividing by the RI constant of the instrument (-1,398,000) gives the d*n*/d*C* of the polymer.

Light scattering measurements were obtained using an ALV-CGS3 system operating with a vertically polarized laser with wavelength λ = 632 nm. The measurements were taken at 20 °C over a range of scattering wave vectors ($q = 4\pi n \sin(\theta/2)/\lambda$, with θ the angle of observation and n the refractive index of the solvent). The Rayleigh ratio, R_θ, was determined using eq. 1,

$$R_\theta = \frac{I_{solution}(\theta) - I_{solvent}(\theta)}{I_{toluene}(\theta)} \cdot \left(\frac{n_{solvent}}{n_{toluene}} \right)^2 \cdot R_{toluene} \quad (1)$$

where $I_{solution}$, $I_{solvent}$ and $I_{toluene}$ are the scattering intensities of the solution, solvent and reference (toluene) respectively, n is the refractive index (n_{water} = 1.333, n_{dmf} = 1.431, $n_{toluene}$ = 1.496) and $R_{toluene}$ the Rayleigh ratio of toluene ($R_{toluene}$ = 1.35 x 10^{-5} cm^{-1} for λ = 632.8 nm).

The optical constant, K, is defined by eq. 2, where N_a is Avogadro number and dn/dC is the incremental refractive index.

$$K = \frac{4\pi^2 n_{solvent}^{\ 2}}{\lambda^4 N_a}\left(\frac{\partial n}{\partial C}\right)^2 \qquad (2)$$

At a given concentration the Rayleigh ratio, R_θ, is related to the apparent molecular weight of the sample, given by eq. 3. It is only at infinite dilutions, where the interactions between scattering particles are negligible, that the apparent molecular weight is equal to the true molecular weight. Multiple concentrations were measured and a plot of linear regression used to determine the apparent molecular weight at conc. = 0 mg/mL. Data and d*n*/d*C* values for all polymers shown in the supplementary information as Figures S10-S15.

$$\frac{KC}{R_\theta} = \frac{1}{M_a}\cdot\left(1+\frac{q^2\cdot R_g^{\ 2}}{3}\right) \qquad (3)$$

3.4.8. DLS/Zetapotential

Dynamic light scattering measurements of resulting polymers and polyplexes at various N/P ratios were carried out using a Malvern nanoZS zetasizer instrument (scattering angle of 173°, 10 mW He-Ne laser). For polyplex formation, appropriate amount of polymer stock solution and DNA stock solution were mixed and made up to a total volume of 1 mL in PBS (final concentration of polymer was 1 mg/mL, in all solutions). The resulting solutions were vortexed, incubated for 30 minutes at room temperature, and analysed at 25 °C. Each sample was run in triplicate and data was acquired using the software (Malvern Zetasizer) provided. Zeta potential measurements were carried out of the same DLS samples at various N/P ratios using the same instrument, and Malvern disposable folded capillary cell (DTS1070) cuvettes.

3.4.9. Ethidium Bromide displacement assay

Polyplex formation of DNA with cationic polymers was followed using quenching of the ethidium bromide fluorescence, as described in the literature. DNA (7.5 µg/mL) and EB (0.4 µg/mL) were dissolved in HEPES buffer, pH 7, and incubated for 10 min at room temperature. 100 µL of the DNA+EB solution was transferred to the wells of a 96-well plate containing different polymer concentrations. Fluorescence was measured after 20 min of incubation with the polymer solution using a Biotek Synergy HTX fluorescence microplate reader (Ex. 525 nm, Em. 605 nm). Control samples containing only DNA and EB were used to calibrate the measurements. Relative fluorescence = $(F_{SAMPLE} - F_{DNA}) / (F_{DNA+EB} - F_{DNA})$.

3.4.10. Agarose gel electrophoresis

Agarose gels (1% w/v) were prepared with agarose and 0.5 × TAE buffer. The solution was cooled on the bench for 5 minutes and 100 µL of 0.5 µg/mL ethidium bromide solution was added. The mixture was poured into the casted agarose tray and a comb inserted. The gel was left to set for a minimum of 30 minutes at room temperature. The agarose gels were run in 0.5× TAE buffer. The final gel was visualized under UV illumination at 365 nm using a UVP benchtop UV transilluminator system. Polyplexes of DNA were prepared at various N/P ratios. DNA stock solution of 60 µg/mL was prepared in PBS, and polymer stock solution of 300 µg/mL. For polyplex formation, the appropriate amount of polymer stock solution and DNA stock solution were mixed and made up to a total volume of 100 µL in PBS (final concentration of DNA was 0.030 µg/µL in all solutions). Polyplexes were vortexed and incubated at room temperature for 30 min. Prior to loading, 30 µL of loading buffer was added to each sample and 20 µL of polyplexes were loaded into the agarose gel wells. Gel electrophoresis was performed at 100 V for 30 minutes.

3.4.11. Atomic Force Microscopy

AFM images were taken using an Asylum Research MFP-3D Stand Alone atomic force microscope with an extended z-range of 40 μm, with closed loop scanning in *x* and *y* over a range of 90 μm. 20 μL of polymer/pDNA complexes in Hepes buffer solution (4 mM Hepes, 10 mM NaCl, and 2 mM $MgCl_2$ (pH 7.4)) containing 0.08 μg of pDNA at various N/P ratios were dropped onto freshly cleaved mica sheets for 5 min, then rinsed with distilled water several times and dried naturally in air overnight. The tapping mode was used for all measurements.

3.4.12. Cell culture and polymer toxicity

HEK293T cells were cultured in DMEM medium supplemented with 10% fetal bovine serum, % of 2 mM glutamine and 1% penicillin/streptomycin. The cells were grown as adherent monolayers at 310 K under a 5% CO2 humidified atmosphere and passaged at approximately 70–80% confluence. For cell viability evaluation, HEK293T cells were seeded in a 96 well plate at a density of 1×10^4 cells per well. After 16 hours, the culture medium was replaced by fresh media containing a series of dilution of the polymers (2, 0.8, 0.2, 0.08, 0.02 mg/mL), prepared from stock solutions in PBS. Following 24 hours incubation, the medium was removed and replaced with fresh medium. The cells were then incubated with a freshly prepared solution of XTT (0.2 mg/mL^{-1}) and N-methyl dibenzopyrazine methyl sulfate (250 μM) in medium for 16 hours. Absorbance of the samples was finally measured using a plate reader at 450 nm and 650 nm. The data presented are representative of a minimum of two independent experiments where each sample was measured in triplicate. Errors reported correspond to the standard deviation of the mean.

3.4.13. *In vitro* transfection

Polyplex samples were prepared prior to incubation with the cells, *via* mixing of plasmid DNA solution (final $concentration_{DNA}$ = 100 μg/mL) with the appropriate amount of

polymer predissolved in sterile water (N/P ratio = 20), and left to complex at room temperature for one hour. HEK293T cells were seeded in a 24 well plate at a density of 1 × 10^5 cells per well. After 16 hours, the culture medium was replaced by Optimem® cell culture media (Thermo Fisher Scientific) without fetal bovine serum. After one hour, the media was replaced by fresh Optimem® media containing the polyplex solutions (final $concentration_{DNA}$ = 10 μg/mL), the cells left to incubate for 5 hours under 5% CO_2 humidified atmosphere, then the media replaced with fresh culture media containing fetal bovine serum. Following overnight incubation, cells were washed with PBS, trypsinised, centrifuged, re-dispersed in ice-cold PBS and filtered into FACS tubes for analysis. Intracellular fluorescence was quantified using a BD LSR II cytometer (BD Biosciences) at excitation 488 nm and emission 525 nm. The geometric mean fluorescence was used as the sample value. The data in presented are representative of two separate experiments where each sample was measured in duplicate (n = 4). All errors reported correspond to the standard deviation from the mean

Appendix to Chapter 3

^{1}H NMR spectrum of macromonomer, ^{1}H NMR spectra and SEC chromatogram of linear PEtOx control, thiol-yne polymerisation concentration study SEC chromatograms and kinetic SEC data, hyperbranched polymer DB calculation, PEtOx hydrolysis kinetics data, SEC/DLS/SLS data for p(EI-*co*-EtOx) copolymers, additional polyplex AFM images, flow cytometry dot plots and histograms.

3.5. References

(1) Somia, N.; Verma, I. M., Gene therapy: Trials and tribulations, *Nature Reviews Genetics* **2000**, *1*, 91.

(2) Putnam, D., Polymers for gene delivery across length scales, *Nat. Mater.* **2006**, *5*, 439.

(3) Griesenbach, U.; Alton, E., Gene transfer to the lung: Lessons learned from more than 2 decades of CF gene therapy, *Adv. Drug Del. Rev.* **2009**, *61*, 128.

(4) Johnson, L. A.; Morgan, R. A.; Dudley, M. E.; Cassard, L.; Yang, J. C.; Hughes, M. S.; Kammula, U. S.; Royal, R. E.; Sherry, R. M.; Wunderlich, J. R.; Lee, C. C. R.; Restifo, N. P.; Schwarz, S. L.; Cogdill, A. P.; Bishop, R. J.; Kim, H.; Brewer, C. C.; Rudy, S. F.; VanWaes, C.; Davis, J. L.; Mathur, A.; Ripley, R. T.; Nathan, D. A.; Laurencot, C. M.; Rosenberg, S. A., Gene therapy with human and mouse T-cell receptors mediates cancer regression and targets normal tissues expressing cognate antigen, *Blood* **2009**, *114*, 535.

(5) Maguire, A. M.; High, K. A.; Auricchio, A.; Wright, J. F.; Pierce, E. A.; Testa, F.; Mingozzi, F.; Bennicelli, J. L.; Ying, G. S.; Rossi, S.; Fulton, A.; Marshall, K. A.; Banfi, S.; Chung, D. C.; Morgan, J. I. W.; Hauck, B.; Zelenaia, O.; Zhu, X. S.; Raffini, L.; Coppieters, F.; De Baere, E.; Shindler, K. S.; Volpe, N. J.; Surace, E. M.; Acerra, C.; Lyubarsky, A.; Redmond, T. M.; Stone, E.; Sun, J. W.; McDonnell, J. W.; Leroy, B. P.; Simonelli, F.; Bennett, J., Age-dependent effects of RPE65 gene therapy for Leber's congenital amaurosis: a phase 1 dose-escalation trial, *Lancet* **2009**, *374*, 1597.

(6) Kaplitt, M. G.; Feigin, A.; Tang, C.; Fitzsimons, H. L.; Mattis, P.; Lawlor, P. A.; Bland, R. J.; Young, D.; Strybing, K.; Eidelberg, D.; During, M. J., Safety and tolerability of gene therapy with an adeno-associated virus (AAV) borne GAD gene for Parkinson's disease: an open label, phase I trial, *Lancet* **2007**, *369*, 2097.

(7) Bowles, D. E.; McPhee, S. W. J.; Li, C. W.; Gray, S. J.; Samulski, J. J.; Camp, A. S.; Li, J.; Wang, B.; Monahan, P. E.; Rabinowitz, J. E.; Grieger, J. C.; Govindasamy, L.; Agbandje-McKenna, M.; Xiao, X.; Samulski, R. J., Phase 1 Gene Therapy for Duchenne Muscular Dystrophy Using a Translational Optimized AAV Vector, *Mol. Ther.* **2012**, *20*, 443.

(8) Jinek, M.; Chylinski, K.; Fonfara, I.; Hauer, M.; Doudna, J. A.; Charpentier, E., A Programmable Dual-RNA-Guided DNA Endonuclease in Adaptive Bacterial Immunity, *Science* **2012**, *337*, 816.

(9) Cong, L.; Ran, F. A.; Cox, D.; Lin, S. L.; Barretto, R.; Habib, N.; Hsu, P. D.; Wu, X. B.; Jiang, W. Y.; Marraffini, L. A.; Zhang, F., Multiplex Genome Engineering Using CRISPR/Cas Systems, *Science* **2013**, *339*, 819.

(10) Yin, H.; Kanasty, R. L.; Eltoukhy, A. A.; Vegas, A. J.; Dorkin, J. R.; Anderson, D. G., Non-viral vectors for gene-based therapy, *Nature Reviews Genetics* **2014**, *15*, 541.

(11) Fischer, D.; Bieber, T.; Li, Y. X.; Elsasser, H. P.; Kissel, T., A novel non-viral vector for DNA delivery based on low molecular weight, branched polyethylenimine: Effect of molecular weight on transfection efficiency and cytotoxicity, *Pharm. Res.* **1999**, *16*, 1273.

(12) Anderson, D. G.; Akinc, A.; Hossain, N.; Langer, R., Structure/property studies of polymeric gene delivery using a library of poly(beta-amino esters), *Mol. Ther.* **2005**, *11*, 426.

(13) Intra, J.; Salem, A. K., Characterization of the transgene expression generated by branched and linear polyethylenimine-plasmid DNA nanoparticles in vitro and after intraperitoneal injection in vivo, *J. Control. Release* **2008**, *130*, 129.

(14) Goula, D.; Remy, J. S.; Erbacher, P.; Wasowicz, M.; Levi, G.; Abdallah, B.; Demeneix, B. A., Size, diffusibility and transfection performance of linear PEI/DNA complexes in the mouse central nervous system, *Gene Ther.* **1998**, *5*, 712.

(15) Wightman, L.; Kircheis, R.; Rossler, V.; Carotta, S.; Ruzicka, R.; Kursa, M.; Wagner, E., Different behavior of branched and linear polyethylenimine for gene delivery in vitro and in vivo, *J. Gene Med.* **2001**, *3*, 362.

(16) Tang, M. X.; Redemann, C. T.; Szoka, F. C., In vitro gene delivery by degraded polyamidoamine dendrimers, *Bioconjugate Chem.* **1996**, *7*, 703.

(17) Godbey, W. T.; Wu, K. K.; Mikos, A. G., Poly(ethylenimine) and its role in gene delivery, *J. Control. Release* **1999**, *60*, 149.

(18) Cortez, M. A.; Godbey, W. T.; Fang, Y. L.; Payne, M. E.; Cafferty, B. J.; Kosakowska, K. A.; Grayson, S. M., The Synthesis of Cyclic Poly(ethylene imine) and

Exact Linear Analogues: An Evaluation of Gene Delivery Comparing Polymer Architectures, *J. Am. Chem. Soc.* **2015**, *137*, 6541.

(19) Konkolewicz, D.; Gray-Weale, A.; Perrier, S., Hyperbranched Polymers by Thiol-Yne Chemistry: From Small Molecules to Functional Polymers, *J. Am. Chem. Soc.* **2009**, *131*, 18075.

(20) Cook, A. B.; Barbey, R.; Burns, J. A.; Perrier, S., Hyperbranched Polymers with High Degrees of Branching and Low Dispersity Values: Pushing the Limits of Thiol–Yne Chemistry, *Macromolecules* **2016**, *49*, 1296.

(21) Hartlieb, M.; Floyd, T.; Cook, A. B.; Sanchez-Cano, C.; Catrouillet, S.; Burns, J. A.; Perrier, S., Well-defined hyperstar copolymers based on a thiol-yne hyperbranched core and a poly(2-oxazoline) shell for biomedical applications, *Polymer Chemistry* **2017**, *8*, 2041.

(22) Barbey, R.; Perrier, S., Synthesis of Polystyrene-Based Hyperbranched Polymers by Thiol-Yne Chemistry: A Detailed Investigation, *Macromolecules* **2014**, *47*, 6697.

(23) Bus, T.; Englert, C.; Reifarth, M.; Borchers, P.; Hartlieb, M.; Vollrath, A.; Hoeppener, S.; Traeger, A.; Schubert, U. S., 3rd generation poly(ethylene imine)s for gene delivery, *J. Mater. Chem. B* **2017**, *5*, 1258.

(24) Rinkenauer, A. C.; Tauhardt, L.; Wendler, F.; Kempe, K.; Gottschaldt, M.; Traeger, A.; Schubert, U. S., A Cationic Poly(2-oxazoline) with High In Vitro Transfection Efficiency Identified by a Library Approach, *Macromol. Biosci.* **2015**, *15*, 414.

(25) Hartlieb, M.; Kempe, K.; Schubert, U. S., Covalently cross-linked poly(2-oxazoline) materials for biomedical applications - from hydrogels to self-assembled and templated structures, *J. Mater. Chem. B* **2015**, *3*, 526.

(26) Fairbanks, B. D.; Scott, T. F.; Kloxin, C. J.; Anseth, K. S.; Bowman, C. N., Thiol-Yne Photopolymerizations: Novel Mechanism, Kinetics, and Step-Growth Formation of Highly Cross-Linked Networks, *Macromolecules* **2009**, *42*, 211.

(27) Hawker, C. J.; Lee, R.; Frechet, J. M. J., One-step synthesis of hyperbranched dendritic polyesters, *J. Am. Chem. Soc.* **1991**, *113*, 4583.

(28) de la Rosa, V. R.; Bauwens, E.; Monnery, B. D.; De Geest, B. G.; Hoogenboom, R., Fast and accurate partial hydrolysis of poly(2-ethyl-2-oxazoline) into tailored linear polyethylenimine copolymers, *Polymer Chemistry* **2014**, *5*, 4957.

(29) Dubin, P. In *Journal of Chromatography Library*; Dubin, P. L., Ed.; Elsevier: 1988; Vol. Volume 40, p xiii.

(30) Perevyazko, I.; Gubarev, A. S.; Tauhardt, L.; Dobrodumov, A.; Pavlov, G. M.; Schubert, U. S., Linear poly(ethylene imine)s: true molar masses, solution properties and conformation, *Polymer Chemistry* **2017**, *8*, 7169.

(31) Striegel, A. M.; Yau, W. W.; Kirkland, J. J.; Bly, D. D. In *Modern Size-Exclusion Liquid Chromatography*; John Wiley & Sons, Inc.: 2009, p i.

(32) Curtis, K. A.; Miller, D.; Millard, P.; Basu, S.; Horkay, F.; Chandran, P. L., Unusual Salt and pH Induced Changes in Polyethylenimine Solutions, *PLoS One* **2016**, *11*.

(33) Niidome, T.; Huang, L., Gene therapy progress and prospects: Nonviral vectors, *Gene Ther.* **2002**, *9*, 1647.

(34) Benjaminsen, R. V.; Mattebjerg, M. A.; Henriksen, J. R.; Moghimi, S. M.; Andresen, T. L., The Possible "Proton Sponge" Effect of Polyethylenimine (PEI) Does Not Include Change in Lysosomal pH, *Mol. Ther.* **2013**, *21*, 149.

(35) Akinc, A.; Thomas, M.; Klibanov, A. M.; Langer, R., Exploring polyethylenimine-mediated DNA transfection and the proton sponge hypothesis, *J. Gene Med.* **2005**, *7*, 657.

(36) Behr, J. P., The proton sponge: A trick to enter cells the viruses did not exploit, *Chimia* **1997**, *51*, 34.

(37) Tse, W. C.; Boger, D. L., A fluorescent intercalator displacement assay for establishing DNA binding selectivity and affinity, *Acc. Chem. Res.* **2004**, *37*, 61.

(38) Frohlich, E., The role of surface charge in cellular uptake and cytotoxicity of medical nanoparticles, *International Journal of Nanomedicine* **2012**, *7*, 5577.

(39) Zhao, X.; Cui, H. X.; Chen, W. J.; Wang, Y.; Cui, B.; Sun, C. J.; Meng, Z. G.; Liu, G. Q., Morphology, Structure and Function Characterization of PEI Modified Magnetic Nanoparticles Gene Delivery System, *PLoS One* **2014**, *9*.

(40) Rackstraw, B. J.; Martin, A. L.; Stolnik, S.; Roberts, C. J.; Garnett, M. C.; Davies, M. C.; Tendler, S. J. B., Microscopic investigations into PEG-cationic polymer-induced DNA condensation, *Langmuir* **2001**, *17*, 3185.

(41) Dunlap, D. D.; Maggi, A.; Soria, M. R.; Monaco, L., Nanoscopic structure of DNA condensed for gene delivery, *Nucleic Acids Res.* **1997**, *25*, 3095.

(42) Li, C.; Ma, C. Y.; Xu, P. X.; Gao, Y. X.; Zhang, J.; Qiao, R. Z.; Zhao, Y. F., Effective and Reversible DNA Condensation Induced by a Simple Cyclic/Rigid Polyamine Containing Carbonyl Moiety, *J. Phys. Chem. B* **2013**, *117*, 7857.

(43) Klemm, A. R.; Young, D.; Lloyd, J. B., Effects of polyethyleneimine on endocytosis and lysosome stability, *Biochem. Pharmacol.* **1998**, *56*, 41.

(44) Kafil, V.; Omidi, Y., Cytotoxic Impacts of Linear and Branched Polyethylenimine Nanostructures in A431 Cells, *Bioimpacts* **2011**, *1*, 23.

(45) Nomoto, T.; Fukushima, S.; Kumagai, M.; Machitani, K.; Arnida; Matsumoto, Y.; Oba, M.; Miyata, K.; Osada, K.; Nishiyama, N.; Kataoka, K., Three-layered polyplex micelle as a multifunctional nanocarrier platform for light-induced systemic gene transfer, *Nature Communications* **2014**, *5*.

(46) Synatschke, C. V.; Schallon, A.; Jerome, V.; Freitag, R.; Muller, A. H. E., Influence of Polymer Architecture and Molecular Weight of Poly(2-(dimethylamino)ethyl methacrylate) Polycations on Transfection Efficiency and Cell Viability in Gene Delivery, *Biomacromolecules* **2011**, *12*, 4247.

(47) Fischer, D.; Li, Y. X.; Ahlemeyer, B.; Krieglstein, J.; Kissel, T., In vitro cytotoxicity testing of polycations: influence of polymer structure on cell viability and hemolysis, *Biomaterials* **2003**, *24*, 1121.

(48) Singh, A. K.; Kasinath, B. S.; Lewis, E. J., Interaction of polycations with cell-surface negative charges of epithelial cells, *Biochim. Biophys. Acta* **1992**, *1120*, 337.

Appendix to Chapter 3

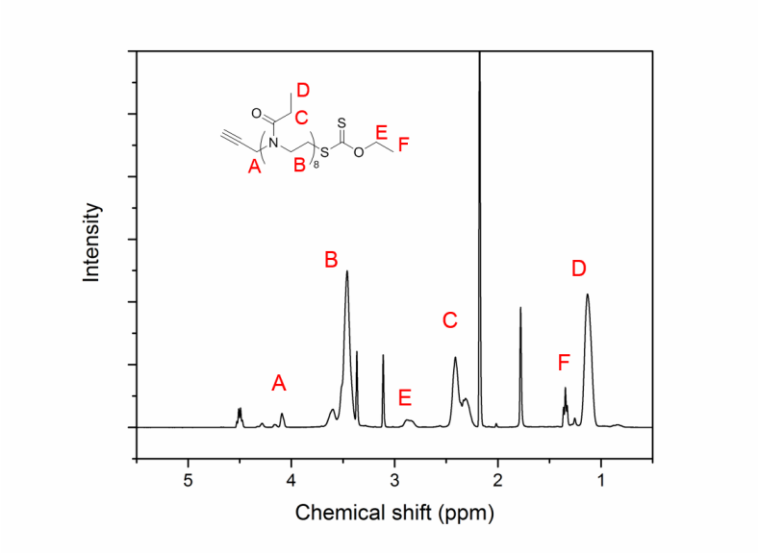

Figure A3.1. ^{1}H NMR spectrum (400 MHz, $CDCl_3$) of xanthate-protected thiol-yne macromonomer synthesized by cationic ring opening polymerization of 2-ethyl-2-oxazoline monomer.

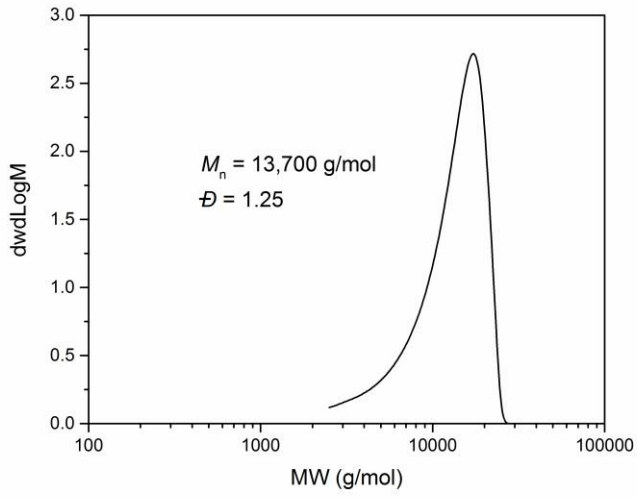

Figure A3.2. Size exclusion chromatogram (DMF +NH_4BF_4 additive eluent, PMMA calibration) of linear POx control polymer synthesized by cationic ring opening polymerization of 2-ethyl-2-oxazoline monomer.

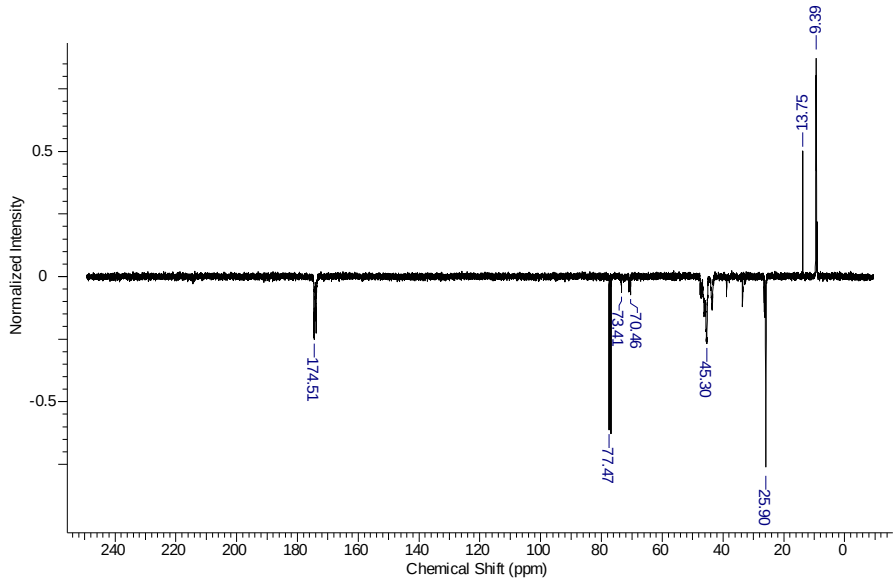

Figure A3.3. ^{13}C NMR spectrum (125 MHz, $CDCl_3$) of thiol-yne macromonomer synthesized by cationic ring opening polymerization of 2-ethyl-2-oxazoline monomer.

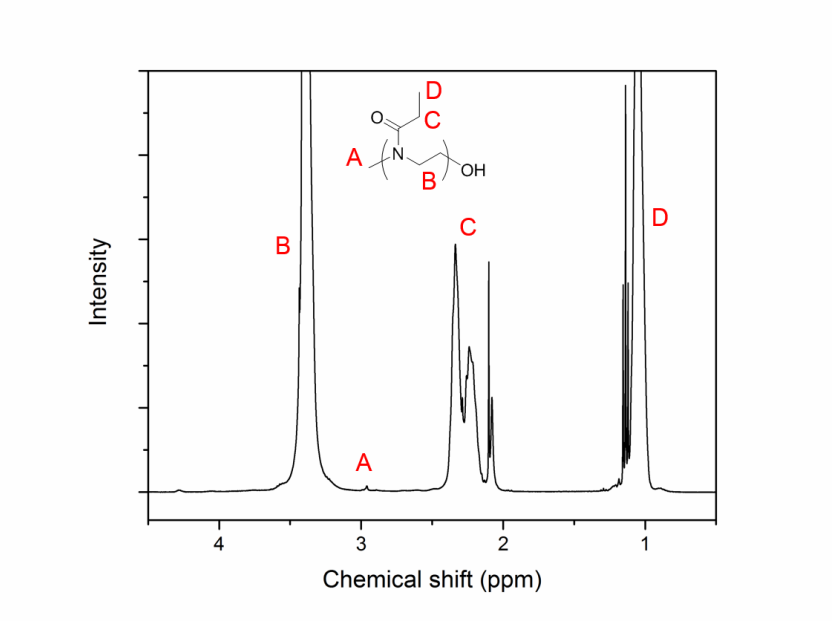

Figure A3.4. ^{1}H NMR spectrum (400 MHz, $CDCl_3$) of linear POx control polymer synthesized by cationic ring opening polymerization of 2-ethyl-2-oxazoline monomer.

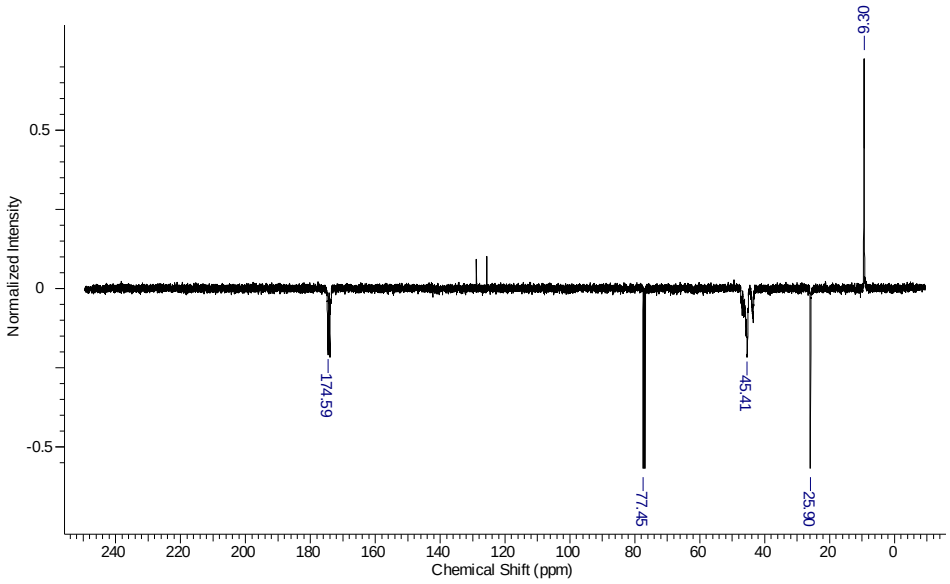

Figure A3.5. ^{13}C NMR spectrum (125 MHz, $CDCl_3$) of thiol-yne hyperbranched POx.

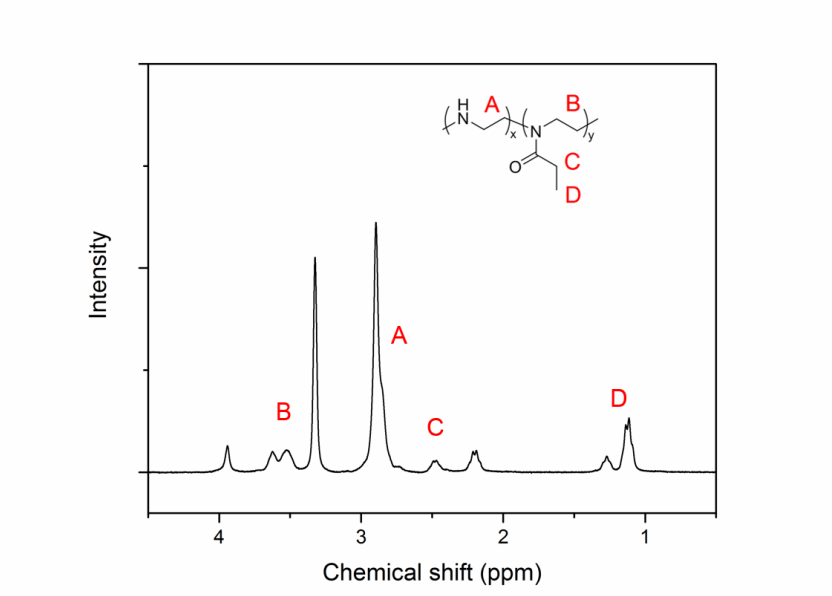

Figure A3.6. ^{1}H NMR spectrum (400 MHz, $CDCl_3$) of linear POx PEI 81% control polymer synthesized by cationic ring opening polymerization of 2-ethyl-2-oxazoline monomer, and subsequent hydrolysis in 1M HCl.

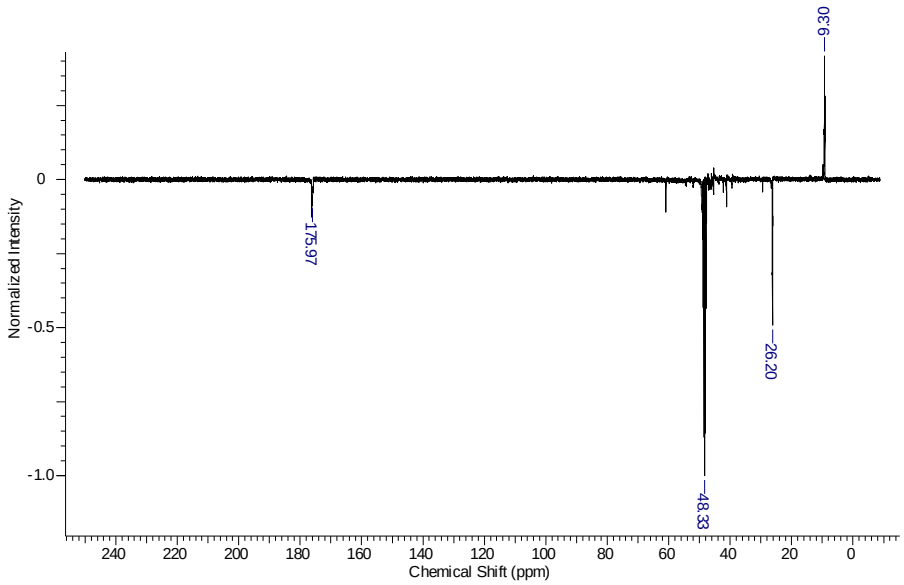

Figure A3.7. ^{13}C NMR spectrum (125 MHz, $CDCl_3$) of hyperbranched POx PEI 76% polymer.

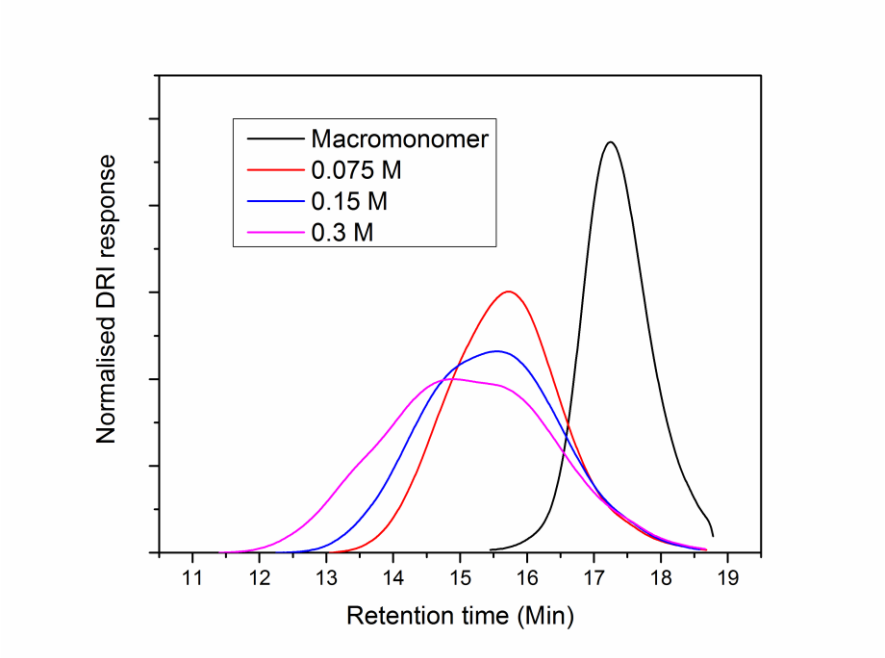

Figure A3.8. Size exclusion chromatogram (DMF + NH_4BF_4 additive eluent, PMMA calibration) of xanthate-protected thiol-yne macromonomer synthesized by cationic ring opening polymerization of 2-ethyl-2-oxazoline monomer, and subsequent hyperbranched polymers formed at various monomer concentrations.

Table A3.1. Size exclusion chromatography data (DMF +NH_4BF_4 additive eluent, PMMA calibration) of xanthate-protected thiol-yne macromonomer synthesized by cationic ring opening polymerization of 2-ethyl-2-oxazoline monomer, and subsequent hyperbranched polymers formed at various monomer concentrations. Degrees of branching (DB) were calculated from ^{1}H NMR spectroscopy (400 MHz, $CDCl_3$) as exemplified in Figure 1d and Figure S6.

	$M_{n,SEC}$ (g/mol)	$M_{w,SEC}$ (g/mol)	$Đ$	DB
Monomer	1200	1500	1.19	
0.075 M	5400	8200	1.51	0.83
0.15 M	5900	10500	1.78	0.83
0.3 M	6800	16400	2.41	0.87

Table A3.2. Size-exclusion chromatography data (DMF +NH_4BF_4 additive eluent, PMMA calibration) for photopolymerisation of poly(2-ethyloxazoline) thiol-yne macromonomer with varying irradiation times.

	$M_{n,SEC}$ (g/mol)	$M_{w,SEC}$ (g/mol)	$Đ$
Monomer	1,200	1,500	1.19
0.5 hr	2,900	4,800	1.67
1 hr	3,900	8,300	2.11
2 hr	4,200	17,000	4.07
4 hr	4,700	23,800	5.10
8 hr	4,700	23,600	5.05
8 hr purified	11,600	28,400	2.45

$$DB = \frac{no.\ of\ dendritic\ units + no.\ of\ terminal\ units}{Total\ no.\ of\ units}$$

$$= \frac{1 - L}{\frac{16.00}{16}}$$

$$= \frac{1 - 0.13}{1}$$

$$= 0.87$$

Figure A3.9. Example of calculation for degree of branching using ^{1}H NMR spectroscopy (400 MHz, $CDCl_3$). Example calculation using NMR spectrum from Figure 1d and reference of 16.00 from $M_{n,NMR}$ of 800 for the macromonomer.

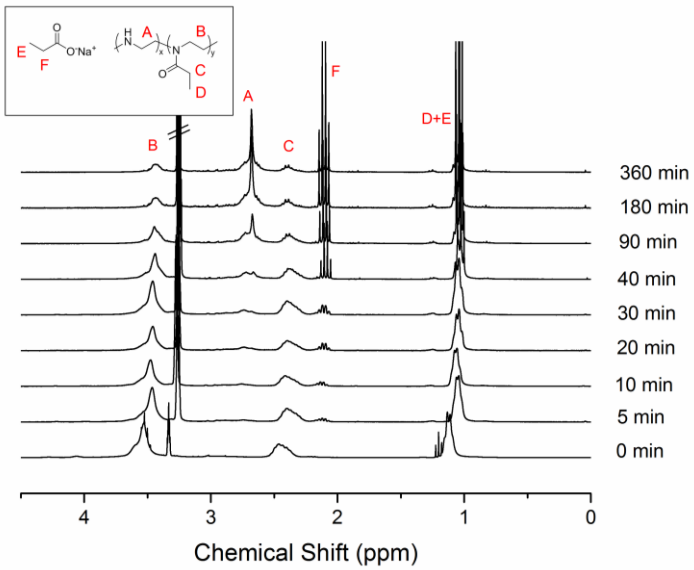

Figure A3.10. Hydrolysis kinetic study of HB POx (^{1}H NMR spectra (400 MHz, $CDCl_3$)) in 1M HCl,

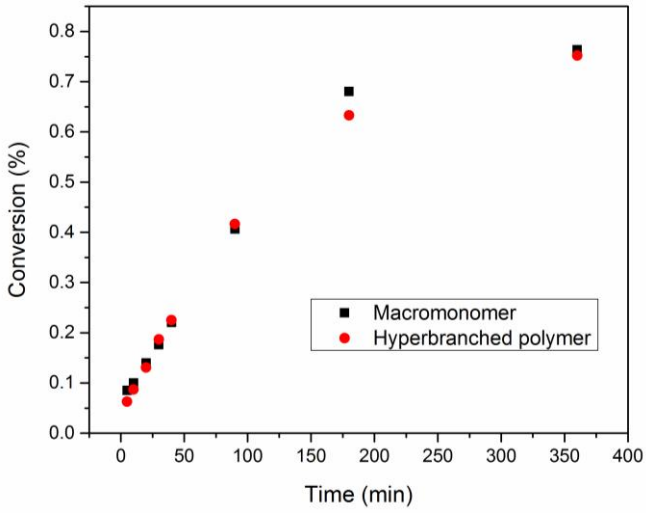

Figure A3.11. Hydrolysis kinetic study of both POx macromonomer and HB PEtOx (^{1}H NMR spectrum (400 MHz, $CDCl_3$)) in 1M HCl, percentage hydrolysis calculated from integral of propionic acid salt in crude hydrolysis product.

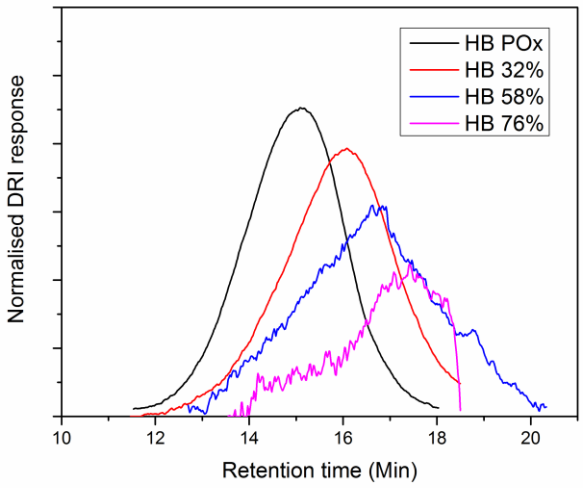

Figure A3.12. Size exclusion chromatograms (DMF +NH_4BF_4 additive eluent, PMMA calibration) of purified hydrolysed hyperbranched polymers and HB POx, showing previously reported low signals and increased retention times due to increased polymer cationic charges.

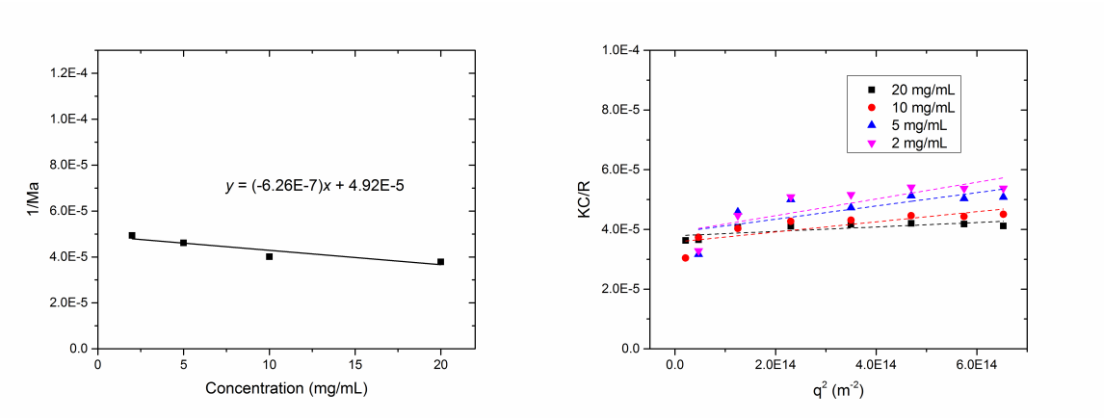

Figure A3.13. Evolution of KC/R of HB POx in water as a function of q^2 and concentration obtained by Static Light Scattering. MW = 20,400 g/mol, d*n*/d*C* = 0.143.

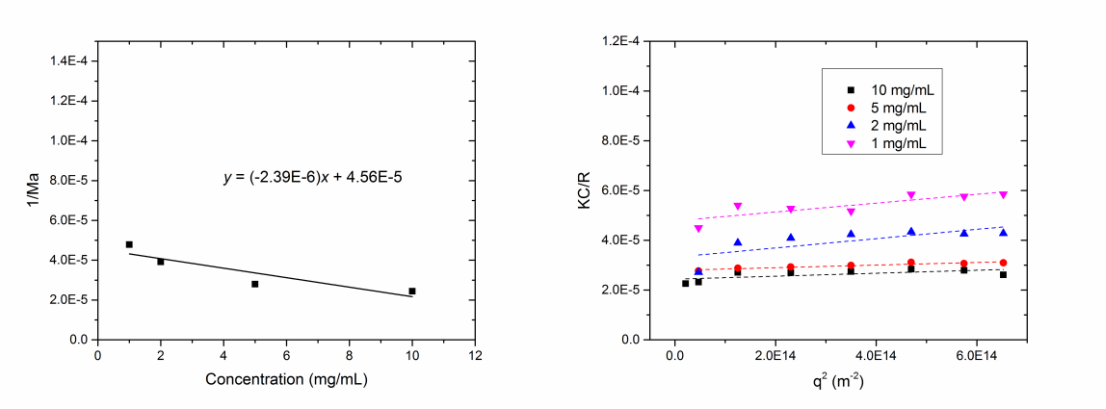

Figure A3.14. Evolution of KC/R of HB 32% in water as a function of q^2 and concentration obtained by Static Light Scattering. MW = 21,900 g/mol, d*n*/d*C* = 0.175.

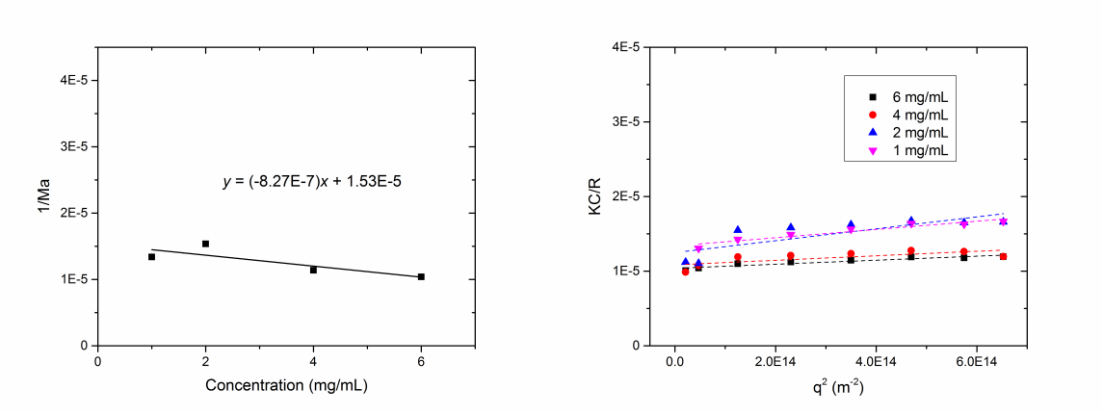

Figure A3.15. Evolution of KC/R of HB 58% in water as a function of q² and concentration obtained by Static Light Scattering. MW = 65,300 g/mol, d*n*/d*C* = 0.185.

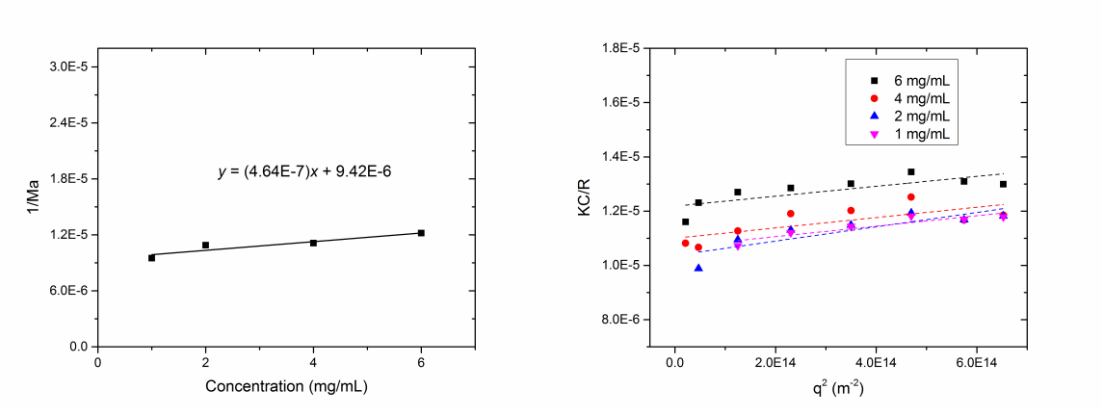

Figure A3.16. Evolution of KC/R of HB 76% in water as a function of q² and concentration obtained by Static Light Scattering. MW = 106,200 g/mol, d*n*/d*C* = 0.198.

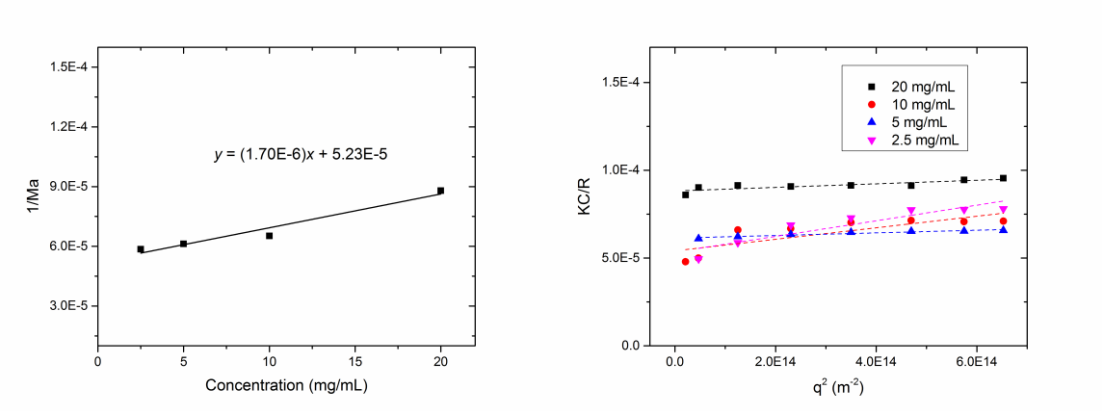

Figure A3.17. Evolution of KC/R of linear POx control in water as a function of q² and concentration obtained by Static Light Scattering. MW = 19,100 g/mol, d*n*/d*C* = 0.143.

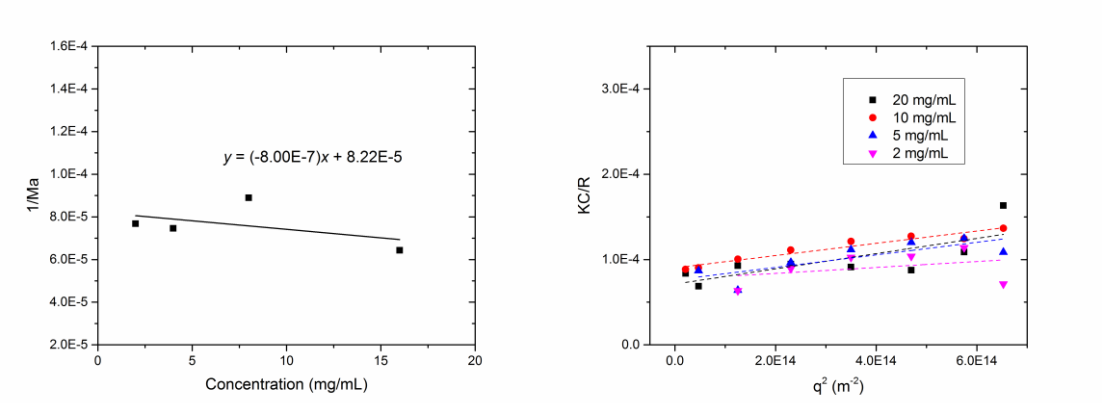

Figure A3.18. Evolution of KC/R of linear POx PEI 81% control in water as a function of q² and concentration obtained by Static Light Scattering. MW = 12,400 g/mol, d*n*/d*C* = 0.128.

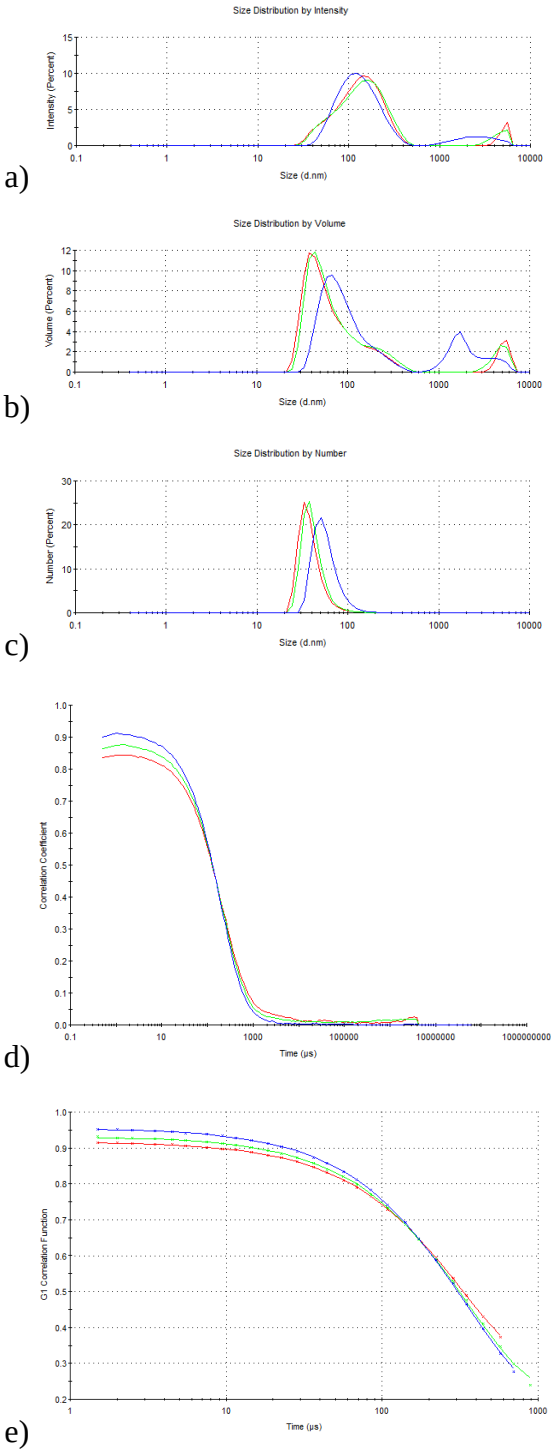

Figure A3.19. Representative DLS data for polyples solutions (HB76 polymer with DNA, N/P 20, three repeats shown), a) intensitie distribution, b) volume distribution, c) number distribution, d) correlalograms, e) cummulants fit.

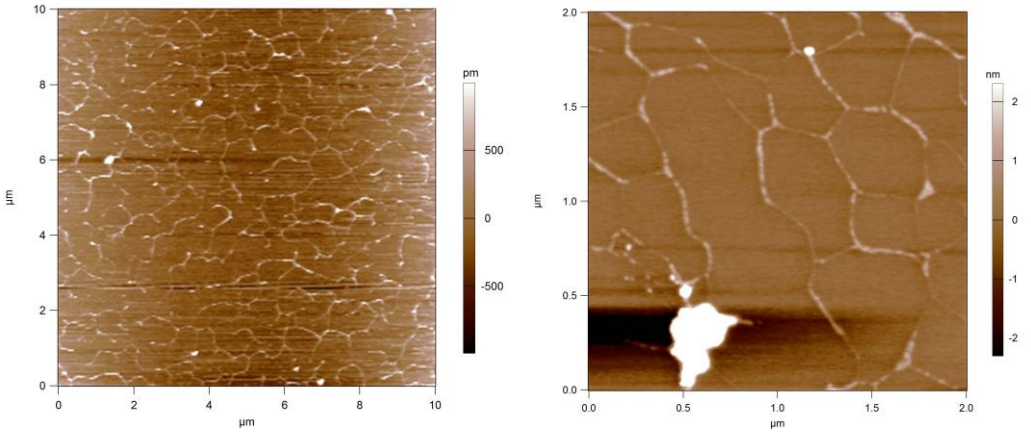

Figure A3.20. AFM images of pDNA on mica surface, at two different resolutions.

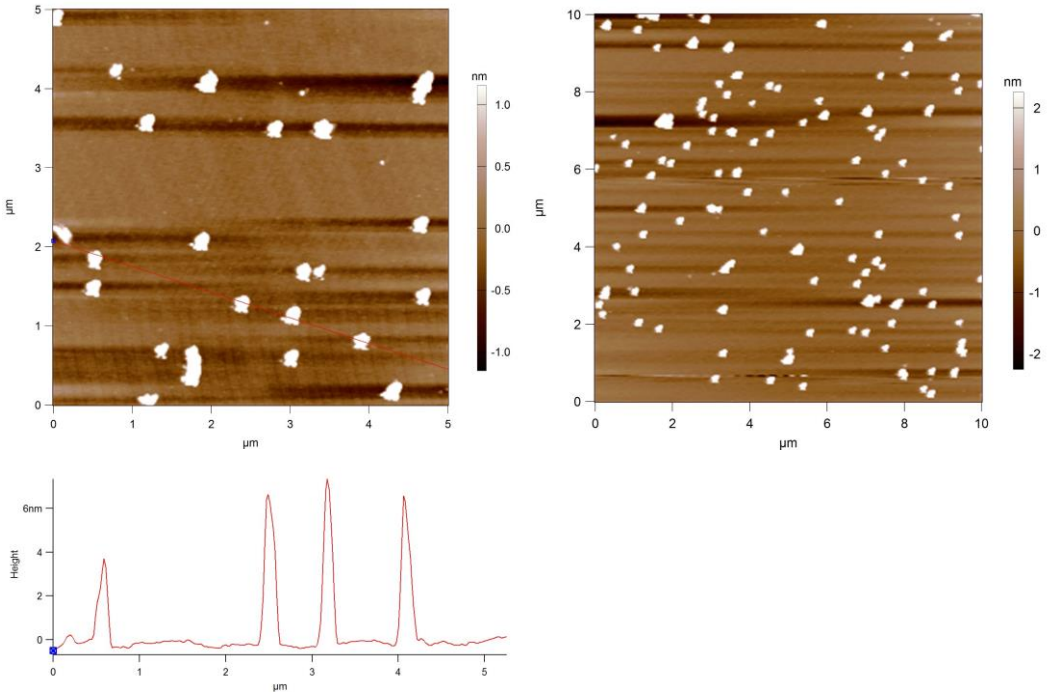

Figure A3.21. AFM images of linear 81% control polymer pDNA polyplex (N/P 20) on mica surface, at two different resolutions. Height profile included.

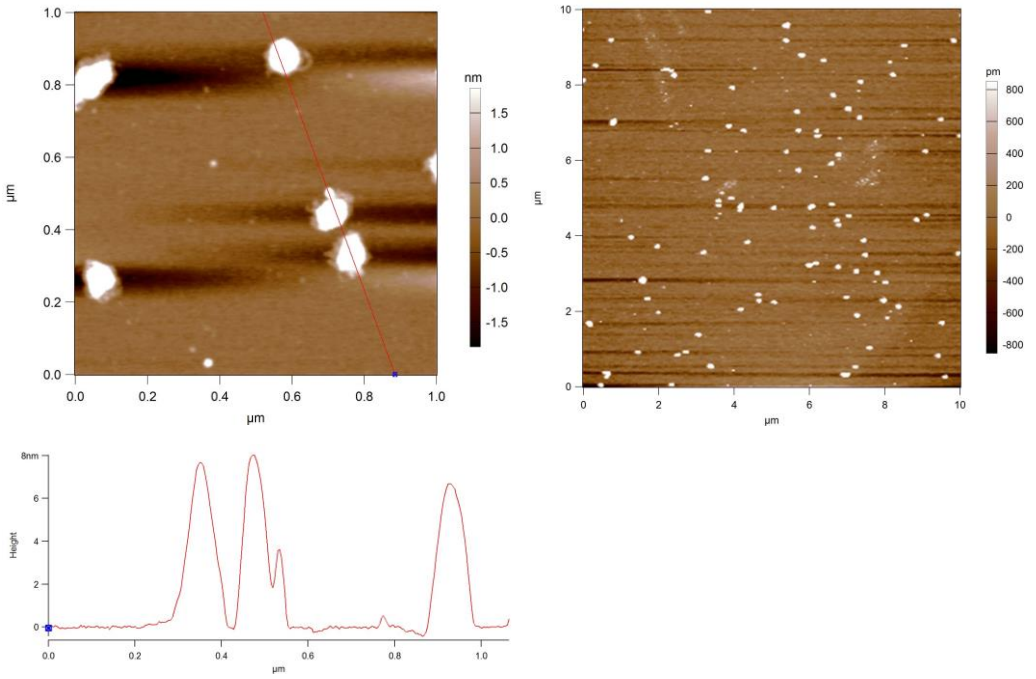

Figure A3.22. AFM images of hyperbranched POx PEI 76% polymer pDNA polyplex (N/P 20) on mica surface, at two different resolutions. Height profile included.

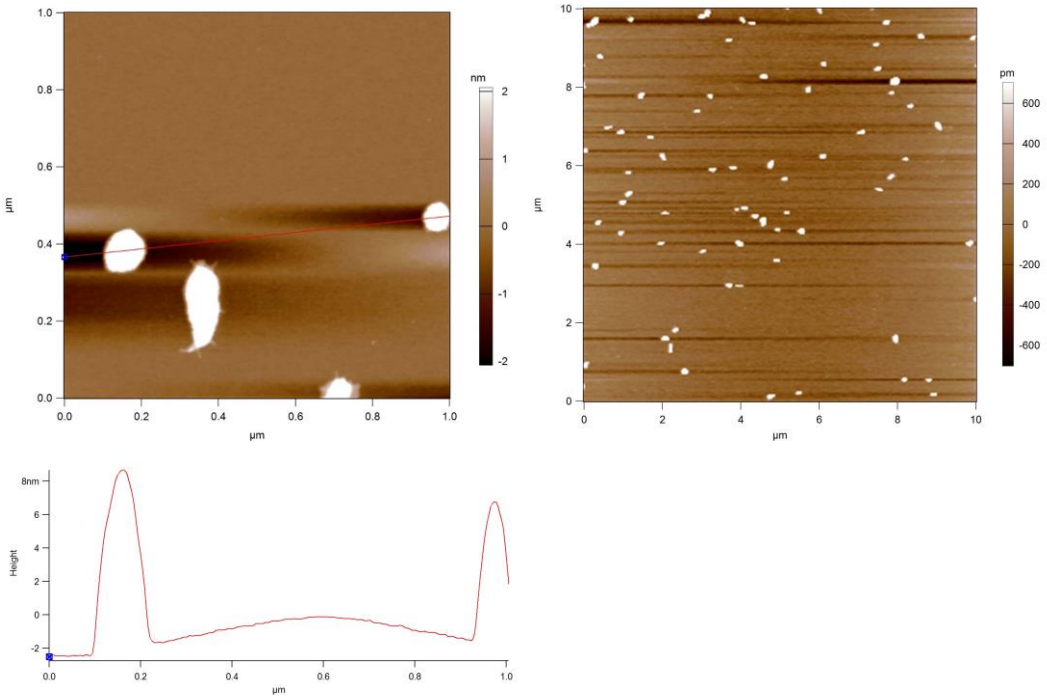

Figure A3.23. AFM images of bPEI polymer pDNA polyplex (N/P 20) on mica surface, at two different resolutions. Height profile included.

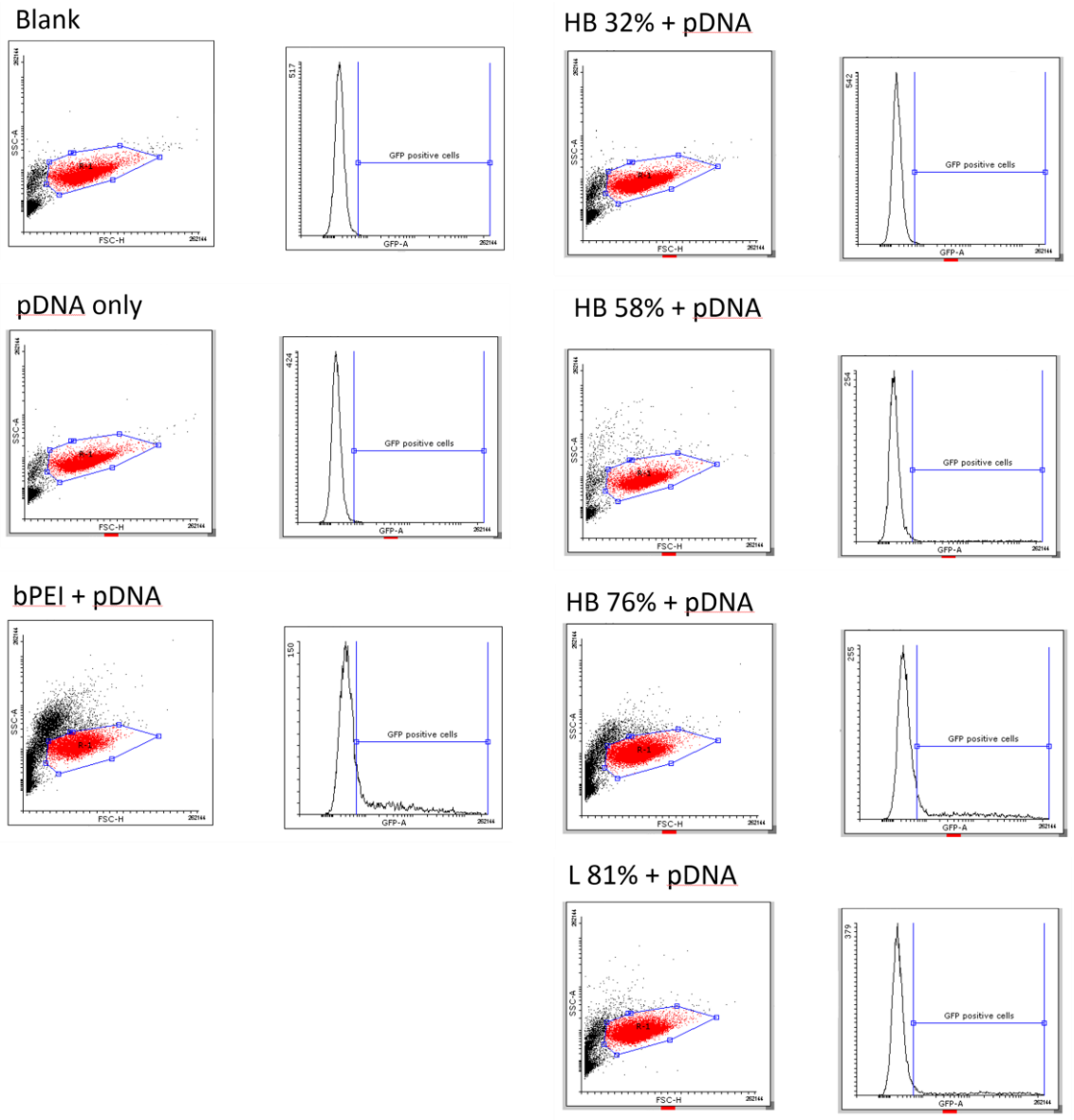

Figure A3.24. Representative (two separate experiments where each sample was measured in duplicate (n = 4)) dot plots and histograms of flow cytometry measurements determining positive GFP-expressing HEK cells after 24 h post-transfection with bPEI and synthesised polymers (all N/P 20).

4.

Cationic and hydrolysable branched polymers by RAFT for complexation and controlled release of dsRNA

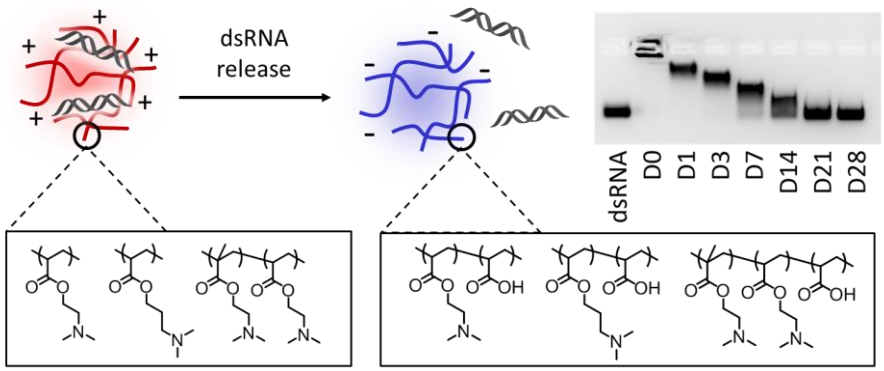

Abstract

The controlled release of nucleic acids from cationic polymers is an important criteria for the design of gene delivery systems, and can be difficult to achieve due to the persistent positive charges required to initially complex the nucleic acids. Here is described the use of highly branched tertiary amine-rich polymers for the complexation and release of dsRNA over a prolonged period of time. Controlled release of dsRNA is obtained via hydrolysis of the polymer side chains and associated change in electrostatic charge. Reversible addition-fragmentation chain transfer (RAFT) polymerization was utilised to synthesise a series of branched polymers of 2-(dimethylamino)ethyl acrylate (DMAEA), 3-(dimethylamino)propyl acrylate (DMAPA), and 2-(dimethylamino)ethyl methacrylate (DMAEMA) (MW ~ 60,000 – 200,000 g/mol, and $Đ$ ~ 2 – 8). The hydrolysis kinetics of all synthesised polymer materials were followed by ^{1}H NMR spectroscopy. Complexation with dsRNA resulted in the formation of polyplex nanoparticles (N/P ratio of 5) with sizes of approximately 400 nm and surface charges of +15 mV. An agarose gel release study showed sustained release of dsRNA from p(DMAEA-*co*-DMAEMA) for a period of more than 2 weeks. Unlike branched PEI commonly used for gene delivery, the majority of these systems showed little toxicity to cells (NIH3T3 fibroblasts). The results point towards pDMAPA and p(DMAEA-*co*-DMAEMA) being promising polymers for the controlled release of oligonucleotides over prolonged periods.

4.1 Introduction

Synthetic vectors that can activate the RNA interference pathway, or transcribe for new proteins, by delivering nucleic acids (dsRNA, siRNA, mRNA, DNA) in target cells are gaining significant attention due to a number of potential advantages over viral vectors.[1] Particular benefits of synthetic vectors over viral vectors include: low immunogenicity,[2] high nucleotide loading,[3] as well as ease and reproducibility of production.[4] Yet, there are many barriers associated with gene-based therapies, which at the moment limits greatly the number of products successfully passing through clinical trials. These include degradation of nucleic acids by nucleases in physiological fluids as well as the short half-life of naked plasmid DNA *in vivo*, which was estimated to be in the region of 10 minutes post systemic injection.[1,5] Synthetic vectors partly mediate these limitations by protecting nucleotides from enzymatic degradation, whilst also avoiding renal clearance and non-specific interactions with serum proteins and extracellular compounds. In addition, synthetic vehicles need to extravasate from the vasculature, promote cell internalisation of otherwise negatively charged non-endocytosable nucleic acid biomolecules, and finally release the therapeutic nucleic acid in the intracellular environment. The latter is increasingly identified as a difficult hurdle to overcome as the strong electrostatic interactions between cationic synthetic systems and negatively charged oligonucleotides make it difficult to release the therapeutic cargo, dramatically decreasing the transfection yields.[6-8]

Thanks to advances in polymer and materials chemistry, stimuli responsive gene delivery systems have made significant progress in the last few years.[9,10] These systems are able to respond to various stimuli and either trigger release of the transported nucleic acid, or promote endosomal escape of the carrier to the cell cytoplasm.[11] Examples of endogenous stimuli include: intracellular changes in pH environment,[12] change in redox environment,[13] temperature difference,[14] or the presence of enzymatic triggers;[15] while exogenous stimuli include: light,[16] ultrasound,[17] or even magnetism.[18]

A major shortcoming of these stimuli-responsive systems lies in the toxicity of the cationic polymers remaining after the oligonucleotide release. In response, increasing attention is being directed towards developing degradable or charge altering polymers

with biocompatible by-products. Degradability can either be introduced in the polymer backbone, or through degradable polymer side chains. In the early 2000's, the Langer group prepared poly(β-amino esters) *via* Michael addition step growth polymerisation of diamines and diacrylates, resulting in cationic polymers with a degradable backbones and cationic groups for DNA complexation.[19,20] In another example, Saltzman *et al*. encapsulated genetic material in poly(lactic-co-glycolic acid) (PLGA) to deliver siRNA efficiently through cervical mucus barrier in mice models.[21] Backbone degradable polymers based on oligo(carbonate-*b*-α-amino ester)s were also shown to be efficient gene delivery vectors.[22] Introduction of polymer degradability through the polymer side chains, leading to biocompatible and non-toxic degradation products, has also been studied extensively by the group of Hennink among others.[23-25] The degradable side chain route however also has the added advantage of being able to incorporate a change in functionality and/or charge with side chain degradation. For example, polymers synthesised from 2-(dimethylamino)ethyl acrylate (DMAEA) have been investigated for the complexation and release of nucleic acids *via* hydrolysis of the ester connection between acrylate backbone and side chains.[26-28] Poly(DMAEA) proved to be an attractive polymer for non-viral gene delivery whose initial structure combines hydrolysable side chains with cationic groups. Upon hydrolysis, cationic side chains turn into negatively charged acrylic acid moeities which enhance nucleic acid release *via* electrostatic repulsion. The self-catalysed hydrolysis of pDMAEA in water was initially reported to reach a limiting degree of hydrolysis of 60 to 70 % after one week in aqueous conditions at room temperature.[29] More recent studies confirmed that the hydrolysis and nucleic acid release occurs rapidly (1 to 10 hours[28]), and is consistent with a self-catalysed mechanism at a rate that is independent of pH, salt concentration, or any other external stimulus.[27,30-32] A number of strategies have been employed to lengthen this release time, but it is yet to be extended past 72 hours.[33,34]

Sustained release of nucleic acids for inducing RNA interference is acknowledged as a major challenge for the gene delivery field, in the context of both human therapies and agrochemical applications. For example, in mammalian biological systems, slow release is needed when considering drug eluting device coatings/stents, local injection hydrogel

systems, or implantable macroscale devices.[35-37] In the agrochemical sector this nucleic acid slow release is useful for one application sprays, and also seed coatings. Here, the prolonged protection and sustained release of dsRNA from synthetic polymers prepared via reversible addition-fragmentation chain transfer (RAFT) polymerisation is reported. Highly branched polymers of 2-(dimethylamino)ethyl acrylate (DMAEA), 3-(dimethylamino)propyl acrylate (DMAPA), 2-(dimethylamino)ethyl methacrylate (DMAEMA), and also statistical copolymers of DMAEA and DMAEMA were synthesised using di(ethylene glycol) diacrylate (DEGDA) or ethyleneglycol dimethacrylate (EGDMA) as cross-linkers. Two different synthetic routes will be attempted in order to slow the side chain hydrolysis of tertiary amine containing polymers. Firstly, by polymerising DMAPA, a monomer with a propyl chain rather than the ethyl of DMAEA. Secondly, by copolymerising DMAEA with DMAEMA, a non-hydrolysing equivalent monomer.[38] The branched polymers were characterized using multi-detector size exclusion chromatography (SEC) and their hydrolysis kinetics were followed with ^{1}H NMR spectroscopy. Polyplex formation and dsRNA release was then investigated using agarose gel electrophoresis. Finally, polymer cytotoxicity was determined before and after side chain hydrolysis in relation to a model fibroblast cell line.

4.2 Results and Discussion

4.2.1 Synthesis of highly branched polymers by RAFT

RAFT polymerisation was used to synthesise a series of highly branched polymers from a range of tertiary amine-containing vinyl monomers and divinyl branching comonomers (**Scheme 4.1**). Reaction temperature, initiator, chain transfer agent (CTA), and branching comonomer, were varied depending on monomer composition. Acrylate monomers (DMAEA, DMAPA and DEGDA) were polymerised at 70 ºC using PABTC as CTA, and ACVA as initiator. Methacrylate monomers (DMAEMA and EGDMA) were polymerised at 90 ºC using CPAETC as CTA, and VA088 as initiator. Copolymers of acrylate and methacrylate were polymerised at 70 ºC using CPAETC as CTA and ACVA

as initiator. Either EGDMA or DEGDA was used as branching comonomer depending on the major proportion of monomer being acrylate or methacrylate. Having a branching monomer with similar reactivity as the main monomer feed increases its insertion into the backbone during the propagation step. Based on previous work, a degree of polymerisation (DP) of 50 with 0.95 – 2.5 branching monomers per CTA was targeted in order to form soluble highly branched polymers with similar and high molecular weights but without gelation.[39] Linear equivalents of the branched DMAEMA/DMAEA copolymers were also synthesised, in order to identify any possible differences of polymer architecture on rate of hydrolysis.

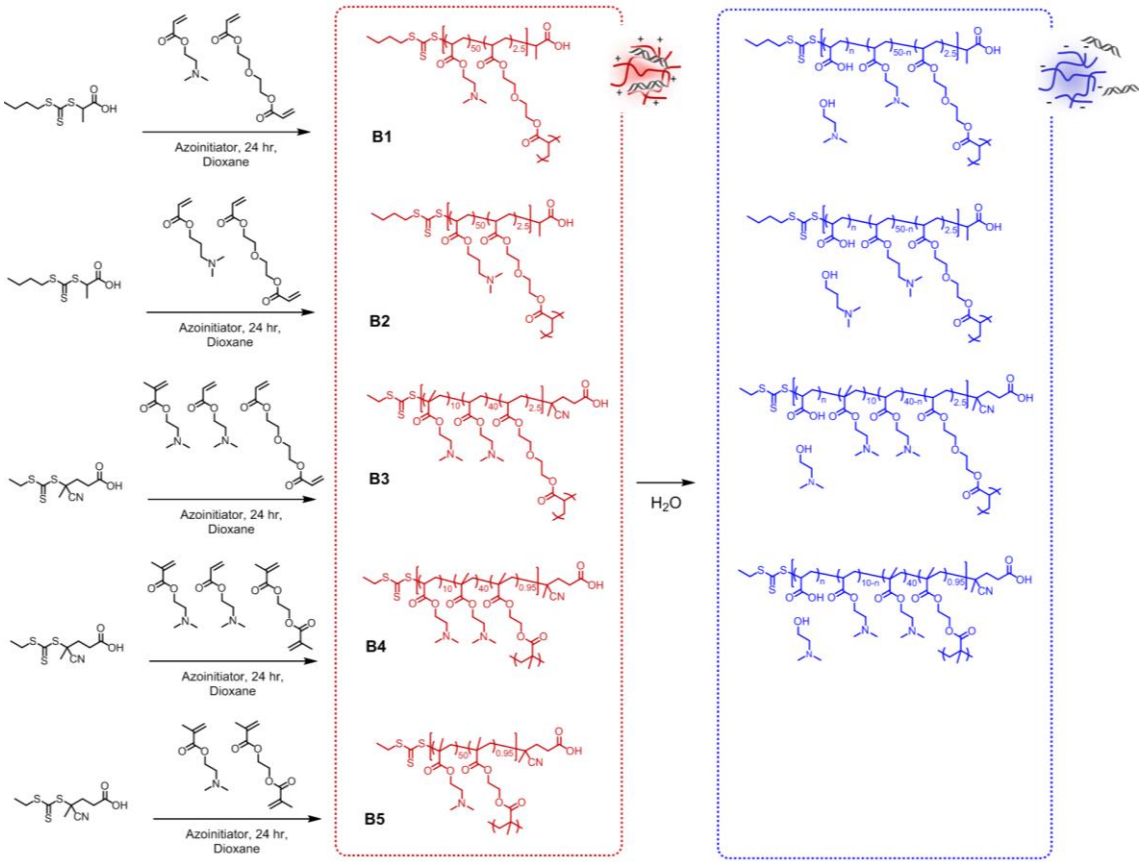

Scheme 4.4. Synthesis of highly branched polymers (**B1**-**B5**) via RAFT polymerisation of tertiary amine-containing monomers (DMAEA, DMAPA, and DMAEMA) and divinyl branching monomers along with decomposition products from hydrolysis in aqueous/physiological conditions.

SEC traces for the resulting branched polymers show a broad molecular weight distribution, as expected for branched polymerisation systems (**Figure 4.1a**). The molecular weights of the polymers were determined to be between 100,000 – 200,000 g/mol using light scattering detection SEC, as seen in **Table 4.1**. Information about the branched nature of the polymers was extracted from the intrinsic viscosity values measured by the viscometry detector. The Kuhn-Mark-Houwink-Sakurada α values for each polymer was calculated from plotting the log of intrinsic viscosity against the log of molecular weight (α = gradient) (**Figure 4.1b**). An α value of between 0.6 and 0.8 corresponds to random coil in good solvent whereas lower values indicates more dense structures close to the hard sphere model typically used for branched or star architectures. **Table 4.1** shows the α values obtained for the synthesised polymers. For most linear polymers α values typically fall between 0.6 – 0.8. The synthesised branched polymers had α values of between 0.36 – 0.53 as expected for more dense globular structures. ^{1}H NMR spectra of the purified polymers are shown in **Figure 4.1c**, however because of the branched nature of the polymers it was not possible to get molecular weight values from the NMR spectra.

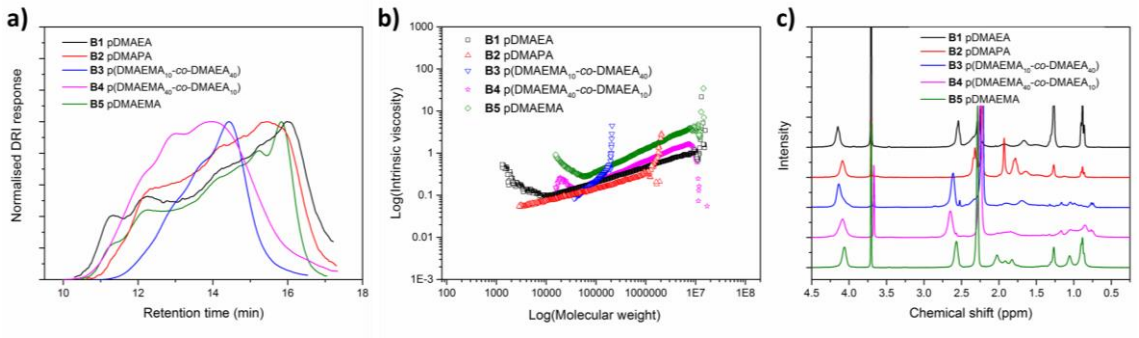

Figure 4.1. a) Size-exclusion chromatograms (normalised DRI detector response vs retention time) for the branched polymers; **b)** Kuhn-Mark-Houwink-Sakurada (KMHS) plots of log intrinsic viscosity against log molecular weight from SEC viscosity detector in $CHCl_3$ eluent; **c)** ^{1}H NMR spectra of tertiary amine containing highly branched polymers in deuterated chloroform.

Table 4.6. Characterisation of branched and linear polymers prepared in this study, including compositions, molecular weights, dispersity, and Kuhn-Mark-Houwink-Sakurada alpha values.

Sample	Structure	M1 : M2 : M3 : B : CTA [a]	$M_{n,SEC}$ (g/mol) [b]	$M_{w,SEC}$ (g/mol) [b]	$Đ$ [b]	$M_{w,MALLS}$ (g/mol) [c]	α [d]
B1	p(DMAEA$_{50}$-*co*-DEGDA$_{2.5}$)	0 : 50 : 0 : 2.5 : 1	19,000	268,000	14	299,000	0.36
B2	p(DMAPA$_{50}$-*co*-DEGDA$_{2.5}$)	0 : 0 : 50 : 2.5 : 1	22,000	168,000	7.6	193,000	0.53
B3	p(DMAEMA$_{10}$-*co*-DMAEA$_{40}$-*co*-DEGDA$_{1.5}$)	10 : 40 : 0 : 1.5 : 1	18,100	31,100	1.7	66,600	0.53
B4	p(DMAEMA$_{40}$-*co*-DMAEA$_{10}$-*co*-EGDMA$_{1.5}$)	40 : 10 : 0 : 1.5 : 1	17,600	54,900	3.1	134,000	0.42
B5	p(DMAEMA$_{50}$-*co*-EGDMA$_{0.95}$)	50 : 0 : 0 : 0.95 : 1	27,000	218,000	8.2	275,000	0.41
L1	p(DMAEMA$_{10}$-*co*-DMAEA$_{40}$)	10 : 40 : 0 : 0 : 1	7,300	9,000	1.24	8,200	0.56
L2	p(DMAEMA$_{40}$-*co*-DMAEA$_{10}$)	40 : 10 : 0 : 0 : 1	7,100	9,800	1.37	8,400	0.61

[a] Ratio of monomer 1 (DMAEMA) to monomer 2 (DMAEA) to monomer 3 (DMAPA) to brancher (EGDMA or DEGDA) to CTA. [b] From $CHCl_3$ SEC, DRI detector, linear PS standard. [c] Absolute molecular weight from light scattering detection on $CHCl_3$ SEC. [d] α = Kuhn-Mark-Houwink-Sakurada parameter, from $CHCl_3$ SEC viscometry detector.

4.2.2 Determination of DMAEMA and DMAEA reactivity ratios

To better understand the copolymerisation of DMAEA and DMAEMA, the kinetics of their polymerisation was studied using ^{1}H NMR spectroscopy. A statistical copolymer of DP 50 containing 50% DMAEA and 50% DMAEMA was targeted (see polymerisation conditions in appendix). The conversion rate of each monomer, reported in **Figure 4.2a**, shows that the methacrylate is incorporated into the polymer faster than the acrylate. This trend, expected in the case of acrylate and methacrylate copolymerisations, could lead to slightly gradient like nature of the polymer.[40] For example, differences in monomer reactivity ratios in the copolymerisation of butyl acrylate and methyl methacrylate of rBA

= 0.36 and rMMA = 2.07 (rBA x rMMA = 0.75) lead to a copolymer with a higher proportion of MMA incorporation in the beginning of the polymerisation.[41]

To further investigate the possible gradient-like nature of the copolymers of DMAEA and DMAEMA, the reactivity ratios of this comonomer system have been determined in typical RAFT conditions using three different calculation methods based on the same experimental data. For this purpose, a series of copoplymers containing 10%, 30%, 50%, 70%, and 90% of DMAEA were prepared. DP 50 was targeted and the polymerization were stopped at less than 10% total monomer conversion. The reactivity ratios were then calculated using the Fineman Ross method (rDMAEMA = 2.55 and rDMAEA = 0.93), the Kelen Tudos linearization method (rDMAEMA = 2.29, rDMAEA = 0.71), and using a non-linear regression method based on a data fit of the copolymer equation (rDMAEMA = 2.13, rDMAEA = 0.69) (see appendix). The last method, generalized by Van Herk in the 1990's, is considered to be more accurate as is doesn't rely of linearization of the data.[42,43] **Figure 4.2b** shows the plot of monomer incorporation ratio against monomer feed ratio and the non-linear regression fit of the data which gives values for the reactivity ratios. All three methods give values which are in good agreement, and indicate that DMAEMA has a tendency for self-propagation. The multiplication of reactivity ratios (rDMAEMA x rDMAEA = 1.47) indicates a slight gradient tendency in the polymerisation.[44] However, when many chains (DP = 50) with slight monomer gradient are linked together in a statistical manner (as in the branched polymer synthesis), the effect of the gradient in the branched polymers should be greatly reduced.

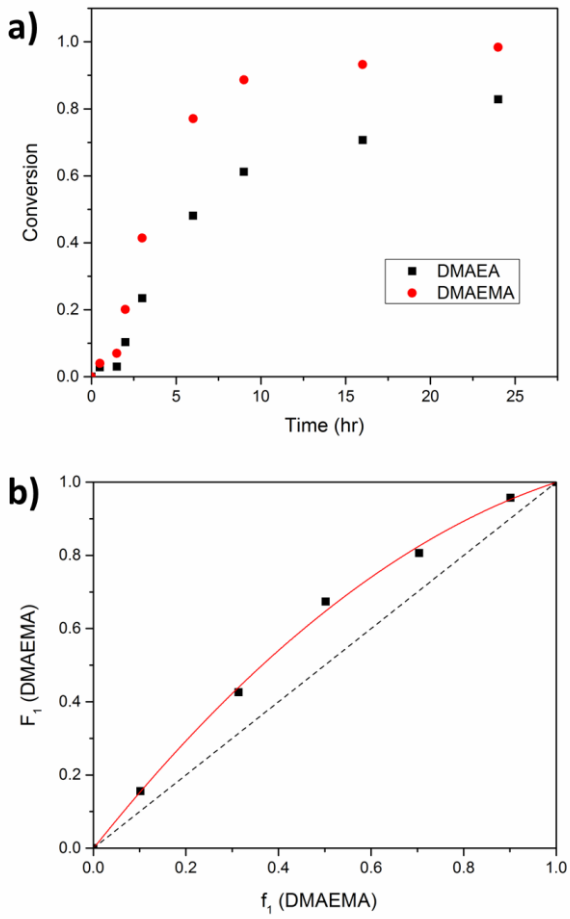

Figure 4.6. a) Monomer conversion against time for a statistical copolymer of DP = 50 containing 50 % DMAEA and 50 % DMAEMA, as determined by ^{1}H NMR spectroscopy; **b)** Monomer incorporation ratio (F_1) against monomer feed ratio (f_1) (dots), including the non-linear regression fit of the data (red curve, giving rDMAEMA = 2.13, rDMAEA = 0.69), dashed line represents $F_1 = f_1$.

4.2.3. Polymer hydrolysis kinetic study

The self-catalysed hydrolysis of pDMAEA in water was first reported in 1989, and was found to reach a limiting degree of hydrolysis of ~ 60 or 70 % after one week in aqueous conditions at room temperature.[29] More recent studies have also found the hydrolysis to occur rapidly, and to be consistent with a self-catalysed mechanism at a rate that is independent of pH, salt concentration, or any other external stimulus.[27,30-32] The hydrolysis kinetics of the branched tertiary amine-containing polymers were studied

using ^{1}H NMR spectroscopy in D_2O (pH ~ 7.4). **Figure 4.3a** shows the ^{1}H NMR spectra of branched p(DMAEMA$_{10}$-*co*-DMAEA$_{40}$) over a period of 20 days. ^{1}H NMR spectra of hydrolysis study of remaining polymers can be found in the appendix. The hydrolysis of DMAEA units in the polymer results in the appearance of sharp peaks at ~3.7 ppm, 2.9 ppm, and 2.6 ppm, due to the creation of dimethylaminoethanol hydrolysis product. Integration of these peaks in comparison with the peak 4.2 ppm representing the total sum of monomer units was used to calculate the percentage hydrolysis. The resulting hydrolysis kinetic profiles are presented in **Figure 4.3b**. Branched pDMAEA hydrolyses relatively fast at first (40 % hydrolysed after 17 hours), then slows down to reach approximately 70 % hydrolysis after 20 days. As expected, the methacrylate polymer pDMAEMA does not shown any significant sign of hydrolysis after 20 days. While branched p(DMAEMA$_{10}$-*co*-DMAEA$_{40}$) hydrolyses with a similar initial rate as pDMAEA homopolymer, introduction of 20% of methacrylate unit in p(DMAEMA$_{10}$-*co*-DMAEA$_{40}$) resulted in an hydrolysis rate that is relatively similar to pDMAEA homopolymer in the first few hours, but which only reaches 50 % hydrolysis after 20 days. Branched pDMAPA reached a similar value of around 50 % hydrolysis after 20 days, but with a slower initial gradient. Branched copolymer p(DMAEMA$_{40}$-*co*-DMAEA$_{10}$) showed very little hydrolysis and reaches a plateau of around 5 % hydrolysis after 3 days.

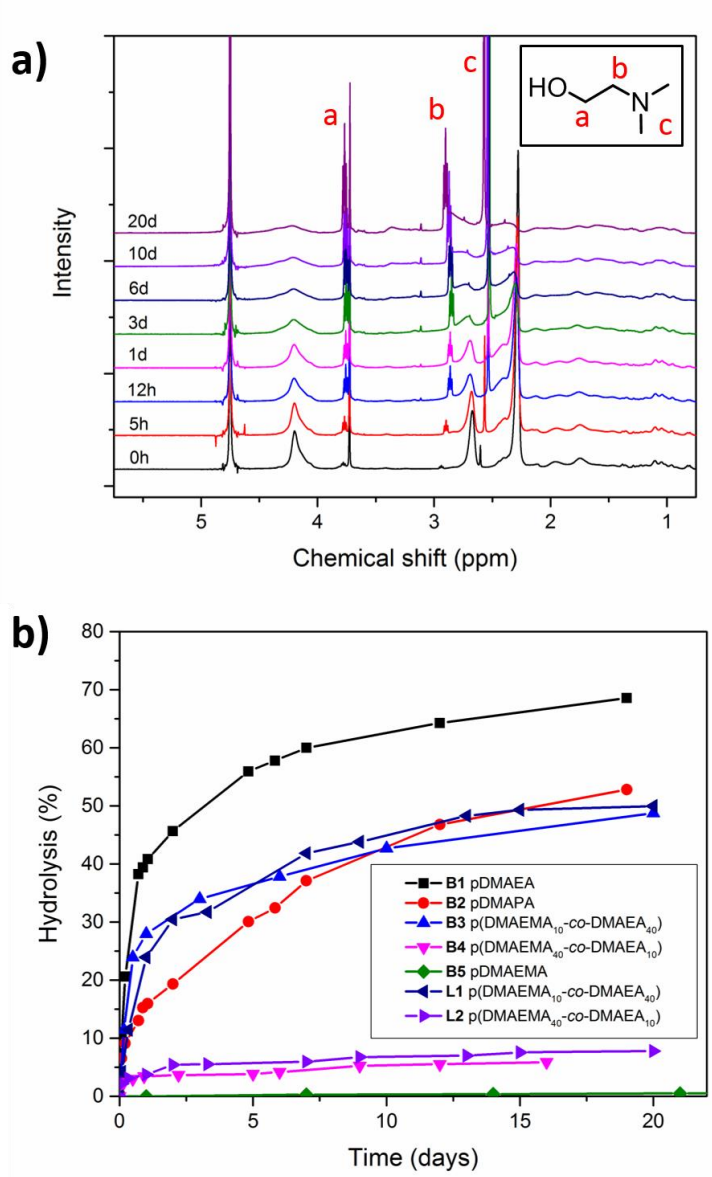

Figure 4.3. a) Hydrolysis of branched p(DMAEMA$_{10}$-*co*-DMAEA$_{40}$) in D_2O (pH ~7.4) as determined using ^{1}H NMR spectroscopy; (other polymers shown in appendix); **b)** Hydrolysis kinetics of synthesised branched and linear polymers in D_2O (pH ~7.4) determined using ^{1}H NMR spectroscopy.

One hypothesis is that the hydrolysis of DMAEA in methacrylate acrylate copolymers is slowed by the more hydrophobic nature of the polymer backbone associated with methacrylate introduction. This is exemplified by the copolymer of 20% DMAEA (**B4** and **L2**) proceeding to 5% hydrolysis instead of the expected value or around 15-20%.

It is worth noting that hydrolysis of 50% of the side chains of these polymers would result in zwitterionic polymers with an overall neutral charge, thus losing their ability to complex negatively charge dsRNA. Therefore, the two systems reaching 50% hydrolysis after a period of weeks, both p(DMAEMA$_{10}$-*co*-DMAEA$_{40}$) and pDMAPA, were thought to be good candidates for slow dsRNA release.

4.2.4. Polyplex formation and dsRNA release

Complexation of the branched polymers with dsRNA to form polyplexes was characterised by DLS and zetapotential measurements, as well as agarose gel electrophoresis. The later technique showed complete complexation of dsRNA by all the branched polymers for N/P ratios of either 1 or 2 (**Figure A4.7**). Therefore, an N/P ratio of 5 was chosen to characterise polyplex physiochemical properties in terms of size and surface charge (**Table 4.2**).

Table 4.7. Size and surface charge (zetapotential) of polyplexes formed by complexation of dsRNA with polymers at N/P = 5, as measured by dynamic light scattering and electrophoretic light scattering.

Polyplex (N/P 5)	Zetapotential (mV)	Size by number (d.nm)	PDI
B1 pDMAEA	+15.1 ±1.4	488.9 ±87.1	0.53
B2 pDMAPA	+14.8 ±1.3	456.8 ±123.1	0.41
B3 p(DMAEMA$_{10}$-*co*-DMAEA$_{40}$)	+15.3 ±1.5	448.4 ±65.3	0.85
B4 p(DMAEMA$_{40}$-*co*-DMAEA$_{10}$)	+15.8 ±1.3	336.9 ±45.8	0.55
B5 pDMAEMA	+15.0 ±1.3	399.7 108.9	0.33
L1 p(DMAEMA$_{10}$-*co*-DMAEA$_{40}$)	+14.3 ±1.3	541.1 ±100.6	0.58
L2 p(DMAEMA$_{40}$-*co*-DMAEA$_{10}$)	+15.7 ±1.4	488.7 ±90.5	0.47

All of the synthesised polymers appeared to form polyplexes with an overall positive charge of between 14 to 16 mV. Polyplex sizes were also found to be similar, with most polyplex diameters measured between 300 and 500 nm. The polydispersity values (**Table 4.2**) indicate a very broad distribution of sizes for the polyplexes in solution. Representative intensity distributions, volume distributions, number distributions, correlallograms, and cummulants fits can be found in the appendix. It is worth noting that this set of values represents a crude estimation of the real size of the polyplexes, as measurement by DLS is subject to significant error when assuming spherical shape.

Next, an agarose gel electrophoresis experiment was designed to correlate polymer side chain hydrolysis and charge reversal of the polymers to an observable release of dsRNA. Polyplexes were formed in sterile water at an N/P ratio of 5, and divided into separate microtubes for each sample time point, following which the samples were frozen at the appropriate time before being simultaneously analysed by agarose gel electrophoresis.

Pictures of the gels are shown in **Figure 4.4**. When the dsRNA is bound in a positively charged polyplex nanoparticle, the dsRNA band can be seen at the top of the gels in the well. Whereas negatively charged unbound dsRNA will move through the gel, resulting in a band at the bottom of the gel. It can be seen that all the synthesised polymers form strongly bound dsRNA polyplexes on day 0, apart from branched pDMAEA homopolymer which has already started to release the dsRNA over the course of sample preparation and/or gel preparation (**Figure 4.4a**). Both linear and branched p(DMAEMA$_{10}$-*co*-DMAEA$_{40}$) (**Figure 4.4b** and **4.4c** respectively) start to release dsRNA after one day, and continue to release dsRNA over the course of more than 14 days as the polymer slowly hydrolyses and the band corresponding to dsRNA moves down the gel towards the location of uncomplexed dsRNA. For these samples, complete dissociation from the dsRNA is observed after 21 days. Branched p(DMAPA) homopolymer showed a slower initial release (**Figure 4.4d**) with dsRNA remaining complexed for three days prior to releasing dsRNA. Full dissociation of dsRNA from the polymer was observed after 14 days. Both linear and branched p(DMAEMA$_{40}$-*co*-DMAEA$_{10}$) show no dsRNA release over the course of the study (**Figure 4.4e** and **4.4f**), which is consistent with the very low percentage of hydrolysis for these polymers.

Accordingly, branched pDMAEMA homopolymer, which does not undergo hydrolysis of the side chains, showed no dsRNA release.

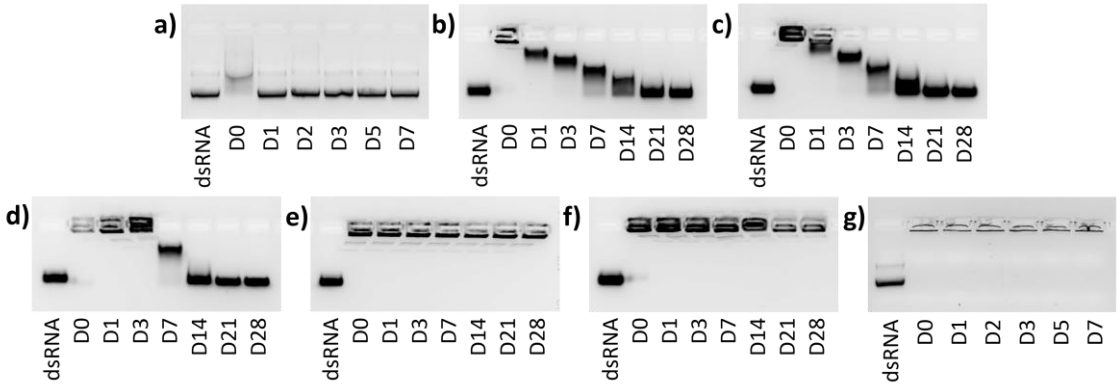

Figure 4.4. Agarose gel electrophoresis assay of branched cationic polymer – dsRNA polyplex nanoparticles (all at N/P ratio 5) over time periods up to 28 days; **a)** branched pDMAEA; **b)** linear p(DMAEMA$_{10}$-*co*-DMAEA$_{40}$); **c)** branched p(DMAEMA$_{10}$-*co*-DMAEA$_{40}$); **d)** branched pDMAPA; **e)** linear p(DMAEMA$_{40}$-*co*-DMAEA$_{10}$); **f)** branched p(DMAEMA$_{40}$-*co*-DMAEA$_{10}$); **g)** branched pDMAEMA.

Overall, the results appear in accordance with the hydrolysis kinetic profiles of the polymers, and confirm the potential of the synthesised polymers for gene delivery applications. Branched pDMAPA shows potential for delayed gene delivery applications, where release of oligonucleotides is required approximately one week after application. To the best of our knowledge, this study is the first to characterise the hydrolysis of pDMAPA and demonstrate its use for oligonucleotide complexation and controlled release.

Copolymers of DMAEA and DMAEMA appear to be better suited for extended release of oligonucleotides, as they were shown to release dsRNA from day 1 to past day 14. This slow release profile can be attributed to the presence of non-hydrolysable DMAEMA groups, which remain positively charged throughout the degradation process. These polymers show dsRNA release for over two weeks, which is a significant improvement

over the pDMAEA and pDMAPA release profiles. Such sustained dsRNA release profiles would be useful for single injection gene silencing over periods of weeks.

The ability of the synthesised branched polymers to protect dsRNA from nuclease degradation in soil applications was also studied. Polyplexes were formed in sterile water at an N/P ratio of 5 with a final concentration of 1 mg/mL dsRNA, then incubated in live soil or enzyme free soil. A protocol for the extraction of dsRNA from the soil was carried out after the appropriate incubation period, and finally and agarose gel was run in order to determine whether the recovered dsRNA was intact (**Figure A4.13** and **A4.14**). The results show that uncomplexed dsRNA is degraded in soil after one day, but when the dsRNA is condensed in a polyplex with branched pDMAEMA, pDMAPA, or pDMAEA, it is protected from enzymatic degradation for up to seven days.

4.2.5. Polymer cytotoxicity

The hydrolysis of pDMAEA into biocompatible and non-cytotoxic poly(acrylic acid) (pAA) and N,N-dimethylamino ethanol (DMAE) is a feature used in biomedical applications. PAA has been shown to be non-toxic to mammalian cell lines both *in vitro* and also *in vivo*,[45,46] While DMAE is approved and safely used in the cosmetics and the neutraceutical industries. Toxicity of synthesised polymers was investigated before and after hydrolysis against a model non-cancerous cell line, NIH-3T3 fibroblast. Branched polyethylenimine (bPEI), commonly used for gene delivery purposes, was also included for comparison. **Figure 4.5a** shows the relative percentage of viable cells following 24 hours incubation with the polymers before hydrolysis. Branched pDMAEMA and p(DMAEMA$_{40}$-*co*-DMAEA$_{10}$) showed a toxicity profile similar to that of bPEI, with complete death of the cells at concentrations above 50 μg/mL. Branched pDMAPA and p(DMAEMA$_{10}$-*co*-DMAEA$_{40}$) showed a less toxic profile with zero cell survival at concentrations above 200 μg/mL and 2 mg/mL, respectively. In contrast, the other polymers appeared to be relatively non-cytotoxic under the conditions tested. The trend of polymer toxicities appear to match the trend of hydrolysis profiles with the more hydrolysable polymers being less toxic. This can be attributed to the conversion of

potentially toxic cationic polymers into biocompatible poly(acrylic acid) over the time of the experiment.

Figure 4.5b shows the toxicity profiles determined for the same polymers but after a 2 week pre-incubation in water at room temperature, following which polymers are expected to be almost completely hydrolysed. As expected, the non-hydrolysable polymers pDMAEMA and bPEI, have similar toxicity profiles to before incubation in water. The branched copolymer with majority DMAEMA monomer, p(DMAEMA$_{40}$-*co*-DMAEA$_{10}$), showed a slightly reduced toxicity compared to the non-hydrolysed version, which can be attributed to the hydrolysis of the small amount of DMAEA units. All other polymers tested showed no toxicity under the conditions studied, illustrating the conversion from toxic cationic polymer to non-toxic pAA.

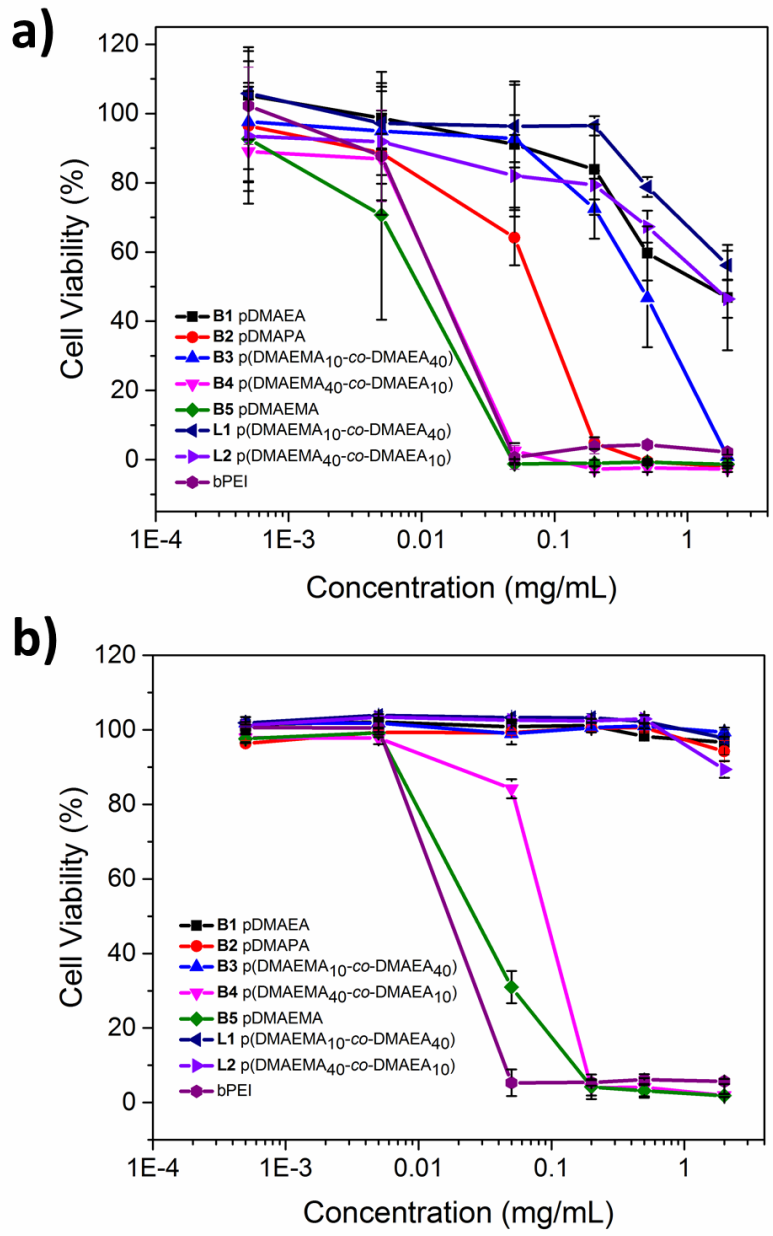

Figure 4.5. NIH-3T3 cell viability following 24h incubation in the presence of branched and linear polymers, as determined using XTT assay; **a)** initial polymers; **b)** polymers pre-incubated for 2 weeks in D2O at pH ~ 7.4.

4.3. Conclusions

Highly branched polymers were synthesised with RAFT polymerisation of hydrolysable acrylate monomers containing tertiary amine functionality (DMAEA, DMAPA), non-hydrolysable methacrylate counterpart (DMAEMA), and branching divinyl comonomers (EGDMA and DEGDA). The highly branched nature of these polymers was characterised using multi-detector SEC, and the copolymers were found to have a slightly gradient nature from calculation of the monomer reactivity ratios of the DMAEA and DMAEMA. Hydrolysis kinetics of the polymers were studied with ^{1}H NMR spectroscopy, and showed pDMAPA and p(DMAEMA-*co*-DMAEA) to have hydrolysis profiles favourable for extended release of dsRNA compared to the fast hydrolysing pDMAEA. All the materials were shown to form polyplexes in presence of dsRNA and were characterized by DLS and agarose electrophoresis gels. The dsRNA release profiles of polyplex nanoparticles were also determined using agarose gel electrophoresis and both branched pDMAPA and p($DMAEMA_{10}$-*co*-$DMAEA_{40}$) showed excellent prolonged release of oligonucleotide in aqueous conditions. Finally, the polymer cytotoxicity to NIH-3T3 fibroblast cell line was determined both before and after side chain hydrolysis. The most promising materials, pDMAPA and p($DMAEMA_{10}$-*co*-$DMAEA_{40}$), show negligible toxicity in the appropriate concentration range (50 - 200 μg/mL) even before complete hydrolysis to biocompatible p(acrylic acid). Whereas non-hydrolysable branched pDMAEMA, bPEI, and also branched p($DMAEMA_{40}$-*co*-$DMAEA_{10}$), had significant toxicity with zero cell proliferation above concentrations of 50 μg/mL. These polymeric materials show great potential for therapeutic nucleic acid delivery as polyplexes, but could also represent an improved material for hydrogel formulations, nucleic acid releasing films, or other implantable or injestable polymeric constructs for controlled release.

4.4. Experimental

4.4.1. Materials

2-(dimethylamino)ethyl acrylate (DMAEA), 2-(dimethylamino)ethyl methacrylate (DMAEMA), 3-(dimethylamino)propyl acrylate (DMAPA), ethyleneglycol dimethacrylate (EGDMA), di(ethylene glycol) diacrylate (DEGDA), 4,4′-Azobis(4-cyanovaleric acid) (ACVA), 1,1′-Azobis(cyclohexanecarbonitrile) (VA088), polyethylenimine branched (bPEI, Mw ~25,000 by LS, Mn ~10,000 by SEC), Agarose, Ethidium bromide solution (500 μg/mL in H_2O), were all obtained from Sigma-Aldrich. All other materials were purchased from Fisher Scientific, or Sigma-Aldrich. dsRNA was provided by Syngenta. 2-(((butylthio)-carbonothioyl)thio)propanoic acid (PABTC) was prepared according to a previously reported procedure.[47] (4-cyano pentanoic acid)yl ethyl trithiocarbonate (CPAETC) was prepared according to a previously reported procedure.[48] 50X Tris-Acetate-EDTA (TAE) buffer for gel electrophoresis was made up at concentration of 2.0M Tris acetate (Sigma Aldrich) and 0.05M EDTA (Sigma Aldrich) in deionised water, pH 8.2 - 8.4, stored at room temperature. Gel loading buffer for samples (colourless) was made up at 30% (vol/vol) glycerol (Sigma Aldrich) in deionised water and stored at room temperature. 2,3-Bis(2-methoxy-4-nitro-5-sulfophenyl)-2H-tetrazolium-5-carboxanilide inner salt (XTT sodium salt), and Phenazine methosulfate (PMS) were obtained from Sigma.

4.4.2. Characterisation

Size Exclusion Chromatography (SEC) was performed in $CHCl_3$, using an Agilent 390-LC MDS instrument equipped with differential refractive index (DRI), viscometry, dual angle light scattering, and dual wavelength UV detectors. The system was equipped with 2 x PLgel Mixed D columns (300 x 7.5 mm) and a PLgel 5 μm guard column. The eluent was $CHCl_3$ with 2% TEA (trimethylamine) additive, and samples were run at 1 mL/min at 30 °C. Analyte samples were filtered through a nylon membrane with 0.22 μm pore size before injection. Apparent molar mass values ($M_{n,SEC}$ and $M_{w,SEC}$) and dispersity ($Đ$) of synthesized polymers were determined by DRI detector and conventional polystyrene

(Agilent EasyVials) calibration and using Agilent SEC software. The absolute/true molecular weight ($M_{w,MALLS}$) and the intrinsic viscosity (IV) were determined by triple-detection SEC method using Agilent software and considering 100% polymer mass recovery (knowing the concentration). The Kuhn-Mark-Houwink-Sakurada parameter α, relating to polymer conformation in solution was determined from the gradient of the double logarithmic plot of intrinsic viscosity as a function of molecular weight, using Agilent SEC software. Proton nuclear magnetic resonance spectra (^{1}H NMR) were recorded on a Bruker Advance 400 or 300 spectrometer (400 MHz or 300 MHz) at 27 °C, with chemical shift values (δ) reported in ppm, and the residual proton signal of the solvent used as internal standard. Proton-decoupled carbon nuclear magnetic resonance spectra (^{13}C NMR) were recorded on a Bruker Advance 400 (100 MHz) at 27 °C in $CDCl_3$, with chemical shift values (δ) reported in ppm, and the residual proton signal of the solvent used as internal standard (δC 77.16). Fourier transform infrared spectra (FTIR) were recorded on a Bruker Alpha FTIR ATR.

4.4.3. Synthesis of branched acrylates pDMAEA and pDMAPA

Conditions for polymerisations can be found in Supporting Information.

For a typical polymerisation in which [M]: [DEGDA]: [PABTC]: [I] = 50: 2.5: 1: 0.1, PABTC (33.3 mg, 0.140 mmol), DMAEA (1 g, 6.98 mmol), DEGDA (74.8 mg, 0.35 mmol), ACVA (3.9 mg, 0.0140 mmol), and dioxane (1.19 mL) were added to a vial deoxygenated by bubbling with nitrogen and left to stir in an oil bath at 70 °C. After a predetermined time, the solution was removed from the oil bath and the polymer precipitated in hexane (x3), and dried under vacuum. $M_{w,MALLS}$ = 299,000 g/mol, $Đ_{,RI}$ = 14 ($CHCl_3$ SEC, multi-detector). ^{1}H NMR spectrum (400 MHz, $CDCl_3$, δ ppm): 4.15 (m, 2H, -C(O)O-C**H$_2$**-CH_2-NMe_2), 2.55 (m, 2H, -C(O)O-CH_2-C**H$_2$**-NMe_2), 2.27 (m, 6H, -CH_2-N**Me$_2$**), 2.11−0.91 (m, 3H, backbone). ^{13}C NMR spectrum (100 MHz, $CDCl_3$, δ ppm): 174.28 (-**C**(O)O-), 62.33 (-C(O)O-**C**H_2-CH_2-), 57.52 (-**C**H_2-$N(CH_3)_2$), 45.71 (-$N(\mathbf{C}H_3)_2$), 41.28 (backbone tertiary), 67.07 (backbone -**C**H2-). FTIR ν cm^{-1}: 2948 (medium, C-H alkane), 2821 and 2768 (medium, N-CH_3 amine), 1728 (strong, C=O

ester), 1455 (medium, C-H alkane), 1251 (medium, C-N, amine), 1153 (strong, C-O ester).

4.4.4. Synthesis of branched methacrylate pDMAEMA

For a typical polymerisation in which [M]: [EGDMA]: [CPAETC]: [I] = 50: 0.95: 1: 0.025, CPAETC (33.5 mg, 0.127 mmol), DMAEMA (1 g, 6.36 mmol), EGDMA (24.0 mg, 0.121 mmol), VA-088 (0.777 mg, 0.00318 mmol), and dioxane (0.974 mL) were added to a vial deoxygenated by bubbling with nitrogen and left to stir in an oil bath at 90 °C. After a predetermined time, the solution was removed from the oil bath and the polymer precipitated in hexane (x3), and dried under vacuum. $M_{w,MALLS}$ = 275,000 g/mol, $Đ_{,RI}$ = 8.2 ($CHCl_3$ SEC, multi-detector). ^{1}H NMR spectrum (400 MHz, $CDCl_3$, δ ppm): 4.07 (m, 2H, -C(O)O-C**H$_2$**-CH_2-NMe_2), 2.57 (m, 2H, -C(O)O-CH_2-C**H$_2$**-NMe_2), 2.29 (m, 6H, -CH_2-N**Me$_2$**), 2.17−0.74 (m, 5H, backbone). ^{13}C NMR spectrum (100 MHz, $CDCl_3$, δ ppm): 177.36 (-**C**(O)O-), 63.03 (-C(O)O-**C**H_2-CH_2-), 57.09 (-**C**H_2-N(CH_3)$_2$), 45.79 (-N(**C**H_3)$_2$), 44.73 (backbone quaternary), 67.09 (backbone -**C**H_2-), 18.47 (backbone -**C**H_3). FTIR ν cm^{-1}: 2944 (medium, C-H alkane), 2820 and 2769 (medium, N-CH_3 amine), 1722 (strong, C=O ester), 1455 (medium, C-H alkane), 1270-1265 (medium, C-N, amine), 1153 (strong, C-O ester).

4.4.5. Synthesis of branched copolymer p(DMAEMA$_{40}$-*co*-DMAEA$_{10}$)

For a typical polymerisation in which [DMAEMA]: [DMAEA]: [EGDMA]: [CTA]: [I] = 40: 10: 1.5: 1: 0.05, CPAETC (21.06 mg, 0.0801 mmol), DMAEMA (0.503 g, 3.204 mmol), DMAEA (0.115 g, 0.801 mmol), EGDMA (23.76 mg, 0.120 mmol), ACVA (1.12 mg, 0.0040 mmol), and dioxane (0.673 mL) were added to a vial deoxygenated by bubbling with nitrogen and left to stir in an oil bath at 70 °C. After a predetermined time, the solution was removed from the oil bath and the polymer precipitated in hexane (x3), and dried under vacuum. $M_{w,MALLS}$ = 134,000 g/mol, $Đ_{,RI}$ = 3.1 ($CHCl_3$ SEC, multi-detector). ^{1}H NMR spectrum (400 MHz, $CDCl_3$, δ ppm): 4.13 (m, 2H, -C(O)O-C**H$_2$**-CH_2-NMe_2), 2.69 (m, 2H, -C(O)O-CH_2-C**H$_2$**-NMe_2), 2.29 (m, 6H, -CH_2-N**Me$_2$**), 2.18−0.77

(m, 5H, backbone). ^{13}C NMR spectrum (100 MHz, $CDCl_3$, δ ppm): 177.31 (-**C**(O)O-), 63.02 (-C(O)O-**C**H_2-CH_2-), 57.07 (-**C**H_2-N(CH_3)$_2$), 45.78 (-N(**C**H_3)$_2$), 44.70 (backbone tertiary), 67.08 (backbone -**C**H_2-), 18.46 (backbone -**C**H_3). FTIR ν cm^{-1}: 2944 (medium, C-H alkane), 2820 and 2769 (medium, N-CH_3 amine), 1722 (strong, C=O ester), 1455 (medium, C-H alkane), 1263-1270 (medium, C-N, amine), 1144 (strong, C-O ester).

4.4.6. Synthesis of branched copolymer p(DMAEMA$_{10}$-*co*-DMAEA$_{40}$)

For a typical polymerisation in which [DMAEMA]: [DMAEA]: [DEGDA]: [CTA]: [I] = 10: 40: 1.5: 1: 0.05, CPAETC (21.06 mg, 0.0801 mmol), DMAEMA (0.126 g, 0.801 mmol), DMAEA (0.458 g, 3.204 mmol), DEGDA (25.68 mg, 0.120 mmol), ACVA (1.12 mg, 0.0040 mmol), and dioxane (0.713 mL) were added to a vial deoxygenated by bubbling with nitrogen and left to stir in an oil bath at 70 °C. After a predetermined time, the solution was removed from the oil bath and the polymer precipitated in diethyl ether (x3), and dried under vacuum. $M_{w,MALLS}$ = 66,600 g/mol, $Đ_{,RI}$ = 1.7 ($CHCl_3$ SEC, multi-detector). ^{1}H NMR spectrum (400 MHz, $CDCl_3$, δ ppm): 4.17 (m, 2H, -C(O)O-C**H$_2$**-CH_2-NMe_2), 2.65 (m, 2H, -C(O)O-CH_2-C**H$_2$**-NMe_2), 2.28 (m, 6H, -CH_2-N**Me$_2$**), 2.05−0.85 (m, 3H, backbone). ^{13}C NMR spectrum (100 MHz, $CDCl_3$, δ ppm): ^{13}C NMR spectrum (100 MHz, $CDCl_3$, δ ppm): 174.26 (-**C**(O)O-), 62.35 (-C(O)O-**C**H_2-CH_2-), 57.53 (-**C**H_2-N(CH_3)$_2$), 45.72 (-N(**C**H_3)$_2$), 67.08 (backbone -**C**H_2-), 19.17 (backbone tertiary). FTIR ν cm^{-1}: 2944 (medium, C-H alkane), 2820 and 2767 (medium, N-CH_3 amine), 1726 (strong, C=O ester), 1455 (medium, C-H alkane), 1263 (medium, C-N, amine), 1155 (strong, C-O ester).

4.4.7. DLS/Zetapotential

Dynamic light scattering measurements of resulting polymers and polyplexes at various N/P ratios were carried out using a Malvern NanoZS Zetasizer instrument (scattering angle of 173°, 10 mW He-Ne laser). For polyplex formation: appropriate amount of polymer stock solution and DNA stock solution were mixed and made up to a total

volume of 1 mL in DI water (final concentration of polymer was 1 mg/mL, in all solutions). The resulting solutions were vortexed incubated for 30 minutes at room temperature and were analysed at 25°C. Each sample was run in triplicate and data was acquired using the software (Malvern Zetasizer) provided. Zeta potential measurements were carried out of the same DLS samples at various N/P ratios using the same instrument, and Malvern disposable folded capillary cell (DTS1070) cuvettes.

4.4.8. Agarose gel electrophoresis

Agarose gels (1% w/v) were prepared with agarose and 1 × TAE buffer with DNAse/RNAse free water. The solution was cooled on the bench for 5 minutes and 100 µL of 0.5 µg/mL ethidium bromide solution was added. The mixture was poured into the casted agarose tray and a comb inserted. The gel was left to set for a minimum of 30 minutes at room temperature. The agarose gels were run in 1× TAE buffer. The final gel was visualized under UV illumination at 365 nm using a UVP benchtop UV transilluminator system. Polyplexes of dsRNA were prepared at various N/P ratios. dsRNA stock solution of 60 µg/mL was prepared sterile water, and polymer stock solution of 300 µg/mL. For polyplex formation: appropriate amount of polymer stock solution and dsRNA stock solution were mixed and made up to a total volume of 100 µL (final concentration of dsRNA was 0.030 µg/µL, in all solutions). Polyplexes were vortexed and incubated at room temperature for 30 minutes. Prior to loading, 30 µL of loading buffer was added to each sample and 20 µL of polyplexes were loaded into the agarose gel wells. Gel electrophoresis was performed at 100 V for 30 minutes.

4.4.9. Agarose gel dsRNA release study

Polyplexes were formed in sterile water at an N/P ratio of 5 with a final concentration of 1 mg/mL dsRNA. Samples were then divided into separate microtubes for each sample time point and stored at room temperature, until the microtubes were frozen at the appropriate time. When all the time points has been collected, samples were defrosted diluted to 100 µg/mL dsRNA. Prior to loading, loading buffer was added to each sample

and 20 µL of polyplexes were loaded into the agarose gel wells. Gel electrophoresis was performed at 100 V for 20 minutes on a 1% agarose gel containing ethidium bromide.

4.4.10. Cell culture

NIH-3T3 mouse fibroblast cells were obtained from the Sigma-Aldrich and used between passages 5 and 15. Cells were grown in DMEM (Dulbecco's Modified Eagle Medium) supplemented with 10% of bovine calf serum, 1% of 2 mM glutamine and 1% penicillin/streptomycin. The cells were grown as adherent monolayers at 310 K under a 5% CO2 humidified atmosphere and passaged at approximately 70–80% confluence.

4.4.11. In vitro toxicity assays

NIH-3T3 mouse fibroblast cells were seeded in a 96 well plate at a density of 1×10^4 cells per well. After 16 hours, the culture medium was replaced by fresh media containing a series of dilution of the polymers. Following 24 hours incubation, the medium was removed and replaced with fresh medium. The cells were incubated with a freshly prepared solution of XTT (0.2 mg/mL) and N-methyl dibenzopyrazine methyl sulfate (250 µM) in medium for 16 hours. Absorbance of the samples was finally measured using a plate reader at 450 nm and 650 nm. The data presented are representative of a minimum of two independent experiments where each sample was measured in triplicate. Errors reported correspond to the standard deviation of the mean. For toxicity assays of polymers after 2-week hydrolysis, the polymers were incubated in sterile water (pH ~7.4) at concentrations of 8 mg/mL. Before incubating with cells, hydrolysed polymer solution was diluted to the appropriate concentration in media.

4.4.12. Polyplex soil stability assay

Polyplexes were formed in sterile water at an N/P ratio of 5 with a final concentration of 1 mg/mL dsRNA. 200 µL of polyplexes were mixed with 0.5 g soil (live soil containing

enzymes, and also sterilised soil (sterilisation conditions: 200 ˚C, 2 hr)) in 2 mL microtubes. Separate microtubes were used for each sample time point and stored at room temperature. At the appropriate time, the reaction was stopped by addition of 1 mL trireagent, vortexing, and incubating for 5 minutes, before storing the sample time point at -20 ˚C.

4.4.13. dsRNA extraction

dsRNA was extracted from the soil in order to analyse the dsRNA by agarose gel electrophoresis. Polyplex/soil/trireagent samples were defrosted, 200 µL of chloroform added, and incubated for 3 minutes at room temperature. Samples were then centrifuged for 15 minutes at 12000 g and 4 ˚C. Supernatant was added to new microtube, isopropanol added (1/1 ratio) to precipitate the RNA, and incubated at for 10 minutes at room temperature. Microtubes were then centrifuged at 12000 g and 4 ˚C for 10 minutes. Supernatant was removed and 500 µL of 70 % ethanol (in RNAse free water) added to the pellet, then centrifuged for 5 minutes at 12000 g and 4 ˚C. The supernatant was removed and the pellet left to dry for 10 minutes before being suspended in 200 µL of RNAse free water. These RNA samples were then enriched for dsRNA following a LiCl purification protocol. LiCl (8M, 67 µL) was added to the 200 uL RNA samples, which were mixed on ice, and incubated for 30 minutes at -20 ˚C. Microtubes were then centrifuged for 20 minutes at 14000 g and 4 ˚C, the supernatant was brought to a new microtube, and LiCl (8M, 133.5 µL) was added. The samples were mixed on ice, incubated for 30 minutes at -20 ˚C, and then centrifuged for 20 minutes at 14000 g and 4 ˚C. The supernatant was removed, the dsRNA pellet washed with 70% ethanol (in RNAse free water, 150 µL), and then centrifuged for 5 minutes at 12000 g and 4 ˚C. The supernatant was removed and the dsRNA pellet left to dry for 5 minutes before being suspended in 20 µL of RNAse free water. These final dsRNA samples were analysed by spectrophotometry (NanoPhotometer NP60 spectrophotometer), and agarose gel electrophoresis. Gel electrophoresis was performed at 100 V for 20 minutes on a 1% agarose gel (1x TAE buffer) containing ethidium bromide.

Appendix to Chapter 4

Polymerisation conditions, linear polymer equivalent SEC chromatograms, polymerisation kinetic data of DMEAMA DMAEA copolymerisation, polymerisation conditions and data for reactivity ratio calculation polymerisations, agarose gel images of polyplex formation, further ^{1}H NMR spectra of polymer hydrolysis, polyplex dsRNA soil stability study agarose gel images.

4.5. References

(1) Yin, H.; Kanasty, R. L.; Eltoukhy, A. A.; Vegas, A. J.; Dorkin, J. R.; Anderson, D. G., Non-viral vectors for gene-based therapy, *Nature Reviews Genetics* **2014**, *15*, 541.

(2) Bessis, N.; GarciaCozar, F. J.; Boissier, M. C., Immune responses to gene therapy vectors: influence on vector function and effector mechanisms, *Gene Ther.* **2004**, *11*, S10.

(3) Thomas, C. E.; Ehrhardt, A.; Kay, M. A., Progress and problems with the use of viral vectors for gene therapy, *Nature Reviews Genetics* **2003**, *4*, 346.

(4) Bouard, D.; Alazard-Dany, N.; Cosset, F. L., Viral vectors: from virology to transgene expression, *Br. J. Pharmacol.* **2009**, *157*, 153.

(5) Kawabata, K.; Takakura, Y.; Hashida, M., The Fate of Plasmid DNA After Intravenous-Injection in Mice - Involvement of Scavenger Receptors in its Hepatic-Uptake, *Pharm. Res.* **1995**, *12*, 825.

(6) Pack, D. W.; Hoffman, A. S.; Pun, S.; Stayton, P. S., Design and development of polymers for gene delivery, *Nat. Rev. Drug Discov.* **2005**, *4*, 581.

(7) Kanasty, R.; Dorkin, J. R.; Vegas, A.; Anderson, D., Delivery materials for siRNA therapeutics, *Nat. Mater.* **2013**, *12*, 967.

(8) Miyata, K.; Kakizawa, Y.; Nishiyama, N.; Harada, A.; Yamasaki, Y.; Koyama, H.; Kataoka, K., Block catiomer polyplexes with regulated densities of charge and disulfide cross-linking directed to enhance gene expression, *J. Am. Chem. Soc.* **2004**, *126*, 2355.

(9) Boyer, C.; Bulmus, V.; Davis, T. P.; Ladmiral, V.; Liu, J. Q.; Perrier, S., Bioapplications of RAFT Polymerization, *Chem. Rev.* **2009**, *109*, 5402.

(10) Cobo, I.; Li, M.; Sumerlin, B. S.; Perrier, S., Smart hybrid materials by conjugation of responsive polymers to biomacromolecules, *Nat. Mater.* **2015**, *14*, 143.

(11) Mura, S.; Nicolas, J.; Couvreur, P., Stimuli-responsive nanocarriers for drug delivery, *Nat. Mater.* **2013**, *12*, 991.

(12) Rozema, D. B.; Lewis, D. L.; Wakefield, D. H.; Wong, S. C.; Klein, J. J.; Roesch, P. L.; Bertin, S. L.; Reppen, T. W.; Chu, Q.; Blokhin, A. V.; Hagstrom, J. E.; Wolff, J. A., Dynamic PolyConjugates for targeted in vivo delivery of siRNA to hepatocytes, *Proc. Natl. Acad. Sci. U. S. A.* **2007**, *104*, 12982.

(13) Wu, M. Y.; Meng, Q. S.; Chen, Y.; Zhang, L. X.; Li, M. L.; Cai, X. J.; Li, Y. P.; Yu, P. C.; Zhang, L. L.; Shi, J. L., Large Pore-Sized Hollow Mesoporous Organosilica for Redox-Responsive Gene Delivery and Synergistic Cancer Chemotherapy, *Adv. Mater.* **2016**, *28*, 1963.

(14) Takeda, N.; Nakamura, E.; Yokoyama, M.; Okano, T., Temperature-responsive polymeric carriers incorporating hydrophobic monomers for effective transfection in small doses, *J. Control. Release* **2004**, *95*, 343.

(15) Saurer, E. M.; Jewell, C. M.; Kuchenreuther, J. M.; Lynn, D. M., Assembly of erodible, DNA-containing thin films on the surfaces of polymer microparticles: Toward a layer-by-layer approach to the delivery of DNA to antigen-presenting cells, *Acta Biomater.* **2009**, *5*, 913.

(16) Kostiainen, M. A.; Smith, D. K.; Ikkala, O., Optically triggered release of DNA from multivalent dendrons by degrading and charge-switching multivalency, *Angew. Chem. Int. Ed.* **2007**, *46*, 7600.

(17) Shapiro, G.; Wong, A. W.; Bez, M.; Yang, F.; Tam, S.; Even, L.; Sheyn, D.; Ben-David, S.; Tawackoli, W.; Pelled, G.; Ferrara, K. W.; Gazit, D., Multiparameter evaluation of in vivo gene delivery using ultrasound-guided, microbubble-enhanced sonoporation, *J. Control. Release* **2016**, *223*, 157.

(18) McBain, S. C.; Yiu, H. H. P.; Dobson, J., Magnetic nanoparticles for gene and drug delivery, *International Journal of Nanomedicine* **2008**, *3*, 169.

(19) Lynn, D. M.; Anderson, D. G.; Putnam, D.; Langer, R., Accelerated discovery of synthetic transfection vectors: Parallel synthesis and screening of degradable polymer library, *J. Am. Chem. Soc.* **2001**, *123*, 8155.

(20) Lynn, D. M.; Langer, R., Degradable poly(beta-amino esters): Synthesis, characterization, and self-assembly with plasmid DNA, *J. Am. Chem. Soc.* **2000**, *122*, 10761.

(21) Woodrow, K. A.; Cu, Y.; Booth, C. J.; Saucier-Sawyer, J. K.; Wood, M. J.; Saltzman, W. M., Intravaginal gene silencing using biodegradable polymer nanoparticles densely loaded with small-interfering RNA, *Nat. Mater.* **2009**, *8*, 526.

(22) McKinlay, C. J.; Vargas, J. R.; Blake, T. R.; Hardy, J. W.; Kanada, M.; Contag, C. H.; Wender, P. A.; Waymouth, R. M., Charge-altering releasable transporters (CARTs) for the delivery and release of mRNA in living animals, *Proc. Natl. Acad. Sci. U. S. A.* **2017**, *114*, E448.

(23) Luten, J.; Akeroyd, N.; Funhoff, A.; Lok, M. C.; Talsma, H.; Hennink, W. E., Methacrylamide polymers with hydrolysis-sensitive cationic side groups as degradable gene carriers, *Bioconjugate Chem.* **2006**, *17*, 1077.

(24) Funhoff, A. M.; van Nostrum, C. F.; Janssen, A.; Fens, M.; Crommelin, D. J. A.; Hennink, W. E., Polymer side-chain degradation as a tool to control the destabilization of polyplexes, *Pharm. Res.* **2004**, *21*, 170.

(25) Veron, L.; Ganee, A.; Charreyre, M. T.; Pichot, C.; Delair, T., New hydrolyzable pH-responsive cationic polymers for gene delivery: A preliminary study, *Macromol. Biosci.* **2004**, *4*, 431.

(26) Truong, N. P.; Gu, W. Y.; Prasadam, I.; Jia, Z. F.; Crawford, R.; Xiao, Y.; Monteiro, M. J., An influenza virus-inspired polymer system for the timed release of siRNA, *Nature Communications* **2013**, *4*.

(27) Truong, N. P.; Jia, Z. F.; Burges, M.; McMillan, N. A. J.; Monteiro, M. J., Self-Catalyzed Degradation of Linear Cationic Poly(2-dimethylaminoethyl acrlyate) in Water, *Biomacromolecules* **2011**, *12*, 1876.

(28) Truong, N. P.; Jia, Z. F.; Burgess, M.; Payne, L.; McMillan, N. A. J.; Monteiro, M. J., Self-Catalyzed Degradable Cationic Polymer for Release of DNA, *Biomacromolecules* **2011**, *12*, 3540.

(29) McCool, M. B.; Senogles, E., The Self-Catalyzed Hydrolysis of Poly(N,N-Dimethylaminoethyl Acrylate), *Eur. Polym. J.* **1989**, *25*, 857.

(30) Cotanda, P.; Wright, D. B.; Tyler, M.; O'Reilly, R. K., A comparative study of the stimuli-responsive properties of DMAEA and DMAEMA containing polymers, *J. Polym. Sci., Part A: Polym. Chem.* **2013**, *51*, 3333.

(31) Zhao, W.; Fonsny, P.; FitzGerald, P.; Warr, G. G.; Perrier, S., Unexpected behavior of polydimethylsiloxane/poly(2-(dimethylamino)ethyl acrylate) (charged) amphiphilic block copolymers in aqueous solution, *Polymer Chemistry* **2013**, *4*, 2140.

(32) Sun, F. X.; Feng, C.; Liu, H. Y.; Huang, X. Y., PHEA-g-PDMAEA well-defined graft copolymers: SET-LRP synthesis, self-catalyzed hydrolysis, and quaternization, *Polymer Chemistry* **2016**, *7*, 6973.

(33) Tran, N. T. D.; Jia, Z. F.; Truong, N. P.; Cooper, M. A.; Monteiro, M. J., Fine Tuning the Disassembly Time of Thermoresponsive Polymer Nanoparticles, *Biomacromolecules* **2013**, *14*, 3463.

(34) Tran, N. T. D.; Truong, N. P.; Gu, W. Y.; Jia, Z. F.; Cooper, M. A.; Monteiro, M. J., Timed-Release Polymer Nanoparticles, *Biomacromolecules* **2013**, *14*, 495.

(35) Pecot, C. V.; Calin, G. A.; Coleman, R. L.; Lopez-Berestein, G.; Sood, A. K., RNA interference in the clinic: challenges and future directions, *Nature Reviews Cancer* **2011**, *11*, 59.

(36) Tanaka, T.; Mangala, L. S.; Vivas-Mejia, P. E.; Nieves-Alicea, R.; Mann, A. P.; Mora, E.; Han, H. D.; Shahzad, M. M. K.; Liu, X. W.; Bhavane, R.; Gu, J. H.; Fakhoury, J. R.; Chiappini, C.; Lu, C. H.; Matsuo, K.; Godin, B.; Stone, R. L.; Nick, A. M.; Lopez-Berestein, G.; Sood, A. K.; Ferrari, M., Sustained Small Interfering RNA Delivery by Mesoporous Silicon Particles, *Cancer Res.* **2010**, *70*, 3687.

(37) Wolfram, J.; Shen, H.; Ferrari, M., Multistage vector (MSV) therapeutics, *J. Control. Release* **2015**, *219*, 406.

(38) Van de Wetering, P.; Zuidam, N.; Van Steenbergen, M.; Van der Houwen, O.; Underberg, W.; Hennink, W., A mechanistic study of the hydrolytic stability of poly (2-(dimethylamino) ethyl methacrylate), *Macromolecules* **1998**, *31*, 8063.

(39) Rosselgong, J.; Armes, S. P.; Barton, W. R.; Price, D., Synthesis of branched methacrylic copolymers: comparison between RAFT and ATRP and effect of varying the monomer concentration, *Macromolecules* **2010**, *43*, 2145.

(40) Moad, G.; Solomon, D. H. *The Chemistry of Radical Polymerization*; Elsevier Science, 2005.

(41) Roos, S. G.; Muller, A. H. E.; Matyjaszewski, K., Copolymerization of n-butyl acrylate with methyl methacrylate and PMMA macromonomers: Comparison of reactivity ratios in conventional and atom transfer radical copolymerization, *Macromolecules* **1999**, *32*, 8331.

(42) Vanherk, A. M., Least-Squares Fitting by Visualization of the Sum of Squares Space, *J. Chem. Educ.* **1995**, *72*, 138.

(43) vanHerk, A. M.; Droge, T., Nonlinear least squares fitting applied to copolymerization modeling, *Macromol. Theory Simul.* **1997**, *6*, 1263.

(44) Odian, G. *Principles of polymerization*; John Wiley & Sons, 2004.

(45) Wang, Q.; Bao, Y. P.; Zhang, X. H.; Coxon, P. R.; Jayasooriya, U. A.; Chao, Y. M., Uptake and Toxicity Studies of Poly-Acrylic Acid Functionalized Silicon Nanoparticles in Cultured Mammalian Cells, *Advanced Healthcare Materials* **2012**, *1*, 189.

(46) Xiong, L. Q.; Yang, T. S.; Yang, Y.; Xu, C. J.; Li, F. Y., Long-term in vivo biodistribution imaging and toxicity of polyacrylic acid-coated upconversion nanophosphors, *Biomaterials* **2010**, *31*, 7078.

(47) Ferguson, C. J.; Hughes, R. J.; Nguyen, D.; Pham, B. T. T.; Gilbert, R. G.; Serelis, A. K.; Such, C. H.; Hawkett, B. S., Ab initio emulsion polymerization by RAFT-controlled self-assembly, *Macromolecules* **2005**, *38*, 2191.

(48) Larnaudie, S. C.; Brendel, J. C.; Jolliffe, K. A.; Perrier, S., Cyclic Peptide-Polymer Conjugates: Grafting-to vs Grafting-From, *J. Polym. Sci., Part A: Polym. Chem.* **2016**, *54*, 1003.

Appendix to Chapter 4

Table A4.1. Experimental conditions used for the synthesis of the branched polymers and copolymers, and also linear equivalents.

Sample	Branched pDMAEA	Branched pDMAPA	Branched pDMAEMA	Branched p(DMAEMA$_{40}$)	Branched p(DMAEMA$_{10}$)	Linear p(DMAEMA$_{40}$)	Linear p(DMAEMA$_{10}$)
[M]:[M]:[B]:[CTA]:[I]	50:0:2.5:1:0.1	50:0:2.5:1:0.1	50:0:0.95:1:0.025	40:10:1.5:1:0.05	10:40:1.5:1:0.05	40:10:0:1:0.05	10:40:0:1:0.05
Mass DMAEMA (mg)	-	-	1000	503	125.8	503	125.8
Mass DMAPA (mg)	-	333	-	-	-	-	-
Mass DMAEA (mg)	1000	-	-	114.6	458.2	114.6	458.2
Brancher	DEGDA	DEGDA	EGDMA	EGDMA	DEGDA	-	-
Mass Brancher (mg)	74.8	22.7	24	23.76	25.68	-	-
CTA	PABTC	PABTC	CPAETC	CPAETC	CPAETC	CPAETC	CPAETC
Mass CTA (mg)	33.3	10.1	33.5	21.06	21.06	21.06	21.06
Initiator	ACVA	ACVA	VA-088	ACVA	ACVA	ACVA	ACVA
Mass Initiator (mg)	3.9	1.2	0.78	1.12	1.12	1.12	1.12
Solvent	Dioxane	Dioxane	Dioxane	Dioxane	Dioxane	Dioxane	Dioxane
Temperature (°C)	70	70	90	70	70	70	70
Time (hr)	24	24	24	24	24	24	24
V. total (mL)	2.245	0.681	2.045	1.33	1.33	1.333	1.333

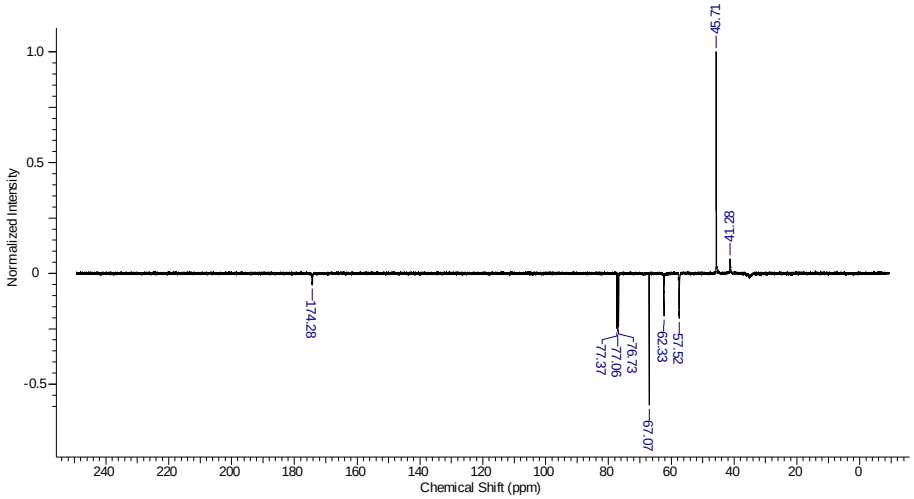

Figure A4.1. ^{13}C NMR spectrum of highly branched pDMAEA in deuterated chloroform.

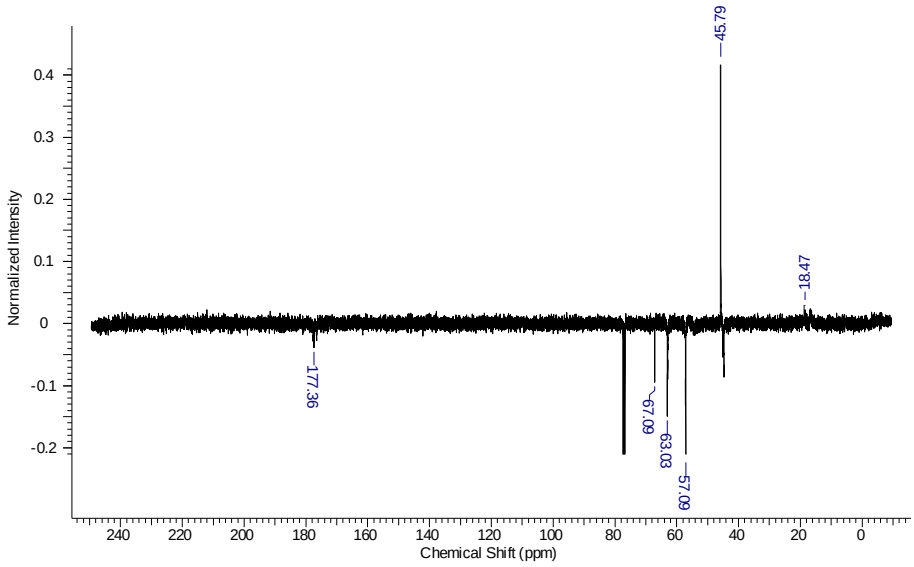

Figure A4.2. ^{13}C NMR spectrum of highly branched pDMAEMA in deuterated chloroform.

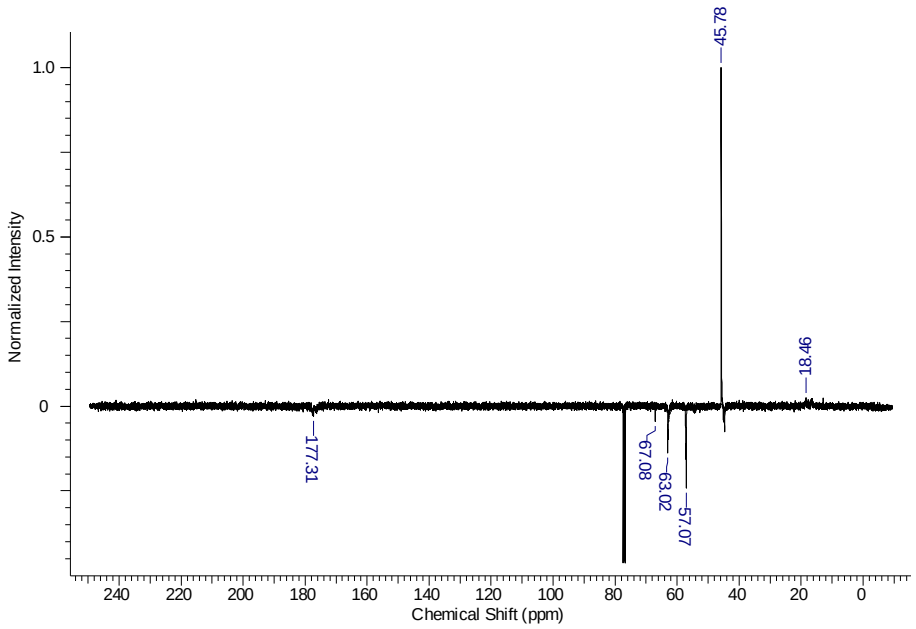

Figure A4.3. ^{13}C NMR spectrum of highly branched copolymer p(DMAEMA$_{40}$-*co*-DMAEA$_{10}$) in deuterated chloroform.

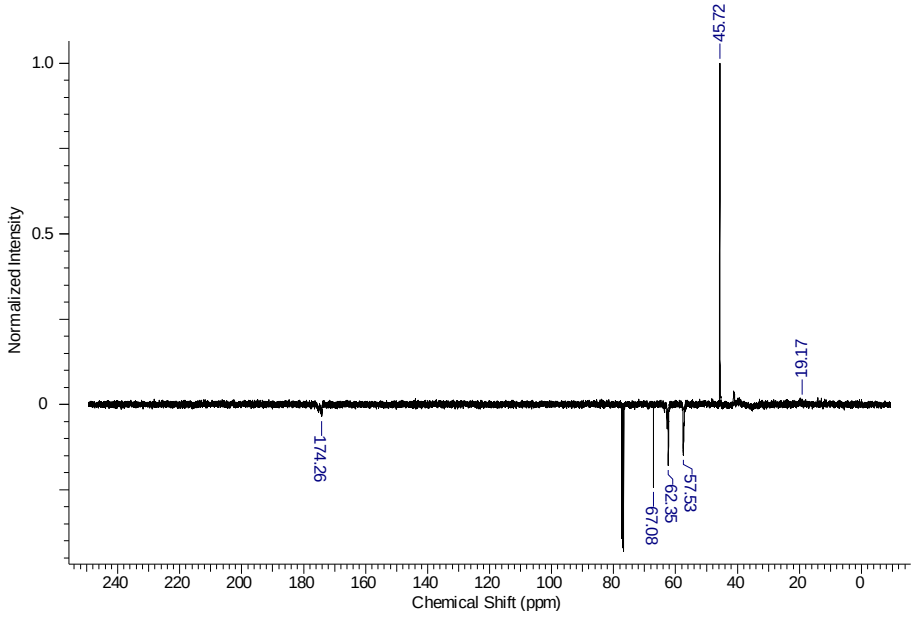

Figure A4.4. ^{13}C NMR spectrum of highly branched copolymer p(DMAEMA$_{10}$-*co*-DMAEA$_{40}$) in deuterated chloroform.

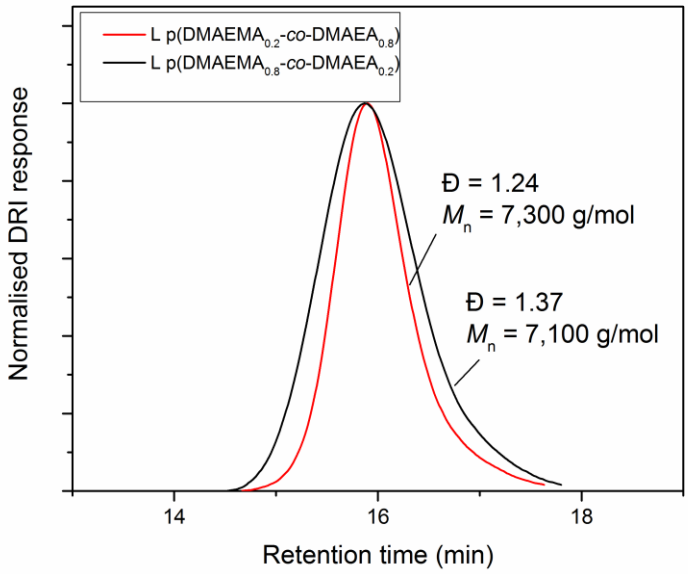

Figure A4.5. Size exclusion chromatograms of linear copolymers of DMAEMA and DMAEA by RAFT (From $CHCl_3$ SEC, DRI detector, linear PS standard).

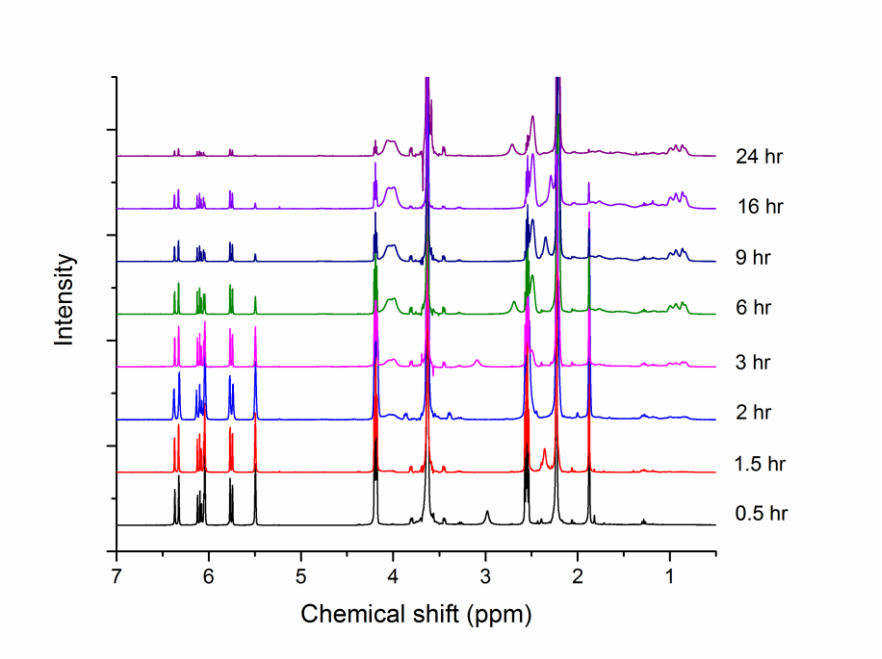

Figure A4.6. Polymerisation kinetic analysis *via* ^{1}H NMR Spectroscopy of copolymerisation of DMAEMA and DMAEA (DP 50, 50:50 ratio), CPAETC RAFT agent, ACVA initiator at 70 ^{o}C.

Table A4.2. Polymerisation kinetic analysis *via* ^{1}H NMR Spectroscopy of copolymerisation of DMAEMA and DMAEA (DP 50, 50:50 ratio), CPAETC RAFT agent, ACVA initiator at 70 ^{o}C.

Time (hr)	Conv. DMAEMA (%)	Conv. DMAEA (%)	Total conv. (%)
0	0	0	0
0.5	4.0	2.8	3.7
1.5	7.0	3.0	5.3
2	20	10	16
3	41	23	33
6	77	48	63
9	89	61	75
18	93	71	82
24	98	83	91

Table A4.3. Experimental conditions used for the synthesis of the linear DMAEMA DMAEA copolymers (used for NMR kinetic study, and reactivity ratio calculations).

Sample	Linear p(DMAEMA$_{10}$-co-DMAEA$_{90}$)	Linear p(DMAEMA$_{30}$-co-DMAEA7$_{0}$)	Linear p(DMAEMA$_{50}$-co-DMAEA$_{50}$)	Linear p(DMAEMA$_{70}$-co-DMAEA$_{30}$)	Linear p(DMAEMA$_{90}$-co-DMAEA$_{10}$)
[M]:[M]:[CTA]:[I]	5:45:1:0.05	15:35:1:0.05	25:25:1:0.05	35:15:1:0.05	45:5:1:0.05
Mass DMAEMA (mg)	31.4	94.3	157.2	220.1	283
Mass DMAEA (mg)	257.8	200.5	143.2	57.3	28.6
CTA	CPAETC	CPAETC	CPAETC	CPAETC	CPAETC
Mass CTA (mg)	10.53	10.53	10.53	10.53	10.53
Initiator	ACVA	ACVA	ACVA	ACVA	ACVA
Mass Initiator (mg)	0.56	0.56	0.56	0.56	0.56
Solvent	Dioxane	Dioxane	Dioxane	Dioxane	Dioxane
Temperature (^{o}C)	70	70	70	70	70
Time (hr)	24	24	24	24	24
V. total (mL)	0.667	0.667	0.667	0.667	0.667

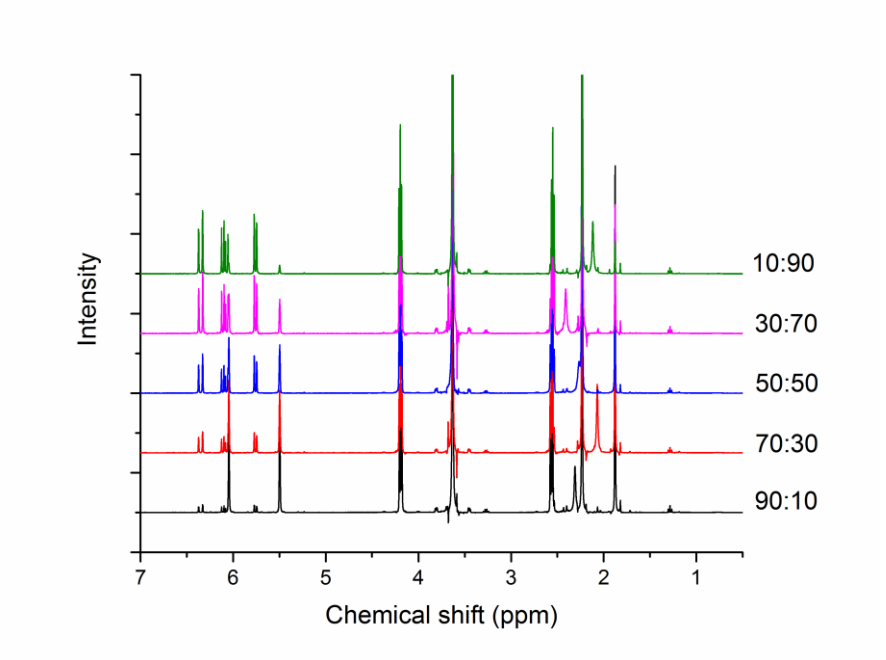

Figure A4.7. Time 0 hour, ^{1}H NMR spectra for the synthesis of the linear DMAEMA DMAEA copolymers (used for reactivity ratio calculations).

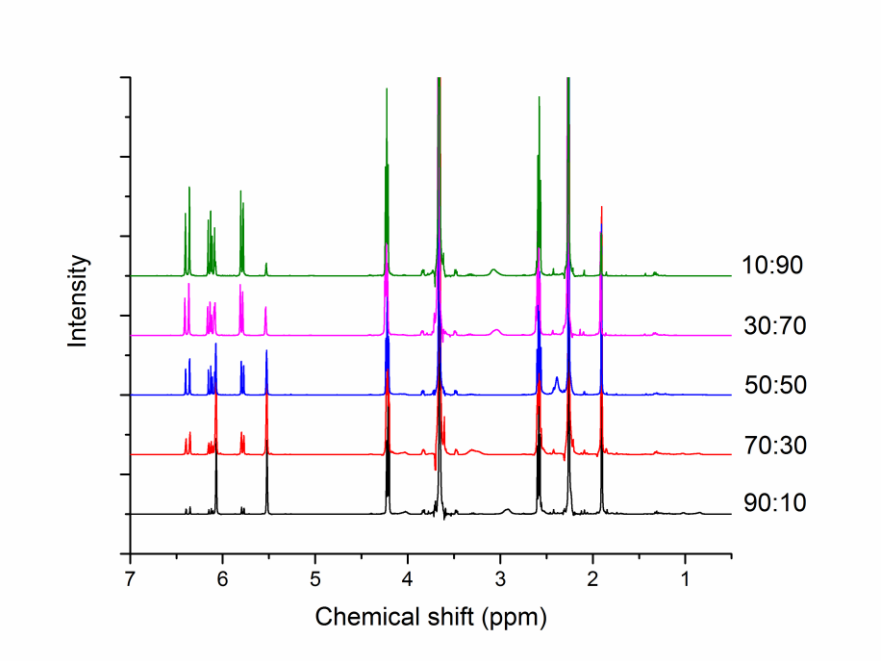

Figure A4.8. Time 1 hour, ^{1}H NMR spectra for the synthesis of the linear DMAEMA DMAEA copolymers (used for reactivity ratio calculations).

Table A4.4. Parameters from the synthesis of the linear DMAEMA DMAEA copolymers (used for reactivity ratio calculations).

f_1 (DMAEMA)	f_2 (DMAEA)	F_1 (DMAEMA)	F_2 (DMAEA)	Total conv. (%)
0.000	1.000	0.000	1.000	-
0.102	0.898	0.156	0.844	9.5
0.314	0.686	0.426	0.574	5.8
0.502	0.498	0.674	0.326	5.2
0.704	0.296	0.806	0.194	6.9
0.901	0.099	0.957	0.043	6.5
1.000	0.000	1.000	0.000	-

The monomer feed ratio and incorporation ratios were then used to calculate reactivity ratios by the Fineman-Ross method, Kelen-Tudos method, and by fitting with a non-linear least squares fit (solver in MS Excel) of the copolymer equation: $F_1 = \frac{r_1 f_1^2 + f_1 f_2}{r_1 f_1^2 + 2 f_1 f_2 + r_2 f_2^2}$

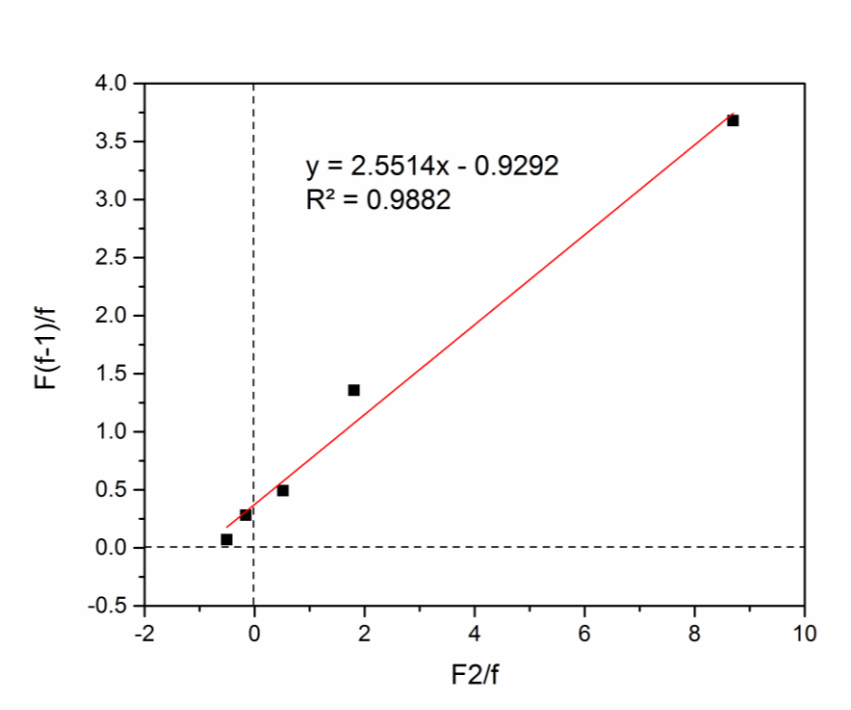

Figure A4.9. Fineman-Ross plot for estimation of reactivity ratios for linear copolymerisation of DMAEMA and DMAEA (DP 50, 50:50 ratio), CPAETC RAFT agent, ACVA initiator at 70 ^{o}C.

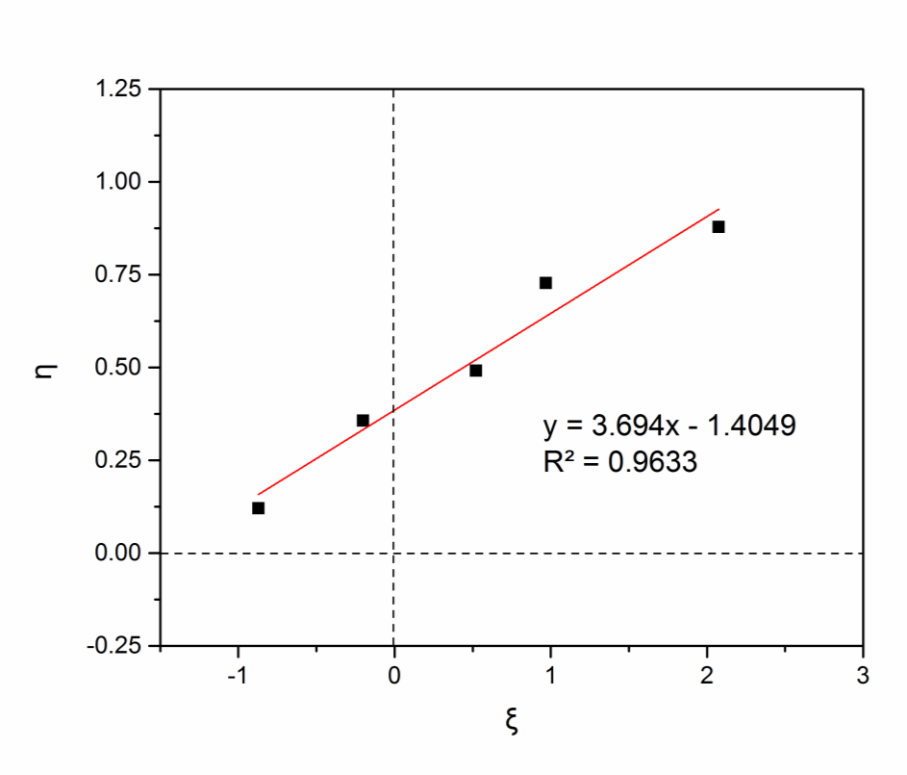

Figure A4.10. Kelen-Tudos plot for estimation of reactivity ratios for linear copolymerisation of DMAEMA and DMAEA (DP 50, 50:50 ratio), CPAETC RAFT agent, ACVA initiator at 70 ^{o}C.

Table A4.5. Reactivity ratio values acquired (from three different methods) for linear copolymerisation of DMAEMA and DMAEA (DP 50, 50:50 ratio), CPAETC RAFT agent, ACVA initiator at 70 ^{o}C.

	Non linear least squares	Fineman Ross	Kelen Tudos
r_1 (DMAEMA)	2.13	2.55	2.29
r_2 (DMAEA)	0.69	0.93	0.71

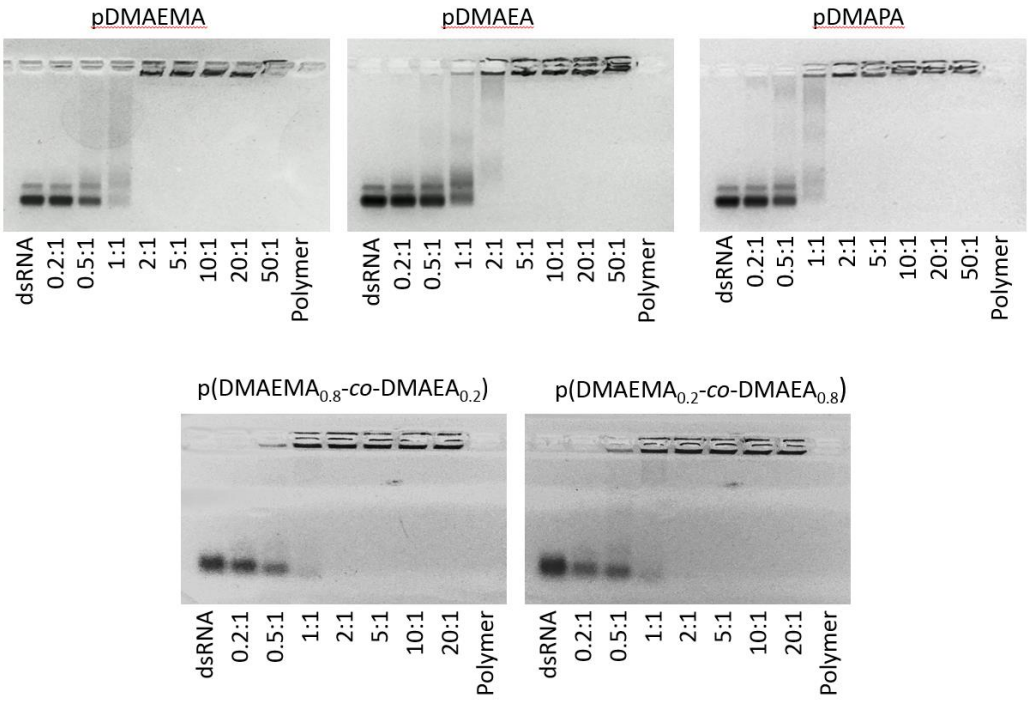

Figure A4.11. Agarose gel electrophoresis images of polyplex formation of synthesised branched polymers with dsRNA, with varying N/P ratios.

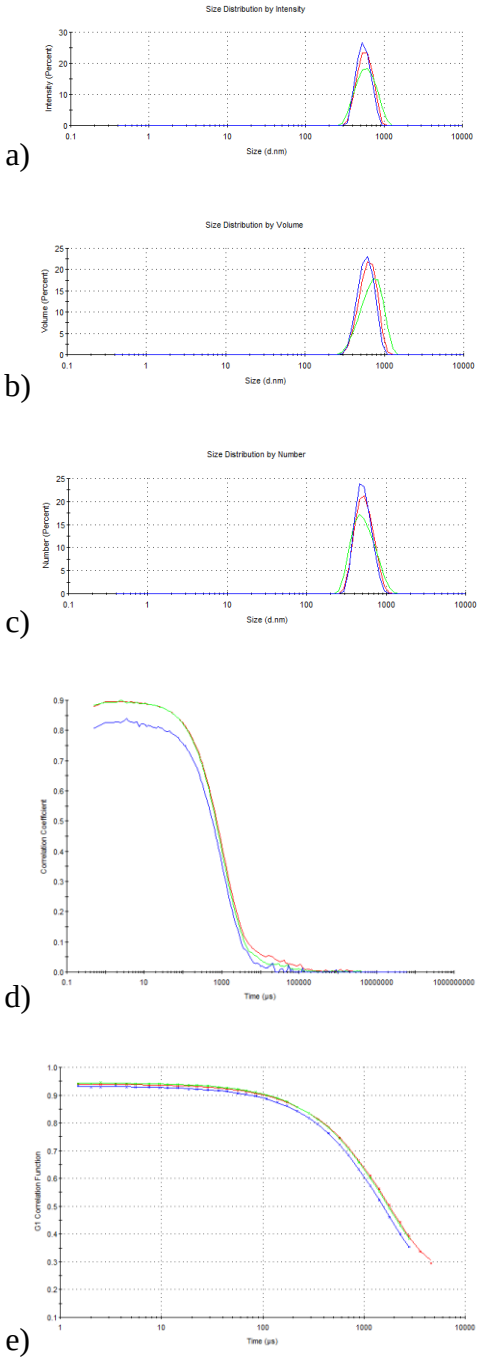

Figure A4.12. Representative DLS data for polyples solutions (branched DMAEMA with dsRNA, N/P 20, three repeats shown), a) intensitie distribution, b) volume distribution, c) number distribution, d) correlalograms, e) cummulants fit.

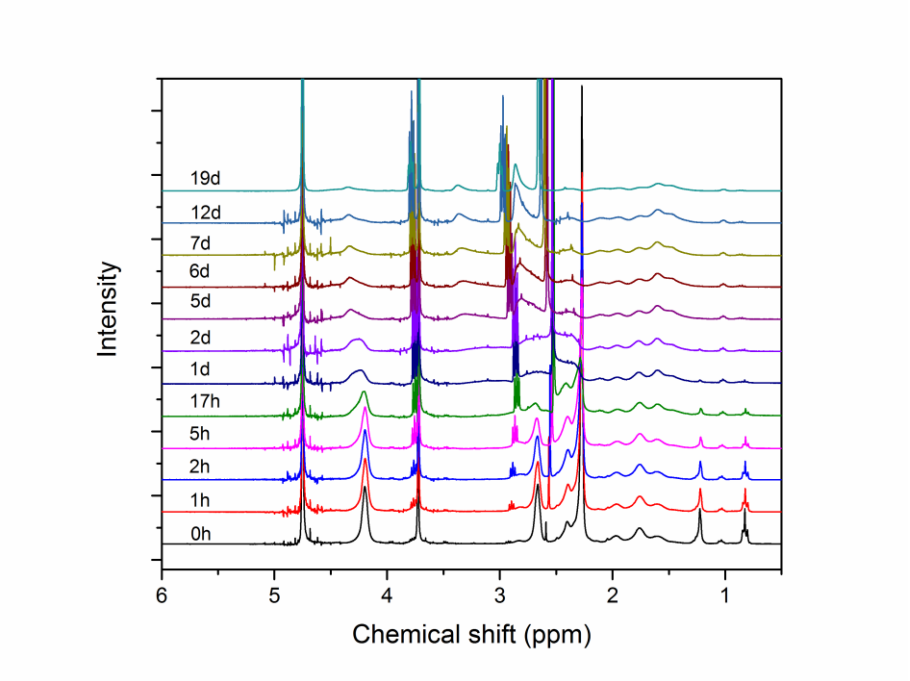

Figure A4.13. Hydrolysis of branched pDMAEA in D_2O (pH ~7.4) determined using ^1H NMR spectroscopy.

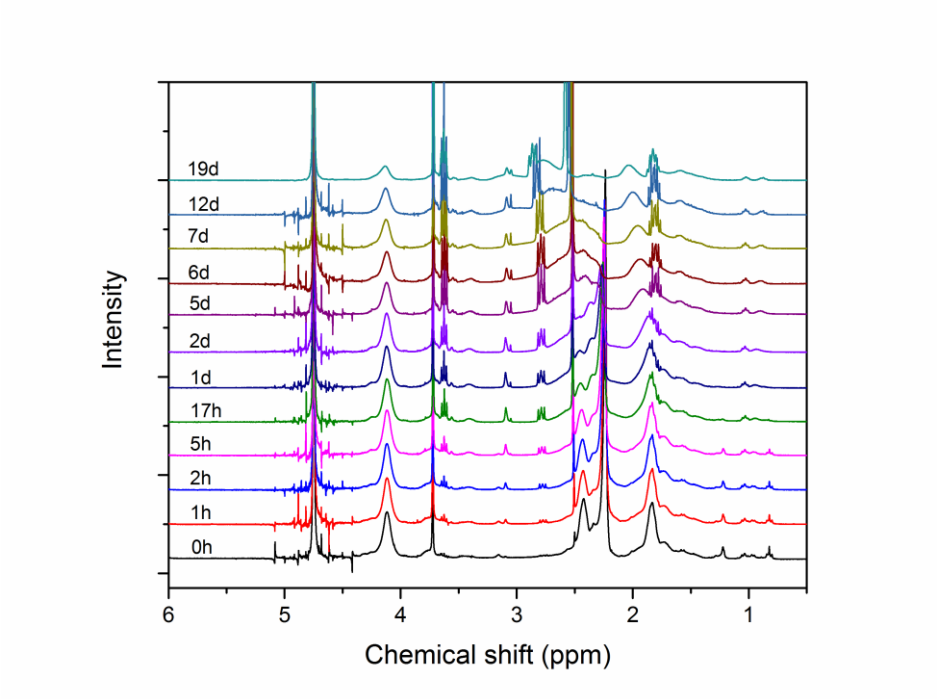

Figure A4.14. Hydrolysis of branched pDMAPA in D_2O (pH ~7.4) determined using ^1H NMR spectroscopy.

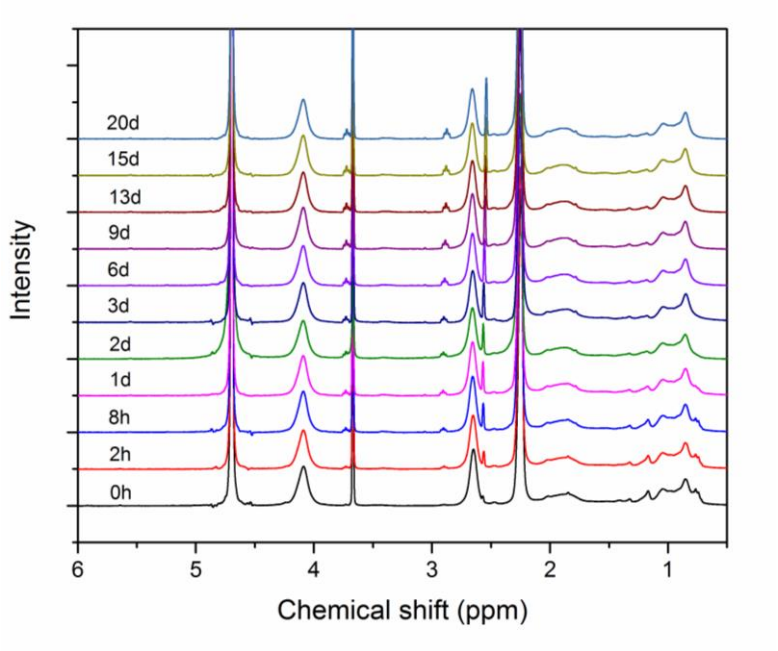

Figure A4.15. Hydrolysis of linear p(DMAEMA$_{40}$-*co*-DMAEA$_{10}$) in D_2O (pH ~7.4) determined using ^{1}H NMR spectroscopy.

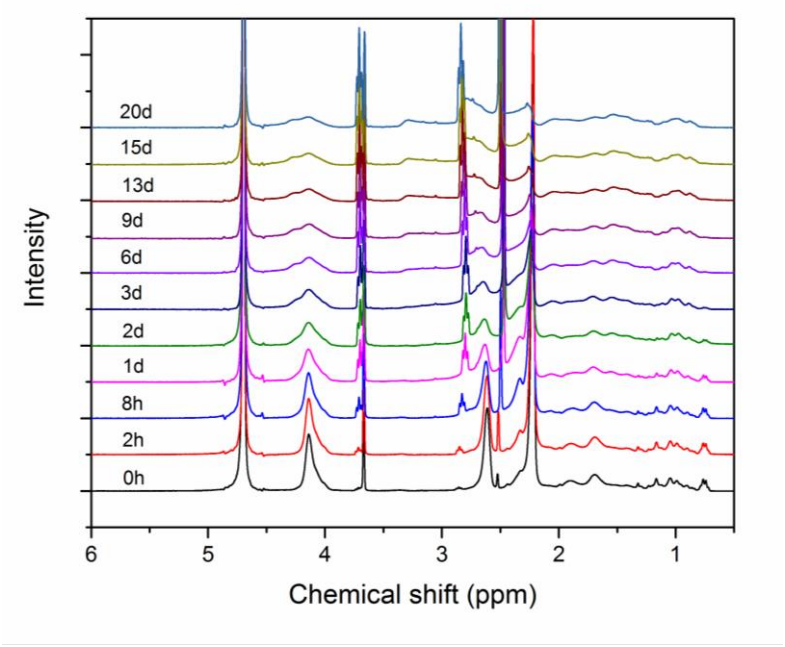

Figure A4.16. Hydrolysis of linear p(DMAEMA$_{10}$-*co*-DMAEA$_{40}$) in D_2O (pH ~7.4) determined using ^{1}H NMR spectroscopy.

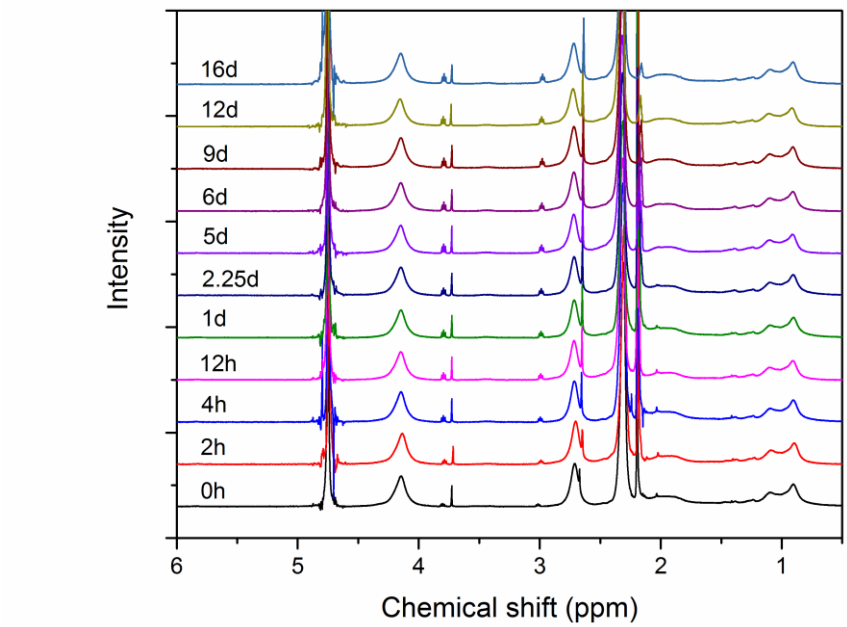

Figure A4.17. Hydrolysis of branched p(DMAEMA$_{40}$-*co*-DMAEA$_{10}$) in D_2O (pH ~7.4) determined using ^1H NMR spectroscopy.

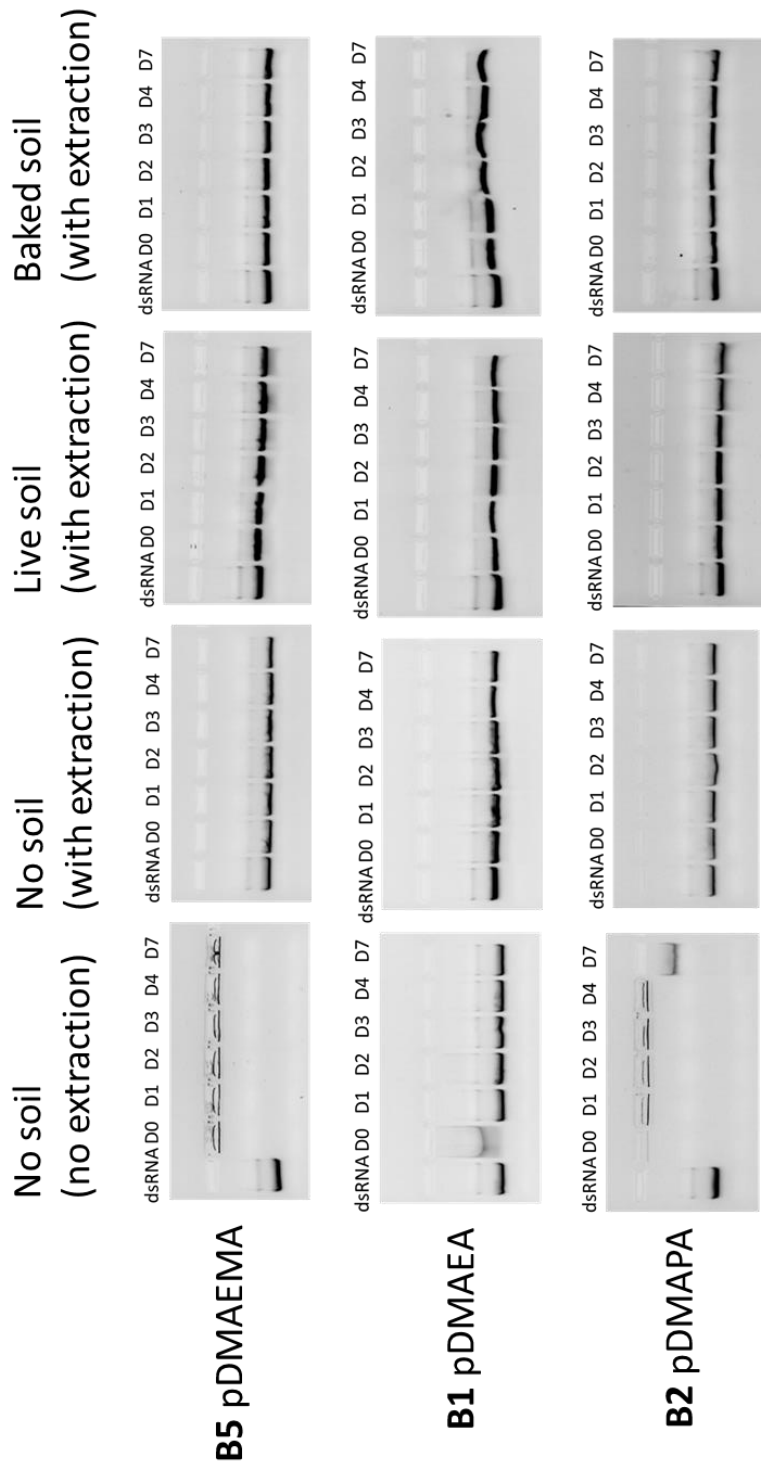

Figure A4.18. Polyplex soil stability assay (dsRNA protection), polyplexes were formed in sterile water at an N/P ratio of 5 with a final concentration of 1 mg/mL dsRNA, incubated in live soil or enzyme free soil, then dsRNA was extracted and run on an agarose gel.

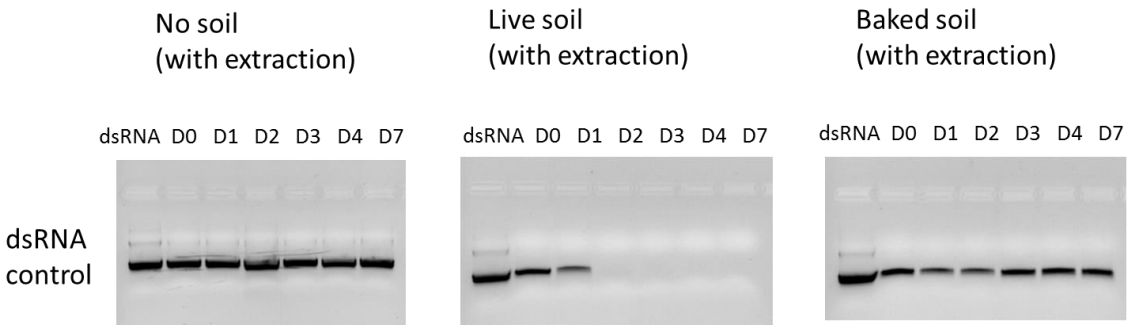

Figure A4.19. Control dsRNA soil stability assay, with a final concentration of 1 mg/mL dsRNA, incubated in live soil or enzyme free soil, then dsRNA was extracted and run on an agarose gel.

5.

Branched poly(trimethylphosphonium ethylacrylate-co-PEGA) by RAFT: alternative to cationic polyammoniums for nucleic acid complexation

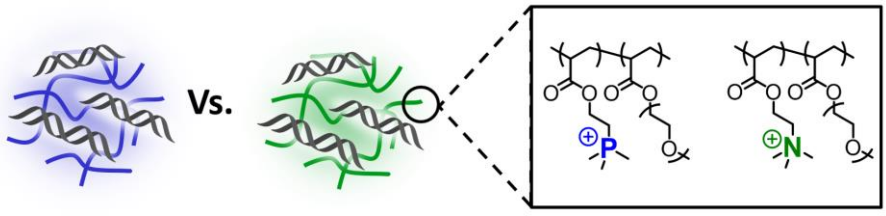

Abstract

Cationic and highly branched poly(trimethylphosphonium ethylacrylate-*co*-PEGA) (p(TMPEA-*co*-PEGA)), and its ammonium equivalent, have been synthesised from post-polymerisation modification of a poly(bromo ethylacrylate-*co*-PEGA) (p(BEA-*co*-PEGA)) precursor polymer produced using reversible addition fragmentation chain transfer (RAFT) polymerisation. The cationic polymers were evaluated for their ability to complex nucleic acids, i*n vitro* cytotoxicityas well as GFP pDNA transfection efficiency. The results show RAFT copolymerisation of BEA and PEGA is a simple route to polyphosphoniums showing reduced cytotoxicities and higher transfection efficiencies than their polyammonium alternatives.

5.1 Introduction

The development of polymeric materials for non-viral gene delivery applications has become a prolific area of research over the last two decades.[1] These compounds facilitate the use of nucleic acids such as siRNA, mRNA, and plasmid DNA as therapeutics to treat a range of diseases with currently limited traditional small molecule therapeutic options.[2] Historically, non-viral gene delivery polymers have been cationic polymers or lipids that can compact negatively charged nucleotides to form nanoparticle polyplexes, which can be uptaken by cells. Commonly utilised systems include polyethyleneimine (PEI), chitosan, polylysine (PLL), and poly(dimethylaminoethyl methacrylate) (pDMAEMA).[3,4] The vast majority of polymer based nucleic acid delivery systems rely on amine-based cationic moieties to complex the phosphate groups of the desired polynucleotides. Although polyamines and polyammoniums show good ability to complex nucleotides, they also have significant cytotoxic effects arising either immediately from the free cationic amine polymer or as a delayed toxicity associated with the intracellular processing of polyplexes.[5-8]

A number of strategies have been used to circumvent or alter the cytotoxicity of polyamine non-viral vectors, most of which include variation of the amine pK_a or introduction of PEG units.[9] Using a cationic heterocycle, for example pyridinium or

imidazolium, was shown to result in a better dispersion of the positive charge over the ring and a decreased toxicity.[10] However, the use of non-nitrogen centred cations for nucleic acid complexation has yet to be thoroughly explored.[11] Phosphonium containing compounds are generally less toxic than their ammonium equivalents due to differences in ionic radius and charge distribution.[11-13] In addition, phosphonium based lipids have been shown to transfect cells with high efficacies and lower toxicity than ammonium analogues.[14] Interestingly, the few polymeric phosphonium materials reported so far in the literature showed a similar trend in relation to toxicity.[15-18] Yet, this was only studied in the case of linear polymers.

Phosphonium containing polymers are beginning to be investigated as delivery vectors, showing good transfection capabilities but with lower toxicities, the monomers used are either styrene based or required multistep syntheses and purification. The group of Long,[17,18] conducted research involving phosphonium containing monomers for nucleic acid complexation using modified styrene monomers, which can be difficult to polymerise, often require high temperatures and high initiator concentrations. Fréchet *et al.*,[15] and also Mantiovanni *et al.*,[16] synthesised phosphonium containing monomers with triethylene glycol spacers between the (meth)acrylate group and the phosphonium moieties. While these monomers showed excellent promise for gene delivery applications, they typically require multistep syntheses and purification. Poly(bromo ethylacrylate) (pBEA) has recently been shown to be an excellent reactive precursor material for post polymerisation modification with a variety of functionalities, including phosphonium moeities.[19] The monomer is compatible with controlled radical polymerisation techniques such as Reversible Addition Fragmentation Chain Transfer (RAFT) polymerisation, which enable great control of molecular weight as well as access to complex architectures.[20,21] In addition, RAFT polymerisation with divinyl comonomers allows simple access to branched architectures,[22] which have been shown to be more efficient gene delivery vectors than linear polymers.[23-25] In this chapter, the facile synthesis of branched phosphonium containing polymers using RAFT and a post-polymerisation modification strategy is reported. The highly branched p(TMPEA-*co*-PEGA), and its ammonium equivalent, were investigated for their ability to complex

DNA, toxicity of the polymers, and their potential to transfect cells *in vitro* with GFP plasmid DNA.

5.2 Results and discussion

5.2.1 Highly branched polymer synthesis

RAFT polymerisation was first used to synthesise highly branched structures by our group in 2005,[22,26,27] following the considerable work of Sherrington *et al.*,[28-30] who developed facile and versatile branched polymeric systems using free radical polymerisation. Here, the chain transfer agent, 2-(((butylthio)carbonothioyl)thio) propanoic acid (PABTC) is employed to copolymerise bromoethyl acrylate (BEA) and poly(ethylene glycol) acrylate (PEGA) with cross-linker diethyleneglycol diacrylate (DEGDA) to form soluble highly branched polymers in a one-pot methodology (**Figure 5.1a**). A molar ratio of 80:20 BEA:PEGA was chosen, which achieves similar weight ratio (and therefore charge to PEG ratio) as previous reports in the literature,[15,16] but from a facile copolymerisation strategy and post-polymerisation modification. The RAFT polymerisation was conducted at 70 ^{o}C in dioxane, with the conditions [BEA]: [PEGA]: [DEGDA]: [CTA]: [I] = 40: 10: 2.5: 1: 0.1, and reached conversions of > 90 % in 24 hrs with no macroscopic gelation. Size exclusion chromatography (SEC) showed a broad molecular weight distribution and high molecular weights (M_w = 127,900 g/mol, $Đ$ = 5.4) for the resulting polymers, as expected for highly branched polymeric systems (**Figure 5.1b**).

Information about the branched nature of these polymers and their globular conformation in solution can be obtained from viscometry detection on the SEC system. **Figure 5.1b** shows the Kuhn-Mark-Houwink-Sakurada (KMHS) double Log plot of intrinsic viscosity against molecular weight. The gradient of the line (α value) gives information about the extent of polymer branching by inferring information about the polymer entanglements in solution. Linear polymers entangle more than branched polymers of similar molecular weight, leading to higher viscosity values which increase with increasing molecular weight more than equivalent branched systems. Linear polymers typically have α values

of ~ 0.7. Here, linear p(BEA-*co*-PEG) was found to have α = 0.6 - 0.7 (see supporting info) while the highly branched p(BEA-*co*-PEGA) reactive polymer precursor has an α = 0.35, indicating a highly branched polymer with a globular conformation.

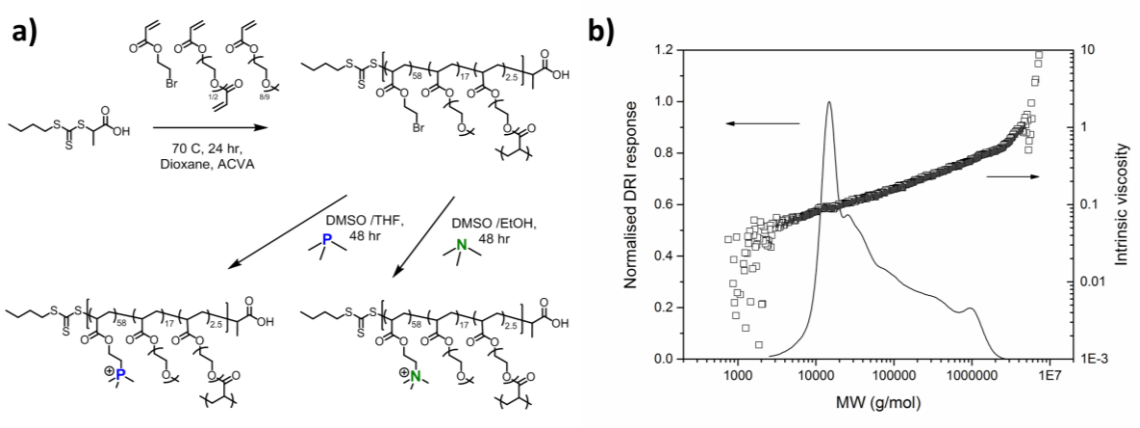

Figure 5.1. a) Reaction scheme for the RAFT polymerisation of BEA and PEGA with crosslinker DEGDA, and subsequent post-polymerisation modification with trimethylamine and trimethylphosphine; **b)** size exclusion chromatogram of p(BEA-*co*-PEGA) precursor polymer from refractive index detector, including KMHS plot of p(BEA-*co*-PEGA) from viscometry detector (DMF, PMMA calibration, Mn = 127,900 g/mol, Đ = 5.4, α = 0.35).

5.2.2 Post polymerisation modification

With the highly branched reactive polymer precursor in hand, post-polymerisation modification with trimethylamine and trimethylphosphine in DMSO/ethanol and DMSO/THF solvent mixtures, respectively, was used to form structurally equivalent polyphosphoniums and polyammoniums. Due to the highly charged nature of the resulting cationic polymers, purification from excess nucleophile could be achieved by precipitation of the charged polymer in THF. The lack of solubility in organic solvents of the resulting polymers, however, presented difficulties with characterisation of the molecular weight distribution using SEC. Using ^{1}H NMR spectroscopy, substitution of the BEA alkyl halide with trimethylamine and trimethylphosphine nucleophiles was shown to proceed to high degrees of substitution (> 95 %) (**Figure 5.2**, **A5.3** and **A5.4**),

which agrees with previously reported results.[19] Phosphorous (^{31}P) NMR spectroscopy confirmed the presence of phosphonium moieties on the purified polymer (**Figure A5.5**). In addition, elemental analysis was carried out to confirm the structure of both precursor BEA copolymer and post-polymerisation modified polymers (**Table A5.2**). In the case of p(TMAEA-*co*-PEGA) appearance of nitrogen confirmed successful substitution. However, the technique was unable to provide a quantitative assessment of substitution value, as the generation of highly charged cationic moieties, leads to the bromine anion being retained in the polymer as a counterion. Electrophoretic light scattering (zetapotential) measurments were employed to determine the charge of branched p(BEA-*co*-PEGA) precursor, and substituted polymers (**Table A5.3** and **Figure A5.6**). The charge increases from -3.05 mV for p(BEA-*co*-PEGA) to positively charged, p(TMAEA-*co*-PEGA) = +41.1 mV, p(TMPEA-*co*-PEGA) = +40.6 mV, further demonstrating substitution.

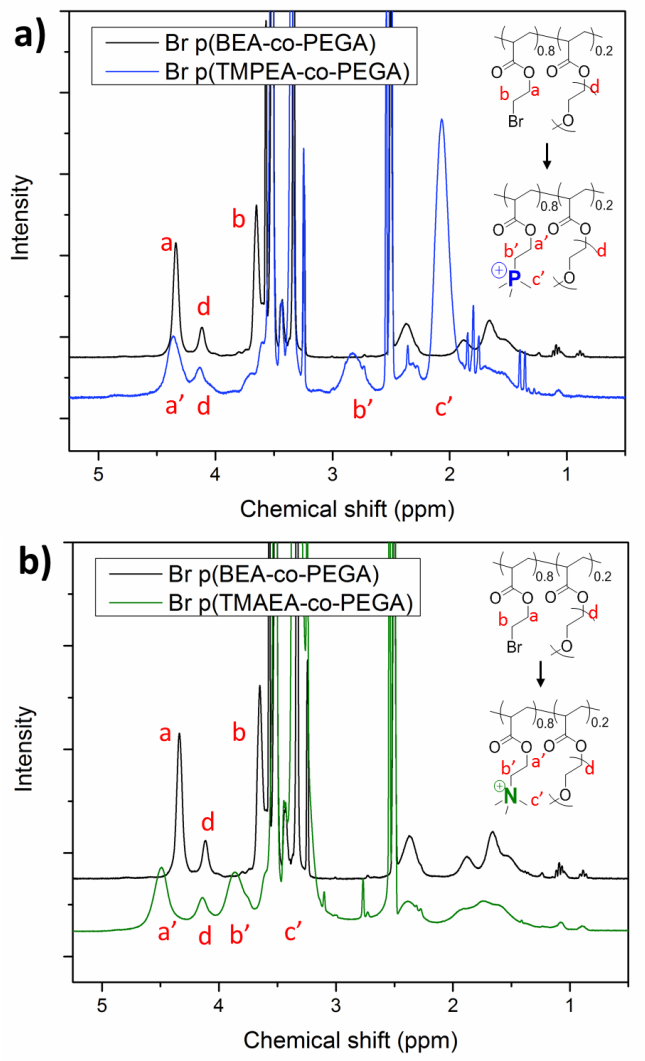

Figure 5.7. a) ^{1}H NMR spectra in DMSO-d_6 of branched p(BEA-*co*-PEGA) before and after substitution to form p(TMPEA-*co*-PEGA), **b)** ^{1}H NMR spectra in DMSO-d_6 of branched p(BEA-*co*-PEGA) before and after substitution to form p(TMAEA-*co*-PEGA).

5.2.3 DNA complexation

Ability of the synthesised highly branched polymers to complex DNA was investigated using a combination of agarose gel electrophoresis, DLS, and zetapotential measurements. The formation of polyplexes at various N/P ratios, where N refers to nitrogens in the polymer/vector and P refers to negatively charged phosphate groups in

the nucleic acid, was tested.[31] For clarity, the different charge ratios are referred to as either P^+/P for phosphonium polymers or N^+/P quaternary ammonium polymers here. **Figure 5.3a** and **5.3b** show the agarose gel retardation assays for branched p(TMPEA-*co*-PEGA) and p(TMAEA-*co*-PEGA) respectively, with both polymers showing complexation of DNA at a charge ratio value of 2.

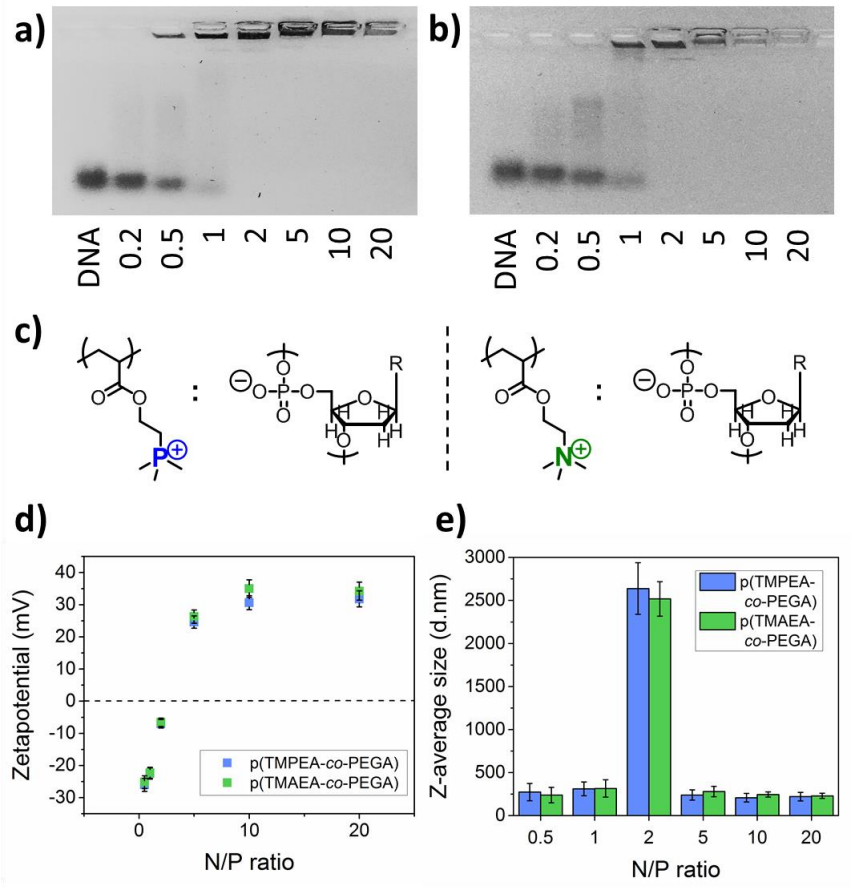

Figure 5.3. a) p(TMPEA-*co*-PEGA) polyplex formation with DNA as characterised by agarose gel electrophoresis at varying P^+/P charge ratios; **b)** p(TMAEA-*co*-PEGA) polyplex formation with DNA as characterised by agarose gel electrophoresis at varying N^+/P charge ratios; **c)** structures of repeating units; **d)** surface charge (zetapotential) and **e)** size of polyplexes formed with DNA at varying N^+/P or P^+/P ratios as measured by dynamic light scattering and electrophoretic light scattering, respectively.

The overall size and surface charge of formed polyplexes was then determined using zetapotential and DLS measurements at various charge ratios (**Figure 5.3d** and **5.3e**). At low P^+/P and N^+/P ratios, observation of negatively charged polyplex nanoparticles with

sizes of apporiximately 200 nm demonstrate the incomplete complexation of the oligonucleotide by both polymers, as excess of nucleic acid accounts for the negative charge observed. At a charge ratio of 2, both p(TMPEA-*co*-PEGA) and p(TMAEA-*co*-PEGA) form aggregates with sizes of over 2 μm with approximately neutral overall charges (~ -5mV from zetapotential). At higher ratio values, branched polymers complex all the nucleic acid and form electrostatically stabilised charged polyplexes with sizes of around 200 nm and a surface charge of approximately +40 mV. Taken together, these results show that both p(TMPEA-*co*-PEGA) and p(TMAEA-*co*-PEGA) have very similar ability to complex nucleic acids.

The ability of the highly branched p(TMPEA-*co*-PEGA) and p(TMAEA-*co*-PEGA) to protect nucleic acids from degradation in soil applications was investigated. Polyplexes (N/P 5) were incubated in live soil or enzyme free soil. The nucleic acids were extracted from the soil after the appropriate incubation period, and then an agarose gel was run to compare to the non-degraded pristine nucleic acid (**Figure A5.8**). Uncomplexed nucleic acid is degraded in soil after one day, but when complexed to branched p(TMPEA-*co*-PEGA) and p(TMAEA-*co*-PEGA), it seems to be protected soil related degradation for, potentially, up to 21 days.

5.2.4 Polymer toxicity and transfection *in vitro*

Difference in the toxicity and pDNA transfection efficiency of phosphonium-containing cationic polymers, as compared to ammonium equivalents, was investigated next. Acute toxicity of the polymers was assessed *in vitro* using 3T3 fibroblast cell line as model. Cells were incubated with the polymers (0.5 μg/mL – 2 mg/mL) for 24 hr and viability was assessed using a typical protocol for the XTT assay (**Figure 5.4a**). At concentrations of 5 μg/mL and below, all polymers present cell viability above 80%. While bPEI shows significant toxicity at concentrations above 50 μg/mL, both p(TMPEA-co-PEGA) and p(TMAEA-co-PEGA) showed no adverse effects to cell viability at concentration as high as 0.5 and 0.2 mg/mL, respectively. The fact that phosphonium polymer is observed to be less toxic than the ammonium-containing equivalent is in accordance with previous

report in the literature. For example, Stekar *et al.* first reported that trimethylphosphonium cationic headgroups in phospholipids had lower cytotoxicity in mouse models compared to equivalent ammonium choline phospholipids, while the lipids also retained similar antineoplastic activity in both *in vitro* and *in vivo* induced carcinoma models.[12] A similar increase in cell viability was observed for triethylphosphonium polymers as compared to triethylammonium polymers, for a range of polymer concentrations.[15]

The polymers were finally assessed for their propensity to help deliver plasmid DNA encoding for green fluorescent protein (GFP) in cells. This was done by incubating model HEK293T cells with polyplexes, at a N/P ratio of 20, for 4 h, following which the cells were allowed to further grow for 16 hours prior to cellular fluorescence quantificatino using flow cytometry. The results, shown in **Figure 5.4b**, show that polyplexes of branched p(TMPEA-*co*-PEGA) enhance transfection efficiency by a factor of approximately six times as compared to naked pDNA. Interestingly, the transfection efficiency of branched p(TMAEA-*co*-PEGA) was shown to only increase the efficiency of naked pDNA by a factor of 3. Such a higher transfection for the phosphonium polymer when compared to the ammonium polymer follows the same trend as previously reported in the literature.[15] Both of the synthesised branched polymers showed lower transfection compared to commercial branched PEI. This is potentially due to the p(TMPEA-*co*-PEGA) and p(TMAEA-*co*-PEGA) polymers being too hydrophilic, and subsequently being unable to efficiently enter cells *via* endocytosis – a process which typically requires a balance of cationic charge and hydrophobicity.[32] Long *et al.* reported a similar trend, where polymers with hydrophobic alkyl moieties attached to phosphonium cations had higher transfection efficiencies compared to more hydrophilic substituents.[17]

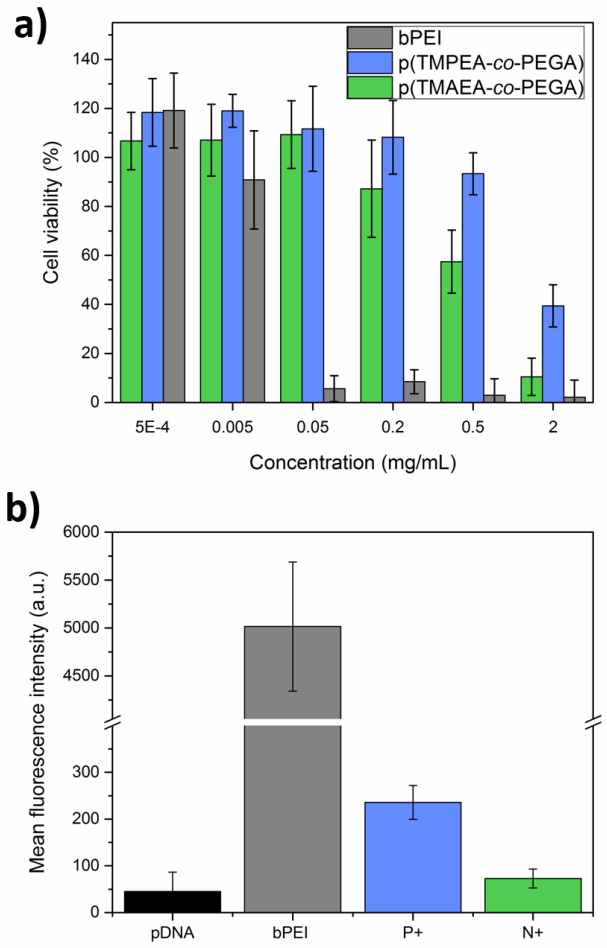

Figure 5.4.. a) Cytotoxicity as determined by the percentage of cell viability for 3T3 fibroblast cells treated with branched p(TMPEA-*co*-PEGA), branched p(TMAEA-*co*-PEGA), and bPEI for 24 hours at 37 °C. **b)** Intracellular fluorescence in HEK-293T cells following incubation with polyplexes of GFP-plasmid DNA and branched p(TMPEA-*co*-PEGA), branched p(TMAEA-*co*-PEGA) or bPEI (N/P 20, 10 µg/mL DNA concentration in well) for 4 hours at 37 °C and overnight incubation in polyplex-free media, as measured by flow cytometry.

5.3 Conclusions

In conclusion, this chapter demonstrated the facile synthesis of highly branched cationic poly(trimethylphosphonium ethylacrylate-*co*-PEGA) using a simple post-polymerisation modification strategy of a p(bromo ethylacrylate-*co*-PEGA) precursor polymer produced

using RAFT polymerisation. This synthesis represents a significant improvement/simplification of current phosphonium containing polymer synthetic methods. The phosphonium and ammonium containing polymers were evaluated for ability to complex nucleic acids, polymer cytotoxicity, and pDNA transfection. The results show that phosphonium-bearing polymers have increased biocompatibility and higher transfection efficiencies when compared to their exact ammonium equivalents. While transfection efficiencies were lower than those observed with commercial bPEI, their much lower toxicity highlights them as promising alternatives for gene delivery applications.

5.4 Experimental

5.4.1 Materials

Poly(ethylene glycol) methyl ether acrylate with average M_n = 480 (PEGA), di(ethylene glycol) diacrylate (DEGDA), 4,4′-azobis(4-cyanovaleric acid) (ACVA), trimethylamine solution (31-35 wt. % in ethanol 4.2 M), trimethylphosphine solution (1.0 M in THF), polyethylenimine branched (bPEI, Mw ~25,000 by LS, Mn ~10,000 by SEC), agarose, ethidium bromide solution (500 μg/mL in H_2O), deoxyribonucleic acid (DNA, low molecular weight from salmon sperm), were all obtained from Sigma-Aldrich. All other materials were purchased from Fisher Scientific. Green fluorescent protein (GFP) expressing plasmid DNA (pWPI) Addgene plasmid #12254. Bromoethyl acrylate was synthesised according to a previously published procedure.[19] 2-(((Butylthio)-carbonothioyl)thio)propanoic acid (PABTC) was prepared according to a previously reported procedure.[33] 50X Tris-Acetate-EDTA (TAE) buffer for gel electrophoresis was made up at concentration of 2.0M Tris acetate (Sigma Aldrich) and 0.05M EDTA (Sigma Aldrich) in deionised water, pH 8.2 - 8.4, and stored at room temperature. Agarose loading buffer for samples (colourless) was made up at 30% (vol/vol) glycerol (Sigma Aldrich) in deionised water, and stored at room temperature. 2,3-Bis(2-methoxy-4-nitro-5-sulfophenyl)-2H-tetrazolium-5-carboxanilide inner salt (XTT sodium salt), and Phenazine methosulfate (PMS) were obtained from Sigma-Aldrich.

5.4.2 Characterisation

Size Exclusion Chromatography (SEC) was performed in DMF, using an Agilent 390-LC MDS instrument equipped with differential refractive index (DRI), viscometry, dual angle light scattering, and dual wavelength UV detectors. The system was equipped with 2 x PLgel Mixed D columns (300 x 7.5 mm) and a PLgel 5 μm guard column. The eluent was DMF with 5 mmol NH_4BF_4 additive, and samples were run at 1 mL/min at 50 °C. Analyte samples were filtered through a nylon membrane with 0.22 μm pore size before injection. Apparent molar mass values ($M_{n,SEC}$ and $M_{w,SEC}$) and dispersity ($Đ$) of synthesized polymers were determined by DRI detector and conventional calibration using Agilent SEC software. Poly(methyl methacrylate) (PMMA) standards (Agilent EasyVials) were used for calibration. The Kuhn-Mark-Houwink-Sakurada parameter α, relating to polymer conformation in solution was determined from the gradient of the double logarithmic plot of intrinsic viscosity as a function of molecular weight, using the SEC viscometry detector and Agilent SEC software. Proton nuclear magnetic resonance spectra (^{1}H NMR) were recorded on a Bruker Advance 400 or 300 spectrometer (400 MHz or 300 MHz) at 27 °C, with chemical shift values (δ) reported in ppm, and the residual proton signal of the solvent used as internal standard. Proton-decoupled carbon nuclear magnetic resonance spectra (^{13}C NMR) were recorded on a Bruker Advance 400 (100 MHz) at 27 °C in $CDCl_3$, with chemical shift values (δ) reported in ppm, and the residual proton signal of the solvent used as internal standard (δC 77.16). Phosphorous ^{31}P NMR spectroscopy was performed on a Bruker Advance 400 (162 MHz) in DMSO-d6, at 27 °C, with chemical shift values (δ) reported in ppm. Fourier transform infrared spectra (FTIR) were recorded on a Bruker Alpha FTIR ATR. Elemental analyses for CHN were carried out on a CE440 CHN elemental analyser, and bromine was analysed using classical oxygen flask methods by Warwick Analytical Service.

5.4.3 Polymer synthesis

For a typical polymerisation, with the conditions [BEA]: [PEGA]: [DEGDA]: [CTA]: [I] = 40: 10: 2.5: 1: 0.1, CTA (10.7 mg, 0.0447 mmol), BEA (0.319 g, 1.78 mmol), PEGA

(0.214 g, 0.446 mmol), DEGDA (23.9 mg, 0.112 mmol), ACVA (1.25 mg, 0.00447 mmol), and dioxane (0.445 mL) were added to a vial deoxegenated by bubbling with nitrogen and left to stir in an oil bath at 70 °C. After a predetermined time, the solution was removed from the oil bath and the polymer precipitated in diethyl ether (x3), and dried under vacuum. M_w = 127,900 g/mol, $Đ$ = 5.4 (DMF SEC, +NH_4BF_4 additive eluent, PMMA calibration). ^{1}H NMR spectrum (400 MHz, DMSO-d_6, δ ppm): 4.34 (m, 2H, -C(O)O-C**H$_2$**-CH_2-Br), 4.12 (m, 2H, -C(O)O-C**H$_2$**-CH_2-O-), 3.65 (m, 2H, -C(O)O-CH_2-C**H$_2$**-Br), 3.52 (m, 32H, -C**H$_2$**- (PEG)), 3.24 (s, 3H, -(CH_2-CH_2-O)-C**H$_3$**), 2.39−1.54 (m, 3H, backbone), 0.89 (t, 3H, -C**H$_3$** (CTA)). ^{13}C NMR spectrum (100 MHz, $CDCl_3$, δ ppm): 173.79 (-**C**(O)O-), 70.26 (-**C**H_2- (PEG)), 66.82 (-C(O)O-**C**H_2-), 30.82 (-**C**H_2-Br), 41.23 (backbone tertiary), 39.91 (backbone -**C**H2-). FTIR ν cm^{-1}: 2867 (medium, C-H alkane), 1728 (strong, C=O ester), 1447 (medium, C-H alkane), 1093 (strong, C-O-C PEG). 569 (weak, C-Br). Elemental analysis shown in **Table A5.2**.

In order to further characterise the branched nature of the synthesised polymers, two linear p(BEA-co-PEGA) polymers were synthesised to give a comparison for the KMHS intrinsic viscosity vs molecular weight plots, and associated α values. The polymerisation conditions were identical to the above branched polymers, but without DEGDA crosslinker (conditions and characterisation data can be seen in **Table A5.1**, and **Figures A5.1** and **A5.2**). M_n = 9,700 g/mol, $Đ$ = 1.12; and M_n = 16,800 g/mol, $Đ$ = 1.32; (DMF SEC, +NH_4BF_4 additive eluent, PMMA calibration). ^{1}H NMR spectrum (400 MHz, DMSO-d_6, δ ppm): 4.34 (m, 2H, -C(O)O-C**H$_2$**-CH_2-Br), 4.12 (m, 2H, -C(O)O-C**H$_2$**-CH_2-O-), 3.65 (m, 2H, -C(O)O-CH_2-C**H$_2$**-Br), 3.52 (m, 32H, -C**H$_2$**- (PEG)), 3.24 (s, 3H, -(CH_2-CH_2-O)-C**H$_3$**), 2.39−1.54 (m, 3H, backbone), 0.89 (t, 3H, -C**H$_3$** (CTA)). ^{13}C NMR spectrum (100 MHz, $CDCl_3$, δ ppm): 174.90 (-**C**(O)O-), 70.19 (-**C**H_2- (PEG)), 65.52 (-C(O)O-**C**H_2-), 31.32 (-**C**H_2-Br), 41.28 (backbone tertiary), 22.87 (backbone -**C**H2-). FTIR ν cm^{-1}: 2880 (medium, C-H alkane), 1725 (strong, C=O ester), 1440 (medium, C-H alkane), 1095 (strong, C-O-C PEG), 576 (weak, C-Br).

5.4.4 Post-polymerisation modification

Typical post-polymerization substitution of branched p(BEA-co-PEGA) with trimethylamine: p(BEA-co-PEGA) (0.10 g of polymer, 0.447 mmol of BEA units) was dissolved in 2 mL of DMSO in a small vial with a stirrer bar, to which was added 2.5 equivalents of trimethylamine (4.2 M in ethanol, 266 μL, 1.12 mmol) and stirred for 48 h under a nitrogen atmosphere. Upon completion, the solution was concentrated by nitrogen flow, purified by precipitation into THF, and dried under vacuum, to give the desired p(TMAEA-co-PEGA). ^{1}H NMR (400 MHz, DMSO-d_6, ppm): δ = 4.53 (m, 2H, -C(O)O-C**H$_2$**-CH$_2$-NMe$_3$), 4.12 (m, 2H, -C(O)O-C**H$_2$**-CH$_2$-O-), 3.91 (m, 2H, -C(O)O-CH$_2$-C**H$_2$**-NMe$_3$), 3.52 (m, 32H, -C**H$_2$**- (PEG)), 3.34 (m, 9H, CH$_2$-CH$_2$-N**Me$_3$**), 3.24 (s, 3H, -(CH$_2$-CH$_2$-O)-C**H$_3$**), 2.41−1.51 (m, 3H, backbone), 0.89 (m, 3H, -C**H$_3$** (CTA)). ^{13}C NMR spectrum (100 MHz, CDCl$_3$, δ ppm): 174.04 (-**C**(O)O-), 70.22 (-**C**H$_2$- (PEG)), 64.00 (-C(O)O-CH$_2$-**C**H$_2$-), 58.92 (-C(O)O-**C**H$_2$-CH$_2$-), 53.42 (-N(**C**H$_3$)$_3$), 40.85 (backbone tertiary), 39.73 (backbone -**C**H2-). FTIR ν cm^{-1}: 2871 (medium, C-H alkane), 1728 (strong, C=O ester), 1477 (medium, C-H alkane), 1248 (medium, C-N, amine), 1092 (strong, C-O-C PEG). Elemental analysis shown in **Table A5.2**.

Typical post-polymerization substitution of branched p(BEA-co-PEGA) with trimethylphosphine: p(BEA-co-PEGA) (0.10 g of polymer, 0.447 mmol of BEA units) was disolved in 2 mL of DMSO in a small vial with a stirrer bar, to which was added 2.5 equiv of trimethylphosphine (1 M in THF, 1.12 mL, 1.12 mmol) and stirred for 48 h under a nitrogen atmosphere. Upon completion, the solution was concentrated by nitrogen flow, purified by precipitation into THF, and dried under vacuum, to give the desired p(TMPEA-co-PEGA). ^{1}H NMR (300 MHz, DMSO-d_6, ppm): δ = 4.36 (m, 2H, -C(O)O-C**H$_2$**-CH$_2$-PMe$_3$), 4.13 (m, 2H, -C(O)O-C**H$_2$**-CH$_2$-O-), 3.51 (m, 32H, -C**H$_2$**- (PEG)), 3.24 (s, 3H, -(CH$_2$-CH$_2$-O)-C**H$_3$**), 2.83 (m, 2H, -C(O)O-CH$_2$-C**H$_2$**-PMe$_3$), 2.07 (m, 9H, CH$_2$-CH$_2$-P**Me$_3$**), 2.46−1.44 (m, 3H, backbone), 1.06 (m, 3H, -C**H$_3$** (CTA)). ^{13}C NMR spectrum (100 MHz, CDCl$_3$, δ ppm): 174.13 (-**C**(O)O-), 70.23 (-**C**H$_2$- (PEG)), 60.64 (-C(O)O-CH$_2$-**C**H$_2$-), 54.87 (-C(O)O-**C**H$_2$-CH$_2$-), 40.84 (backbone tertiary), 39.93 (backbone -**C**H2-), 8.99 (-P(**C**H$_3$)$_3$). FTIR ν cm^{-1}: 2897 (medium, C-H alkane), 1728

(strong, C=O ester), 1420 (medium, C-H alkane), 1087 (strong, C-O-C PEG), 971 (strong, P-CH_3). Elemental analysis shown in **Table A5.2**.

5.4.5 DLS/Zetapotential

Dynamic light scattering measurements were carried of resulting polymers and polyplexes at various N/P ratios using a Malvern nanoZS zetasizer instrument (scattering angle of 173°, 10 mW He-Ne laser). For polyplex formation: appropriate amount of polymer stock solution and DNA stock solution were mixed and made up to a total volume of 1 mL in DI water (final concentration of polymer was 1 mg/mL, in all solutions). The resulting solutions were vortexed incubated for 30 minutes at room temperature and were analysed at 25°C. Each sample was run in triplicate and data was acquired using the software (Malvern Zetasizer) provided. Zeta potential measurements were carried out on the same DLS samples at various N/P ratios using the same instrument, and Malvern disposable folded capillary cell (DTS1070) cuvettes.

5.4.6 Agarose gel electrophoresis

Agarose gels (1% w/v) were prepared with agarose and 1 × TAE buffer. The solution was cooled on the bench for 5 minutes and 100 µL of 0.5 µg/mL ethidium bromide solution was added. The mixture was poured into the casted agarose tray and a comb inserted. The gel was left to set for a minimum of 30 minutes at room temperature. The agarose gels were run in 1× TAE buffer. The final gel was visualized under UV illumination at 365 nm using a UVP benchtop UV transilluminator system. Polyplexes of DNA were prepared at various N/P ratios. DNA stock solution of 60 µg/mL was prepared in PBS, and polymer stock solution of 300 µg/mL. For polyplex formation: appropriate amount of polymer stock solution and DNA stock solution were mixed and made up to a total volume of 100 µL in PBS (final concentration of DNA was 0.030 µg/µL, in all solutions). Polyplexes were vortexed and incubated at room temperature for 30 minutes. Prior to loading, 30 µL of loading buffer was added to each sample and 20 µL of polyplexes were

loaded into the agarose gel wells. Gel electrophoresis was performed at 100 V for 30 minutes.

5.4.7 Cell culture

3T3 mouse endothelial cells were obtained from the European Collection of Cell Cultures (ECACC) and used between passages 5 and 25, grown in DMEM (Dulbecco's Modified Eagle Medium) supplemented with 10% of fetal calf serum, 1% of 2 mM glutamine. The cells were grown as adherent monolayers at 310 K under a 5% CO2 humidified atmosphere and passaged at approximately 70–80% confluence.

5.4.8 Cytotoxicity assays

For cell viability evaluation, 3T3 cells were seeded in a 96 well plate at a density of 1×10^4 cells per well. After 16 hours, the culture medium was replaced by fresh media containing a series of dilution of the polymers (2, 0.8, 0.2, 0.08, 0.02 mg/mL), prepared from stock solutions in media. Following 24 hours incubation, the medium was removed and replaced with fresh medium. The cells were incubated with a freshly prepared solution of XTT (0.2 mg/mL^{-1}) and N-methyl dibenzopyrazine methyl sulfate (250 µM) in medium for 16 hours. Absorbance of the samples was finally measured using a plate reader at 450 nm and 650 nm. The data presented are representative of a minimum of two independent experiments where each sample was measured in triplicate. Errors reported correspond to the standard deviation of the mean.

5.4.9 *In vitro* transfection

Polyplex samples were prepared prior to incubation with the cells, via mixing of plasmid DNA solution (final $concentration_{DNA}$ = 100 µg/mL) with the appropriate amount of polymer predissolved in sterile water (N/P ratio = 20), and left to complex at room temperature for one hour. HEK293T cells were seeded in a 24 well plate at a density of 1

$\times 10^5$ cells per well. After 16 hours, the culture medium was replaced by Optimem® cell culture media (Thermo Fisher Scientific) without fetal bovine serum. After one hour, the media was replaced by fresh Optimem® media containing the polyplex solutions (final $concentration_{DNA}$ = 10 µg/mL), the cells left to incubate for 5 hours under 5% CO_2 humidified atmosphere, then the media replaced with fresh culture media containing fetal bovine serum. Following overnight incubation, cells were washed with PBS, trypsinised, centrifuged, re-dispersed in ice-cold PBS and filtered into FACS tubes for analysis. Intracellular fluorescence was quantified using a BD LSR II cytometer (BD Biosciences) at excitation 488 nm and emission 525 nm. The geometric mean fluorescence was used as the sample value. The data in presented are representative of two separate experiments where each sample was measured in duplicate (n = 4). All errors reported correspond to the standard deviation from the mean

5.4.10 Polyplex soil stability assay

Polyplexes were formed in sterile water at an N/P ratio of 5 with a final concentration of 1 mg/mL dsRNA. 200 µL of polyplexes were mixed with 0.5 g soil (live soil containing enzymes, and also sterilised soil (sterilisation conditions: 200 ˚C, 2 hr)) in 2 mL microtubes. Separate microtubes were used for each sample time point and stored at room temperature. At the appropriate time, the reaction was stopped by addition of 1 mL trireagent, vortexing, and incubating for 5 minutes, before storing the sample time point at -20 ˚C.

5.4.11 dsRNA extraction

dsRNA was extracted from the soil in order to analyse the dsRNA by agarose gel electrophoresis. Polyplex/soil/trireagent samples were defrosted, 200 µL of chloroform added, and incubated for 3 minutes at room temperature. Samples were then centrifuged for 15 minutes at 12000 g and 4 ˚C. Supernatant was added to new microtube, isopropanol added (1/1 ratio) to precipitate the RNA, and incubated at for 10 minutes at room temperature. Microtubes were then centrifuged at 12000 g and 4 ˚C for 10 minutes.

Supernatant was removed and 500 µL of 70 % ethanol (in RNAse free water) added to the pellet, then centrifuged for 5 minutes at 12000 g and 4 ˚C. The supernatant was removed and the pellet left to dry for 10 minutes before being suspended in 200 µL of RNAse free water. These RNA samples were then enriched for dsRNA following a LiCl purification protocol. LiCl (8M, 67 µL) was added to the 200 uL RNA samples, which were mixed on ice, and incubated for 30 minutes at -20 ˚C. Microtubes were then centrifuged for 20 minutes at 14000 g and 4 ˚C, the supernatant was brought to a new microtube, and LiCl (8M, 133.5 µL) was added. The samples were mixed on ice, incubated for 30 minutes at -20 ˚C, and then centrifuged for 20 minutes at 14000 g and 4 ˚C. The supernatant was removed, the dsRNA pellet washed with 70% ethanol (in RNAse free water, 150 µL), and then centrifuged for 5 minutes at 12000 g and 4 ˚C. The supernatant was removed and the dsRNA pellet left to dry for 5 minutes before being suspended in 20 µL of RNAse free water. These final dsRNA samples were analysed by spectrophotometry (NanoPhotometer NP60 spectrophotometer), and agarose gel electrophoresis. Gel electrophoresis was performed at 100 V for 20 minutes on a 1% agarose gel (1x TAE buffer) containing ethidium bromide.

Appendix to Chapter 5

Table of polymerisation conditions, linear polymer SEC chromatograms and KMHS plots, p(TMPEA-*co*-PEGA) and p(TMAEA-*co*-PEGA) ^{1}H NMR spectra for degree of substitution, p(TMPEA-*co*-PEGA) ^{31}P NMR spectrum, elemental analysis data, branched polymer DLS and zetapotential, ^{1}H NMR spectroscopy hydrolysis resistance study for branched p(TMPEA-*co*-PEGA), polyplex soil stability assay.

5.5 References

(1) Whitehead, K. A.; Langer, R.; Anderson, D. G., Knocking down barriers: advances in siRNA delivery, *Nat. Rev. Drug Discov.* **2009**, *8*, 129.

(2) Fire, A.; Xu, S. Q.; Montgomery, M. K.; Kostas, S. A.; Driver, S. E.; Mello, C. C., Potent and specific genetic interference by double-stranded RNA in Caenorhabditis elegans, *Nature* **1998**, *391*, 806.

(3) Kanasty, R.; Dorkin, J. R.; Vegas, A.; Anderson, D., Delivery materials for siRNA therapeutics, *Nat. Mater.* **2013**, *12*, 967.

(4) Yin, H.; Kanasty, R. L.; Eltoukhy, A. A.; Vegas, A. J.; Dorkin, J. R.; Anderson, D. G., Non-viral vectors for gene-based therapy, *Nature Reviews Genetics* **2014**, *15*, 541.

(5) Godbey, W. T.; Ku, K. K.; Hirasaki, G. J.; Mikos, A. G., Improved packing of poly(ethylenimine)/DNA complexes increases transfection efficiency, *Gene Ther.* **1999**, *6*, 1380.

(6) Lv, H. T.; Zhang, S. B.; Wang, B.; Cui, S. H.; Yan, J., Toxicity of cationic lipids and cationic polymers in gene delivery, *J. Control. Release* **2006**, *114*, 100.

(7) Godbey, W. T.; Wu, K. K.; Mikos, A. G., Poly(ethylenimine)-mediated gene delivery affects endothelial cell function and viability, *Biomaterials* **2001**, *22*, 471.

(8) Wolfert, M. A.; Dash, P. R.; Nazarova, O.; Oupicky, D.; Seymour, L. W.; Smart, S.; Strohalm, J.; Ulbrich, K., Polyelectrolyte vectors for gene delivery: Influence of cationic polymer on biophysical properties of complexes formed with DNA, *Bioconjugate Chem.* **1999**, *10*, 993.

(9) Pack, D. W.; Hoffman, A. S.; Pun, S.; Stayton, P. S., Design and development of polymers for gene delivery, *Nat. Rev. Drug Discov.* **2005**, *4*, 581.

(10) Ilies, M. A.; Seitz, W. A.; Caproiu, M. T.; Wentz, M.; Garfield, R. E.; Balaban, A. T., Pyridinium-based cationic lipids as gene-transfer agents, *Eur. J. Org. Chem.* **2003**, 2645.

(11) Rose, V. L.; Mastrotto, F.; Mantovani, G., Phosphonium polymers for gene delivery, *Polymer Chemistry* **2017**, *8*, 353.

(12) Stekar, J.; Nossner, G.; Kutscher, B.; Engel, J.; Hilgard, P., Synthesis, Antitumor-Activity, and Tolerability of Phospholipids Containing Nitrogen Homologs, *Angewandte Chemie-International Edition in English* **1995**, *34*, 238.

(13) Strasak, T.; Maly, J.; Wrobel, D.; Maly, M.; Herma, R.; Cermak, J.; Mullerova, M.; St'astna, L. C.; Curinova, P., Phosphonium carbosilane dendrimers for biomedical applications - synthesis, characterization and cytotoxicity evaluation, *Rsc Advances* **2017**, *7*, 18724.

(14) Guenin, E.; Herve, A. C.; Floch, V.; Loisel, S.; Yaouanc, J. J.; Clement, J. C.; Ferec, C.; des Abbayes, H., Cationic phosphonolipids containing quaternary phosphonium and arsonium groups for DNA transfection with good efficiency and low cellular toxicity, *Angew. Chem. Int. Ed.* **2000**, *39*, 629.

(15) Ornelas-Megiatto, C.; Wich, P. R.; Frechet, J. M. J., Polyphosphonium Polymers for siRNA Delivery: An Efficient and Nontoxic Alternative to Polyammonium Carriers, *J. Am. Chem. Soc.* **2012**, *134*, 1902.

(16) Rose, V. L.; Shubber, S.; Sajeesh, S.; Spain, S. G.; Puri, S.; Allen, S.; Lee, D. K.; Winkler, G. S.; Mantovani, G., Phosphonium Polymethacrylates for Short Interfering RNA Delivery: Effect of Polymer and RNA Structural Parameters on Polyplex Assembly and Gene Knockdown, *Biomacromolecules* **2015**, *16*, 3480.

(17) Hemp, S. T.; Allen, M. H.; Green, M. D.; Long, T. E., Phosphonium-Containing Polyelectrolytes for Nonviral Gene Delivery, *Biomacromolecules* **2012**, *13*, 231.

(18) Hemp, S. T.; Smith, A. E.; Bryson, J. M.; Allen, M. H.; Long, T. E., Phosphonium-Containing Diblock Copolymers for Enhanced Colloidal Stability and Efficient Nucleic Acid Delivery, *Biomacromolecules* **2012**, *13*, 2439.

(19) Barlow, T. R.; Brendel, J. C.; Perrier, S., Poly(bromoethyl acrylate): A Reactive Precursor for the Synthesis of Functional RAFT Materials, *Macromolecules* **2016**, *49*, 6203.

(20) Boyer, C.; Bulmus, V.; Davis, T. P.; Ladmiral, V.; Liu, J. Q.; Perrier, S., Bioapplications of RAFT Polymerization, *Chem. Rev.* **2009**, *109*, 5402.

(21) Cobo, I.; Li, M.; Sumerlin, B. S.; Perrier, S., Smart hybrid materials by conjugation of responsive polymers to biomacromolecules, *Nat. Mater.* **2015**, *14*, 143.

(22) Liu, B. L.; Kazlauciunas, A.; Guthrie, J. T.; Perrier, S., One-pot hyperbranched polymer synthesis mediated by reversible addition fragmentation chain transfer (RAFT) polymerization, *Macromolecules* **2005**, *38*, 2131.

(23) Anderson, D. G.; Akinc, A.; Hossain, N.; Langer, R., Structure/property studies of polymeric gene delivery using a library of poly(beta-amino esters), *Mol. Ther.* **2005**, *11*, 426.

(24) Wightman, L.; Kircheis, R.; Rossler, V.; Carotta, S.; Ruzicka, R.; Kursa, M.; Wagner, E., Different behavior of branched and linear polyethylenimine for gene delivery in vitro and in vivo, *J. Gene Med.* **2001**, *3*, 362.

(25) Ahmed, M.; Narain, R., Progress of RAFT based polymers in gene delivery, *Prog. Polym. Sci.* **2013**, *38*, 767.

(26) Liu, B. L.; Kazlauciunas, A.; Guthrie, J. T.; Perrier, S., Influence of reaction parameters on the synthesis of hyperbranched polymers via reversible addition fragmentation chain transfer (RAFT) polymerization, *Polymer* **2005**, *46*, 6293.

(27) Semsarilar, M.; Ladmiral, V.; Perrier, S., Highly Branched and Hyperbranched Glycopolymers via Reversible Addition-Fragmentation Chain Transfer Polymerization and Click Chemistry, *Macromolecules* **2010**, *43*, 1438.

(28) Isaure, F.; Cormack, P. A. G.; Graham, S.; Sherrington, D. C.; Armes, S. P.; Butun, V., Synthesis of branched poly(methyl methacrylate)s via controlled/living polymerisations exploiting ethylene glycol dimethacrylate as branching agent, *Chem. Commun.* **2004**, 1138.

(29) O'Brien, N.; McKee, A.; Sherrington, D. C.; Slark, A. T.; Titterton, A., Facile, versatile and cost effective route to branched vinyl polymers, *Polymer* **2000**, *41*, 6027.

(30) Slark, A. T.; Sherrington, D. C.; Titterton, A.; Martin, I. K., Branched methacrylate copolymers from multifunctional comonomers: the effect of multifunctional monomer functionality on polymer architecture and properties, *J. Mater. Chem.* **2003**, *13*, 2711.

(31) Felgner, P. L.; Barenholz, Y.; Behr, J. P.; Cheng, S. H.; Cullis, P.; Huang, L.; Jessee, J. A.; Seymour, L.; Szoka, F.; Thierry, A. R.; Wagner, E.; Wu, G., Nomenclature for synthetic gene delivery systems, *Hum. Gene Ther.* **1997**, *8*, 511.

(32) Nelson, C. E.; Kintzing, J. R.; Hanna, A.; Shannon, J. M.; Gupta, M. K.; Duvall, C. L., Balancing Cationic and Hydrophobic Content of PEGylated siRNA Polyplexes Enhances Endosome Escape, Stability, Blood Circulation Time, and Bioactivity in Vivo, *Acs Nano* **2013**, *7*, 8870.

(33) Ferguson, C. J.; Hughes, R. J.; Nguyen, D.; Pham, B. T. T.; Gilbert, R. G.; Serelis, A. K.; Such, C. H.; Hawkett, B. S., Ab initio emulsion polymerization by RAFT-controlled self-assembly, *Macromolecules* **2005**, *38*, 2191.

Appendix to Chapter 5

Table A5.1. Polymerisation conditions for both branched and linear BEA PEGA copolymers, and characterisation data from SEC and NMR spectroscopy.

Polymer	Conditions	DRI SEC			TD SEC		^{1}H NMR		
	[BEA]:[PEGA]:[DEGDA]:[CTA]:[I]	M_n (g/mol)	M_w (g/mol)	$Đ$	M_w (g/mol)	α	DP BEA	DP PEGA	M_n (g/mol)
Branched	40:10:2.5:1:0.1	23,600	127,900	5.41	220,900	0.35	58	17	-
Linear	64:16:0:1:0.1	9,700	10,800	1.12	13,900	0.6	39	9	11,300
Linear	240:60:0:1:0.1	16,800	22,100	1.32	31,800	0.78	160	35	45,400

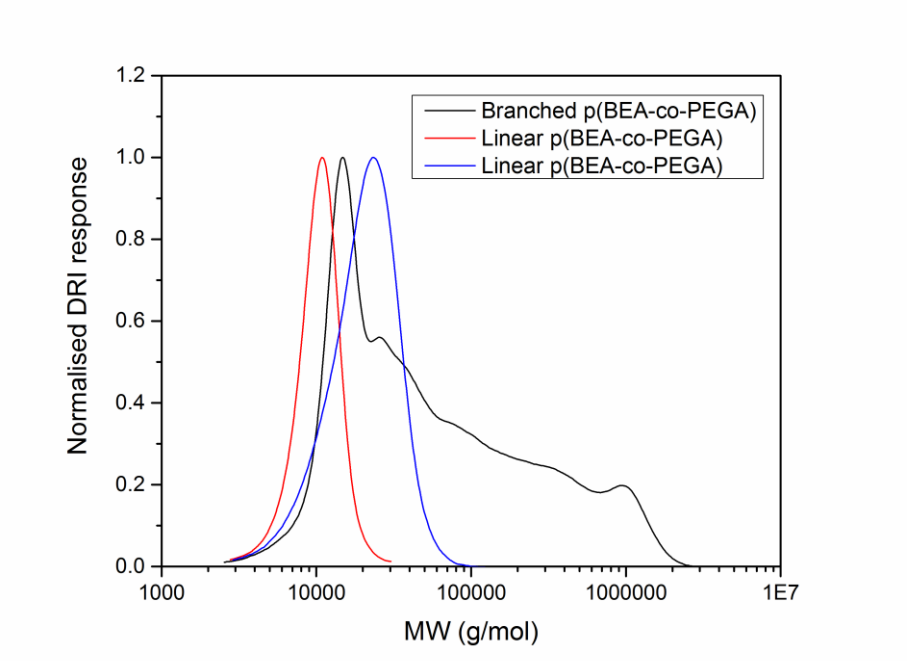

Figure A5.1. Size exclusion chromatograms of branched and linear p(BEA-co-PEGA) precursor polymers from refractive index detector (DMF, PMMA calibration, Mn = 127,900 g/mol, Đ = 5.4).

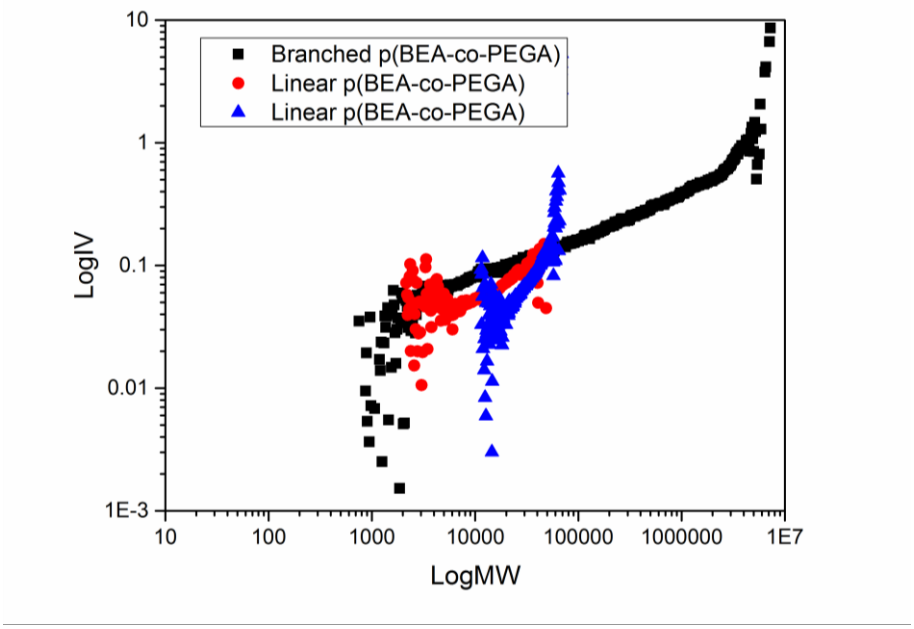

Figure A5.2. KMHS plot of branched and linear p(BEA-co-PEGA) precursor polymers from viscometry detector in DMF.

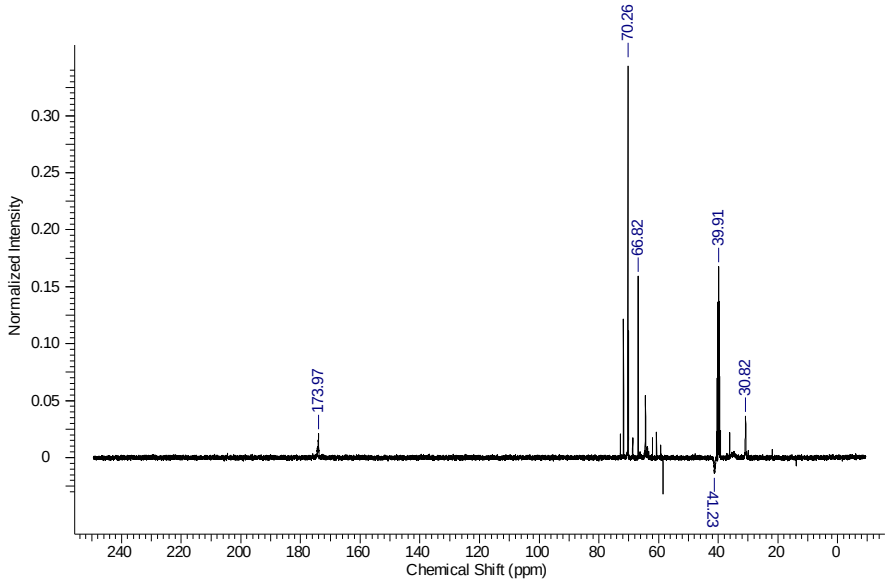

Figure A5.3. ^{13}C NMR spectrum of branched p(BEA-co-PEGA) precursor polymer in deuterated DMSO.

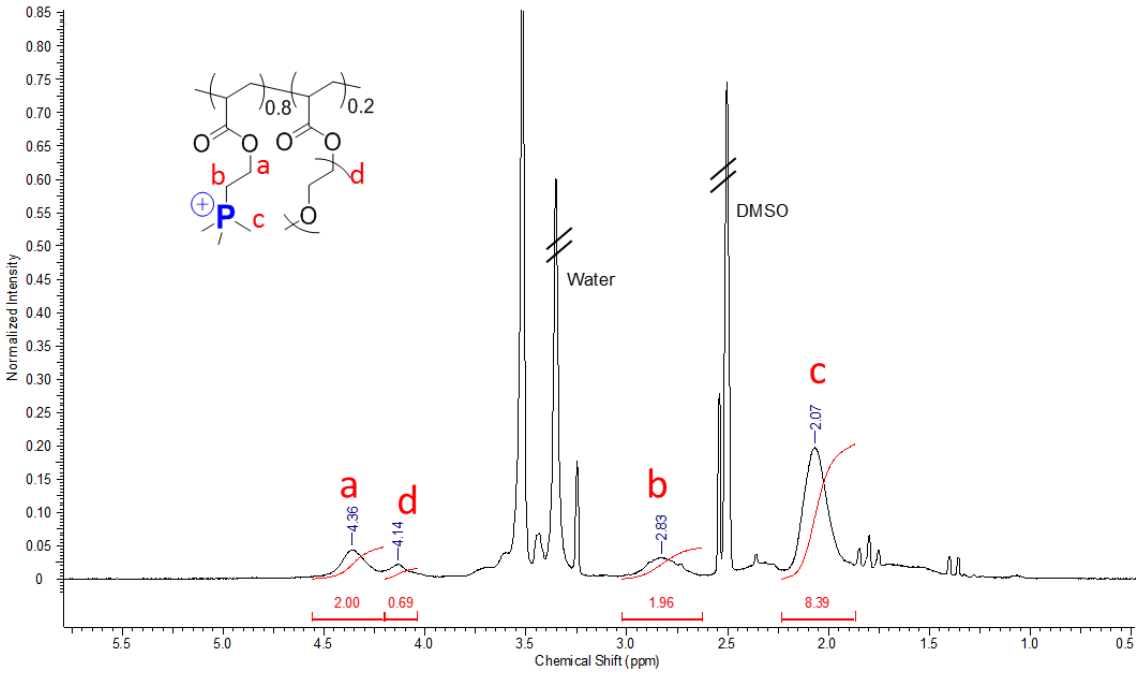

Figure A5.4. ^{1}H NMR in DMSO-d6 of branched p(TMPEA-co-PEGA).

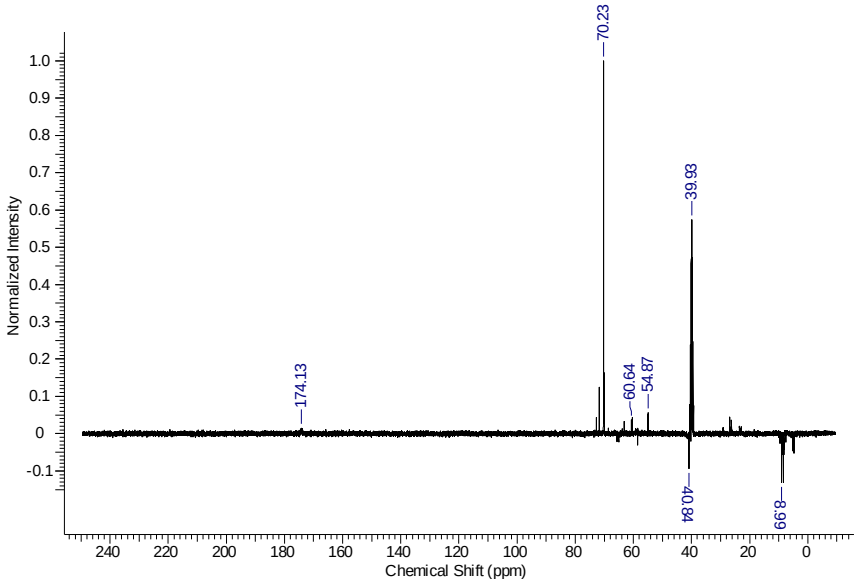

Figure A5.5. ^{13}C NMR in DMSO-d6 of branched p(TMPEA-co-PEGA).

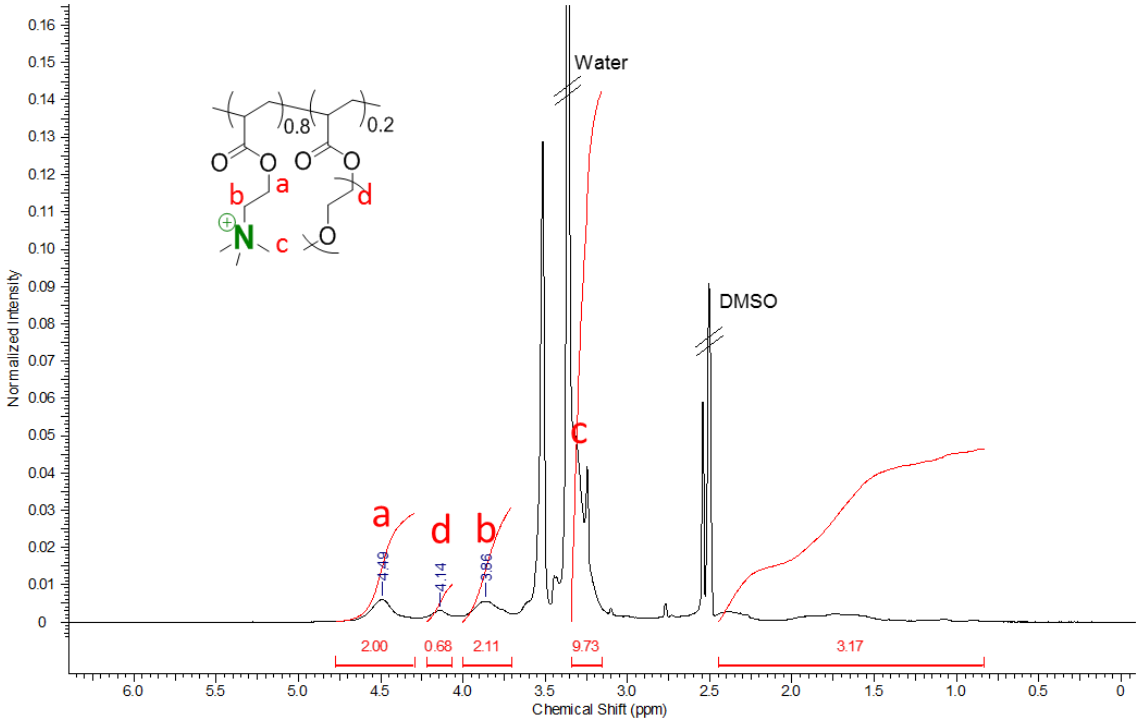

Figure A5.6. ^{1}H NMR in DMSO-d6 of branched p(TMAEA-co-PEGA).

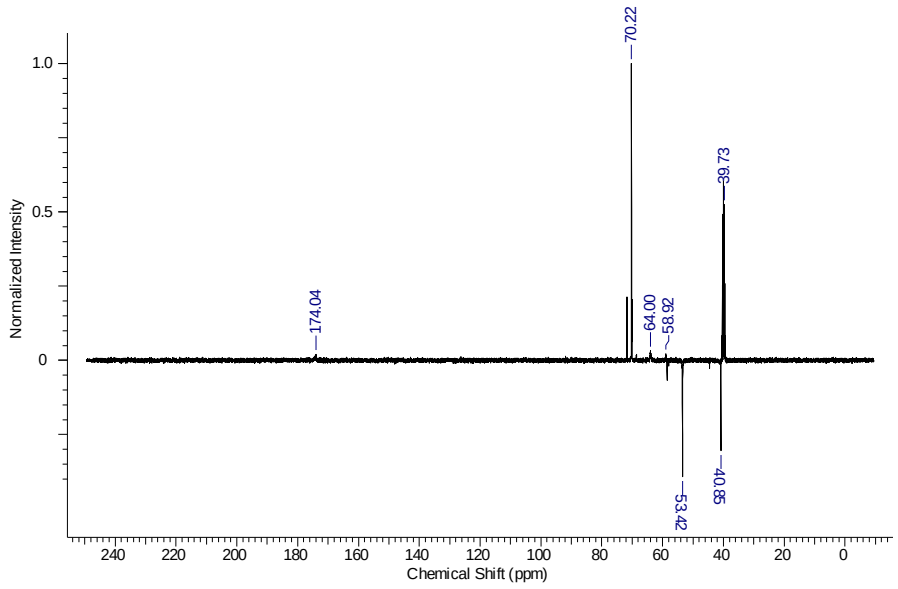

Figure A5.7. ^{13}C NMR in DMSO-d6 of branched p(TMAEA-co-PEGA).

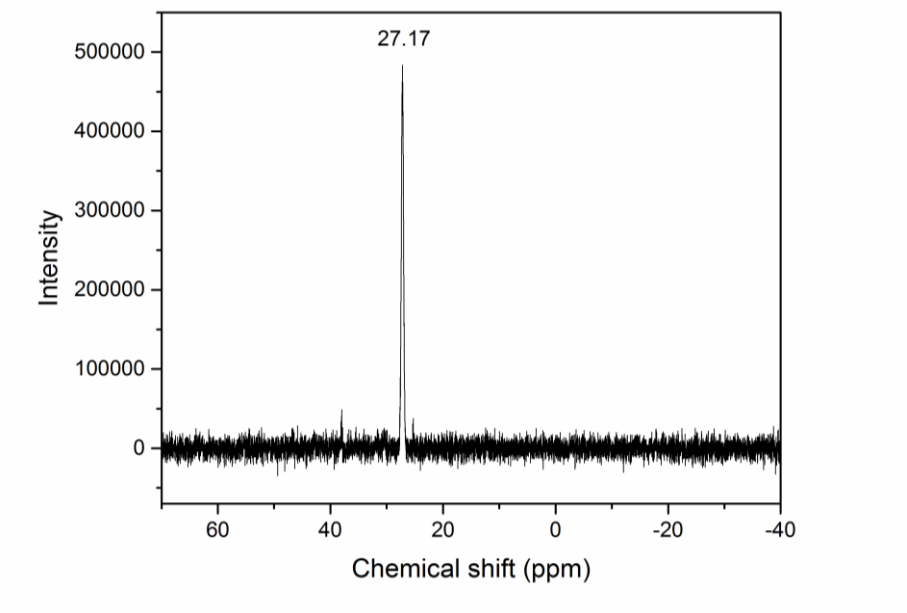

Figure A5.8. Phosphorous (^{31}P) NMR spectrum of branched p(TMPEA-co-PEGA) confirming the presence of phosphonium moieties on the purified polymer.

Table A5.2. Elemental analysis results for branched BEA PEGA copolymer, and post-polymerisation modified polymers, branched p(TMPEA-coPEGA) and p(TMAEA-co-PEGA).

Polymer	**C (%)**		**H (%)**		**N (%)**		**Br (%)**		**S (%)**	
	Calc.	Found	Calc.	Found	Calc.	Found	Calc.	Found	Calc.	Found
Branched p(BEA-co-PEGA) $C_{445.5}H_{739}Br_{40}O_{198.25}S_3$	42.60	41.95	5.93	6.08	0.00	0.00	25.45	24.91	0.77	1.01
Branched p(TMAEA-co-PEGA) $C_{565.5}H_{1099}Br_{40}N_{40}O_{198.25}S_3$	45.51	40.45	7.42	7.79	3.75	3.10	21.42	19.88	0.64	1.99
Branched p(TMPEA-co-PEGA) $C_{565.5}H_{1099}Br_{40}O_{198.25}P_{40}S_3$	43.53	38.04	7.10	7.22	0.00	0.00	20.48	19.21	0.62	1.10

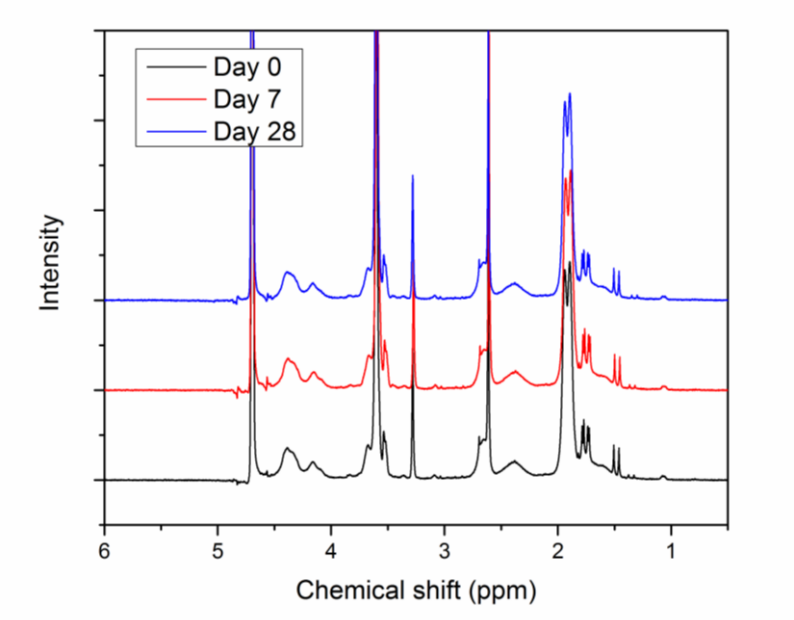

Figure A5.9. Proton (^{1}H) NMR spectra of branched p(TMPEA-co-PEGA) in D2O over 4 weeks at room temperature and pH 7, confirming no hydrolysis of polymer side chains occurring.

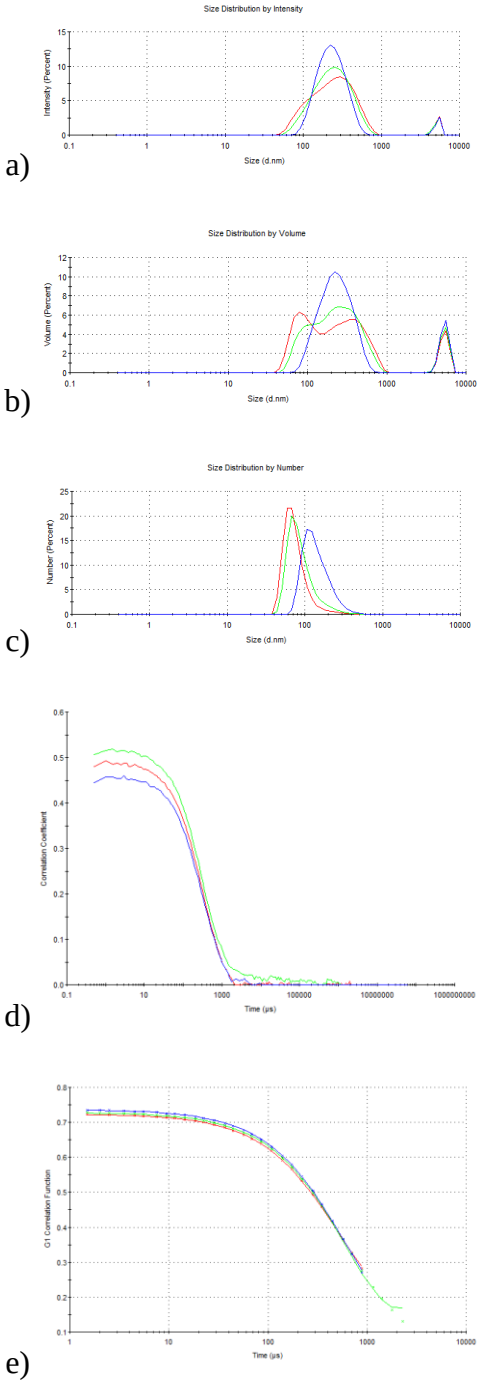

Figure A5.10. Representative DLS data for polyples solutions (branched p(TMPEA-co-PEGA) with DNA, N/P 10, three repeats shown), a) intensitie distribution, b) volume distribution, c) number distribution, d) correlalograms, e) cummulants fit.

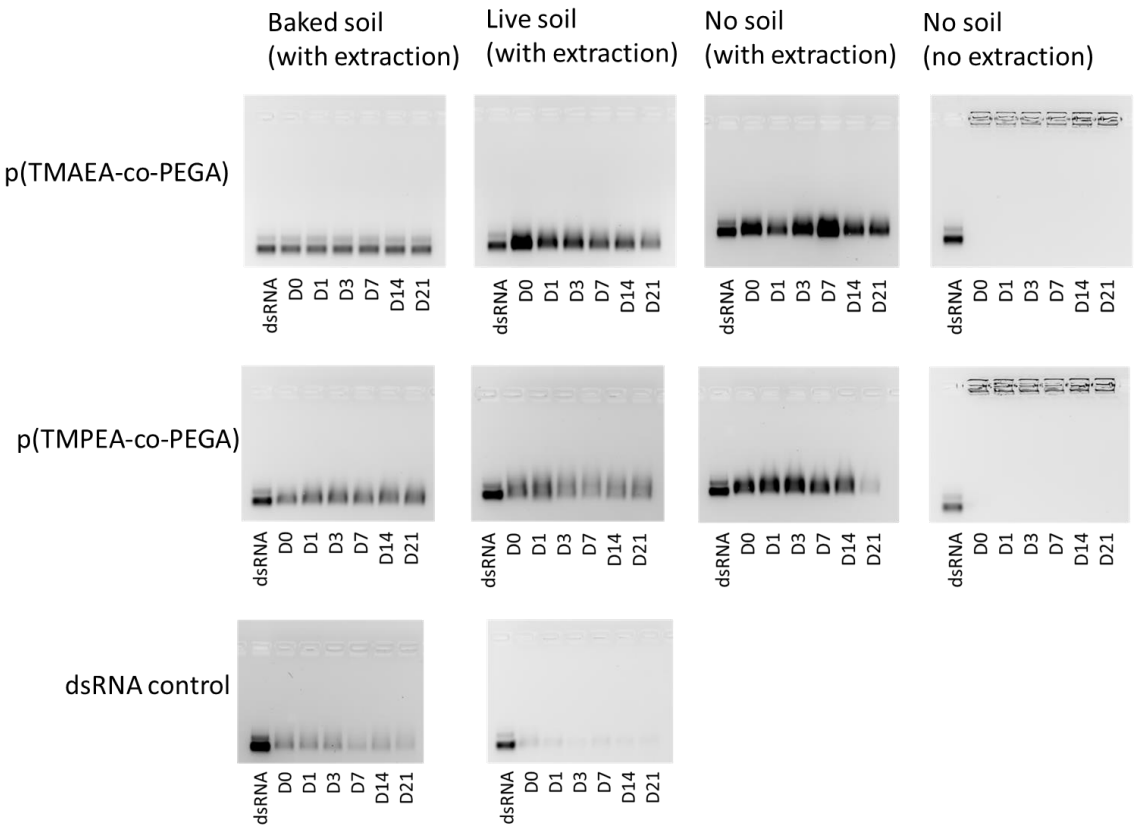

Figure A5.11. Polyplex soil stability assay (dsRNA protection), polyplexes were formed in sterile water at an N/P ratio of 5 with a final concentration of 1 mg/mL dsRNA, incubated in live soil or enzyme free soil, then dsRNA was extracted and run on an agarose gel.

Conclusions and future perspectives

The objective of this work was to utilise advanced polymer synthesis methods to synthesise a range of new cationic polymers with well controlled branched architectures and different charged moieties for nucleic acid delivery applications. The synthesised polymers ability to complex nucleic acids, the resulting polyplex morphology, initial polymer toxicity, and associated gene transfection efficiencies were also investigated.

Chapter 2 describes a method for the preparation of hyperbranched polymers with high degrees of branching, predictable molecular weights and narrow molecular weight distributions, involving slow monomer addition of a thiol/yne monomer to multifunctional core molecules in the presence of photoinitiator and UV irradiation. A small thiol/yne monomer was synthesized via simple esterification, giving a route to high purity monomers. Copolymerisation with multifunctional alkyne or alkene molecules was found to lower dispersity of the resulting hyperbranched polymers, whilst maintaining very high degrees of branching. This Chapter outlined a new process for the synthesis of hyperbranched polymers of remarkably well-controlled molecular weight and molecular weight distributions, with very high degrees of branching.

Synthesis of hyperbranched polyethyleneimine containing structures by AB_2 chemistry is reported for the first time in Chapter 3. This strategy allowed for the preparation of hyperbranched polymers, from macromolecular monomer units, with degrees of branching in the region of dendrimers. The synthetic strategy allowed synthesis of AB_2 hyperbranched PEI structures with only secondary amines, and well defined branching patterns, unachievable via the ring opening polymerisation of aziridine. The GFP plasmid DNA polyplex nanoparticles were analysed by DLS, zetapotential, and AFM. Hyperbranched poly(ethyleneimine-*co*-oxazoline) and bPEI from small positively charged particles, and linear forms were found to form larger aggregates. Differences were also found in polymer *in vitro* cytotoxicity due to polymer architecture, with poly(ethyleneimine-*co*-oxazoline)s having much reduced toxicity compared to bPEI, and the hyperbranched poly(ethyleneimine-*co*-oxazoline) having reduced toxicity compared to the linear equivalent. Delivery of pDNA encoding for GFP was assessed with in vitro

assays. Poly(ethyleneimine-*co*-oxazoline) copolymer with high percentages of ethyleneimine units were found to have transfection efficiencies slightly lower than the commercial standard 25K branched PEI. In agreement with the literature, it is believed that the compact hyperbranched polymer conformation contributes, in some extent, to both the improved toxicity and also high transfection efficiencies.

Chapter 4 is a study outlining the syntheisis of highly branched polymers by RAFT polymerisation of hydrolysable amine containing monomers: DMAEA, DMAPA, DMAEMA, and also copolymers of DMAEA and DMAEMA. The highly branched nature of these polymers was characterised using multi detector size exclusion chromatography. Hydrolysis kinetics of the polymers studied with ^{1}H NMR spectroscopy, showed pDMAPA and p(DMAEMA-co-DMAEA) to have hydrolysis profiles favourable for extended release of dsRNA compared to the fast hydrolysing pDMAEA. The release of dsRNA from polyplex nanoparticles was followed with agarose gel electrophoresis and both pDMAPA and p(DMAEMA-co-DMAEA) showed excellent release kinetics for prolonged oligonucleotide release in aqueous conditions. The highly branched polymeric materials synthesised in this study show great potential for therapeutic dsRNA delivery.

Chapter 5 involves the facile synthesis of highly branched and cationic poly(trimethylphosphonium ethylacrylate-*co*-PEGA), and its ammonium equivalent, using a simple post-polymerisation modification strategy of a p(bromo ethylacrylate-*co*-PEGA) precursor polymer produced using RAFT polymerisation. This synthesis represents a significant improvement/simplification of current phosphonium containing polymer synthetic methods. The results show polyphosphoniums have increased biocompatibility compared to their ammonium equivalents while maintaining the same ability to complex nucleic acids.

The presented thesis has demonstrated a range of polymer synthesis methods including, RAFT polymerisation, thiol-yne polymerisation, and oxazoline polymerisation, to access highly branched and hyperbranched polymer architectures. The polymers were investigated for their ability to bind, protect, and deliver nucleic acids with particular attention to effect of polymer architecture. However, different aspects of this work could be pursued further.

Additional exploration of the thiol-yne polymerisations in Chapter 2 would be beneficial, in order to achieve higher molecular weights. Further work of this project could look at incorporating additional functionality into small molecule thiol-yne monomers for use with the slow monomer addition polymerisation procedure.

To expand upon Chapter 3, alternative plasmid DNA molecules would be investigated. In particular, it would be good to investigate plasmid with therapeutic effect for a particular disease, rather than the GFP reporter gene used in this study. Further work could also look at alternative *in vitro* cell lines, and potentially *in vivo* mouse models. The possibility of reaching full hydrolysis of the hyperbranched poly(oxazoline) would also be interesting, in order to further compare the effect of amine type and polymer architecture on nucleic acid delivery.

Further work on Chapter 4 would look at creating DMAEMA DMAEA copolymers of additional monomer ratios, and comparing the hydrolysis rates to expand the window of nucleic acid controlled release. It would also be beneficial to study the in vitro transfection efficiencies of nucleic acid polyplexes of these polymers, in order to correlate nucleic acid release to biologic effect. Another exciting avenue of research could look at using confocal microscopy to study the intracellular pathway and nucleic acid release of the described polymer systems. This would be achieved with Forster resonance energy transfer (FRET) imaging, by attaching the FRET donor dye to the polymer and the quencher to the nucleic acid, release of the nucleic acid could then be followed in the intracellular environment.

In Chapter 5, it was concluded that the highly branched p(TMPEA-*co*-PEGA) and p(TMAEA-*co*-PEGA) polymers were too hydrophilic to efficiently enter cells *via* endocytosis – a process which typically requires a balance of cationic charge and hydrophobicity – leading to low pDNA transfection efficiencies. Additional work on Chapter 5 would therefore look at varying proportions of PEGA and charged monomer, and also investigating the effect of cationic monomer substituent on gene transfection. Another avenue of research would be to also investigate arsonium and sulfonium cationic monomers in comparison to ammonium and phosphonium.